

**Macro- and microfossils from the Upper Cretaceous
sedimentary rocks of Hornby Island, British Columbia, Canada**

by

Sandy Melvin Stuart McLachlan
B.A., University of Victoria, 2010
CRMP, University of Victoria, 2013

A Thesis Submitted in Partial Fulfillment
of the Requirements for the Degree of

MASTER OF SCIENCE

in the School of Earth and Ocean Science

© Sandy Melvin Stuart McLachlan, 2017
University of Victoria

All rights reserved. This thesis may not be reproduced in whole or in part, by
photocopy or other means, without the permission of the author.

**Macro- and microfossils from the Upper Cretaceous
sedimentary rocks of Hornby Island, British Columbia, Canada**

by

Sandy Melvin Stuart McLachlan
B.A., University of Victoria, 2010
CRMP, University of Victoria, 2013

Supervisory Committee

Dr. Vera Pospelova, Co-Supervisor,
(School of Earth and Ocean Sciences)

Dr. Richard Hebda, Co-Supervisor,
(School of Earth and Ocean Sciences)

Dr. Eileen van der Flier-Keller, Departmental Member
(School of Earth and Ocean Sciences)

Abstract

Heteromorph ammonites and dinoflagellate cysts from the Upper Cretaceous Northumberland Formation on Hornby Island, British Columbia, Canada are examined. The collection and preparation of new material has enabled the recognition of eleven species of which only three have been reported from the locality. Of these taxa represented from three heteromorph ammonite families in the study area, five are new occurrences and three are new to science. This expansion of the Hornby Island ammonite fauna is presented alongside a pioneering taxonomic survey of dinoflagellate cysts from the same rocks. Together, these macro- and microfossils reinforce a late Campanian age for the Northumberland Formation with the upper extent of the section approaching the Campanian-Maastrichtian boundary (CMB) interval. The palaeoecology and evolutionary relationships of these heteromorph ammonoids are considered with new insights into their ontogenetic development and neritic palaeoenvironmental circumstances. The dinoflagellate cysts and associated terrestrial palynomorphs have also allowed for enhanced palaeoenvironmental reconstruction and depositional setting inference. The scope of the studied material, and the presence of key index taxa, enables refined biostratigraphy and a stronger basis for correlation of the Hornby Island succession with neighboring coeval biotic provinces.

Table of Contents

Supervisory Committee	ii
Abstract	iii
Table of Contents	iv
List of Tables	vi
List of Figures	vii
List of Plates	xii
Dedication	xxi
Chapter 1 Introduction.....	1
1.1 Thesis structure	1
Chapter 2 Reassessment of the late Campanian (Late Cretaceous) heteromorph ammonite fauna from Hornby Island, British Columbia, with implications for the taxonomy of the Diplomoceratidae and Nostoceratidae	2
2.1 Contribution of authors	2
2.2 Abstract	2
2.3 Introduction and geological setting.....	3
2.4 Materials and methods	9
2.5 Institutional abbreviations.....	12
2.6 Morphological abbreviations	12
2.7 Systematic Palaeontology	12
2.7.1 Family Baculitidae Gill, 1871.....	13
2.7.2 Family Diplomoceratidae Spath, 1926	19
2.7.3 Family Nostoceratidae Hyatt, 1894	58
2.8 Discussion	88
2.9 Summary	91
2.10 Acknowledgments	92
Chapter 3 General Discussion	93
3.1 Heteromorph ammonite taphonomy	93
3.2 Heteromorph ammonite polymorphism.....	95
3.3 Heteromorph ammonoid ontogeny and palaeoecology	98
3.4 Heteromorph ammonoid evolutionary progression	101
3.5 Heteromorph ammonoid palaeobiogeography.....	103

Chapter 4 Late Campanian (Late Cretaceous) dinoflagellate cysts from Hornby Island, British Columbia with implications for Nanaimo Group biostratigraphy and palaeoenvironmental reconstructions	106
4.1 Abstract	106
4.2 Materials and methods	106
4.3 Morphological abbreviations	114
4.4 Systematic Palaeontology	114
4.5 Discussion	168
4.5.1 Age interpretation	168
4.5.2 Dinoflagellate cyst zones	171
4.5.3 Palaeoenvironmental and paleolatitudinal reconstructions.....	172
4.6 Acknowledgments	177
4.7 Taxonomic entities.....	177
Chapter 5 Conclusion	182
5.1 Summary of research	182
References	183
Appendix I List of heteromorph ammonite specimens.....	233
Appendix II Heteromorph ammonite specimen measurements	254
Appendix III <i>Nostoceras</i> (<i>Nostoceras</i>) species	266
Appendix IV Glossary of heteromorph ammonite terms.....	271
Appendix V Palynological counts data.....	274
Appendix VI Palynomorph relative abundances	277

List of Tables

- Table 2.1.** Dichotomous key for identification of species belonging to the genus *Solenoceras* Conrad, 1860..... 51
- Table 2.2.** Qualitative and quantitative characters applicable to the description of helical whorls belonging to species within the genus *Nostoceras* Hyatt, 1894..... 61
- Table 4.1.** Stratigraphic distribution of dinoflagellate cyst taxa within the Northumberland Formation on Hornby Island in order of lowest occurrence. Dotted line denotes the 4.4 km separation along strike between northwestern and southeastern coastal exposures. 112

List of Figures

- Figure 2.1.** **A**, location of the Georgia Basin (red) within British Columbia, western Canada. **B**, location of Hornby Island (red) within the Georgia basin. **C**, geology and topography of Hornby Island adapted from Katnick & Mustard (2001, 2003). Co = Collishaw Point, M = Manning Point, P = Phipps Point, S = Shingle Spit. 5
- Figure 2.2.** Schematic framework of the Northumberland Formation on Hornby Island with heteromorph ammonite taxon ranges. Points denote isolated occurrences. Grey denotes imprecision. Chronostratigraphy inferred from Haggart *et al.* (in prep). Magnetostratigraphy chron assignments (C33n, C32n.2n) inferred from Raub *et al.* in Ward *et al.* (2012). F = Foraminiferal zones of McGugan in Muller & Jeletzky (1970). M = Molluscan zones of Haggart *et al.* (2009, 2012). Lithostratigraphy modified from Katnick (2001). ST = stratigraphic level above base of section. D = DeCourcy Formation. G = Geoffrey Formation. Many of the heteromorph taxa are represented as float specimens and thus species ranges have no absolute horizon of physical first or last occurrence. 8
- Figure 2.3.** Diagrams illustrating the application of the Elbow Axis Model of measurement introduced herein. **A**, the Elbow Axis Model and apical angle measurement applied to a mature nostoceratid conch. **B**, the Elbow Axis Model and limb divergence measurement applied to a segment of recurvature in a diplomoceratid conch. See page 12 for abbreviations. 10
- Figure 2.4.** **A**, lateral measurements across a 180° section of helical whorl. **B**, measurement of curvature along an open gyroconic whorl. See page 12 for abbreviations. 10
- Figure 2.5.** Sutural lobe incision elements. Numbers indicate order as a function of magnitude. Arrow denotes third-order lobe incision bordered by two lobules. 11
- Figure 2.6. A–D**, *Fresvillia constricta* Kennedy, 1986a. **A**, suture line, RBCM.2, Wh = 2.5 mm; **B**, shaft cross-section and lobe positioning, RBCM.2, Wh = 2.5 mm; **C**, suture line, RBCM.3, Wh = 5.5 mm; **D**, shaft cross-section and lobe positioning, RBCM.3, Wh = 5.5 mm. 19
- Figure 2.7. A, B**, reconstruction of *Diplomoceras (Diplomoceras) cylindraceum* (Defrance, 1816) conch based on Hornby Island material. **A**, shell in early development, arrow denotes point of transition from helical to planispiral coiling, grey bands denote periodic

- constrictions; **B**, generalized inference of limb orientation in a mature conch and position of final septum (P). Numbers indicate ontogenetic order of limbs..... 30
- Figure 2.8.** Variation in Ci and Wh with developmental progression in *Diplomoceras* (*Diplomoceras*) *cylindraceum* (Defrance, 1816). Black points denote definitive values. Opacity denotes values extrapolated from specimen surfaces marked by shell absence or deformation. Point size denotes precision, larger points less precise. 31
- Figure 2.9. A–C**, limb cross-section and lobe positioning throughout ontogeny in *Diplomoceras* (*Diplomoceras*) *cylindraceum* (Defrance, 1816). **A**, RBCM.5, Wh = 1.9 mm; **B**, RBCM.11, Wh = 8.3 mm; **C**, RBCM.23, Wh = 55 mm. 32
- Figure 2.10. A–C**, suture line developmental progression in *Diplomoceras* (*Diplomoceras*) *cylindraceum* (Defrance, 1816). **A**, RBCM.5, Wh = 1.9 mm; **B**, RBCM.11, Wh = 8.3 mm; **C**, RBCM.23, Wh = 55 mm, tips of preceding folioles (grey) illustrate septal approximation. 33
- Figure 2.11. A, B**, *Exiteloceras* (*Exiteloceras*) *densicostatum* sp. nov. partial suture line and partial lateral lobe. **A**, partial suture line of holotype RBCM.25, Wh = 7 mm; **B**, partial lateral lobe of paratype RBCM.28, Wh = 30 mm. 39
- Figure 2.12. A–C**, *Exiteloceras* (*Neancyloceras*) aff. *bipunctatum* (Schlüter, 1872). **A**, suture line, RBCM.29, Wh = 2.7 mm; **B**, suture line, RBCM.29, Wh = 4.6 mm; **C**, whorl cross-section and lobe positioning, RBCM.29, Wh = 4.6 mm. 42
- Figure 2.13. A–C**, complete reconstruction of *Phylloptychoceras horitai* Shigeta & Nishimura, 2013 based on Hornby Island material. **A**, juvenile shell dorsal view in relation to tertiary limb; **B**, juvenile shell lateral view in relation to tertiary limb; **C**, generalized inference of limb orientation in a mature conch and position of final septum (P). Dashed lines indicate ventral position of siphuncle. 49
- Figure 2.14. A–D**, *Phylloptychoceras horitai* Shigeta & Nishimura, 2013 suture line, limb cross-section, and lobe positioning. **A**, suture line, RBCM.42, Wh = 3 mm; **B**, limb cross-section and lobe positioning, RBCM.42, Wh = 3 mm; **C**, suture line, RBCM.51, Wh = 6.7 mm; **D**, limb cross-section and lobe positioning, RBCM.51, Wh = 6.7 mm. 50
- Figure 2.15. A, B**, *Solenoceras* cf. *reesidei* Stephenson, 1941. **A**, suture line, RBCM.66, Wh = 3.4 mm; **B**, limb cross-section and lobe positioning, RBCM.66, Wh = 3.4 mm. **C–G**, *Solenoceras exornatus* sp. nov. **C**, suture line, paratype RBCM.54, Wh = 3 mm; **D**, limb

- cross-section and lobe positioning, paratype RBCM.54, Wh = 3 mm; **E**, partial suture line, paratype RBCM.59, Wh = 6 mm; **F**, limb cross-section and lobe positioning with grey area denoting body chamber, paratype RBCM.59, Wh = 6 mm; **G**, partial suture line, holotype RBCM.53, Wh = 6 mm..... 56
- Figure 2.16.** Suture line of *Nostoceras (Didymoceras?) adrotans* sp. nov., paratype CDM No. 2008.1.102 HUN, Wh = 18 mm..... 68
- Figure 2.17. A–C**, suture line of *Nostoceras (Nostoceras) hornbyense* (Whiteaves, 1895). **A**, RBCM.76, helical Wh = 17.9 mm; **B**, penultimate septum, RBCM.79, penultimate limb Wh = 20 mm, tips of preceding folioles (grey) illustrate septal approximation; **C**, penultimate septum, CDM No. 2008.1.17 HUN, penultimate limb Wh = 28 mm. 81
- Figure 2.18. A, B**, whorl cross-section and lobe positioning in *Nostoceras (Nostoceras) hornbyense* (Whiteaves, 1895) and *Nostoceras (Nostoceras) aff. pauper* (Whitfield, 1892). **A**, *N. (N.) hornbyense* (Whiteaves, 1895), RBCM.76, Wh = 18 mm; **B**, *N. (N.) aff. pauper* (Whitfield, 1892), RBCM.88, Wh = 5.7 mm. Dotted lines indicate adjacent whorl surfaces. Arrows indicate sites of preceding whorl impression..... 82
- Figure 2.19.** Penultimate limb and body chamber variation in Ci and Wh within *Nostoceras (Didymoceras?) adrotans* sp. nov and *Nostoceras (Nostoceras) hornbyense* (Whiteaves, 1895). Circular and square points denote D₁–V₁ and D₃–V₃ values, respectively. *N. (D.?) adrotans* values (black) are presented in contrast with *N. (N.) hornbyense* antidimorph values indicated by macroconches (red) and microconches (blue). Opacity denotes values extrapolated from specimens marked by shell absence or deformation. 83
- Figure 2.20. A, B**, suture line of *Nostoceras (Nostoceras) aff. pauper* (Whitfield, 1892). **A**, RBCM.88, Wh = 5.8 mm; **B**, RBCM.92, Wh = 15 mm, tips of preceding folioles (grey) illustrate septal approximation..... 88
- Figure 2.21.** Palaeogeographic map of North America during the latest Campanian modified from Blakey (2014). **A–I**, inferred positions of regional localities correlative with the *Nostoceras (Nostoceras) hyatti* global Assemblage Zone. **A**, Kaguyak Formation, Alaska; **B**, Matanuska Formation, Alaska; **C**, Northumberland Formation, Hornby Island; **D**, Rosario Formation, Baja California; **E**, Perras Shale, Coahuila, Mexico; **F**, Pierre Shale, Colorado; **G**, Nacatoch Sand, Texas; **H**, Saratoga Chalk, Arkansas; **I**, Ripley Formation, Tennessee; **J**, Navesink Formation, New Jersey. Locations **A–D** are poorly constrained due to uncertainties in tectonic translation..... 90

Figure 4.1. **A**, location of the Georgia Basin (red) within British Columbia, western Canada. **B**, location of Hornby Island (red). **C**, geology and topography of Hornby Island adapted from Katnick & Mustard (2001, 2003) with locations of concretionary mudstone matrix samples (red points) marked across the extent of Northumberland Formation coastal outcrop (black). Dark red zones denote float sample localities. Solid points denote in situ samples..... 107

Figure 4.2. Schematic framework of the Northumberland Formation on Hornby Island, modified from McLachlan & Haggart (in prep), with plotted stratigraphic positions of matrix samples and dinoflagellate cyst zonation. Grey denotes imprecision of float samples. Chronostratigraphy inferred from Haggart *et al.* (in prep). Magnetostratigraphy chron assignments inferred from Raub *et al.* in Ward *et al.* (2012). DC = dinoflagellate cyst ecozones. F = foraminiferal zones of McGugan in Muller & Jeletzky (1970). M = molluscan zones of McLachlan & Haggart (in prep). Lithostratigraphy modified from Katnick (2001). ST = stratigraphic level above base of section. D = DeCourcy Formation. G = Geoffrey Formation. 109

Figure 4.3. **A–I**, schematic diagrams illustrating the plexus of morphologies corresponding to various areoligeracean cyst taxa within the Hornby Island section as expressed through ventral margin ornamentation. **A**, *Circulodinium* cf. *colliveri*; **B**, *Circulodinium?* sp.; **C**, *Cyclonephelium* spp.; **D–F**, *Areoligera* spp.; **G, H**, *Glaphyrocysta–Membranophoridium* spp. plexus; **I**, *Renidinium* spp. 117

Figure 4.4. **A, B**, inferred tabulation and areoligeracean cyst measurement model modified from Clarke & Verdier (1967) applied to schematic diagrams of *Canningia diezeugmenis* sp. nov. **A**, inferred tabulation of dorsal surface; **B**, imposed measurement parameters on dorsal surface with ectophragm texture and support structure distribution indicated in posterolateral quadrant. Grey area denotes ectocoel..... 120

Figure 4.5. Known chronostratigraphic ranges of selected dinoflagellate cysts referable to forms present within the Hornby Island assemblage as plotted over 30 Ma spanning the Late Cretaceous. Yellow band denotes inferred age interval of the Northumberland Formation on Hornby Island. Solid bar terminations denote absolute range horizons. 171

Figure 4.6. Absolute abundance of dinoflagellate cysts and terrestrial palynomorphs within the Hornby Island subsample suite based on counts data. Subsamples ascending in order of stratigraphic succession. 172

Figure 4.7. Relative abundance of dinoflagellate cysts and terrestrial palynomorph constituents within the Hornby Island subsample suite based on counts data. Subsamples ascending in order of stratigraphic succession. D/T = dinoflagellate cysts to terrestrial palynomorph ratio. 176

List of Plates

- Plate 2.1. A–D, *Fresvillia constricta* Kennedy, 1986a. A, ammonitella and juvenile shaft, left F, RBCM.1, arrow denotes nepionic constriction, scale bar = 500 µm; B, ammonitella and juvenile shaft, left F, RBCM.1, scale bar = 2 mm; C, shaft fragment with suture line exposed, right F, RBCM.2; D, shaft fragment with suture line exposed, D, RBCM.3, arrow denotes the position of the only observed constriction in the suite. E–O, *Diplomoceras (Diplomoceras) cylindraceum* (Defrance, 1816). E, helical whorl fragment, RBCM.4; F, G, helical whorl volution, right and left F, RBCM.5; H, one-half helical whorl volution, V, RBCM.6; I, helical whorl volution, right F, RBCM.7; J–L, one-half helical whorl volution, right F, V and left F, RBCM.8; M, helical whorl volution, left F, RBCM.9; N, O, final helical whorl volution transitioning to primary limb and primary elbow, left F and D, RBCM.10, scale bar = 5 mm. 18**
- Plate 2.2. A–J, *Diplomoceras (Diplomoceras) cylindraceum* (Defrance, 1816). K, *Diplomoceras (Diplomoceras) cf. cylindraceum* (Defrance, 1816). A, secondary limb fragment with suture line exposed and costal plications on internal mould, D, RBCM.11; B, secondary limb fragment, left F, RBCM.12; C, secondary elbow and limb fragment, right F, RBCM.13; D, secondary elbow and partial limb, right F, RBCM.14; E, secondary elbow and partial limb, left F, RBCM.15; F, secondary elbow and partial limbs, right F, RBCM.16; G, secondary elbow and partial limbs, left F, RBCM.17; H, secondary elbow and partial limbs, left F, RBCM.18; I, secondary elbow and partial limbs, right F, RBCM.19; J, secondary elbow, left F, RBCM.20. K, *Diplomoceras (Diplomoceras) cf. cylindraceum* (Defrance, 1816), probable aberrant gyroconic whorl, left F, RBCM.21. Scale bar = 1 cm. 28**
- Plate 2.3. A–F, *Diplomoceras (Diplomoceras) cylindraceum* (Defrance, 1816). A, tertiary elbow leading into quaternary limb, left F, RBCM.22; B, C, quaternary limb fragment with suture line exposed and costal plications on internal mould, left and right F, RBCM.23; D, E, quaternary limb fragment, D and left F, RBCM.24; F, tertiary elbow and partial limbs, right F, QBM No. P2015.173. Scale bar = 1 cm. 30**
- Plate 2.4. A–D, *Exiteloceras (Exiteloceras) densicostatum* sp. nov. E–L, *Exiteloceras (Neancyloceras) aff. bipunctatum* (Schlüter, 1872). A, one and one-half volutions of phragmocone, left F, holotype RBCM.25, matrix retained in the inferred position of the primary limb; B, body chamber fragment, left F, paratype RBCM.26; C, whorl fragment, left F, paratype RBCM.27; D, partial whorl and body chamber, right F, paratype RBCM.28. E–L, *Exiteloceras (Neancyloceras) aff. bipunctatum* (Schlüter, 1872). E,**

partial whorl and body chamber, left F, RBCM.29; **F**, partial whorl and body chamber, left F, RBCM.30; **G–J**, whorl fragment, D, right F, V, and left F, RBCM.31; **K**, whorl fragment, left F, RBCM.32; **L**, whorl fragment, left F, RBCM.33. Scale bars = 1 cm..... 39

Plate 2.5. A–Z, *Phylloptychoceras horitai* Shigeta & Nishimura, 2013. **A**, ammonitella and primary limb, V, RBCM.34, arrow denotes nepionic constriction, scale bar = 500 µm; **B**, RBCM.34, V, scale bar = 1 mm; **C, D**, partial primary through tertiary limbs, V to right F transition, RBCM.35; **E**, partial secondary and tertiary limbs, right F, RBCM.36; **F**, partial secondary and tertiary limbs, V to left F transition, RBCM.37; **G**, partial secondary and tertiary limbs, right F, RBCM.38; **H**, partial tertiary and quaternary limbs, left F, RBCM.39; **I, J**, tertiary elbow internal mould, left and right F, RBCM.40; **K**, partial tertiary and quaternary limbs, left F, RBCM.41; **L**, partial tertiary and quaternary limbs, right F, RBCM.42; **M**, partial primary through quaternary limbs, V to right F transition, RBCM.43; **N**, secondary through partial quaternary limbs, V to left F transition, RBCM.44; **O**, secondary through partial quaternary limbs, V to left F transition, RBCM.45, scale bar = 5 mm; **P**, quaternary limb and partial elbow, right F, RBCM.46; **Q, R**, quaternary elbow and partial body chamber, right F and V, CDM No. 2013.84.1; **S**, fifth-order elbow and partial body chamber, right F, RBCM.47; **T**, fifth-order elbow and partial body chamber, right F, RBCM.48; **U, V**, partial fifth-order elbow and body chamber, right F and V, RBCM.49; **W**, partial fifth-order limb and body chamber, right F, RBCM.50; **X**, partial quaternary and fifth-order limbs, left F, RBCM.51; **Y, Z**, fifth-order limb and body chamber, left F and V, RBCM.52, scale bar = 1 cm..... 47

Plate 2.6. A–X, *Solenoceras exornatus* sp. nov. **A, B**, penultimate limb and body chamber, V and left F, holotype RBCM.53, arrow denotes position of spinous ornamentation; **C**, spines on body chamber, V, holotype RBCM.53; **D, E**, penultimate limb fragment, left F and V, paratype RBCM.54; **F–H**, penultimate limb fragment, V, right F and D, paratype RBCM.55; **I**, penultimate limb fragment, right F, paratype RBCM.56; **J**, penultimate limb fragment, left F, paratype RBCM.57, scale bar = 5 mm; **K–N**, penultimate limb and body chamber, right F and three V sides, paratype RBCM.58; **O**, penultimate limb and partial body chamber, left F, paratype RBCM.59; **P**, penultimate limb and body chamber, left F, paratype RBCM.60; **Q**, penultimate limb and body chamber, left F, paratype RBCM.61. Arrow denotes pre-apertural construction. **R**, penultimate limb and body chamber, left F, paratype RBCM.62; **S–U**, penultimate limb and body chamber fragment, right F and two V sides, paratype RBCM.63; **V, W**, penultimate limb and body chamber, left F and V, paratype RBCM.64; **X**, penultimate limb, D, RBCM.65. **Y**, *Solenoceras* cf.

reesidei Stephenson, 1941, penultimate limb and body chamber, right F, RBCM.66, scale bar = 1 cm. 55

Plate 2.7. A–J, *Nostoceras (Didymoceras?) adrotans* sp. nov. **A**, torsional penultimate limb and body chamber, right F, holotype RBCM.67; **B–E**, penultimate limb and partial body chamber with two parallel rows of spines, right F, two V sides and D, paratype RBCM.68; **F–H**, penultimate limb, torsional left F, V and right F, paratype CDM No. 2008.1.102 HUN; **I, J**, penultimate limb and body chamber with single row of spines, left F and V, paratype RBCM.69. Scale bar = 1 cm. 66

Plate 2.8. A–K, *Nostoceras (Didymoceras?) adrotans* sp. nov. **A**, penultimate limb and partial body chamber, left F, paratype RBCM.70; **B**, penultimate limb and partial body chamber, right F, paratype RBCM.71; **C, D**, penultimate limb and partial body chamber with two rows of alternating spines, right F and V, paratype RBCM.72; **E**, body chamber with two parallel rows of nodes, V, paratype RBCM.73; **F, G**, body chamber with no spinous protuberances, V and right F, paratype RBCM.74; **H–K**, penultimate limb and body chamber, right F, two V sides and left F, paratype RBCM.75. Scale bar = 1 cm. 67

Plate 2.9. A–K, *Nostoceras (Nostoceras) hornbyense* (Whiteaves, 1895). **A**, initial shaft and two whorl volutions, V, GSC No. 139086, arrow denotes earliest constriction, scale bar = 5 mm; **B**, five and one-half whorl volutions, V and right F umbilical, RBCM.76; **C**, one whorl volution, right F umbilical, RBCM.77, scale bar = 1 cm; **D–K**, microconchs; **D**, four partial volutions, penultimate limb and body chamber, left F, RBCM.78; **E–G**, two and one-half slightly dislocated volutions, penultimate limb and body chamber, left F and two V sides, CDM No. 2008.1.82 HUN; **H**, penultimate limb and body chamber, left F, QBM No. P2015.171; **I**, penultimate limb and body chamber, right F, QBM No. P2015.172; **J, K**, penultimate limb and body chamber, right F and V, RBCM.79, scale bar = 1 cm. 77

Plate 2.10. A–H, *Nostoceras (Nostoceras) hornbyense* (Whiteaves, 1895) microconchs; C, D, *redux* Ludvigsen & Beard (1994, fig. 80, 1998, fig. 91). **A**, four partial whorl volutions, V, RBCM.80; **B**, penultimate limb and body chamber, left F, RBCM.81. Arrow denotes encrusted anomiid bivalve on body chamber; **C**, three and one-half whorl volutions, penultimate limb and body chamber, left F, CDM No. 998.1.866 COP. Arrow denotes forward-projected ventrolateral apertural margin and sinuous lirae; **D**, three and one-half whorl volutions, penultimate limb and body chamber, V, CDM No. 998.1.866 COP; **E**, impression of final whorl volution, penultimate limb and body chamber, left F, CDM No. 2008.1.17 HUN; **F, G**, penultimate limb and body chamber with two alternating rows of

- spines, right F and V, RBCM.82; **H**, penultimate limb and body chamber, right F, RBCM.83. Scale bar = 1 cm. 79
- Plate 2.11. A–G, *Nostoceras (Nostoceras) hornbyense*** (Whiteaves, 1895) microconches. **A**, penultimate limb and body chamber, right F, CDM No. 2008.1.1 HUN; **B, C**, penultimate limb and body chamber, right F and V, RBCM.84; **D**, two dislocated partial whorls, penultimate limb and body chamber, left F, RBCM.85; **E**, two whorl volutions, V, QBM No. P2015.170; **F, G**, penultimate limb and body chamber, left F and V, CDM No. 2008.1.15 HUN. Scale bar = 1 cm. 80
- Plate 2.12. A–K, *Nostoceras (Nostoceras) aff. pauper*** (Whitfield, 1892). **A, B**, one and one-half helical whorl volutions, right F umbilical and V, RBCM.86; **C, D**, one and one-half helical whorl volutions, right F umbilical and V, RBCM.87; **E**, five helical whorl volutions and partial body chamber, V, RBCM.88; **F**, two partial helical whorl volutions and body chamber, left F, RBCM.89; **G**, two partial helical whorl volutions and body chamber, left F, RBCM.90; **H**, two partial helical whorl volutions and weathered body chamber, right F, RBCM.91; **I, J**, two and one-half helical whorl volutions, right F umbilical and V, RBCM.92; **K**, partial final helical whorl volution and body chamber, left F, RBCM.93. Scale bar = 1 cm. 87
- Plate 4.1.** Bright-field photomicrographs and epifluorescence imaging of selected gonyaulacacean dinoflagellate cysts. **A, B, *Aireiana salicta***. **A**, subsample 15-766, slide A, surficial focus; **B**, subsample 16-368, slide C, surficial focus. **C, D, *Cordosphaeridium callosum***, subsample 16-366, slide A. **C**, mid-focus; **D**, surficial focus. **E, F, *Cordosphaeridium* spp.**, subsample 15-766, slide C. **E**, mid-focus; **F**, archaeopyle in focus. **G–I, *Neoeurysphaeridium?* sp.**, subsample 15-756, slide A. **G**, mid-focus; **H**, distal process openings in focus; **I**, epifluorescence. Scale bars = 10 µm. 142
- Plate 4.2.** Bright-field photomicrographs and epifluorescence imaging of selected peridiniacean dinoflagellate cysts. **A–E, *Alterbidinium?* spp.** **A–C**, subsample 14-269, slide B; **A**, I_{2a} archaeopyle; **B**, mid-focus; **C**, epifluorescence; **D, E**, subsample 14-269, slide A; **D**, I_{1–3a} archaeopyle; **E**, epifluorescence. **F–I, *Bohaidina* spp.** **F**, I_{1–3a} archaeopyle, subsample 14-269, slide B; **G–I**, subsample 14-269, slide A; **G**, dorsal view; **H**, ventral view; **I**, ventral view, epifluorescence. Scale bars = 10 µm. 143
- Plate 4.3.** Bright-field photomicrographs of selected areoligeracean dinoflagellate cysts. **A, B, *Areoligera "circumcoronata"***, subsample 14-271, slide B. **A**, dorsal view; **B**, ventral view. **C, D, *Areoligera* spp.**, subsample 16-367, slide A. **C**, dorsal view; **D**, ventral view. **E, *Areosphaeridium?* sp.**, subsample 14-271, slide B. **F, *Glaphyrocysta*–**

Membranophoridium spp., subsample 14-274, slide A, ventral view. **G, H**, *Glaphyrocysta–Membranophoridium* spp., subsample 15-765, slide D. **G**, dorsal view; **H**, mid-focus. **I**, *Senoniasphaera* cf. *protrusa*, subsample 14-273, slide A, mid-focus. Scale bars = 10 µm. 144

Plate 4.4. Bright-field photomicrographs and epifluorescence imaging of the areoligeracean dinoflagellate cyst *Canningia diezeugmenis* sp. nov. **A–E**, holotype, subsample 14-273, slide A, England Finder reference V38/3. **A**, dorsal view; **B**, mid-focus; **C**, ventral view; **D**, closeup of antapical region, arrow denotes ectophragm perforations; **E**, mid-focus, epifluorescence. **F**, paratype, subsample 16-368, slide E, England Finder reference S38/2, mid-focus, operculum. **G–I**, paratype, subsample 16-368, slide E, England Finder reference W33/3. **G**, dorsal view; **H**, mid-focus; **I**, ventral view. Scale bars = 10 µm. . 145

Plate 4.5. Bright-field photomicrographs of selected peridiniacean dinoflagellate cysts. **A**, *Andalusiella gabonensis*, subsample 15-766, slide C. **B, C**, *Cerodinium diebelii*. **B**, subsample 15-757, slide C; **C**, subsample 14-269, slide B. **D**, *Cerodinium glabrum*, subsample 15-759, slide A. **E**, *Cerodinium* cf. *leptodermum*, subsample 14-271, slide A. **F**, *Lejeuniacysta* cf. *hyalina*, subsample 15-757, slide C. **G**, *Lejeuniacysta* sp., subsample 15-757, slide C. **H, I**, *Palaeocystodinium golzowense*. **H**, subsample 15-767, slide A; **I**, subsample 14-274, slide A. Scale bars = 10 µm. 146

Plate 4.6. Bright-field photomicrographs of selected areoligeracean dinoflagellate cysts. **A–C**, *Circulodinium?* sp., subsample 16-368, slide E. **A**, dorsal view; **B**, mid-focus; **C**, ventral view. **D**, *Circulodinium colliveri*, subsample 16-368, slide E. **E, F**, *Cyclonephelium* spp., subsample 16-364, slide B. **E**, dorsal view; **F**, ventral view. **G–I**, *Renidinium* spp., subsample 15-766, slide C. **G**, dorsal view; **H**, mid-focus; **I**, ventral view. Scale bars = 10 µm. 147

Plate 4.7. Bright-field photomicrographs of selected cladopyxiinean dinoflagellate cysts. **A–C**, *Cladopyxidium paucireticulatum*, subsample 14-272, slide A. **A**, dorsal view; **B**, mid-focus; **C**, ventral view. **D, E**, *Cladopyxidium* sp., subsample 14-271, slide B. **D**, dorsal view; **E**, mid-focus. **F**, *Glyphanodinium facetum*, subsample 14-274, slide B, mid-focus. Scale bars = 10 µm. 148

Plate 4.8. Bright-field photomicrographs and epifluorescence imaging of selected gonyaulacacean dinoflagellate cysts. **A–C**, *Coronifera oceanica sensu* Schiøler & Wilson (2001), subsample 16-368, slide E. **A**, mid-focus; **B**, basal process periphragm in focus; **C**, mid-focus, epifluorescence. **D**, *Hystriodinium pulchrum*, subsample 14-273, slide B.

- E, F**, *Trichodinium* cf. *erinaceoides*, subsample 14-273, slide B. **E**, dorsal view, **F**, dorsal view, epifluorescence. Scale bars = 10 μ m. 149
- Plate 4.9.** Bright-field photomicrographs and epifluorescence imaging of selected cladopyxiinean and gonyaulacacean dinoflagellate cysts. **A–D**, *Druggidium?* cf. *discretum*, subsample 14-271, slide A. **A**, dorsal view; **B**, mid-focus; **C**, ventral view; **D**, dorsolateral view, subsample 14-273, slide A. **E, F**, *Druggidium?* sp., subsample 16-363, slide B. **E**, dorsolateral? view; **F**, mid-focus. **G, H**, *Gonyaulacysta?* sp., subsample 15-758, slide C. **G**, dorsolateral view; **H**, dorsolateral view, epifluorescence. **I**, *Leptodinium* sp., dorsolateral view, subsample 15-761, slide C. Scale bars = 10 μ m. 150
- Plate 4.10.** Bright-field photomicrographs of selected gonyaulacacean and goniodomacean dinoflagellate cysts. **A, B**, *Dapsilidinium* cf. *pseudocolligerum*, subsample 15-755, slide D. **A**, surficial view; **B**, mid-focus. **C**, *Hystrichosphaeridium recurvatum*, subsample 14-273, slide B, apical view, **D**, *Hystrichosphaeridium tubiferum*, apical view, subsample 14-269, slide A. **E**, *Minisphaeridium latiricum*, subsample 14-272, slide B, mid-focus. **F, G**, *Minisphaeridium* sp., subsample 15-766, slide C. **F**, mid-focus; **G**, surficial view. **H**, *Oligosphaeridium complex*, subsample 15-767, slide A, apical view. **I**, *Tanyosphaeridium xanthiopyxides*, subsample 14-272, slide A, precingular plate margin of apical archaeopyle in focus. Scale bars = 10 μ m. 151
- Plate 4.11.** Bright-field photomicrographs of selected ptychodiscacean dinoflagellate cysts. **A**, *Alisogymnium euclaense*, subsample 15-766, slide C. **B**, *Amphigymnium cooksoniae*, subsample 14-269, slide B. **C**, *Dinogymnium acuminatum*, subsample 14-271, slide A. **D**, *Dinogymnium* cf. *aerlicum*, subsample 16-362, slide B. **E**, *Dinogymnium avellana*, subsample 15-755, slide D. **F**, *Dinogymnium cretaceum*, subsample 15-755, slide D. **G**, *Dinogymnium longicorne*, subsample 14-269, slide B. **H**, *Dinogymnium* sp. A, subsample 15-756, slide A. **I**, *Dinogymnium* sp. B, subsample 15-756, slide A. Scale bars = 10 μ m. 152
- Plate 4.12.** Bright-field photomicrographs of selected gonyaulacacean dinoflagellate cysts. **A**, *Diphyes colligerum*, subsample 14-271, slide A. **B–F**, *Diphyes* spp.? **B, C**, subsample 15-766, slide C; **B**, antapical view; **C**, apical view; **D–F**, subsample 14-272, slide B; **D**, antapical view; **E**, mid-focus; **F**, apical view. Scale bars = 10 μ m. 153
- Plate 4.13.** Bright-field photomicrographs of selected cladopyxiinean and goniodomacean dinoflagellate cysts. **A–C**, *Eisenackia?* sp., subsample 14-271, slide A. **A**, surficial view; **B**, one-quarter focus; **C**, mid-focus. **D–F**, *Microdinium carpentierae*. **D, E**, subsample 15-768, slide A; **D**, dorsal view; **E**, mid-focus; **F**, subsample 15-760, slide D, apical view.

- G–I**, *Microdinium mariae*, subsample 14-272, slide B. **G**, dorsal view, one-quarter focus; **H**, mid-focus; **I**, ventral view. Scale bars = 10 μm 154
- Plate 4.14.** Bright-field photomicrographs of selected goniodomacean and gonyaulacacean dinoflagellate cysts. **A–E**, *Fibrocysta* spp. **A**, **B**, subsample 14-274, slide B; **A**, dorsolateral view; **B**, ventrolateral view; **C**, subsample 14-269, slide B, surficial view; **D**, **E**, subsample 14-269, slide B; **D**, dorsolateral view; **E**, ventrolateral view. **F**, **G**, *Litosphaeridium* spp., subsample 14-273, slide B; **F**, apical view; **G**, surficial view. **H**, **I**, *Polysphaeridium* spp. subsample 16-367, slide B; **H**, precingular plate margin of apical archaeopyle in focus; **I**, surficial view. Scale bars = 10 μm 155
- Plate 4.15.** Bright-field photomicrographs and epifluorescence imaging of selected peridiniacean dinoflagellate cysts. **A**, **B**, *Geiselodinium geiseltense*, subsample 15-760, slide D. **A**, dorsal view; **B**, dorsal view, epifluorescence. **C**, **D**, *Isabelidinium bakeri*. **C**, subsample 15-764, slide A dorsolateral view; **D**, subsample 14-272, slide B, dorsolateral view. **E**, **F**, *Isabelidinium weidichii*, subsample 15-758, slide C. **E**, dorsal view; **F**, mid-focus, epifluorescence. **G**, *Spinidinium densispinatum*, subsample 14-272, slide A, dorsal view. **H**, **I**, *Spinidinium echinoideum*, subsample 14-272, slide A. **H**, mid-focus; **I**, mid-focus, epifluorescence. Scale bars = 10 μm 156
- Plate 4.16.** Bright-field photomicrographs of selected gonyaulacacean dinoflagellate cysts. **A–C**, *Hafniasphaera delicata*, subsample 16-366, slide B. **A**, dorsolateral view; **B**, mid-focus; **C**, ventral view. **D**, **E**, *Hafniasphaera* cf. *delicata*, subsample 14-272, slide A. **D**, dorsolateral view; **E**, ventral view. **F**, *Hafniasphaera septata*, subsample 14-269, slide B, dorsolateral view. **G–I**, *Spiniferites* sp. A, subsample 14-269, slide A. **G**, dorsolateral view; **H**, mid-focus; **I**, ventral view, one-quarter focus. Scale bars = 10 μm 157
- Plate 4.17.** Bright-field photomicrographs of selected gonyaulacacean dinoflagellate cysts. **A**, *Impagidinium rigidaseptatum*, subsample 14-273, slide B, dorsal view. **B**, **C**, *Impagidinium* cf. *scabrosum*, subsample 14-272, slide A. **B**, dorsolateral view; **C**, mid-focus. **D–F**, *Impagidinium* cf. *sphaericum–multiplex* of de Coninck (1968), subsample 15-760, slide A. **D**, dorsolateral view; **E**, mid-focus; **F**, ventrolateral view. **G**, *Impagidinium* spp., subsample 15-755, slide C, one-quarter focus, dorsal view. **H**, *Pterodinium cingulatum* sensu Antonescue et al. (2001a), subsample 15-759, slide C, dorsal view. **I**, *Unipontidinium aquaeductus*, subsample 14-272, slide B, dorsolateral view. Scale bars = 10 μm 158
- Plate 4.18.** Bright-field photomicrographs of selected gonyaulacacean dinoflagellate cysts. **A**, **B**, *Florentinia ferox*, subsample 14-272, slide B. **A**, surficial view with precingular plate

- margin of apical archaeopyle in focus; **B**, mid-focus. **C**, **D**, *Florentinia laciniata*, subsample 15-763, slide A. **C**, dorsal view; **D**, mid-focus. **E**, **F**, *Kleithriasphaeridium perforatum*, subsample 14-272, slide A. **E**, dorsolateral view; **F**, ventral view. Scale bars = 10 μm 159
- Plate 4.19.** Bright-field photomicrographs and epifluorescence imaging of selected ceratiacean dinoflagellate cysts. **A**, **B**, *Odontochitina* cf. *nuda*, subsample 16-368, slide C. **A**, dorsal view; **B**, ventral view. **C**, **D**, *Odontochitina* cf. *tabulata*, subsample 14-269, slide B. **C**, dorsolateral view, one-quarter focus; **D**, ventrolateral view. **E**, **F**, *Xenascus ceratioides*, subsample 14-269, slide B. **E**, mid-focus; **F**, mid-focus, epifluorescence. Scale bars = 10 μm 160
- Plate 4.20.** Bright-field photomicrographs and epifluorescence imaging of selected gonyaulacacean dinoflagellate cysts. **A–C**, *Phanerodinium belgicum*, sample 15-767, slide B. **A**, dorsal view; **B**, mid-focus; **C**, ventral view. **D**, **E**, *Phanerodinium* cf. *belgicum*, sample 15-768, slide A. **D**, dorsal view; **E**, mid-focus. **F**, *Phanerodinium* sp., dorsolateral view, sample 15-756, slide A. **G–I**, *Phanerodinium?* *turnhoutensis*, sample 15-756, slide A. **G**, dorsal view; **H**, dorsal view, one-quarter focus; **I**, mid-focus, epifluorescence. Scale bars = 10 μm 161
- Plate 4.21.** Bright-field photomicrographs and epifluorescence imaging of selected protoperidiniacean and peridiniacean dinoflagellate cysts. **A–C**, *Protoperidinium* sp. A, sample 15-759, slide C. **A**, dorsal view; **B**, ventral view; **C**, ventral view, epifluorescence. **D–F**, *Protoperidinium* sp. B, sample 16-365, slide B. **D**, dorsal view; **E**, mid-focus; **F**, ventral view, epifluorescence. **G**, **H**, Peridiniacean Group A. **G**, sample 16-362, slide A, dorsal view; **H**, sample 14-269, slide B, ventral view. **I**, Peridiniacean Group B, sample 15-755, slide D, dorsolateral view. Scale bars = 10 μm 162
- Plate 4.22.** Bright-field photomicrographs and epifluorescence imaging of selected peridiniacean dinoflagellate cysts. **A**, **B**, *Laciniadinium arcticum*, sample 14-272, slide B. **A**, surficial view; **B**, surficial view, epifluorescence. **C**, *Laciniadinium firmum*, sample 15-766, slide C, ventral view. **D**, *Laciniadinium rhombiforme*, sample 15-766, slide C, surficial view. **E**, **F**, *Senegalinium?* *simplex*, sample 14-271, slide A. **E**, dorsal view; **F**, dorsal view, epifluorescence. **G–I**, *Trithyrodinium evittii*, sample 14-274, slide A. **G**, dorsal view; **H**, mid-focus; **I**, mid-focus, epifluorescence. Scale bars = 10 μm 163
- Plate 4.23.** Bright-field photomicrographs of selected gonyaulacacean dinoflagellate cysts. **A–C**, *Spiniferella cornuta*. **A**, **B**, sample 15-765, slide C; **A**, ventral view; **B**, mid-focus; **C**, sample 14-272, slide A, dorsal view. **D–H**, *Spiniferites* spp. **D–F**, sample 16-368, slide

E, form with gonal and intergonal processes; **D**, dorsal view; **E**, ventral view; **F**, mid-focus, form with robust gonal processes; **G**, **H**, sample 14-274, slide A, aberrant form, arrow denotes a single, large, distally trifurcated and bifurcated process; **G**, surficial view; **H**, one-quarter focus. **I**, *Nematosphaeropsis* sp., sample 16-368, slide E. Scale bars = 10 μm 164

Plate 4.24. Bright-field photomicrographs and epifluorescence imaging of selected gonyaulacacean, indeterminate, and possible dinoflagellate cysts. **A**, *Xenicodinium delicatum sensu* Slimani *et al.* 2011, sample 15-762, slide A, dorsolateral view. **B**, **C**, Cyst Type A, sample 14-273, slide B. **B**, precingular plate margin of apical archaeopyle in focus; **C**, mid-focus. **D–F**, Cyst Type B, sample 15-755, slide A; **D**, dorsal view; **E**, dorsal view, epifluorescence; **F**, ventral view. **G**, **H**, Cyst Type C, 15-766, slide C; **G**, surficial view; **H**, surficial view, epifluorescence. **I**, Cyst? Type A, sample 16-368, slide E, mid-focus. Scale bars = 10 μm 165

Plate 4.25. Bright-field photomicrographs of selected marine acritarchs and other palynomorphs. **A**, *Palaeostomocystis reticulata*, subsample 15-767, slide B. **B**, *Fromea chytra*, subsample 14-272, slide A. **C**, *Fromea* sp., subsample 14-269, slide A. **D**, *Schizocysta rugosa*, 15-756, slide A. **E**, *Tetrachacysta* sp., subsample 15-766, slide C; **F**, *Horolonginella?* sp., subsample 14-272, slide B. **G**, *Paralecaniella indentata*, subsample 15-766, slide C. **H**, *Michrhystridium* sp., subsample 14-270, slide A. **I**, Foraminifera organic lining, subsample 15-756, slide A. Scale bars = 10 μm 166

Plate 4.26. Bright-field photomicrographs of selected terrestrial miospores and pollen grains. **A**, *Trilobosporites* cf. *humilis*, subsample 14-269, slide B. **B**, *Trilobosporites* sp., subsample 15-767, slide B. **C**, *Appendicisporites* sp., subsample 15-766, slide C. **D**, *Trudopollis* sp., subsample 16-361, slide A. **E**, *Proteacidies* sp., subsample 14-269, slide B. **F**, *Atlantopolis* sp., subsample 16-363, slide A. **G**, *Picea* sp., subsample 15-766, slide C. **H**, *Aquilapollenites* cf. *pseudoaucellatus*, subsample 15-766, slide C. **I**, *Aquilapollenites* sp., subsample 15-755, slide D. Scale bars = 10 μm 167

Dedication

To my parents without whose love and support this work would not have been possible. And to all of those who have experienced the joy of discovery and were whisked away to a place of wonder.

Chapter 1

Introduction

1.1 Thesis structure

Over 85 collection fieldtrips were made within a period of nineteen years to exposures of the Upper Cretaceous Northumberland Formation on Hornby Island on the part of the author with the objective of building a comprehensive faunal and floral assemblage from this interval of Nanaimo Group strata. Macrofossil collection activities were largely non-selective as to produce an accurate representation of the biodiversity within the paleoenvironment. A total of 84 specimens collected have been incorporated into the study which comprises Chapter 2, a taxonomic survey of the heteromorph ammonites present and their biostratigraphic utility. The manuscript comprising Chapter 2 has been accepted by the *Journal of Systematic Palaeontology* on July 23, 2017.

Chapter 3 addresses a broader discussion of the taphonomy, palaeoecology, palaeobiogeography, and evolutionary relationships of the heteromorph ammonite families considered in Chapter 2. Chapter 4 is a separate study which focuses on the organic microfossils of dinoflagellate cysts and other palynomorphs extracted from the mudstone of the same formation. Chapter 5 presents a brief summary of the findings and their significance. The citation style follows that of the *Journal of Systematic Palaeontology*.

Chapter 2

Reassessment of the late Campanian (Late Cretaceous) heteromorph ammonite fauna from Hornby Island, British Columbia, with implications for the taxonomy of the Diplomoceratidae and Nostoceratidae¹

2.1 Contribution of authors

All of the material presented herein—data, analyses, and conclusions—relating to the fossil assemblages reported are those of the student author unless otherwise indicated. The stratigraphic interpretation of the western coastal exposure of the Northumberland Formation is based on the field measurements, illustrations, and lithological observations of Dr. James W. Haggart (Geological Survey of Canada, Vancouver) who also provided editorial review, presentation advice and insights into the geological context of the study area.

2.2 Abstract

Three heteromorph ammonite families are represented within upper Campanian (Upper Cretaceous) strata of the Northumberland Formation exposed on Hornby Island, British Columbia—the Baculitidae, the Diplomoceratidae, and the Nostoceratidae. A variety of species are distinguished within these families, of which only three taxa—*Baculites occidentalis* Meek,

¹ This study was submitted to the *Journal of Systematic Palaeontology* on Dec 29, 2016 and accepted on July 23, 2017 as McLachlan, S. M. S. & Haggart, J. W. Reassessment of the late Campanian (Late Cretaceous) heteromorph ammonite fauna from Hornby Island, British Columbia, with implications for the taxonomy of the Diplomoceratidae and Nostoceratidae.

1862, *Diplomoceras* (*Diplomoceras*) *cylindraceum* (Defrance, 1816), and *Nostoceras* (*Nostoceras*) *hornbyense* (Whiteaves, 1895)—have been reported previously. Over the last decade, large new collections and the further preparation of existing collections has provided new taxonomic and morphometric data for the Hornby Island ammonite fauna, from which new descriptions of heteromorph taxa are formulated. Eleven taxa are recognized, including the newly established species *Exiteloceras* (*Exiteloceras*) *densicostatum* sp. nov., *Nostoceras* (*Didymoceras?*) *adrotans* sp. nov., and *Solenoceras* *exornatus* sp. nov. Morphometric analyses of over 700 specimens demonstrate the considerable phenotypic plasticity of these ammonites, which exhibit a broad spectrum of variability in their ornamentation and shell dimensions. A large population sample of *Nostoceras* (*Nostoceras*) *hornbyense* provides an excellent case study of a member of the Nostoceratidae; the recovery of nearly complete, well-preserved specimens enables the re-evaluation of diagnostic traits within the genus *Nostoceras*. The northeast Pacific *Nostoceras* (*Nostoceras*) *hornbyense* Zone and the global *Nostoceras* (*Nostoceras*) *hyatti* Assemblage Zone are herein regarded as correlative, reinforcing a late Campanian age for the Northumberland Formation.

2.3 Introduction and geological setting

Noted for their enigmatic variation and diversity, heteromorph ammonites have long been regarded as key fossils for correlation of stratigraphic successions in widely separated regions of the globe (e.g. Wiedmann 1969). In western North America, heteromorph ammonites have provided significant biostratigraphic control for more than a century in the correlation of strata of the Upper Cretaceous Nanaimo Group, exposed on southeastern Vancouver Island and adjacent islands in the Strait of Georgia (Whiteaves 1879, 1895, 1903; Usher 1952; Muller & Jeletzky 1970; Ward 1978a). The early description of heteromorph ammonites from the Nanaimo Group provided a basic taxonomic and biostratigraphic framework for Upper Cretaceous strata along the Pacific coast of North America (California: Anderson 1958, Matsumoto 1959a, 1960; southern Alaska: Jones 1963) as well as elsewhere in the circum-North Pacific region, including eastern Russia (Shimizu 1929) and Japan (Yabe 1927; Matsumoto 1938). Since those early efforts, a large body of work on Late Cretaceous heteromorph ammonites has arisen and revision of the Nanaimo Group heteromorph fauna is thus critically needed.

For over 125 years, a large number of amateur collectors and professional palaeontologists have directed their attention toward the molluscan fauna of Hornby Island (e.g. Mustard *et al.* 2003) (Fig. 2.1), in the Strait of Georgia east of Vancouver Island, due mainly to the abundance and conspicuous nature of the macrofossils preserved there which exhibit a high quality of shell preservation. As a result of these efforts, a great number of Nanaimo Group heteromorph ammonites have been obtained from the Hornby Island strata. Concurrently, the lithostratigraphy of the Nanaimo Group succession has been studied at length (e.g. Muller & Jeletzky 1970, Mustard 1994, Katnick & Mustard 2003; Mustard *et al.* 2003; Haggart *et al.* 2011) and biostratigraphic analyses utilizing mollusks (e.g. Usher 1952; Muller & Jeletzky 1970; Ward 1978a; Haggart *et al.* 2005, 2011; Ward *et al.* 2012), terrestrial pollen and spores (Rouse 1957; Rouse *et al.* 1970), foraminifera (McGugan 1962, 1964, 1979, 1982; Sliter 1973), and crinoids (Haggart & Graham *in press*) have established the basis age framework of the succession. More recently, magnetostratigraphic analysis has been undertaken in conjunction with biostratigraphy to further refine basinal correlations (Enkin *et al.* 2001; Ward *et al.* 2012).

In total, ten stratigraphic formations are recognized as comprising the generally-accepted Nanaimo Group succession (Mustard 1994; Katnick & Mustard 2003; Mustard *et al.* 2003), spanning an age range from Santonian through Campanian. Recent biostratigraphic analysis has suggested that the base of the succession likely extends down into the lower Turonian (Haggart 1991, 1994; Haggart *et al.* 2005). Of this overall Nanaimo Group succession, five formations are recognized on Hornby Island (Fig. 2.1), varying from mudstone deposited in shelf to slope environments (Northumberland and Spray formations) to coarse-grained strata (DeCourcy, Geoffrey, and Gabriola formations) deposited in submarine fan channel settings. Virtually all macrofaunal collections made from Hornby Island have come from the Northumberland Formation with only rare instances of specimens occurring in reworked concretionary matrices from within the overlying conglomeratic Geoffrey Formation.

Northumberland Formation strata exposed along the western and southeastern shores of Hornby Island (Fig. 2.1) were mapped originally as either the Spray Formation or the Lambert Formation (Williams 1924; Usher 1952), stratigraphic units considered equivalent to the Northumberland Formation (England 1989). The strata along the western shore were also later assigned to the Spray Formation (Muller & Jeletzky 1970), based on interpretations of fault control on the geology. These interpreted faults are now recognized as facies boundaries,

however, and all of the strata of the western and southeastern shores of Hornby Island are now assigned to the Northumberland Formation (Katnick 2001; Katnick & Mustard 2003; Mustard *et al.* 2003).

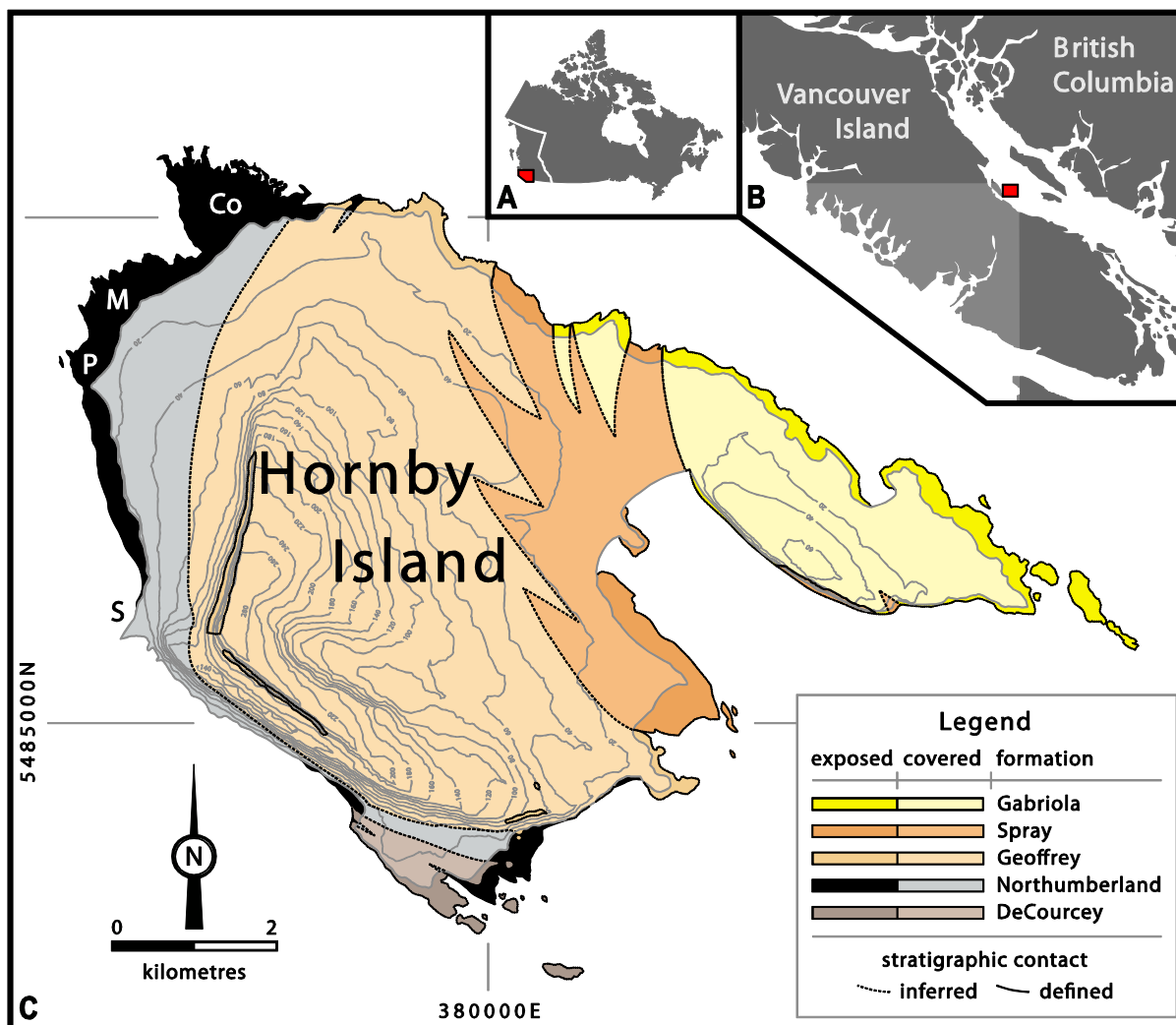
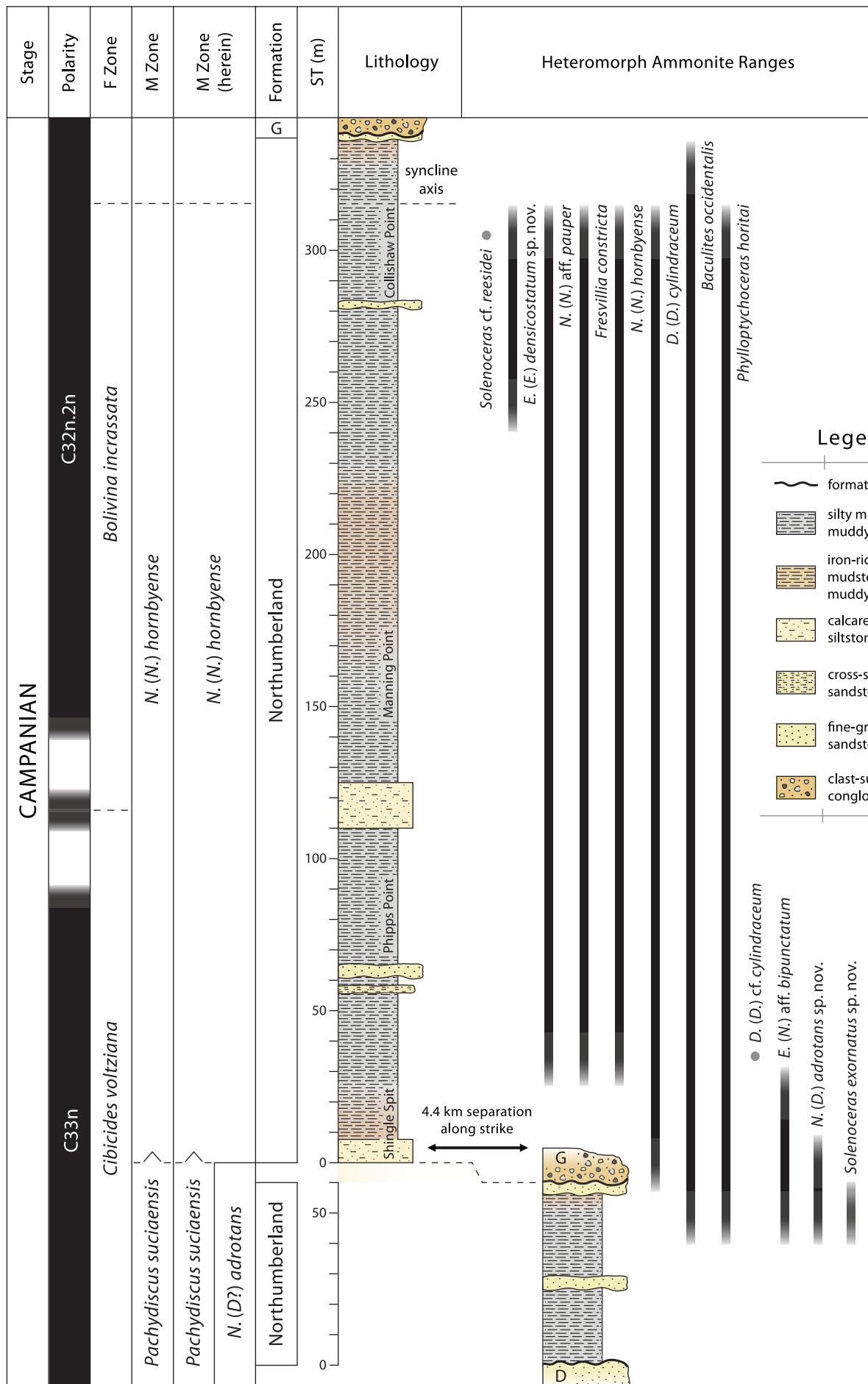


Figure 2.1. **A**, location of the Georgia Basin (red) within British Columbia, western Canada. **B**, location of Hornby Island (red) within the Georgia Basin. **C**, geology and topography of Hornby Island adapted from Katnick & Mustard (2001, 2003). Co = Collishaw Point, M = Manning Point, P = Phipps Point, S = Shingle Spit.

The Northumberland Formation is composed chiefly of massive, dark grey mudstone and occasional siltstone, with thinner sandstone beds and alternating mudstone-sandstone sequences (Mustard 1994; Katnick 2001; Katnick & Mustard 2003; Mustard *et al.* 2003) (Fig. 2.2).

Extensive coastal exposures of the formation are found along the northwestern, western, and southeastern shores of Hornby Island, amounting to nearly 1.85 km² of outcrop at peak low tide (Fig. 2.1C). Northumberland Formation strata dip very gently across the island, in general becoming younger to the east. The formation thins dramatically in a southeasterly direction across the island, due to scouring by the overlying Geoffrey Formation (Katnick 2001; Katnick & Mustard 2003) (Fig. 2.2). Along the western coast, the bulk of the section is readily accessible, with a measured thickness of ~ 335 m. The lowermost section of Northumberland Formation exposed along the southeastern coast has been interpreted as approaching 60 m in overall thickness (Katnick 2001) above its contact with sandstone of the underlying DeCourcy Formation. The top of the southeastern coast section is aligned directly along strike with the base of the west coast section at Shingle Spit, and a composite stratigraphic thickness of the Northumberland Formation on Hornby Island is thus calculated at ~ 395 m (Fig. 2.2).



Legend

- formation contact
- silty mudstone/muddy siltstone
- iron-rich silty mudstone/muddy siltstone
- calcareous siltstone
- cross-stratified sandstone
- fine-grained sandstone
- clast-supported conglomerate

- D. (D.) cf. cylindraceum*
- E. (N.) aff. bipunctatum*
- N. (D.) adrotans* sp. nov.
- Solenoceras exornatus* sp. nov.

4.4 km separation along strike

Figure 2.2. Schematic framework of the Northumberland Formation on Hornby Island with heteromorph ammonite taxon ranges. Points denote isolated occurrences. Grey denotes imprecision.

Chronostratigraphy inferred from Haggart *et al.* (in prep). Magnetostratigraphy and chron assignments (C33n, C32n.2n) inferred from Raub *et al.* in Ward *et al.* (2012). F = foraminiferal zones of McGugan in Muller & Jeletzky (1970). M = molluscan zones of Haggart *et al.* (2009, 2011). Lithostratigraphy modified from Katnick (2001). ST = stratigraphic level above base of section. D = DeCourcy Formation. G = Geoffrey Formation. Many of the heteromorph taxa are represented as float specimens and thus species ranges have no absolute horizon of physical first or last occurrence.

The age of the Northumberland Formation on Hornby Island, as determined through biostratigraphic work based on mollusks (Jeletzky in Muller & Jeletzky 1970) and foraminifera (McGugan 1962, 1979, 1982; Sliter 1973) has placed these rocks as late Campanian to early Maastrichtian. Magnetostratigraphic studies have recognized a considerable temporal expanse of global magnetochron C32n.2n in the upper section of the formation (Raub *et al.* 1998; Enkin *et al.* 2001; Ward *et al.* 2012), also indicating a late Campanian age. Coupled with recent geochemical findings obtained through analysis of $\delta^{13}\text{C}$ excursion (Hasegawa *et al.* 2015), the dataset supports the inference that the top of the section at Collishaw Point terminates below the position of the Campanian-Maastrichtian boundary at ~ C32n.2n.88 (Ogg *et al.* 2016).

A large number of heteromorph ammonites have now been collected from the Northumberland Formation on Hornby Island over the past 100 years. In light of a great volume of new material held in the collections of the Royal British Columbia Museum (RBCM), Victoria, British Columbia, the Geological Survey of Canada (GSC), and the Courtenay and District Museum, Courtenay, British Columbia, we have undertaken a review of the taxonomy and systematics of the heteromorph ammonite fauna from the Northumberland Formation on Hornby Island. The fauna is now understood to be of much greater diversity and importance than previously recognized.

2.4 Materials and methods

Specimen preparation was achieved through use of pneumatic airscribes and rotary tools in matrix removal to expose diagnostic features and enable accurate dimensional measurements. In a select few specimens, shell was removed for the purpose of revealing elements of the suture line. A variety of adhesives were applied to specimens for the purposes of shell repair and consolidation to maintain structural integrity. Paraloid B-72 and Paleo-Bond penetrant stabilizers of low viscosity served to reinforce exfoliating shell material. High viscosity Paraloid B-72 as well as Devcon and System Three brand two-part epoxies were used in specimen reconstruction.

Photography was conducted using Nikon D610 and D7100 cameras with the exception of two minute specimens (see: Plate 6A, B; Plate 17A, B) photographed through a Leica M205A stacking microscope and DFC450 digital camera using Leica Application Suite version 4.2. Composite specimen figures were assembled using Macromedia Fireworks 8 software wherein image modification was limited to the balancing of brightness and contrast through black level adjustments. Vector line tracing of sutural elements was conducted in Adobe Illustrator CS2 over specimen photographs sequentially rotated as to compensate for shell surface curvature. Depending on specimen size, suture photographs were taken with a Fujifilm FinePix XP10 camera either through a 10x hand lens mounted over the aperture or through the 20x/13 ocular lens of a Wild M8 stereoscopic microscope. In circumstances requiring higher resolution imaging, suture photographs were taken through the aforementioned stacking microscope.

Measurements were taken with a digital vernier caliper. Conch elbows were identified as universal points of reference for ontogenetic consistency among many of the taxa considered as presented in the Elbow Axis Model of measurement devised for this study (Fig. 2.3).

Measurements at independent points along straight limb sections and freestanding whorls have also been taken where incomplete material precluded the application of this model (Fig. 2.4). All measurements are intercostal and all averages presented were derived from measured values, where approximation (~) is not otherwise indicated. In instances where shell was not present at a point of measurement but remained intact on an adjacent surface, the shell thickness was recorded and added to the reading obtained from the internal mould to produce a more accurate value. Precise angular readings were obtained through the superimposition of a protractor over specimen photographs using Macromedia Fireworks 8 software.

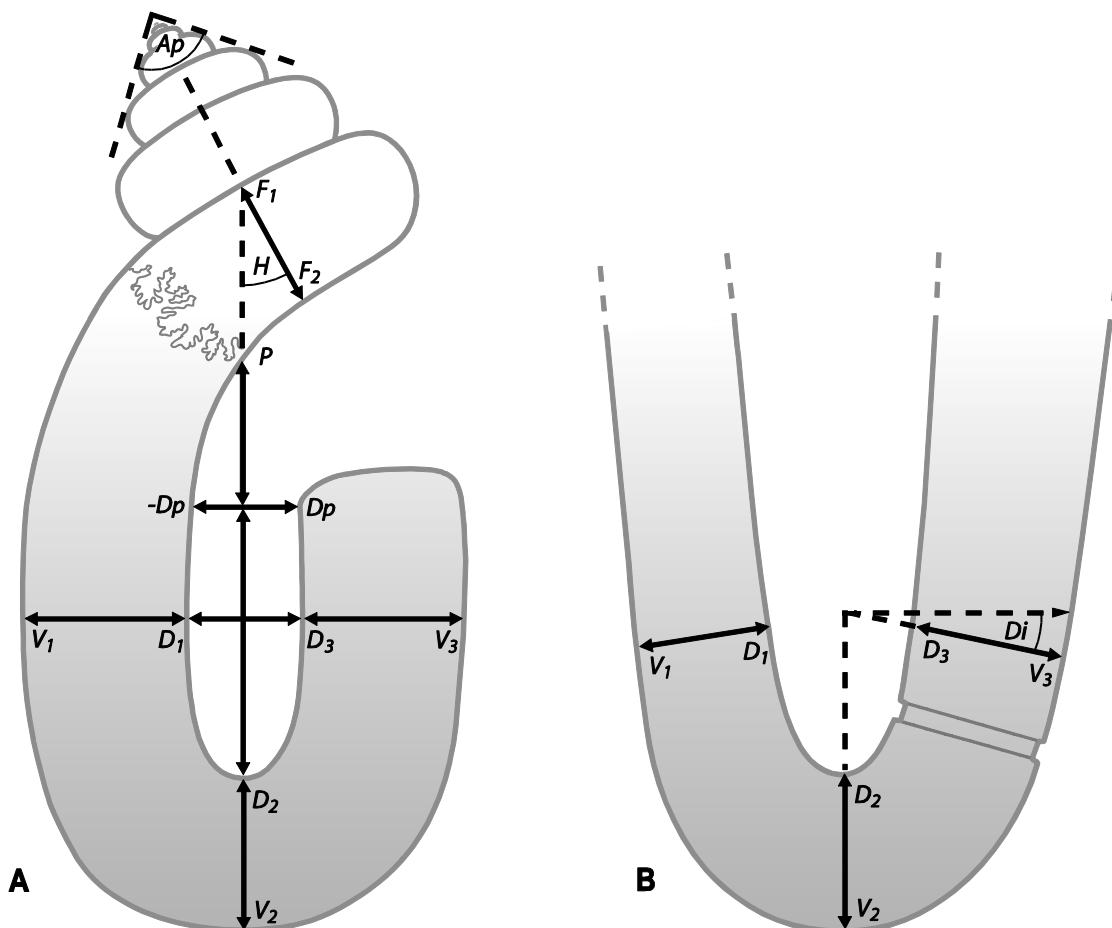


Figure 2.3. Diagrams illustrating the application of the Elbow Axis Model of measurement introduced herein. **A**, the Elbow Axis Model and apical angle measurement applied to a mature nostoceratid conch. **B**, the Elbow Axis Model and limb divergence measurement applied to a segment of recurvature in a diplomoceratid conch. See page 12 for abbreviations.

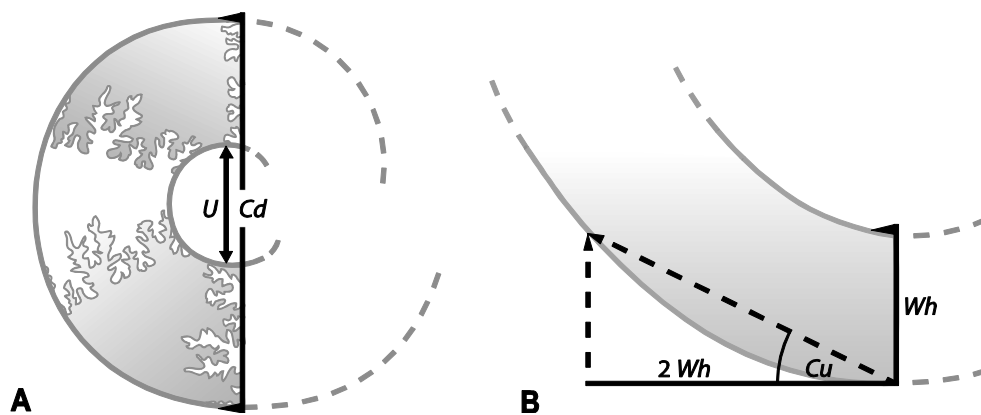


Figure 2.4. **A**, lateral measurements across a 180° section of helical whorl. **B**, measurement of curvature along an open gyroconic whorl. See page 12 for abbreviations.

Measures of sutural geometry and complexity follow the lateral saddle proxy method of Ward *et al.* (2015). Sutural elements relating to septal lobe incision are illustrated in Figure 2.5. Costal index readings in this study only consider costae with dorsoventral continuity; bifurcations and intercalated costae have been disregarded except for counts of costae per quarter revolution where dorsoventral continuity cannot be determined due to visual obstruction from adjacent whorls. Readings are taken along a flank and do not consider interruptions in general growth sequence such as megastriae bordering constrictions; in these circumstances, readings are extrapolated from the spacing of adjacent costae. Fishing line was used to compensate for whorl curvature where necessary when determining costal index readings. In these instances, line was mounted firmly against the whorl, end points were marked along its length and the distance between them measured. Conch expansion rate values were obtained using the formula employed by Olivero & Zinsmeister (1989). In order to obtain an adequate expansion rate reading, shell length was measured adaperturnally over a distance at least twice that of the whorl height from the point of initial measurement.

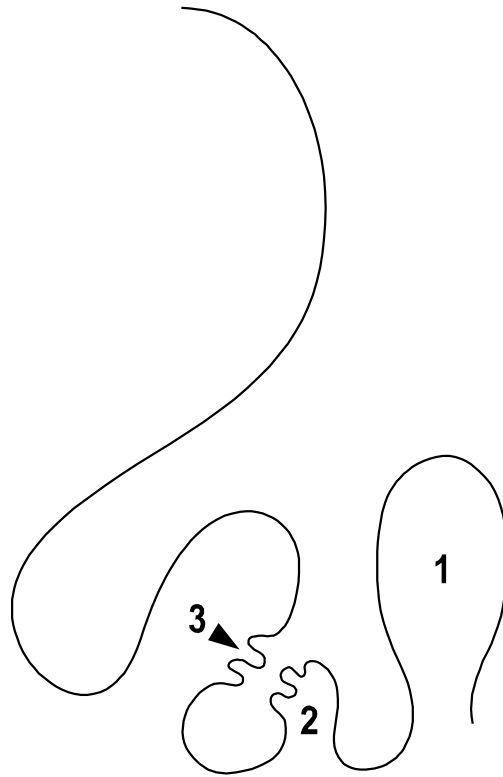


Figure 2.5. Sutural lobe incision elements. Numbers indicate order as a function of magnitude. Arrow denotes third-order lobe incision bordered by two lobules.

2.5 Institutional abbreviations

CAS: California Academy of Science, San Francisco, California, USA; **CDM:** Courtenay and District Museum, Courtenay, British Columbia, Canada; **GZG:** University of Göttingen Geoscience Centre, Göttingen, Germany; **GSC:** National Type Collection, Geological Survey of Canada, Ottawa, Ontario, Canada; **HMG:** Hobetsu Museum, Mukawa, Hokkaido, Japan; **IRSNB:** Royal Belgian Institute of Natural Sciences, Brussels, Belgium; **NJSM:** New Jersey State Museum, Trenton, New Jersey, USA; **QBM:** Qualicum Beach Museum, Qualicum Beach, British Columbia, Canada; **RBCM:** Royal British Columbia Museum, Victoria, British Columbia, Canada; **USNM:** United States National Museum, Washington, District of Columbia, USA.

2.6 Morphological abbreviations

Ap: apical angle; **Cd:** coil diameter of helical whorl; **Ci:** costal index; **Cu:** angle of gyroconic coil curvature; **Cv:** number of costae per quarter revolution transecting the ventrolateral margin. Values in brackets denote the number of costae per 360° revolution which may be obtained through extrapolation expressed as $(Cv \times 4) - 3$ to account for the costae beginning subsequent quarterly increments; **D:** dorsum; **Di:** angle of limb divergence from elbow axis; **F:** flank; **F₁–F₂:** flank-to-flank whorl breadth measurement transversal along helical coiling axis of final revolution; **Fb:** constriction furrow breadth as a measurement of costal interspace; **H:** angle between helical whorl and retroversal axes; **Sc:** sutural complexity; **Sg:** sutural geometry; **U:** umbilical diameter; **V:** venter; **Wb:** whorl breadth; **Wh:** whorl height; **Xr:** whorl expansion rate. Measurement approximations are indicated as follows: **a:** the figure is an extrapolation where a portion of the shell is absent. Sutural terminology follows the system proposed by Wedekind (1916) and reviewed by Kullmann & Wiedmann (1970) where: **E:** external lobe; **I:** internal lobe; **L:** first lateral lobe; **U:** umbilical lobe.

2.7 Systematic Palaeontology

Three heteromorph ammonite families are represented in the Northumberland Formation outcrops on Hornby Island; Baculitidae Gill, 1871, Diplomoceratidae Spath, 1926, and

Nostoceratidae Hyatt, 1894. Eleven species can be distinguished from these families, of which only three taxa—*Baculites occidentalis* Meek, 1862, *Diplomoceras* (*Diplomoceras*) *cylindraceum* (Defrance, 1816), and *Nostoceras* (*Nostoceras*) *hornbyense* (Whiteaves, 1895)—have been reported previously (e.g. Usher 1952; Ludvigsen & Beard 1998; Mustard *et al.* 2003). Accessibility to large collections in recent years has enabled a more detailed and comprehensive taxonomic treatment of the material present within the section. The order in which morphological characters are addressed follows a generalized hierarchy of their taxonomic significance in line with the treatment of Wright *et al.* (1996). This framework is intended to be flexible and serves to provide a systematic basis to ensure consistency in the presentation of observable data within diagnostic and descriptive sections. Open nomenclature follows the methodology outlined by Bengtson (1988) and synonymy and reference lists follow that devised by Matthews (1973). All specimens examined in this study are listed in Appendix I and all measurements obtained are reported in Appendix II. RBCM in-text type specimen numbers are paired with their corresponding institutional accession numbers in both respective appendices.

Order **Ammonoidea** Zittel, 1884

Suborder **Ancyloceratina** Wiedmann, 1966

Superfamily **Turrilitoidea** Gill, 1871

2.7.1 Family **Baculitidae** Gill, 1871

Age. Range: late Albian–early Danian (e.g. Wright *et al.* 1996; Jagt 2012; Landman *et al.* 2012).

Remarks. This conservative family is comprised of at least seven genera of orthoconic heteromorph ammonites characterized by a single straight or curved shaft having developed from a neanoconch of up to two contiguous planispiral coils enveloping the ammonitella (Arkell *et al.* 1957; Wright *et al.* 1996). Helical whorls and instances of recurvature are absent. Apertural margins often possess a forward-projected ventral rostrum. Mature suture lines are generally complex with second or third-order incision elements.

Genus ***Baculites*** de Lamarck, 1799

Type species. *Baculites vertebralis* de Lamarck, 1801 by subsequent designation (Meek 1876).

Age. Range: late Turonian–early Danian (e.g. Wright *et al.* 1996; Machalski & Heinberg 2005).

***Baculites occidentalis* Meek, 1862**

1862 *Baculites occidentalis* Meek: 316.

1952 *Baculites chicoensis* Trask; Usher: 96, pl. 26, figs 1–4.

1952 *Baculites occidentalis* Meek; Usher: 98, pl. 28, fig. 1, pl. 31, fig. 19, text-fig. 4 (*cum syn.*).

1959a *Baculites occidentalis* Meek; Matsumoto: 150, pl. 35, figs 2a–d, 3a–d, pl. 36, fig. 1a–d, pl. 41, fig. 1a–d, pl. 42, figs 1a–c, 2a–c, text-figs 64, 65a, b, 66–71.

1976a *Baculites occidentalis* Meek; Ward: 68, pl. 4–1, figs 8, 9, text-fig. 4–2.

1978b *Baculites occidentalis* Meek; Ward: 1153, pl. 2, figs 5, 6, text-fig. 2 (*cum syn.*).

1991 *Baculites occidentalis* Meek; Haggart: pl. 5, fig. 5 (*redux* Usher 1952, pl. 28, fig. 1).

1996 *Baculites occidentalis* Meek; Haggart: 174, fig. 14.4E (*redux* Usher 1952, pl. 28, fig. 1).

(?)2009 *Baculites* sp. cf. *occidentalis* Meek; Haggart *et al.*: 944, figs 5F.

Types. Plesiotypes GSC Nos. 5952, 5952a, and 5952b as designated from the upper Campanian Northumberland Formation exposed along the northwestern shore of Hornby Island (Usher 1952, p. 98, pl. 28, fig. 1, pl. 31, fig. 19, text-fig. 4).

Occurrence. On Hornby Island, *B. occidentalis* spans nearly the entire stratigraphic section of the upper Campanian Northumberland Formation, from the southeastern shore to Collishaw Point. *B. occidentalis* has also been reported from exposures of the upper Campanian Cedar District Formation on Sucia Island (Usher 1952; Ward 1978a, b), with other North American occurrences in California (Matsumoto 1959a), Alaska (Jones 1963), and possibly Haida Gwaii, British Columbia (Haggart *et al.* 2009).

Remarks. The general description of *B. occidentalis* is herein maintained following previous treatments (Usher 1952; Ward 1987b). Crushed material collected from Haida Gwaii (Haggart *et al.* 2009) may also be assignable to the species. In light of the recently augmented definition of the North Pacific species *Baculites inornatus* Meek, 1862 (Ward *et al.* 2015), the morphometric parameters of *B. occidentalis* and its affinity with other endemic baculitids warrants re-examination.

Genus *Fresvillia* Kennedy, 1986a

Type species. *Fresvillia constricta* Kennedy, 1986a.

Age. Range: early–late Maastrichtian (e.g. Wright *et al.* 1996; Ifrim & Stinnesbeck 2013).

Remarks. Circular cross-sections, discontinuous constrictions and distinctly cuneate septal saddles distinguish members of this presumably straight-shafted genus from all others within the Baculitidae. Mature suture lines are somewhat complex with second-order incision elements. Described only from fragments, *Fresvillia* was originally placed within the family Baculitidae because otherwise comparable polyptychoceratine material is typified by reduced costal prorsiradiancy and a more simplified suture line (Kennedy 1986a).

Fresvillia constricta Kennedy, 1986a

(Pl. 2.1A–D; Fig. 2.6A–D)

1986a *Fresvillia constricta* Kennedy: 62, pl. 14, figs 39–42, text-fig. 10A.

1996 *Fresvillia constricta* Kennedy; Wright *et al.*: 258, fig. 198.1a–c.

(?)1998 *Baculites* sp.; Ludvigsen & Beard: 134, fig. 97.

2010 *Fresvillia constricta* Kennedy; Ifrim *et al.*: 609, figs 5bb–cc, fig. 10w–bb (*cum syn.*).

Types. The holotype is specimen 10254 housed in the IRSNB as designated from the upper Maastrichtian Calcaires à *Baculites* of Manche, France (Kennedy 1986a, p. 62, pl. 14, figs 39–42, text-fig. 10A).

Material. Nineteen shaft fragments extracted from four concretionary matrices—17 from which measurements could be obtained. A single concretion of ~ 415 ml in matrix volume yielded fifteen specimens.

Occurrence. *F. constricta* has been recorded from the Maastrichtian of the Méndez (Ifrim *et al.* 2004, 2017; Stinnesbeck *et al.* 2012) Formation and Cañon del Tule (Ifrim *et al.* 2010) Formation of Mexico as well as from the upper Maastrichtian Calcaires à *Baculites* of northwestern France (Kennedy 1986a). *F. constricta* finds its earliest global occurrence on Hornby Island with specimens having been recovered from exposures of the upper Campanian Northumberland Formation along the western shore from Shingle Spit north to Collishaw Point.

Description. A presumably straight-shafted heteromorph ammonite which maintains a circular cross-section throughout development. The earliest stage is represented by a subcircular protoconch enveloped by an ammonitella comprised of a 360° whorl volution. The Wh of the shaft at the point of emergence from the nepionic constriction is 300 µm (Pl. 2.1A). The largest fragment, RBCM.3, consists of six complete camerae with terminal septal folioles against the body chamber at a Wh of 7.2 mm. The shell bears a smooth external surface with fine growth lirae presumably interrupted periodically by discontinuous, undulatory constrictions in the form of concave liral depressions transecting the venter (Pl. 2.1D). Of the 17 specimens measured, the average Xr is 4.78. Prorsiradially curved lirae on the dorsum and venter are connected sigmoidally along the flanks. The mature suture line displays intricate cuneate lobes and saddles with second-order incision elements (Fig. 2.6C). The highest Sc and Sg values were obtained from RBCM.3 at 54.63 and 6.02, respectively.

Remarks. *F. constricta* differs from *Fresvillia teres* (Forbes, 1846) in having pronounced dorsal constrictions and lacking the annular to ventrally prorsiradiate costae which characterize the latter species (Kennedy & Henderson 1992; Ifrim *et al.* 2004, 2010). The suture line is similar in both species (Ifrim *et al.* 2004, text-fig. 12E–G). Fragments assigned to *F. aff. teres* have been recorded from Alaska (Jones 1963) standing as the only other occurrence of the genus in the Pacific. It is interesting that the genus has not been recognized to date in the extensive and

diverse heteromorph faunas of the North Pacific (Matsumoto 1967, 1977; Matsumoto & Miyauchi 1984; Shigeta *et al.* 2015, 2016).

F. constricta stands in stark contrast to other members of the Baculitidae such as *Baculites occidentalis* which is ubiquitous throughout the Northumberland Formation on Hornby Island (Ward 1978a, b) with increasing abundance upsection to Collishaw Point. *B. occidentalis* differs from *F. constricta* in its ovate cross-section, increasing flank and venter compression with growth, pronounced, undulating costae along the flanks and broader sutural geometry (Ward 1978b). Cross-section shape is consistent throughout development however, ornamental differentiation between the species is difficult at early stages with the distinct, elongated septal saddles of *F. constricta* beginning to emerge at a Wh of 1.2 mm (Pl. 2.1B). The only other juvenile baculitid described from the section presents ammonitella proportions and an apparent Xr nearly identical to that of RBCM.1 (Ludvigsen & Beard 1998, fig. 97). However, aspects of cross-section and sutural geometry are not discernible in this specimen.



Plate 2.1. A–D, *Fresvillia constricta* Kennedy, 1986a. A, ammonitella and juvenile shaft, left F, RBCM.1, arrow denotes nepionic constriction, scale bar = 500 μ m; B, ammonitella and juvenile shaft, left F, RBCM.1, scale bar = 2 mm; C, shaft fragment with suture line exposed, right F, RBCM.2; D, shaft

fragment with suture line exposed, D, RBCM.3, arrow denotes the position of the only observed constriction in the suite. **E–O**, *Diplomoceras (Diplomoceras) cylindraceum* (Defrance, 1816). **E**, helical whorl fragment, RBCM.4; **F, G**, helical whorl volution, right and left F, RBCM.5; **H**, one-half helical whorl volution, V, RBCM.6; **I**, helical whorl volution, right F, RBCM.7; **J–L**, one-half helical whorl volution, right F, V and left F, RBCM.8; **M**, helical whorl volution, left F, RBCM.9; **N, O**, final helical whorl volution transitioning to primary limb and primary elbow, left F and D, RBCM.10, scale bar = 5 mm.

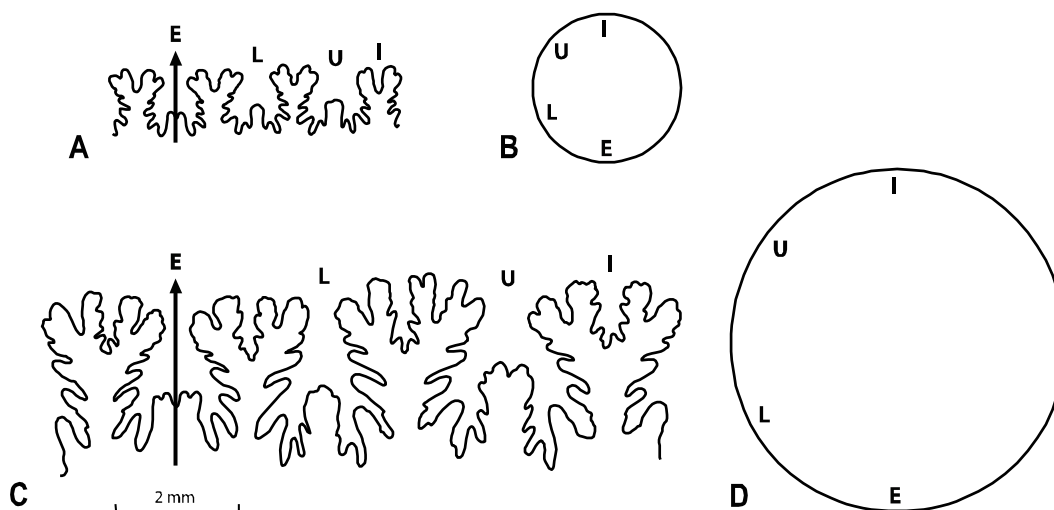


Figure 2.6. **A–D**, *Fresvillia constricta* Kennedy, 1986a. **A**, suture line, RBCM.2, Wh = 2.5 mm; **B**, shaft cross-section and lobe positioning, RBCM.2, Wh = 2.5 mm; **C**, suture line, RBCM.3, Wh = 5.5 mm; **D**, shaft cross-section and lobe positioning, RBCM.3, Wh = 5.5 mm.

2.7.2 Family Diplomoceratidae Spath, 1926

Age. Range: Turonian–late Maastrichtian (e.g. Wright *et al.* 1996).

Remarks. The family is comprised of at least 14 genera of heteromorph ammonites characterized by predominant adherence to planispiral gyroconic and hamitonic coiling (Arkell *et al.* 1957; Wright *et al.* 1996). Helical whorls and irregularities in shell development are not characteristic of the intermediate and mature stages (Shigeta 2014). The presence of post-embryonic limb constrictions has been proposed as a potential diagnostic trait distinguishing these forms from those of the Nostoceratidae (Tanabe *et al.* 1981) although the presence of constrictions in the early stage of *Nostoceras (Nostoceras) hornbyense* (Whiteaves, 1895)

challenges this notion (Pl. 2.8A). Mature suture lines range from somewhat complex to highly florid with second or third-order incision elements.

Subfamily **Diplomoceratinae** Spath, 1926

Emended diagnosis. Heteromorph ammonites characterized by elliptical to polygonal planispiral coiling in early to intermediate stages with helical whorls occurring in the earliest stages in some forms. Mature suture lines are highly complex and florid with third-order incision elements.

Age. Range: Turonian–late Maastrichtian (e.g. Wright *et al.* 1996) with statistical probability above the K-Pg boundary (Wang & Marshall 2004; Landman *et al.* 2014).

Genus **Diplomoceras** Hyatt, 1900

Type species. *Baculites cylindracea* DeFrance, 1816 by subsequent designation (Hyatt 1900).

Emended diagnosis. Heteromorph ammonites beginning with early helical whorls transitioning to predominantly gyroconic, polygonal, or hamiticonic modes of coiling. Whorl cross-section may be circular to subovate. Constrictions may be present and bordered by megastriae. Costae may be fine to coarse and raised. Mature suture lines are complex and florid with third-order incision elements.

Age. Range: late Santonian–late Maastrichtian (e.g. Wright *et al.* 1996; Everhart & Maltese 2010) with statistical probability above the K-Pg boundary (Wang & Marshall 2004; Landman *et al.* 2014).

Remarks. The subgeneric placement of *Glyptoxoceras* within *Diplomoceras* was proposed originally due to similarity in ontogenetic progression and to a lesser extent costal ornamentation (Wiedmann 1962; Klinger 1976). The validity of this placement has now been confirmed herein by implication of the recovery of early helical whorls belonging to *D. (D.) cylindraceum*

establishing an initial helical stage as a common trait uniting both groups as *Diplomoceras* subgenera. Members of *D. (Glyptoxoceras)* differ from those of *D. (Diplomoceras)* in exhibiting a predominance of gyroconic to subgyroconic coiling stemming from contiguous helical whorls with a moderate to high translation rate. Compared to *D. (Diplomoceras)*, *D. (Glyptoxoceras)* has a greater tendency to bear constrictions throughout, and possesses broadly spaced, sharp and raised costae.

Given the present subgeneric reinstatement of *D. (Glyptoxoceras)*, *D. (Diplomoceras)* can be characterized by the possession of four to five subparallel limbs stemming from loose, open helical whorls with a low translation rate. The transitional phase from helical coiling to planispiral hamitonic coiling is marked by gyroconic, polygonal, or ellipsoidal progression. The whorl cross-section is subcircular to subovate and constrictions may occur throughout but are most common following points of limb recurvature. Considerable overlap in Wb/Wh ratio, Ci, and sutural elements has been documented in collections from around the globe, bolstering the argument for *D. (Diplomoceras)* monospecificity (Kennedy 1986a; Klinger & Kennedy 2003a).

The degree of helical axis obliquity to that of the plane of subsequent coiling varies widely in *D. (D.) cylindraceum* and is not a useful character to distinguish *D. (Diplomoceras)* from *D. (Glyptoxoceras)*. The genus *Morewites* Shigeta, 2014, erected following the examination of a single specimen obtained from the lower Campanian Chinomigawa Formation of Hokkaido, exhibits contiguous helical whorls situated at 90° to the gyroconic axis. If a broader population sample of *D. (Glyptoxoceras)* were to demonstrate negligible variation in the expression of this trait, helical axis obliquity could at most be regarded as a valid character for specific diagnosis only.

Subgenus *Diplomoceras (Diplomoceras)* Hyatt, 1900

Type species. *Baculites cylindracea* Defrance, 1816.

Age. Range: late Campanian–late Maastrichtian (e.g. Remin *et al.* 2015; Kurihara *et al.* 2016) with statistical probability above the K-Pg boundary (Wang & Marshall 2004; Landman *et al.* 2014).

Diplomoceras (Diplomoceras) cylindraceum (Defrance, 1816)

(Pls 2.1E–O, 2.2A–J, 2.3A–F; Figs 2.7A, B, 2.8, 2.9A–C, 2.10A–C)

- 1816 *Baculites cylindracea* Defrance: 160.
- v*1903 *Diplomoceras notabile* Whiteaves: 335, pl. 44, figs 4a, b.
- v.1952 *Diplomoceras notabile* Whiteaves; Usher: 109, pl. 29, fig. 2, pl. 30, fig. 1, pl. 31, figs 26, 27.
- v.1952 *Hamites obstrictus* Jimbo; Usher: 100, pl. 26, fig. 7 (*cum syn.*).
- v.1970 *Hamites obstrictus* Jimbo; Jeletzky: pl. 28, fig. 8 (*redux* Usher 1952, pl. 26, fig. 7).
- 1978 *Diplomoceras* cf. *cylindraceum* (Defrance); Magalashvili: 90, pl. 8, figs 1a–c, 2
- (?)1984 *Diplomoceras notabile* Whiteaves; Matsumoto: 31, pl. 8, fig. 3.
- 1986a *Diplomoceras cylindraceum* (Defrance); Kennedy: 51, pl. 4, figs 1, 2, pl. 9, figs 8–10, pl. 10, text-figs 3i–3l, 6, 7g–7m (*cum syn.*).
- 1986b *Diplomoceras cylindraceum* (Defrance); Kennedy: 181, pl. 17, fig. 3, pl. 18, fig. 5, pl. 21, figs 2, 3, 5, 6, pl. 22, fig. 6, pl. 23, figs 1, 2, pl. 24, figs 1–3, pl. 25, figs 1–8, pl. 26, fig. 18; pl. 33, fig. 16, pl. 36, fig. 6, text-figs 9, 10 (*cum syn.*).
- v.1991 *Diplomoceras notabile* Whiteaves; Haggart: pl. 4, fig. 6 (*redux* Usher 1952, pl. 30, fig. 1).
- 1992 *Glyptoxoceras tenuisulcatum* (Forbes, 1846); Kennedy & Henderson: 702, pl. 2, figs 2, 6, 8, 30, text-fig. 2B (*cum syn.*).
- 1992 *Diplomoceras cylindraceum* (Defrance); Kennedy & Henderson: 704, pl. 6, figs 1–3, text-figs 1B, 3 (*cum syn.*).
- 1993 *Diplomoceras cylindraceum* (Defrance); Ward & Kennedy: 49, fig. 42, fig. 43.16, 43.17 (*cum syn.*).
- v.1994 *Diplomoceras cylindraceum* (Defrance); Ludvigsen & Beard: 115, fig. 85.
- v.1996 *Diplomoceras notabile* Whiteaves; Wright *et al.*: 250, fig. 195.3a, b (*redux* Usher 1952, pl. 30, fig. 1).
- v.1998 *Diplomoceras cylindraceum* (Defrance); Ludvigsen & Beard: 133, fig. 96 (*redux* Ludvigsen & Beard 1994, fig. 85).
- 1998 *Diplomoceras cylindraceum* (Defrance); Jagt, pl. 10, fig. 3.

- 2000 *Diplomoceras cylindraceum* (Defrance); Arkadiev *et al.*: 118, pl. 15, fig. 1a–c, pl. 16, figs 7a, b, 8a–c.
- 2001 *Diplomoceras cylindraceum* (Defrance); Klinger *et al.*: 284, pl. 9, figs 8–11 (*cum syn.*).
- v.2003 *Diplomoceras notabile* Whiteaves; Mustard *et al.*: 108, fig. 6G (*redux* Usher 1952, pl. 30, fig. 1).
- 2003 *Diplomoceras cylindraceum* (Defrance); Niebuhr: 268, pl. 1, fig. 8, pl. 4, fig. 1 (*cum syn.*).
- 2004 *Diplomoceras cylindraceum* (Defrance); Goolaerts *et al.*: 321, fig. 4A, figs 6C–E.
- 2004 *Diplomoceras cylindraceum* (Defrance); Summesberger & Kennedy: 178, pl. 6.
- 2009 *Diplomoceras* sp. cf. *tenuisulcatus* (Forbes); Haggart *et al.*: 944, fig. 5E.
- 2009 *Diplomoceras* sp.; Olivero *et al.*: 66, fig. 5c.
- 2010 *Diplomoceras cylindraceum* (Defrance); Odin: 19, fig. 10.
- 2010 *Diplomoceras cylindraceum* (Defrance); Sobral *et al.*: 38, fig. 05E.
- 2010 *Diplomoceras cylindraceum* (Defrance); Goolaerts: pl. 8, fig. 11.
- 2011 *Diplomoceras cylindraceum* (Defrance); Sobral: 46, pl. 9, figs 1, 2.
- 2011 *Diplomoceras cylindraceum* (Defrance); Niebuhr *et al.*: 200, text-fig. 3A (*redux* Niebuhr 2003, pl. 4, fig. 1).
- 2012 *Diplomoceras cylindraceum* (Defrance); Jagt: 160, pl. 38, fig. B.
- 2012 *Diplomoceras cylindraceum* (Defrance) *sensu* Kennedy, 1987, Machalski: 103, pl. 6, pl. 7, figs 1–5, pl. 8, figs 9, 11 (*cum syn.*).
- 2012 *Diplomoceras cylindraceum* (Defrance); Stinnesbeck *et al.*: 719, fig 2E, 3B.
- (?)2013 *Diplomoceras* sp.; Martinioni *et al.*: figs 9g, h.
- 2013 *Diplomoceras cylindraceum* (Defrance); Ifrim & Stinnesbeck: 195, fig. 2.30 (*cum syn.*).
- 2013 *Diplomoceras cylindraceum* (Defrance); Schnoor: 65, 3 figs.
- 2014 *Diplomoceras* sp.; Landman *et al.*: fig. 2A, d (*redux* Macellari 1986, fig. 14.1).
- 2015 *Diplomoceras* cf. *notabile* Whiteaves; Shigeta *et al.*: 119, figs 6G, 7D (*cum syn.*).
- 2015 *Diplomoceras cylindraceum* (Defrance); Ifrim *et al.*: 237, fig. 10S–X (*cum syn.*).
- 2015 *Diplomoceras cylindraceum* (Defrance); Krupp: 78, fig. 1A–C.
- 2015 *Diplomoceras cylindraceum* (Defrance); Landman *et al.*: fig. 19.16i (*redux* Goolaerts 2010, pl. 8, fig. 11).

- 2015 *Diplomoceras lambi* (Spath); Landman *et al.*: fig. 19.16a (*redux* Macelari 1986, fig. 14.1).
- 2015 *Diplomoceras cylindraceum* (Defrance); Remin *et al.*: 844, fig. 3.
- 2016 *Diplomoceras cylindraceum* (Defrance); Pons *et al.*: 217, fig. 6E.
- 2016 *Diplomoceras cylindraceum* (Defrance); Kurihara *et al.*: 117, fig. 3.
- 2017 *Didymoceras* juv. sp.; Ifrim *et al.*: 154, pl. 1, figs 38–68.

Type. Internal mould specimen 10293 housed in the IRSNB is the neotype designated from the upper Maastrichtian Kunrade Limestone of the Maastricht Formation in southeastern Limburg (Kennedy 1986b, p. 181, pl. 24, figs 1–3), following a subsequent literary correction (Machalski 2012).

Emended diagnosis. An hamitonic heteromorph ammonite with four to five subparallel limbs stemming from at least two open, sinistral helical volutions with a low translation rate. Helical whorls may adhere—or deflect obliquely away from—the plane of subsequent planispiral coiling. Whorl cross-section is subcircular to ovate. Constrictions may occur throughout; most commonly following points of limb recurvature. Costal index ranges from 7–18 throughout. Mature suture line is complex and florid with third-order incision elements.

Material. A total of 187 specimens were examined—139 from which measurements could be obtained. The material consists of 122 independent limb sections, 51 partial or complete independent elbows and fourteen helical whorls.

Occurrence. *D. (D.) cylindraceum* is found globally (e.g. Machalski 2012; Ifrim *et al.* 2015) and is the longest ranging heteromorph ammonite in the Late Cretaceous with reliable records from the middle Campanian to the late Maastrichtian (e.g. Remin *et al.* 2015; Kurihara *et al.* 2016). The species has been described previously from the upper Campanian Northumberland Formation on Hornby Island (Whiteaves 1903; Usher 1952), where it occurs throughout the exposures along the western shore from Shingle Spit north to Collishaw Point. Along the southeastern shore, the species is known only from a single isolated occurrence (Pl. 2.11).

Description. Elbow and limb sections can be classified into four and five distinct developmental stages, respectively. The early shell consists of sinistrally coiling helical whorls in at least two open volutions which may adhere (Pl. 2.1I)—or deflect obliquely away from (Pl. 2.1N, O)—the plane of subsequent planispiral coiling. Of 10 specimens, the helical whorls have an average X_r of 9.3 and of seven specimens, an average U/C_d of 0.53. Of nine helical volution sections, the C_i ranges from 7–11 with an average of 8. A sub-gyroconic, primary limb and elbow mark the polygonal transitional phase from helical coiling to that of the hamiticone of later development. Of 33 specimens, overall X_r values range from 1.88–12.7. Based on the phragmacone dimensions and rate of expansion, it is inferred that the conch consisted of five limbs succeeding the early whorls (Fig. 2.7A, B).

Each subsequent limb following the first elbow typically achieves roughly twice the length and twice the W_h of the one preceding it. Constrictions are continuous around the full limb circumference and are often bordered by megastriae. Of 22 specimens, the constriction F_b/W_h ratio ranges from 0.04–0.13, averaging 0.10. Constrictions may be present at any point occurring most frequently, and exhibiting the highest F_b/W_h ratios, on the tertiary limb following recurvature of the elbow. A wide range in C_i is evident across the hamitonic stage: 7–14 for secondary limbs, 9–17 for tertiary limbs, 10–18 for quaternary limbs, and 11–17 for fifth-order limbs (Fig. 2.8). Of 55 limb sections, the average C_i is 13. Costal plications on internal moulds are common in primary and secondary limbs.

Whorl cross-sections range from circular to subovate (Fig. 2.9A–C). The secondary limbs have a somewhat subcircular cross-section producing an average W_b/W_h ratio of 0.89. Of two specimens examined, the average D_i value between primary and secondary limbs is 24° ; of 16 specimens, this value is 13.4° between secondary and tertiary limbs; of three specimens, the average value is 13° between tertiary and quaternary limbs. Tertiary and quaternary limbs possess distinctly subovate cross-sections with lower W_b/W_h ratios averaging 0.82 and 0.85, respectively. Accurate W_b/W_h ratios are impossible to ascertain from fifth-order limb sections as these comprise the mature body chambers, which presumably collapsed following soft tissue decomposition. The mature suture line is highly florid with narrow-stemmed saddles, phylloid folioles, and third-order incision elements (Fig. 2.10C). The highest extrapolated S_c and S_g values were obtained from RBCM.23 at 1499.92 and 62.32, respectively.

Remarks. The Hornby Island material confirms that *Glyptoxoceras tenuisulcatum* (Forbes, 1846) is to be regarded as a junior synonym of *D. (D.) cylindraceum* in representing the early helical whorls of the latter species as is apparent in material comparison (e.g. Forbes 1846, pl. 11, fig. 3a; Kennedy & Henderson, 1992, pl. 2, figs 2, 6, 8). With the nature of costal ornamentation, suture line floridity, and Wb/Wh ratio in *G. tenuisulcatum* considered in relation to that described for *D. (D.) cylindraceum* (Kennedy 1986a), synonymy is consistent with the observation of loose helical and gyroconic whorls in *D. (D.) cylindraceum* previously described and never illustrated (e.g. Matsumoto 1959b; Wiedmann 1962; Klinger 1976). Subparallel limbs prior to a Wh of 5 mm are present on juvenile specimens from Japan (Matsumoto 1984, pl. 8, fig. 3; Matsumoto & Miyauchi 1984, pl. 27, fig. 2) assigned to *Diplomoceras notabile* Whiteaves, 1903. Although the former specimen exhibits limb divergence similar to that observed in the Hornby Island material, the latter specimen presents a strict adherence to hamitonic progression, precluding the possibility of helical whorls and thus an early ontogeny inconsistent with that characteristic of the genus. Material described recently from Argentina (Martinioni *et al.* 2013) consists of questionable internal mould fragments although previous work (Olivero *et al.* 2009) has provided greater evidence for *D. (D.) cylindraceum* in the region.

The species *Diplomoceras maximum* Olivero & Zinsmeister, 1989 was first proposed for material collected in Antarctica which exhibits Ci values ranging from 9–13. *D. maximum* has been considered as a potential zonal indicator for the upper Maastrichtian (Remin 2011). However, other authors came to regard *D. maximum* as a junior synonym of *D. (D.) cylindraceum* based on the species' broad range in Wb/Wh ratio and Ci (Kennedy & Henderson 1992; Ward & Kennedy 1993). As a concept, the species has since been considered valid based on a lower Ci in the mature stage and uniformly in costal spacing throughout development (Remin 2011; Machalski 2012). With the presence of both paucicostate and multicostate ribbing in mature limb sections, the Hornby Island material falls within the acceptable range of Wb/Wh ratio and Ci variation of *D. (D.) cylindraceum*, while underscoring the importance of acquiring material representative of numerous ontogenetic stages as to ascertain consistency in the expression of ornamentation within a population.

The retention of *Diplomoceras lambi* Spath, 1953 is also unjustified due to the range of the *D. (D.) cylindraceum* Wb/Wh ratio and Ci spectrum (Machalski 2012). Phylloid folioles in Antarctic specimens, noted as diagnostic markers of *D. lambi* (Macellari 1986), are observed in

many Hornby Island specimens of subovate cross-section definitively placing the species as a junior synonym of *D. (D.) cylindraceum* (Henderson *et al.* 1992). The observation of deeper septal lobe incision in Hornby Island specimens (Usher 1952) has been considered a distinction that could be at most indicative of a subspecific form (Kennedy 1986a).

Contrary to previous thought (Olivero & Zinsmeister 1989), a uniformly thickened nacreous layer beneath the costae resulting in a smooth internal mould is not a reliable diagnostic trait for the genus. More accurately, a thickened nacreous layer in *D. (D.) cylindraceum* is a commonly observed in post-secondary limb phragmacone onward but is not always present. Internal moulds such as those of specimens RBCM.11 (Pl. 2.2A) and RBCM.23 (Pl. 2.3C) retain evidence of costal undulation. Additionally, body chamber shell beyond the phragmacone is marked by the absence of the smooth layer resulting in pronounced costal plications on internal moulds as exemplified by Antarctic specimen C. 41400 (Spath 1953, pl. 3, fig. 1).

Constrictions in *D. (D.) cylindraceum* have been described by several authors (e.g. Henderson *et al.* 1992; Fatmi & Kennedy 1999) and are noted frequently in the Hornby Island material. Specimens figured from Austria (Kennedy & Summesberger 1986, pl. 15, figs 1, 2) and Antarctica (Olivero & Zinsmeister 1989, fig. 4.4) for instance, show at least one constriction on what are likely secondary limbs consistent with a coarsely costate elbow figured previously from Hornby Island (Usher 1952, pl. 26, fig. 7). Paucicostate and multicostate ribbing in early limb fragments, another feature typical of Hornby Island examples, has been documented in Australian and Danish specimens (Henderson *et al.* 1992; Birkelund 1993). Secondary and tertiary limbs from Hornby Island also reveal varying angles of prorsiradiancy in addition to developmental C_i fluctuations.

D. (D.) cylindraceum has been proposed as a diagnostic marker for the base of the Maastrichtian Stage, based on the succession at Tercis, France (Odin & Lamaurelle 2001). However, the presence of *D. (D.) cylindraceum* in association with Campanian ammonites and inoceramids at a number of localities in Europe, the Americas, and in the North Pacific precludes its utility as a marker for the base of the Maastrichtian (e.g. Remin 2011; Remin *et al.* 2015).

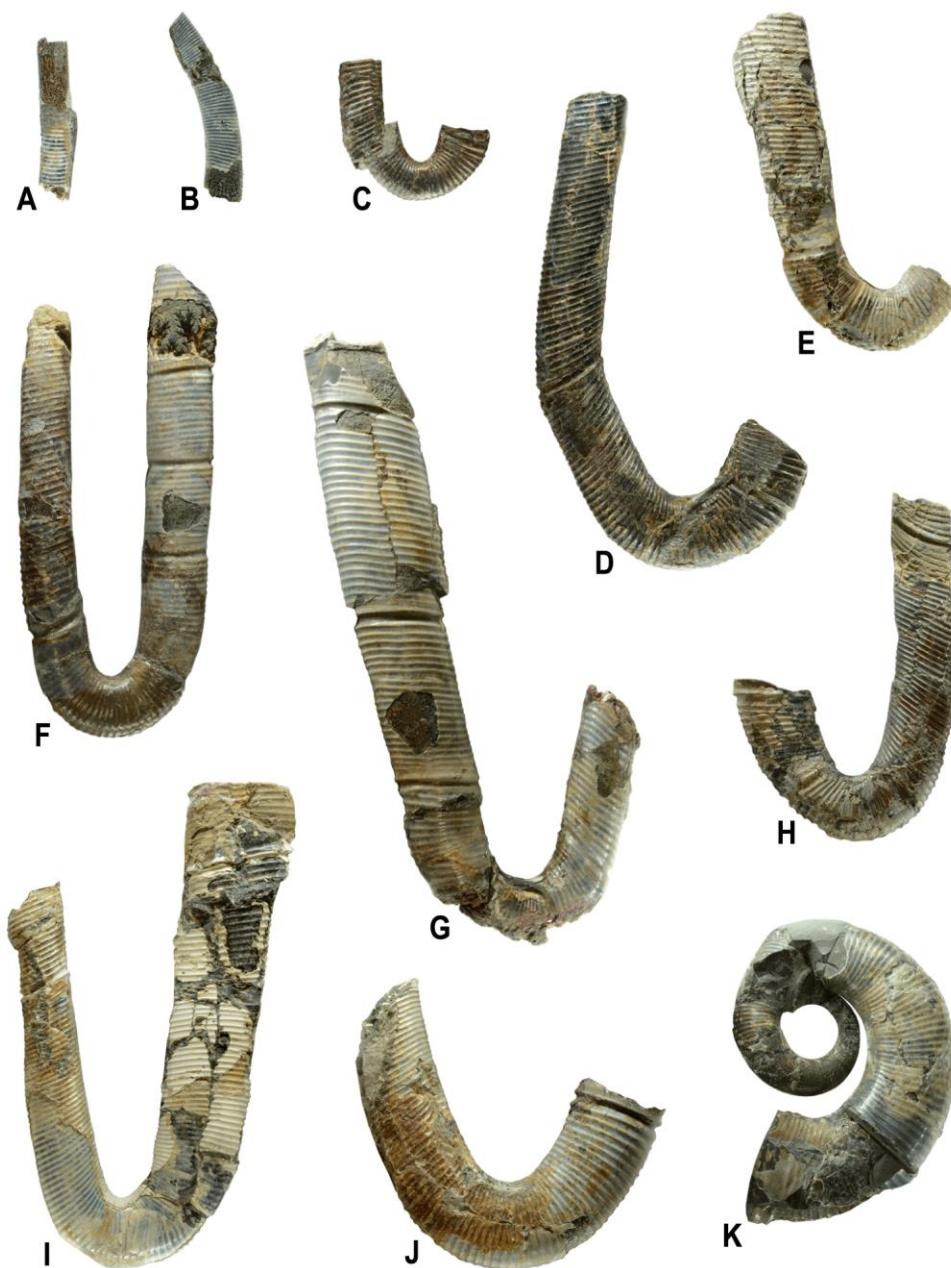


Plate 2.2. A–J, *Diplomoceras* (*Diplomoceras*) *cylindraceum* (Defrance, 1816). A, secondary limb fragment with suture line exposed and costal plications on internal mould, D, RBCM.11; B, secondary limb fragment, left F, RBCM.12; C, secondary elbow and limb fragment, right F, RBCM.13; D, secondary elbow and partial limb, right F, RBCM.14; E, secondary elbow and partial limb, left F, RBCM.15; F, secondary elbow and partial limbs, right F, RBCM.16; G, secondary elbow and partial limbs, left F, RBCM.17; H, secondary elbow and partial limbs, left F, RBCM.18; I, secondary elbow and partial limbs, right F, RBCM.19; J, secondary elbow, left F, RBCM.20. K, *Diplomoceras* (*Diplomoceras*)

cf. *cylindraceum* (Defrance, 1816), probable aberrant gyroconic whorl, left F, RBCM.21. Scale bar = 1 cm.

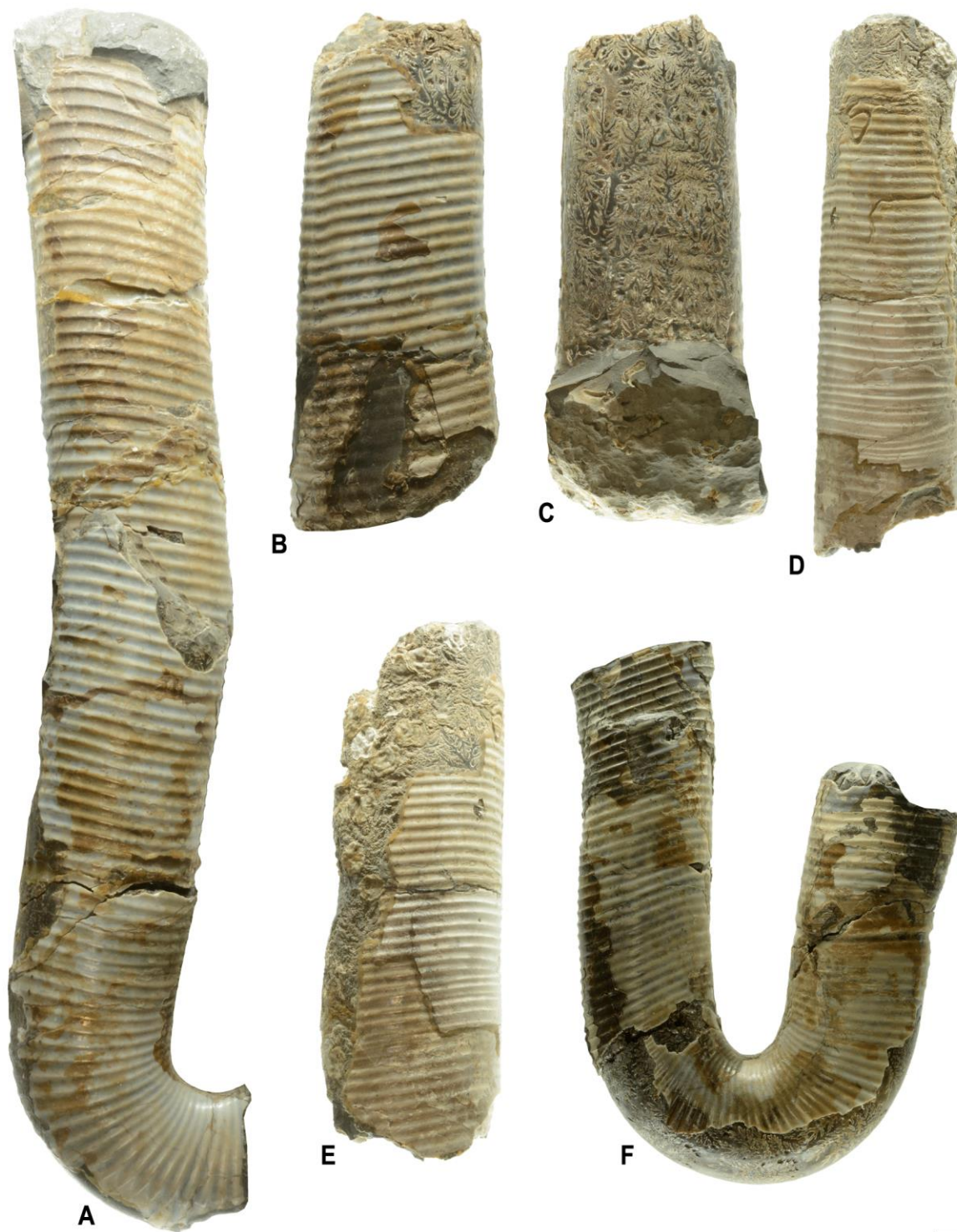


Plate 2.3. A–F, *Diplomoceras (Diplomoceras) cylindraceum* (DeFrance, 1816). **A,** tertiary elbow leading into quaternary limb, left F, RBCM.22; **B, C,** quaternary limb fragment with suture line exposed and costal plications on internal mould, left and right F, RBCM.23; **D, E,** quaternary limb fragment, D and left F, RBCM.24; **F,** tertiary elbow and partial limbs, right F, QBM No. P2015.173. Scale bar = 1 cm.

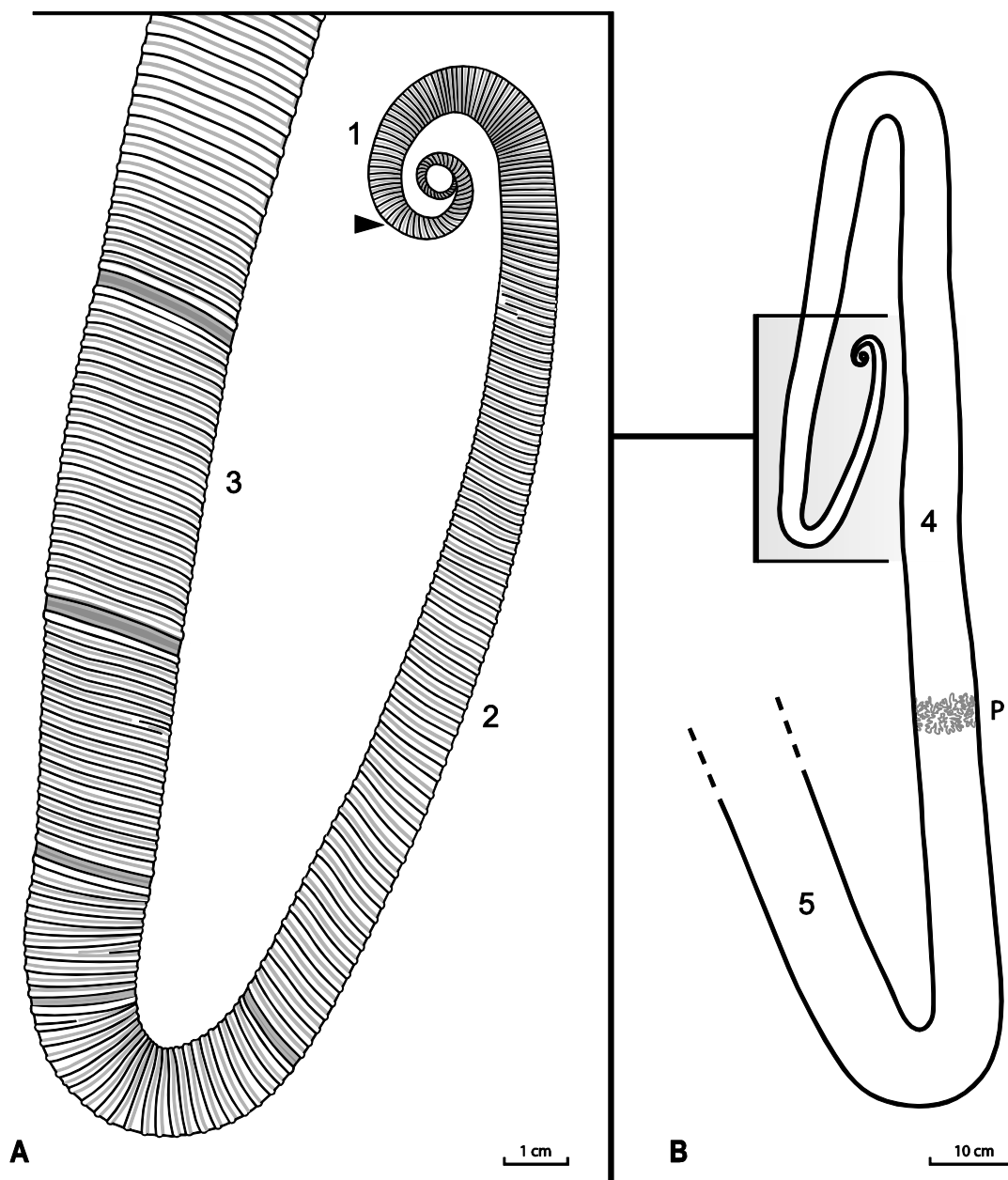


Figure 2.7. A, B, reconstruction of *Diplomoceras (Diplomoceras) cylindraceum* (DeFrance, 1816) conch based on Hornby Island material. **A,** shell in early development, arrow denotes point of transition from helical to planispiral coiling, grey bands denote periodic constrictions; **B,** generalized inference of limb

orientation in a mature conch and position of final septum (P). Numbers indicate ontogenetic order of limbs.

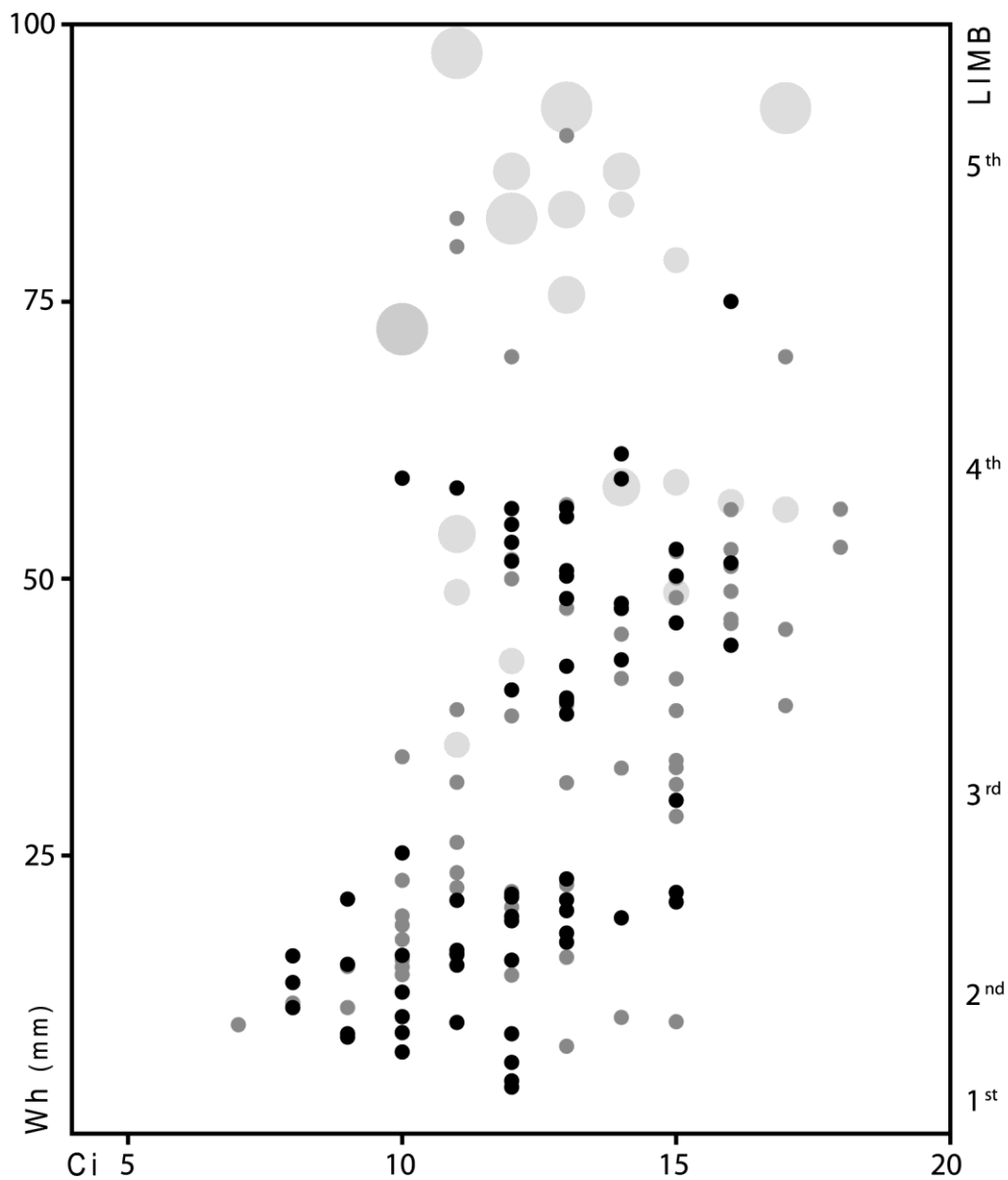


Figure 2.8. Variation in Ci and Wh with developmental progression in *Diplomoceras* (*Diplomoceras*) *cylindraceum* (Defrance, 1816). Black points denote definitive values. Opacity denotes values extrapolated from specimen surfaces marked by shell absence or deformation. Point size denotes precision, larger points less precise.

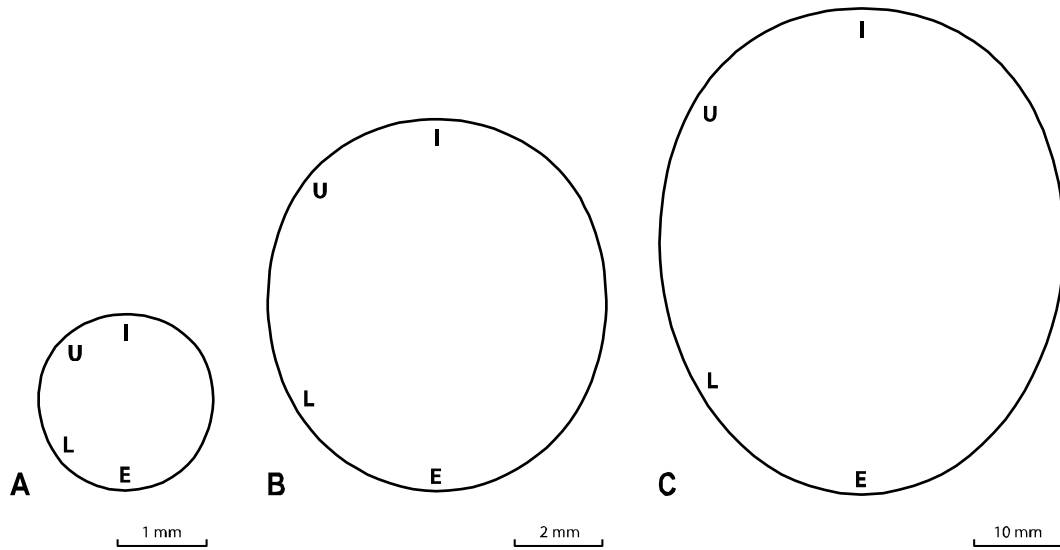


Figure 2.9. A–C, limb cross-section and lobe positioning throughout ontogeny in *Diplomoceras* (*Diplomoceras*) *cylindraceum* (Defrance, 1816). **A**, RBCM.5, Wh = 1.9 mm; **B**, RBCM.11, Wh = 8.3 mm; **C**, RBCM.23, Wh = 55 mm.

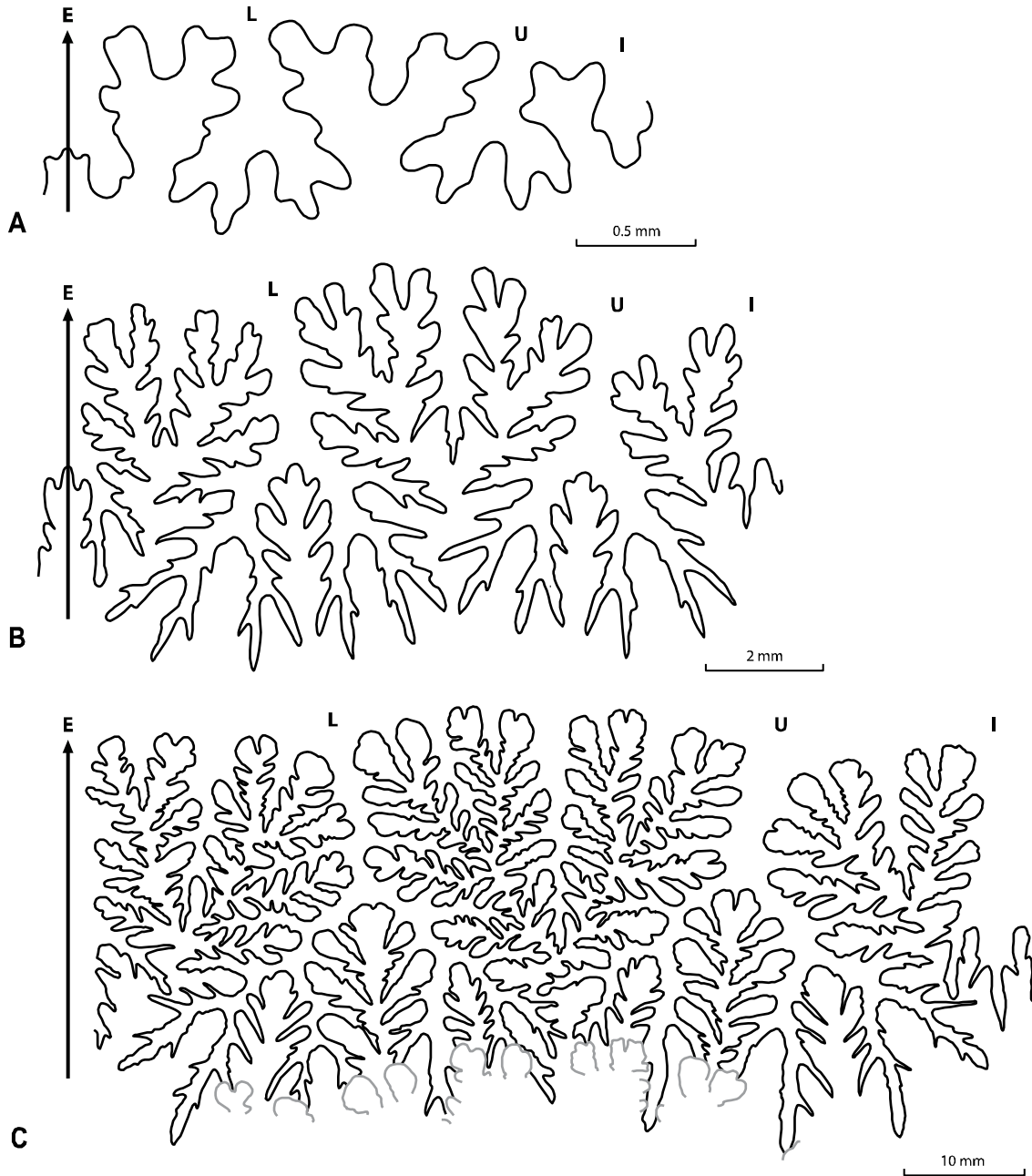


Figure 2.10. A–C, suture line developmental progression in *Diplomoceras (Diplomoceras) cylindraceum* (Defrance, 1816). A, RBCM.5, Wh = 1.9 mm; B, RBCM.11, Wh = 8.3 mm; C, RBCM.23, Wh = 55 mm, tips of preceding folioles (grey) illustrate septal approximation.

Diplomoceras (Diplomoceras) cf. cylindraceum (Defrance, 1816)

(Pl. 2.2K)

Material. A single specimen, RBCM.21, consisting of one and one-half gyroconic volutions.

Occurrence. *D. (D.) cf. cylindraceum* is represented by an isolated occurrence from the upper Campanian Northumberland Formation exposed along the mid-western shore of Hornby Island.

Description. One and one-half discontinuous volutions of gyroconic phragmacone expanding from a Wh of at least 7–26 mm with an 11° ventral lobe offset to the left of the plane of coiling. The dorsum is somewhat flattened on what is otherwise a whorl of subcircular cross-section with a Wb/Wh ratio of 0.94. The largest gyroconic section exhibits an Xr of 12.7 and a Ci of 11.

Remarks. Specimen RBCM.21 stands removed from the overall population of *D. (D.) cylindraceum* represented within the Hornby Island material in the expression of gyroconic coiling in the post-helical stage at a Wh typically characterized by limb development and recurvature. Additionally, the specimen exhibits a flattened dorsum. For these reasons, it cannot be assigned to *D. (D.) cylindraceum* with certainty, although the ventral lobe offset suggests aberrant development with a Wb/Wh ratio, Xr, Ci, and suture line all within the parameters of the species.

Genus *Exiteloceras* Hyatt, 1894

Type species. *Ancyloceras jenneyi* Whitfield, 1877 by subsequent designation (Diener 1925).

Age. Range: late Campanian–late Maastrichtian (e.g. Kennedy *et al.* 2000c; Summesberger *et al.* 2009).

Emended diagnosis. Heteromorph ammonites which are predominantly gyroconic, planispirally coiled, and bilaterally symmetric along their dorsoventral axes. Volutions may be contiguous or discontinuous. Mode of whorl progression may be uniformly gyroconic throughout or with

hamitid, elliptical, or polygonal variance at early stages. Whorl cross-section may be circular to trapezoidal or subquadrate. Constrictions may be independent or associated with megastriae. Costae may be fine and flexuous to coarse and raised. Intercalated costae are common. Ventrolateral ornamentation consists generally of two rows of tubercles or spines. Mature suture line is complex and florid with third-order incision elements.

Remarks. *Exiteloceras* was originally assigned to the Nostoceratidae (Hyatt 1894). Placement of the genus was later retained but with admission of little certainty on the part of some authors (e.g. Kennedy *et al.* 2000c), citing ambiguity surrounding its phylogenetic relationships to other heteromorph ammonite families. However, it appears most appropriate that *Exiteloceras* be moved to the Diplomoceratidae based on the predominance of planispiral coiling among forms assignable to the genus (Cobban 1970; Klinger 1982).

Numerous authors have considered *Axonoceras* Stephenson, 1941 to be synonymous with *Exiteloceras* (Matsumoto 1967; Lewy 1969; Klinger 1982; Wright *et al.* 1996). However, several distinguishing traits suggest taxonomic merit in retaining the group at subgeneric rank. First, mature forms possess coils nearly or directly in contact. Second, based on material described from Texas (Stephenson 1941) and the Atlantic Highlands (Cobban 1974b), *E. (Axonoceras)* is almost always gyroconically coiled, whereas the early coils of *E. (Exiteloceras)* are highly irregular and often hamitid. Additionally, specimens assignable to *E. (Axonoceras)* are distinctly smaller than those belonging to *E. (Exiteloceras)*, exhibiting mature volutions less than 50 mm in diameter (Klinger 1982).

Neancyloceras is considered to bear closer affinity to *Exiteloceras* than to *Pseudoxybeloceras* Wright & Matsumoto, 1954 or *Parasolenoceras* Collignon, 1969, based on its broad, open coils in the early to intermediate stages, in contrast to the latter genera, which are predominantly hamiticonic (Klinger 1982). *Neancyloceras* is herein treated as a subgenus of *Exiteloceras* reserved for forms consisting of several gyroconic volutions which straighten to form a limb in approach to a recurved body chamber (Klinger 1982). *E. (Neancyloceras)* also has a tendency to exhibit broadly spaced, raised costae with low angles of limb curvature.

Members of *E. (Exiteloceras)* are therefore characterized by planispiral whorls varying from hamitid to elliptical or polygonal in the early stages, followed by predominantly discontinuous gyroconic coiling. The late Campanian index species *Exiteloceras (Exiteloceras)*

jennyi (Whitfield, 1877) of the US Western Interior (e.g. Kennedy *et al.* 2000c), Colombia (Föllmi *et al.* 1992) and Mexico (Ifrim *et al.* 2015) typifies the subgenus and is the most widely abundant taxon. The species bears discontinuous whorls that are subelliptical to trapezoidal in cross-section (Scott & Cobban 1965; Wright *et al.* 1996; Kennedy *et al.* 2000c). It is herein proposed that the genus should not exclude constricted forms as suggested previously (Cobban 1974b) and that, in principle, constrictions should only be considered specifically diagnostic if they appear with consistency and uniformity within a population, as would be expected in a genetically based feature.

Subgenus *Exiteloceras* (*Exiteloceras*) Hyatt, 1894

Type species. *Ancyloceras jennyi* Whitfield, 1877 by subsequent designation (Diener 1925).

Age. Constrained to the late Campanian (e.g. Kennedy *et al.* 2000c).

Exiteloceras (*Exiteloceras*) *densicostatum* sp. nov.

(Pl. 2.4A–D; Fig. 2.11A, B)

Types. The type series consists of the holotype RBCM.EH2008.011.00425.001 (RBCM.25) and paratypes RBCM.26–28 from the upper part of the Northumberland Formation, Collishaw Point, Hornby Island, housed in the RBCM.

Diagnosis. A heteromorph ammonite with early limbs arranged polygonally, gradually assuming an elliptical, gyroconic mode of coiling. Whorl cross-section is subovate to subquadrate with an expansion rate averaging 12.69. Flexuous costae possess a high costal index ranging from 9 in the early stages to 18 on the body chamber. Mature suture line is complex and florid marked by a narrow-stemmed lateral saddle and third-order incision elements.

Etymology. Latin, *densicostatum*, densely ribbed.

Material. Four partial specimens consisting of gyroconic whorls and polygonal limb sections of phragmocone and body chamber fragments.

Occurrence. *E. (E.) densicostatum* is restricted to the upper part of the upper Campanian Northumberland Formation exposed at Collishaw Point, Hornby Island.

Description. Early limbs are arranged polygonally and gradually assume an elliptical, gyroconic mode of coiling in later whorls. Limbs are moderately inflated with a depressed dorsum and venter. The whorl cross-section is subovate to subquadrate. The X_r calculated along the earliest preserved limb of specimen RBCM.25 is 13.14, decreasing to 12.24 along a length of approximate equivalence in the subsequent volution. Although the ventral surface is obscured by weathering in specimen RBCM.28, it is apparent that the maximum phragmocone Wh would have approached 31 mm and the mature volution would have easily attained a diameter in excess of 115 mm (Pl. 2.4D). Of the four specimens measured, the average Ca value is 32.5°.

Periodic constrictions are common and may be discontinuous, terminating prior to the dorsolateral or ventrolateral margin with an average Fb/Wh ratio of ~ 0.07. Costae are flexuous and weakly sigmoidal with a Ci of 9 on intermediate growth stages and 18 in approach to the mature volution. Each transverse costa is prorsiradiate on the dorsum, becoming rectiradiate on the dorsolateral margin before abruptly transitioning to rursiradiate at mid-flank and continuing toward the ventrolateral margin (Pl. 2.4C). Periodic intercalated costae are present which may or may not merge at the base of spines on the ventrolateral margin (Pl. 2.4A). Joined by ventrally transverse costae, spines are well developed in all four specimens with a length/Wh ratio varying from 1:6 to 1:7. The mature suture line is florid with narrow-stemmed saddles and third-order incision elements (Fig. 2.11B). The highest extrapolated Sc and Sg values were obtained from RBCM.28 at 698.52 and 41.97, respectively.

Remarks. *E. (E.) densicostatum* possesses the highest Ci of any species within the genus. The numerous costae and high inflation of RBCM.25 is comparable to that of *Exiteloceras (Axonoceras) multicosatus* (Stephenson, 1941) from the upper Campanian Neylandville Marl of Texas. However, the much larger Hornby Island specimens consist of discontinuous, elliptical volutions bearing finer, narrower costae than the Texas examples. On these grounds, *E. (E.)*

densicostatum bears closest affinity to *E. (E.) jenneyi* (Whitfield, 1877) but differs in the intricacy of costal ornamentation and a narrow-stemmed lateral saddle.

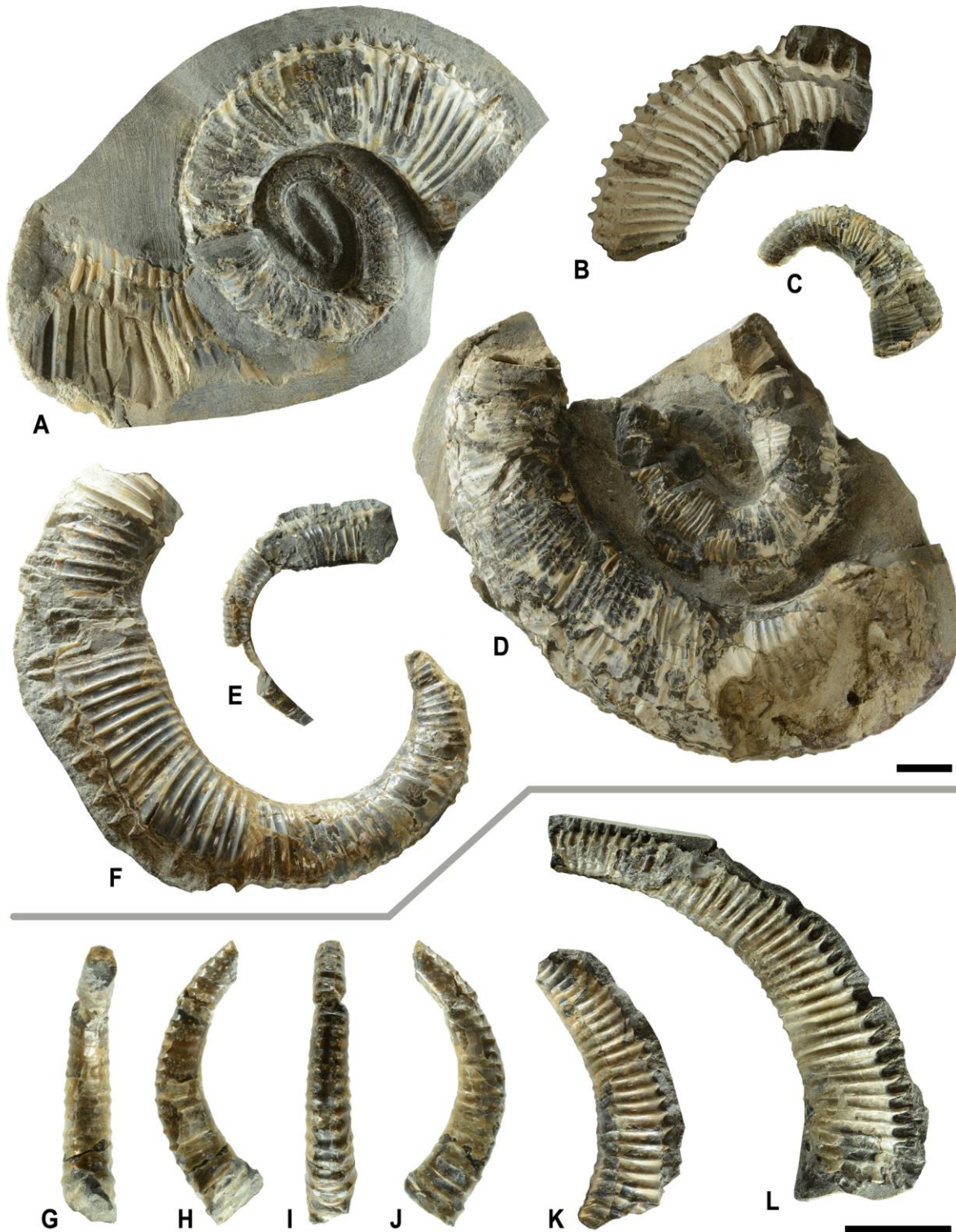


Plate 2.4. A–D, *Exiteloceras* (*Exiteloceras*) *densicostatum* sp. nov. **A**, one and one-half volutions of phragmocone, left F, holotype RBCM.25, matrix retained in the inferred position of the primary limb; **B**, body chamber fragment, left F, paratype RBCM.26; **C**, whorl fragment, left F, paratype RBCM.27; **D**, partial whorl and body chamber, right F, paratype RBCM.28. **E–L, *Exiteloceras* (*Neancyloceras*) aff. *bipunctatum* (Schlüter, 1872).** **E**, partial whorl and body chamber, left F, RBCM.29; **F**, partial whorl and body chamber, left F, RBCM.30; **G–J**, whorl fragment, D, right F, V, and left F, RBCM.31; **K**, whorl fragment, left F, RBCM.32; **L**, whorl fragment, left F, RBCM.33. Scale bars = 1 cm.

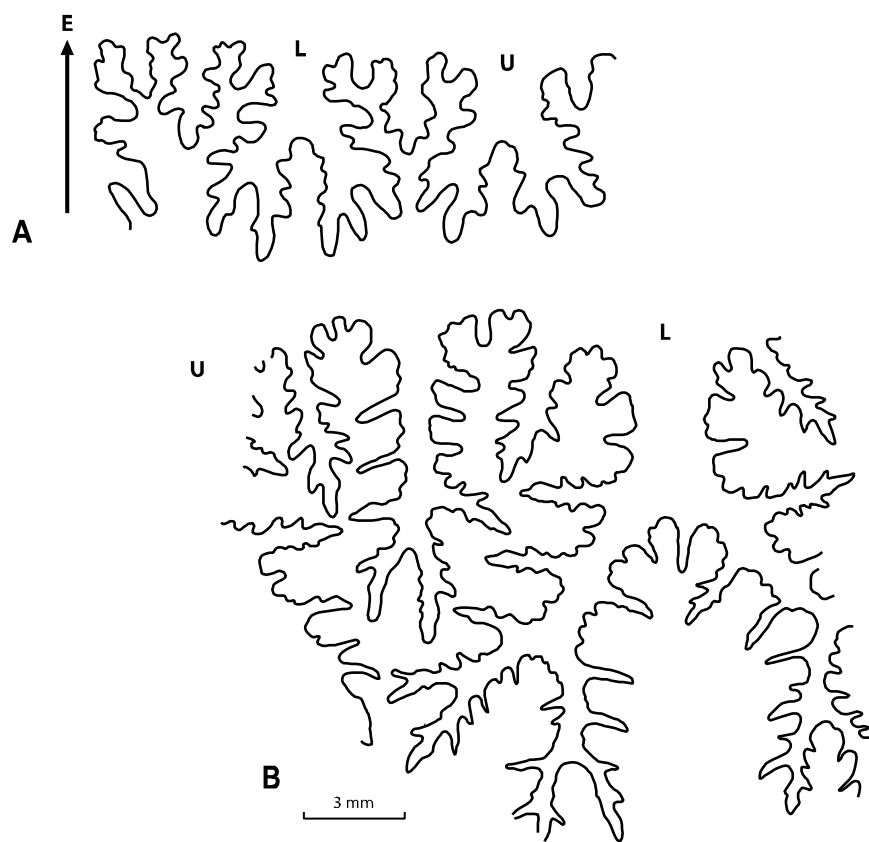


Figure 2.11. A, B, *Exiteloceras* (*Exiteloceras*) *densicostatum* sp. nov. **A**, partial suture line of holotype RBCM.25, Wh = 7 mm; **B**, partial lateral lobe of paratype RBCM.28, Wh = 30 mm.

Subgenus *Exiteloceras* (*Neancyloceras*) Spath, 1926

Type species. *Ancyloceras bipunctatum* Schlüter, 1872.

Age. Range: late Campanian–late Maastrichtian (e.g. Summesberger *et al.* 2009).

Exiteloceras (Neancyloceras) aff. bipunctatum (Schlüter, 1872)

(Pl. 2.4E–L; Fig. 2.12A–C)

Compare:

- 1872 *Ancyloceras bipunctatum* Schlüter: 98, pl. 29, figs 1–3.
- (?)1980 *Neancyloceras bipunctatum* (Schlüter); Błaszkiwicz: 29, pl. 12, fig. 5.
- (?)1980 *Neancyloceras bipunctatum* (Schlüter); Błaszkiwicz: 29, pl. 11, fig. 3.
- 1982 *Neancyloceras bipunctatum* (Schlüter); Tzankov: 20, pl. 5, figs 1–4.
- (?)1986c *Neancyloceras cf. bipunctatum* (Schlüter); Kennedy: 104, pl. 16, fig. 5.
- (?)1995 *Neancyloceras bipunctatum* (Schlüter); Lommerzheim: 66, pl. 7, fig. 7 (*cum syn.*).
- 1999 *Neancyloceras bipunctatum* (Schlüter); Kennedy & Summesberger: 27, pl. 2, fig. 6 (*cum syn.*).
- 2000 *Neancyloceras aff. bipunctatum* (Schlüter); Kuchler: pl. 16, figs 7–9.
- 2009 *Neancyloceras bipunctatum* (Schlüter); Summesberger *et al.*: 171, pl. 1, fig. 4 (*cum syn.*).

Type. The lectotype was initially designated from upper Campanian strata of Ahlten, Germany, erected from the original suite (Błaszkiwicz 1980) upon which the description of the species was based (Schlüter 1872, p. 98, pl. 29, fig. 2). Lectotype status was subsequently reassigned to an alternate specimen selected from the original material (Schlüter 1872, p. 98, pl. 29, fig. 1) and refigured (Klinger 1982, p. 221, fig. 2a); it was deposited in the GZG as specimen GZG.INV.116510 alongside paralectotypes GZG.INV.116510 and GZG.INV.116512.

Material. Eleven partial specimens consisting of whorl phragmocone and body chamber fragments.

Occurrence. *E. (N.) bipunctatum* is known from the upper Campanian strata of Germany (Schlüter 1872), Austria (e.g. Kennedy & Summesberger 1999), Northern Ireland (Hancock 1961), Ukraine (Pasternak 1954), western Belgium (Kennedy 1993), southwestern France (Kennedy 1986c), Bulgaria (Tzankov 1982), and Russia (e.g. Mikhailov 1951; Naidin 1959) with

possible occurrences in northern Spain (Küchler 2000), Poland (Błaszkiwicz 1980), and southwestern Arkansas (Kennedy & Cobban 1993b, d). *E. (N.) bipunctatum* has also been recorded from the upper Maastrichtian Nierental Formation of Austria (Summesberger *et al.* 2009). On Hornby Island, *E. (N.)* aff. *bipunctatum* has been recovered from lower part of the upper Campanian Northumberland Formation exposed along the southeastern to mid-western shore.

Description. Whorl sections are subovate and inflated to moderately compressed (Fig. 2.12C), with an average Wb/Wh ratio of 0.93 among five specimens. Of seven specimens, the average Xr is 9.07 with a Ca value of 16.9°. Periodic constrictions are common and continuous around the circumference in early whorls, diminishing on the dorsum in later development. Constrictions may be bordered by megastriae. Of five specimens, the average Fb/Wh ratio is 0.1. Six distinct constrictions are present over 180° of gyroconic coiling in RBCM.30 (Pl. 2.4F).

Costae are sharp, raised, broadly spaced, and flexuous. Ci values increase with development ranging from 4–9. RBCM.26 has a Ci of 4 at a Wh of 3 mm and RBCM.30 possesses a Ci of 6 at a Wh of 15 mm progressing to 8 at a mature Wh of 19.8 mm. Each transverse costa is prorsiradiate on the dorsum becoming weakly rursiradiate on the dorsolateral margin before sigmoidally transitioning to rectiradiate or weakly prorsiradiate across the flank in continuation toward the ventrolateral margin. Costae transect the venter and join a spine projecting at each ventrolateral margin. The mature portion of RBCM.30 displays some segments where every second costa bears a spine (Pl. 2.4F). The spine length/Wh ratio progresses from 1:6 to 1:7.

The suture line of RBCM.29 is indicative of high floridity at maturity with a narrow-stemmed lateral saddle and second-order incision elements in the early phragmocone (Fig. 2.12B). The highest Sc and Sg values were obtained from RBCM.29 at 412.83 and 50.03, respectively.

Remarks. The gradual curvature of the whorl sections indicates a broad angle of open planispiral coiling. *E. (N.)* aff. *bipunctatum* differs from *E. (N.) bipunctatum* (Schlüter, 1872) in exhibiting greater coil inflation and lacking flared costae, although fragments devoid of independent flared costae in the latter are known (e.g. Klinger 1982, fig. 8A–C). Of the material

examined, there is no evidence of hamiticonic recurvature although the body chamber of RBCM.30 appears to straighten (Pl. 2.4F). Variation in the type material has been underscored (Klinger 1982; Kennedy 1993). If the suture line of *E. (N.) bipunctatum* (Kennedy 1993, text-fig. 3) were reduced three-fold, it would likely appear similar to that of RBCM.29 (Fig. 2.12B). The fragmentary nature of some specimens described from Poland (Błaszkiwicz 1980), France (Kennedy 1986c), and Germany (Lommerzheim 1995) casts uncertainty on whether or not they are assignable to the species.

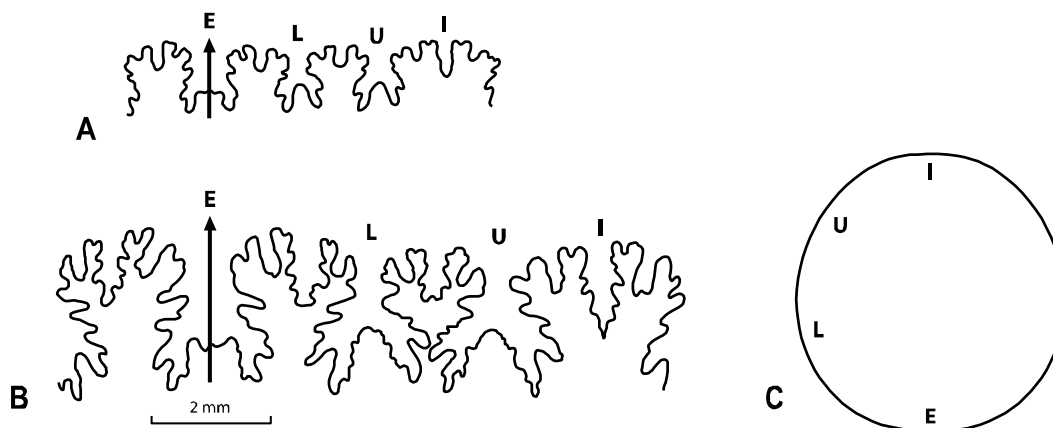


Figure 2.12. A–C, *Exiteloceras* (*Neancyloceras*) aff. *bipunctatum* (Schlüter, 1872). A, suture line, RBCM.29, Wh = 2.7 mm; B, suture line, RBCM.29, Wh = 4.6 mm; C, whorl cross-section and lobe positioning, RBCM.29, Wh = 4.6 mm.

Subfamily **Polyptychoceratinae** Matsumoto, 1938

Emended diagnosis. Heteromorph ammonites encompassing largely hamiticonic forms devoid of helical coiling. Taxa are characterized by one or multiple elongated, straight limbs. Mature suture lines bear second-order incision elements and are less complex than those of the Diplomoceratinae.

Age. Range: late Turonian–late Maastrichtian (e.g. Wright *et al.* 1996).

Genus *Phylloptychoceras* Spath, 1953

Type species. *Ptychoceras siphon* Forbes, 1846.

Emended diagnosis. Heteromorph ammonites comprised of six parallel limbs connected by abruptly recurving elbows. Limbs in close contact with the plane of coiling sinistrally reoriented 90° over the length of the secondary limb. Limbs are circular to subcircular in cross-section. Constrictions may occur at points of limb recurvature being more frequent on the early limbs. Low relief ornamentation is characterized by broadly spaced, rounded costae. The cuneate suture line is distinguished by elongated, narrow-stemmed saddles and a trifold internal lobe.

Age. Range: early–late Maastrichtian (e.g. Jagt *et al.* 2006; Shigeta & Nishimura 2013).

Remarks. *Phylloptychoceras* has been regarded as a subgenus of the Santonian *Polyptychoceras* Yabe, 1927 without consideration of the chronological succession of the former genus in the Maastrichtian (Howarth 1965; Wright *et al.* 1996). The generic distinction made on grounds of a cuneate suture line and subdued costal ornamentation (Jagt *et al.* 2006; Shigeta & Nishimura 2013) has since been upheld (Ikuno & Hurano 2015). Through the recovery of Hornby Island material, it is now understood that *Phylloptychoceras* attained twice the number of limbs typified by *Polyptychoceras sensu* Wright *et al.* (1996). Also, the secondary limb of *Phylloptychoceras* presents a 90° reorientation in the plane of coiling over its length in a manner similar to the developmental progression of *Rhyoptychoceras* Matsumoto, 1977, described from the Coniacian strata of Japan.

***Phylloptychoceras horitai* Shigeta & Nishimura, 2013**

(Pl. 2.5A–Z; Figs 2.13A–C, 2.14A–D)

?1926 *Ptychoceras zelandicum* Marshall: 157.

(?)1958 *Neocyrtochilus bryani* Anderson: 189, pl. 27, fig. 5.

2006 *Phylloptychoceras* cf. *siphon* (Forbes); Jagt *et al.*: 99, pl. 1, figs A–I, text-fig. 2A.

2013 *Phylloptychoceras horitai* Shigeta & Nishimura: 174, figs 1A–Q, 2A–C.

Types. The holotype (HMG-1587a) and paratypes (HMG-1587b-d) as designated from the lower Maastrichtian Hakobuchi Formation along the Tonai-zawa River (Shigeta & Nishimura 2013, p. 174, figs 1A–Q, 2A–C), housed in the HMG.

Emended diagnosis. A heteromorph ammonite comprised of six parallel limbs connected by abruptly recurving elbows. Limbs in close contact, with the plane of coiling sinistrally reoriented 90° over the length of the secondary limb. Limbs are circular to subcircular in cross-section. Constrictions may occur at points of limb recurvature, being more frequent on the early limbs. Low relief ornamentation is characterized by broadly spaced, rounded costae. Mature suture line cuneate, distinguished by elongate, narrow-stemmed saddles and a trifid internal lobe with bifid lateral and umbilical saddles.

Material. Forty-six specimens—40 from which measurements could be obtained. The material consists of independent limbs, elbows, and body chambers ranging from an ammonitella to terminal apertures.

Occurrence. *P. horitai* occurs in the lower Maastrichtian Hakobuchi Formation of Japan (Shigeta & Nishimura 2013) with another likely occurrence in the upper Maastrichtian Merseen Member of the Maastricht Formation type section in the Netherlands (Jagt *et al.* 2006). The species may also occur in the Maastrichtian Moreno Formation of California (Anderson 1958). *P. horitai* finds its earliest occurrence on Hornby Island where it spans nearly the entire stratigraphic section of the upper Campanian Northumberland Formation from the southeastern shore to Collishaw Point.

Description. The fragments examined indicate a shell consisting of six parallel limbs (Fig. 2.13A–C). The earliest stage is represented by a subcircular protoconch enveloped by an ammonitella comprised of a 360° whorl volution. The Wh of the primary limb at the point of emergence from the nepionic constriction is 200 µm (Pl. 2.5A), increasing to a maximum of 9 mm at the aperture of the mature body chamber (Pl. 2.5Y). Of 29 specimens, the average limb X_r is 2.73. Limbs are situated parallel to one another with little to no divergence throughout development. However, a shift in limb orientation occurs after the first elbow over the length of

the secondary limb wherein the plane of coiling is twisted sinistrally 90° (Fig. 2.13A, B). The 90° reorientation is completed just prior to the bend of the second elbow so that the flanks of both primary and secondary limbs rest along the dorsum of the tertiary limb. This is the only discernible developmental variation in the direction of coiling.

Following the planar readjustment, the quaternary limb often deflects from a trajectory parallel to the tertiary limb so that the dorsum is aligned with the flanks of the primary and secondary limbs; this adjustment forms a space to accommodate the two earliest limbs so that limbs remain close to each other. Limb cross-section outlines are circular to subcircular (Fig. 2.14B, D). Of 14 specimens, the average Wb/Wh ratio at the D₁–V₁ transect is 1.09. Among 25 specimens, elbow axes are the site of the lowest Wb/Wh ratio averaging 1.13. Constrictions, if present, generally follow earlier elbows as deep, prorsiradiate, discontinuous furrows terminating at the dorsoventral margin. Of seven specimens exhibiting constrictions, the average Fb/Wh ratio is 0.19.

Costae on the earliest limbs occur as faint, prorsiradiate undulations. Along the fifth- and sixth-order limbs, costae become gradually more prominent appearing rounded and broadly spaced. These costae are depressed along the dorsum and uniformly pronounced along the flanks and across the venter. Prorsiradiate costae with a Ci of 3 vary little throughout development except in approach to an elbow where they become fine, condensed, rectiradiate lirae. The growth pattern of broad, undulating costae is resumed at the opposite point of limb emergence from the elbow. The mature suture line is characterized by a narrow, trifid internal lobe with bifid lateral and umbilical saddles bearing second-order incision elements (Fig. 2.14C). The highest Sc and Sg values were obtained from RBCM.51 at 14.56 and 2.67, respectively.

Remarks. The Hornby Island material facilitates a full conch reconstruction of the species, preserving a complete record of phragmocone development and the progression of the species' distinct suture line. Among these examples, mature sutural elements (Fig. 2.14C) appear virtually identical to those of *P. horitai* described from Japan at the approximately equivalent Wh (Shigeta & Nishimura 2013, fig. 1Q). The suture lines of both examples share the same trigonal angulation and narrow taper of the saddles.

Phylloptychoceras sipho (Forbes, 1846), the type species and only other member of the genus, differs from *P. horitai* mainly in having a higher limb Xr and broad septal saddles with

phylloid lateral margins (e.g. Howarth 1965, pl. 2, fig. 1; Kennedy & Henderson 1992, text-fig. 2d, pl. 4, fig. 7, pl. 5, figs 18–32). The suture line illustrated from material obtained from the Maastrichtian type section (Jagt *et al.* 2006, fig. 2A) appears gradational between *P. siphon* and *P. horitai* at equivalent Wh and may be attributable to intraspecific variability in the former. *P. horitai* also seems to have a more subcircular cross-section than *P. siphon*.

The simple suture lines of juvenile limb sections in *P. horitai* are similar to those of *Phylloptychoceras zelandicum* (Marshall, 1926), as illustrated from a small fragment (Spath 1953, pl. 11, fig. 8). However, a direct phylogenetic relationship is unlikely considering confirmation of a bifid internal lobe and an apparent lack of limb recurvature in the New Zealand forms (Henderson 1970). These traits were considered to be taxonomically significant enough to warrant the reassignment of *P. zelandicum* to the genus *Astreptoceras* Henderson, 1970.

The taxon *Neocyrtochilus bryani* Anderson, 1958, described from California, is probably synonymous with *P. horitai*. It has been suggested that the specimen compares well with those of *P. siphon* at an equivalent developmental stage (Ward & Kennedy 1993), although the species clearly exhibits a more rapid Xr in approach to points of limb recurvature (Kennedy & Henderson 1992, pl. 5, figs 18–32). Based on a fragment consisting of two early parallel limbs, the Californian specimen is too small to assign to *P. horitai* with confidence, let alone provide the basis for the description of a separate taxon.



Plate 2.5. A–Z, *Phylloptychoceras horitai* Shigeta & Nishimura, 2013. A, ammonitella and primary limb, V, RBCM.34, arrow denotes neponic constriction, scale bar = 500 μ m; B, RBCM.34, V, scale bar = 1 mm; C, D, partial primary through tertiary limbs, V to right F transition, RBCM.35; E, partial secondary

and tertiary limbs, right F, RBCM.36; **F**, partial secondary and tertiary limbs, V to left F transition, RBCM.37; **G**, partial secondary and tertiary limbs, right F, RBCM.38; **H**, partial tertiary and quaternary limbs, left F, RBCM.39; **I, J**, tertiary elbow internal mould, left and right F, RBCM.40; **K**, partial tertiary and quaternary limbs, left F, RBCM.41; **L**, partial tertiary and quaternary limbs, right F, RBCM.42; **M**, partial primary through quaternary limbs, V to right F transition, RBCM.43; **N**, secondary through partial quaternary limbs, V to left F transition, RBCM.44; **O**, secondary through partial quaternary limbs, V to left F transition, RBCM.45, scale bar = 5 mm; **P**, quaternary limb and partial elbow, right F, RBCM.46; **Q, R**, quaternary elbow and partial body chamber, right F and V, CDM No. 2013.84.1; **S**, fifth-order elbow and partial body chamber, right F, RBCM.47; **T**, fifth-order elbow and partial body chamber, right F, RBCM.48; **U, V**, partial fifth-order elbow and body chamber, right F and V, RBCM.49; **W**, partial fifth-order limb and body chamber, right F, RBCM.50; **X**, partial quaternary and fifth-order limbs, left F, RBCM.51; **Y, Z**, fifth-order limb and body chamber, left F and V, RBCM.52, scale bar = 1 cm.

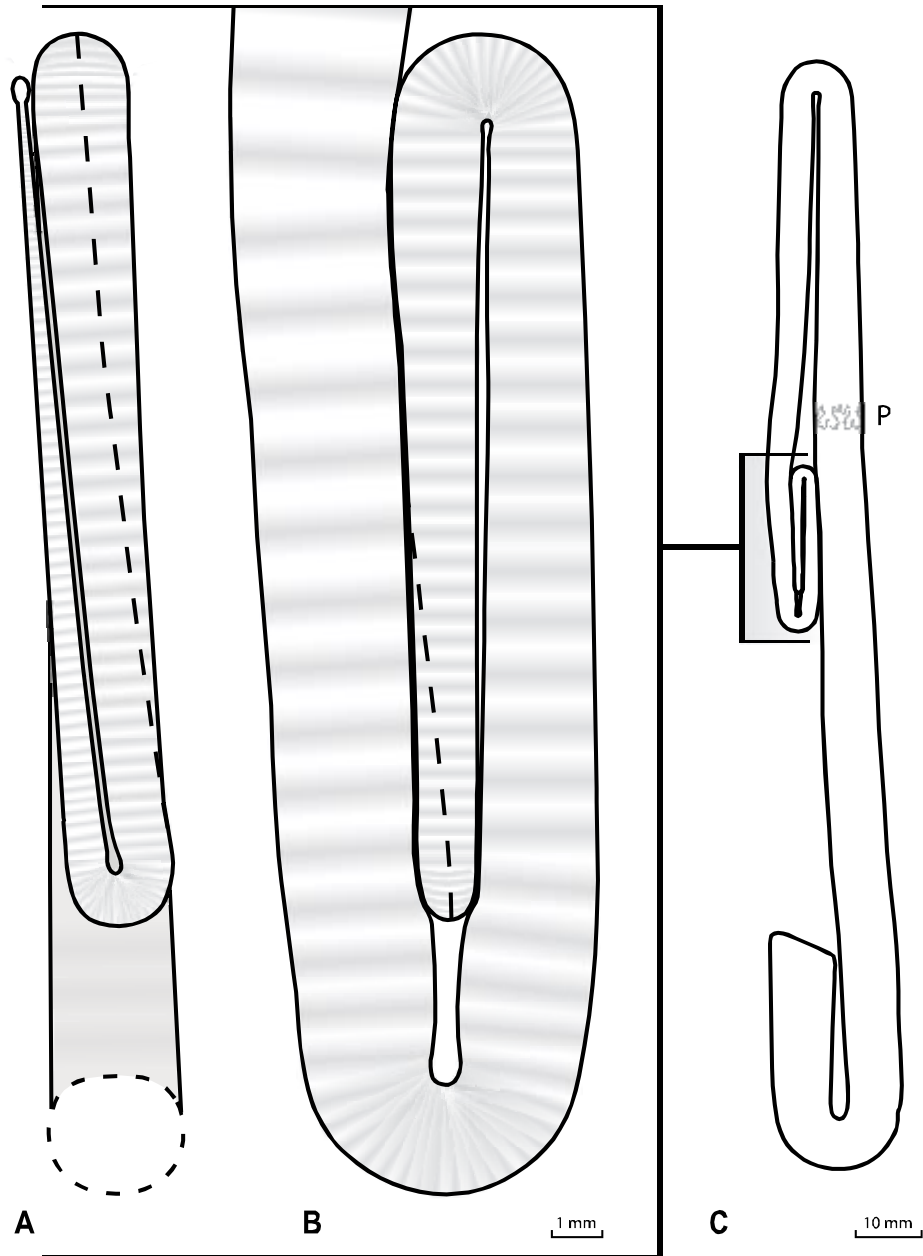


Figure 2.13. A–C, complete reconstruction of *Phylloptychoceras horitai* Shigeta & Nishimura, 2013 based on Hornby Island material. **A**, juvenile shell dorsal view in relation to tertiary limb; **B**, juvenile shell lateral view in relation to tertiary limb; **C**, generalized inference of limb orientation in a mature conch and position of final septum (P). Dashed lines indicate ventral position of siphuncle.

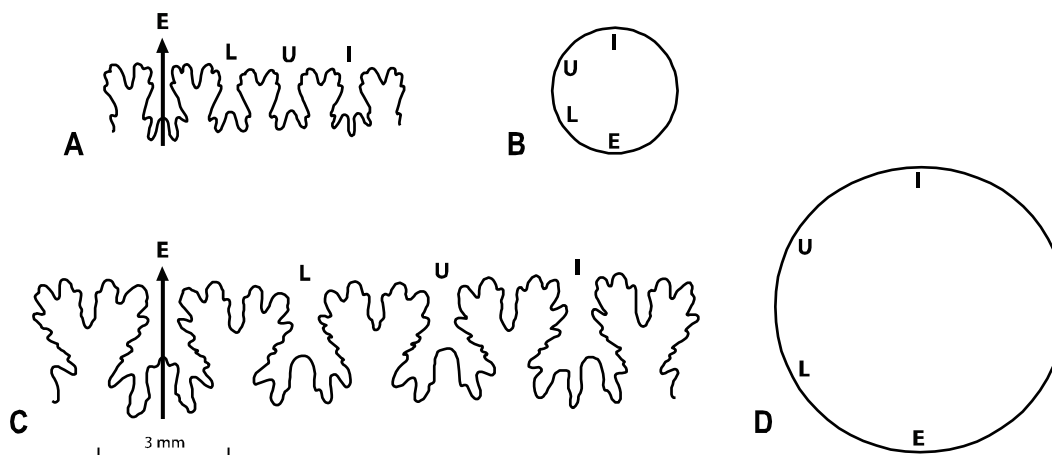


Figure 2.14. A–D, *Phylloptychoceras horitai* Shigeta & Nishimura, 2013. A, suture line, RBCM.42, Wh = 3 mm; B, limb cross-section and lobe positioning, RBCM.42, Wh = 3 mm; C, suture line, RBCM.51, Wh = 6.7 mm; D, limb cross-section and lobe positioning, RBCM.51, Wh = 6.7 mm.

Genus *Solenoceras* Conrad, 1860

Type species. *Hamites annulifer* Morton, 1842 by subsequent designation (Conrad 1860).

Emended diagnosis. Heteromorph ammonites comprised of two parallel limbs in contact and of equal or unequal length presumably succeeding a minute ammonitella. Conches are characterized by a curved initial limb leading to a tight elbow marking the beginning of the body chamber. A small, tear-shaped opening occurs between the limbs at the axis of recurvature. Limb cross-sections range from circular to reniform with that of the body chamber being dependent on the degree of penultimate limb impression often resulting in a contact furrow. Constrictions may or may not be present. Costae may be prorsiradiate to rursiradiate. Small ventrolateral tubercles or spines are generally present throughout. Mature suture line is complex and florid with second-order incision elements.

Age. Range: middle Campanian–early Maastrichtian (e.g. Kennedy *et al.* 2000c; Ifrim *et al.* 2017).

Remarks. Several morphological variables—chiefly those of limb inflation, constrictions, and Ci—have been used to define 11 species belonging to *Solenoceras*, but not without interspecific overlap of certain traits. For this reason, a dichotomous key is presented to assist workers in diagnosing these species (Table 2.1). Species not recognized herein, and which were not subsequently reassigned to the genus *Spiroxybeloceras* Kennedy & Cobban, 1999, are *Solenoceras binodosum* (Haughton, 1925) *sensu* Cooper (1994) and *Solenoceras bembense* Haas, 1943, as these taxa were erected from fragmentary specimens lacking fully articulated parallel limbs.

Table 2.1. Dichotomous key for identification of species belonging to the genus *Solenoceras* Conrad, 1860.

1a	Constrictions present	2.
1b	Constrictions absent	<i>S. mexicanum</i> Anderson, 1958.
2a	Constrictions present on penultimate limb	3.
2b	Constrictions absent on penultimate limb	4.
3a	Constrictions present throughout	5.
3b	Constrictions present throughout and pre-apertural constriction	7.
4a	Multiple constrictions and pre-apertural constriction	<i>S. elegans</i> Kennedy <i>et al.</i> , 2000c.
4b	Pre-apertural constriction only	<i>S. nitidum</i> Cobban, 1974a.
5a	Body chamber laterally compressed	<i>S. texanum</i> (Shumard, 1861).
5b	Body chamber inflated	6.
6a	Penultimate limb cross-section circular	<i>S. bearpawense</i> Kennedy <i>et al.</i> , 2000c.
6b	Penultimate limb venter slightly depressed and narrow	<i>S. larimerense</i> Kennedy <i>et al.</i> , 2000c.
7a	Penultimate limb cross-section circular	8.
7b	Penultimate limb cross-section subovate to depressed reniform	9.
8a	Costal index of 3–5	<i>S. mortoni</i> (Meek & Hayden, 1857).
8b	Costal index of 6 throughout	<i>S. reesidei</i> Stephenson, 1941.
9a	Multiple constrictions on body chamber	<i>S. annulifer</i> (Morton, 1842).
9b	Pre-apertural constriction only	10.
10a	Costal index of 3–5	<i>S. exornatus</i> sp. nov.

Solenoceras exornatus sp. nov.

(Pl. 2.6A–X; Fig. 2.15C–G)

Types. The type series consists of the holotype RBCM.EH2008.011.10210.001 (RBCM.53) and paratypes RBCM.54–65 from the upper Campanian Northumberland Formation, Hornby Island, housed in the RBCM.

Diagnosis. A dual-limbed heteromorph ammonite with a high expansion rate averaging 6.37 on the penultimate limb. Whorl cross-section ranges from ovate to subovate becoming reniform in approach to the body chamber. Constrictions only present on the early portion of the penultimate limb and one preceding a megastria prior to the apertural margin on the body chamber. Conch possesses fine spinous ornamentation. Mature suture line is complex and florid with second-order incision elements.

Etymology. Latin, *exornatus*, embellished or ornamented.

Material. Thirty-two partial specimens—29 from which measurements could be obtained—largely comprised of early limb and body chamber fragments. The most complete specimens consist of two parallel limbs connected by an elbow.

Occurrence. *S. exornatus* is restricted to the lower part of the upper Campanian Northumberland Formation exposed along the southeastern shore of Hornby Island.

Description. The shell consists of two parallel limbs connected by an elbow. Of 14 specimens, the average penultimate limb X_r is 6.79; of six specimens, this value is 6.02 on the body chamber. In holotype RBCM.53 (Pl. 2.6A), the penultimate limb attains twice the W_h over a distance of 36 mm. The body chamber occupies both the largest limb and its preceding elbow. A dorsal furrow is present along the body chamber and accommodates the impressed penultimate limb. The penultimate limb cross-section is oval before flattening in the dorsal region, with an increase in flank breadth toward the elbow (Fig. 2.15F). Of thirteen specimens, the average penultimate limb W_b/W_h ratio is 1.19. The body chamber cross-section is reniform due to penultimate limb impression. The highest W_b/W_h ratio occurs at the elbow axis, averaging 1.37 among five specimens. Due to the curvature and taper of the penultimate limb, it is unlikely that the largest examples exceeded 80 mm in length. A notable degree of size polymorphism is evident from the material available, with definitive elbow axis W_h values ranging from 5.4 to 6.5 mm among six specimens.

Constrictions are clearly visible on the early, curved portion of the penultimate limb and spaced four to six costae apart. Each constriction is preceded by a megastria in the form of a prominently raised adapertural costa. Constrictions weaken with maturation, becoming faint or absent as the dorsum flattens against the body chamber. A distinct constriction precedes a megastria prior to the fine lirae which distinguish the apertural margin (e.g. Pl. 2.6Q). The flanks of both limbs are rounded, possessing costae which become sharper and more pronounced on the body chamber. Costae are prorsiradiate on the penultimate limb, rectiradiate across the elbow, and rursiradiate on the body chamber. The Ci of the penultimate limb ranges from 4 to 5 in the early stages, reducing to 4 or 3 on the body chamber as the dorsum begins to flatten.

Spinous ornamentation occurs throughout. Each costa bears a small spine at the ventrolateral margin and transverse costae cross the flattened venter joining parallel spines (Fig. 20C). Well-preserved penultimate limb sections reveal that these spines typically attain a length equal to 1/8 their associated Wh (e.g. Pl. 2.6I). The mature suture line is complex and florid with narrow-stemmed saddles and intricate second-order incision elements (Fig. 2.15E, G). The highest Sc and Sg values were obtained from RBCM.53 at 39.75 and 5.2, respectively.

Remarks. *S. exornatus* is most similar to *Solenoceras texanum* (Shumard, 1861) but differs in having a more complex suture line and a lower Ci on the body chamber, with more broadly spaced furrows between sharper costae (Stephenson 1941, pl. 77, figs 4, 5). Additionally, *S. texanum sensu* Larson (2016) and *Solenoceras bearpawense* Kennedy *et al.*, 2000c of the US Western Interior differ from *S. exornatus* in being more compressed, having an overall greater Ci and constrictions throughout. *Solenoceras mexicanum* Anderson, 1958, with a possible occurrence reported in the North Pacific (Haggart *et al.* 2009), lacks constrictions altogether and pronounced ornamentation on the smaller limb (Kennedy *et al.* 2000c). Both limbs of *S. mexicanum* have also been noted as circular in cross-section (Anderson 1958) as opposed to those of *S. exornatus*.

Solenoceras elegans Kennedy *et al.*, 2000c is smaller than *S. exornatus* with less inflation and a lower penultimate limb Xr. *S. elegans* also lacks constrictions on the penultimate limb. *Solenoceras reesidei* Stephenson, 1941 is also smaller than *S. exornatus* with a Ci of 6 on the body chamber and constrictions on both limbs (Larson 2016). *Solenoceras multicostatum* Stephenson, 1941 has a similar degree of inflation to that of *S. exornatus* but a notably higher Ci

of 7 or 8 and exhibits constrictions along the full length of the penultimate limb. One specimen assigned to *Solenoceras humei* (Douvillé, 1928) from eastern Egypt (Luger & Gröschke 1989, pl. 49, fig. 4) bears a superficial similarity to *S. exornatus* but constrictions are absent and the limbs are barely appressed. Subsequent authors have placed much of the Egyptian material within the genus *Spiroxybeloceras* due to planispiral coiling in the early stages (Kennedy *et al.* 2000c; Kennedy & Lunn 2000).

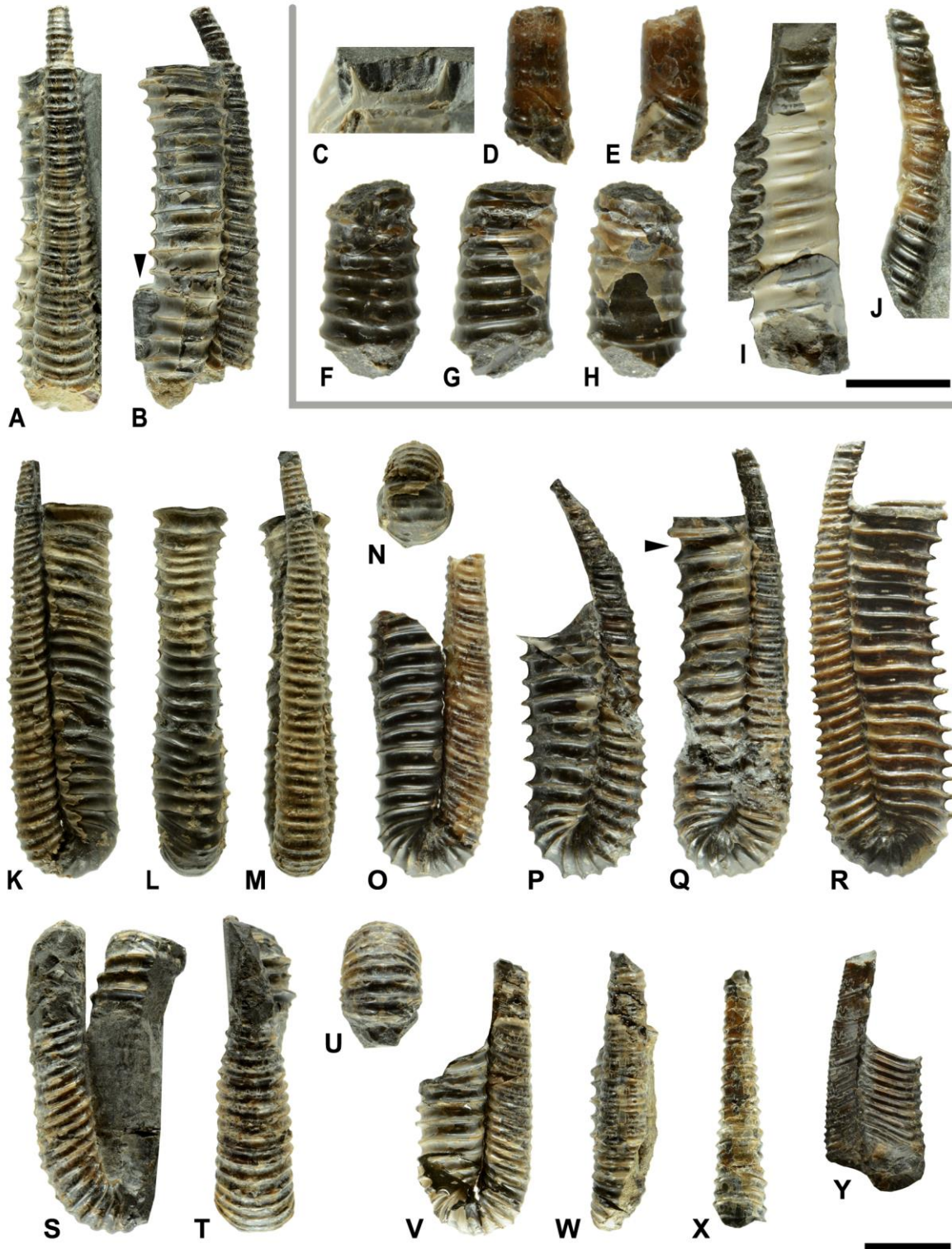


Plate 2.6. A–X, *Solenoceras exornatus* sp. nov. A, B, penultimate limb and body chamber, V and left F, holotype RBCM.53, arrow denotes position of spinous ornamentation; C, spines on body chamber, V, holotype RBCM.53; D, E, penultimate limb fragment, left F and V, paratype RBCM.54; F–H,

penultimate limb fragment, V, right F and D, paratype RBCM.55; **I**, penultimate limb fragment, right F, paratype RBCM.56; **J**, penultimate limb fragment, left F, paratype RBCM.57, scale bar = 5 mm; **K–N**, penultimate limb and body chamber, right F and three V sides, paratype RBCM.58; **O**, penultimate limb and partial body chamber, left F, paratype RBCM.59; **P**, penultimate limb and body chamber, left F, paratype RBCM.60; **Q**, penultimate limb and body chamber, left F, paratype RBCM.61. Arrow denotes pre-apertural construction. **R**, penultimate limb and body chamber, left F, paratype RBCM.62; **S–U**, penultimate limb and body chamber fragment, right F and two V sides, paratype RBCM.63; **V, W**, penultimate limb and body chamber, left F and V, paratype RBCM.64; **X**, penultimate limb, D, RBCM.65. **Y**, *Solenoceras* cf. *reesidei* Stephenson, 1941, penultimate limb and body chamber, right F, RBCM.66, scale bar = 1 cm.

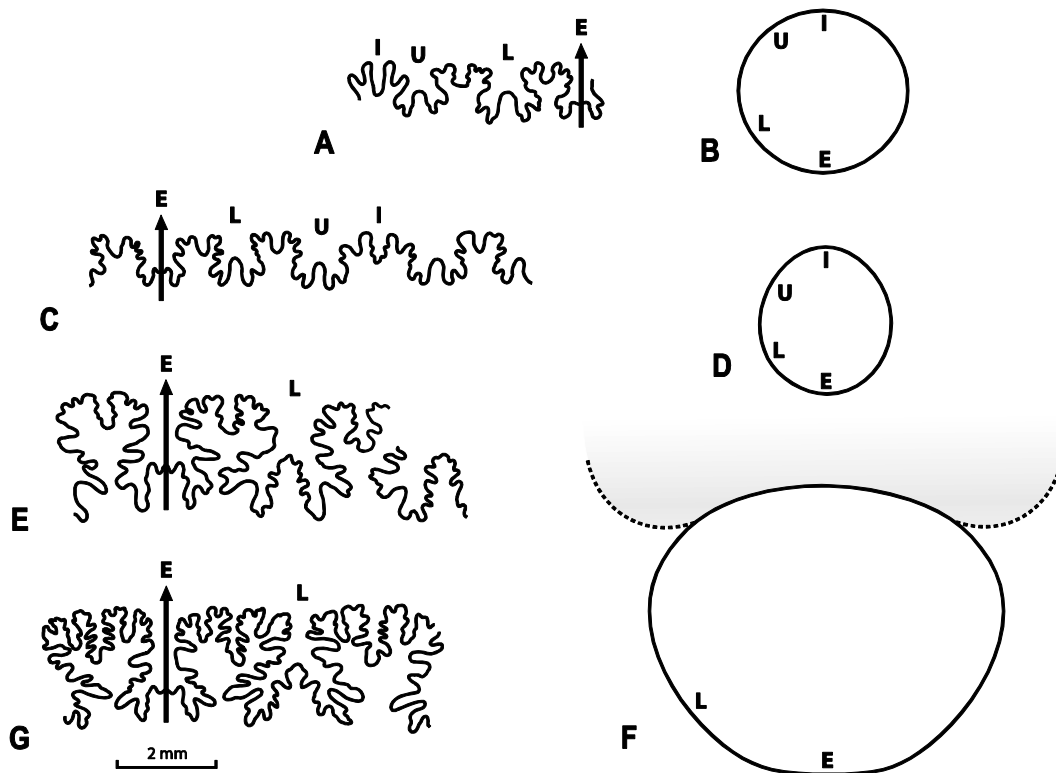


Figure 2.15. **A, B**, *Solenoceras* cf. *reesidei* Stephenson, 1941. **A**, suture line, RBCM.66, Wh = 3.4 mm; **B**, limb cross-section and lobe positioning, RBCM.66, Wh = 3.4 mm. **C–G**, *Solenoceras exornatus* sp. nov. **C**, suture line, paratype RBCM.54, Wh = 3 mm; **D**, limb cross-section and lobe positioning, paratype RBCM.54, Wh = 3 mm; **E**, partial suture line, paratype RBCM.59, Wh = 6 mm; **F**, limb cross-section and lobe positioning with grey area denoting body chamber, paratype RBCM.59, Wh = 6 mm; **G**, partial suture line, holotype RBCM.53, Wh = 6 mm.

Solenoceras cf. reesidei Stephenson, 1941

(Pl. 2.6Y; Fig. 2.15A, B)

Compare:

- 1941 *Solenoceras reesidei* Stephenson: 401, pl. 77, figs 1–3.
- 1969 *Solenoceras cf. S. reesidei* Stephenson; Lewy: 126, pl. 3, fig. 7a, b (*cum syn.*).
- 1993 *Solenoceras cf. reesidei* Stephenson; Giudici & Pallini: 320, pl. 2, figs 2, 3.
- 2000a *Solenoceras cf. S. reesidei* Stephenson; Kennedy *et al.*: 15.
- 2000 *Solenoceras reesidei* Stephenson; Kennedy & Lunn: 469, figs 4.16, 7.1–7.3, 7.5.
- 2001 *Solenoceras reesidei* Stephenson; KÜchler & Odin: 521, pl. 6, fig. 3.
- 2010 *Solenoceras reesidei* Stephenson; Ifrim *et al.*: 610, fig. 5ee, figs 10oo–tt (*cum syn.*).
- 2012 *Solenoceras reesidei* Stephenson; Larson: 13, pl. 4, figs 1–7, 13 (*cum syn.*).
- 2016 *Solenoceras reesidei* Stephenson; Larson: 32, figs 4a–g, m (*redux* Larson 2012, pl. 4, figs 1–7, 13).

Types. The holotype is USNM 77238 as designated from the upper Campanian Neylandville Marl of Texas along with four paratypes listed under the number USNM 77239 (Stephenson 1941, p. 401, pl. 77, figs 1–3) housed in the USNM.

Material. Three specimens consisting of two parallel limbs and two independent limb fragments.

Occurrence. *S. reesidei* is a well-established marker of the late Campanian with occurrences in the Pierre Shale of northern Colorado (Cobban *et al.* 1992; Kennedy *et al.* 2000a) and the Coon Creek Tongue of the Ripley Formation, Tennessee (e.g. Cobban & Kennedy 1994a; Larson 2016) as well as from the Neylandville Marl and the upper Campanian–lower Maastrichtian Nacatoch Sand of Texas (Stephenson 1941). Outside of North America, the species has been recorded from coeval strata in southwestern France (KÜchler & Odin 2001; Odin *et al.* 2001), the Mishash Formation of Israel (Lewy 1969), the Shinarish Formation of northwestern Iraq (Kennedy & Lunn 2000), and the Poggiardo Limestone of Italy (Giudici & Pallini 1993). Most recently, the species has been recovered from the upper Campanian–lower Maastrichtian of the Méndez Formation (Ifrim *et al.* 2004, 2017) and lower Maastrichtian Cañon del Tule Formation

(Ifrim *et al.* 2010) of Mexico. On Hornby Island, *S. cf. reesidei* is known from a single isolated concretion from the upper part of the upper Campanian Northumberland Formation exposed at Collishaw Point.

Description. The most complete specimen, RBCM.66, exhibits penultimate limb phragmocone which is subcircular in cross-section with no indication of dorsal compression (Fig. 2.15B). There are two constrictions present on the penultimate limb and none on the body chamber. Very little original shell is retained on the penultimate limb but a clear Ci of 6 from can be discerned from the internal mould plications. A Ci of 7 and a moderate degree of lateral compression characterizes the right flank—and only preserved portion—of the body chamber. Ventrolateral ornamentation cannot be observed due to shell absence. The suture line approaching maturity is marked by a broad lateral saddle and sparse, underdeveloped second-order incision elements (Fig. 2.15A). The highest Sc and Sg values were obtained from RBCM.66 at 9.55 and 2.11, respectively.

Remarks. The fragmented Hornby Island specimens cannot be assigned to *S. reesidei* with complete confidence due to low Ci and suture line inconsistencies. RBCM.66 (Pl. 2.6Y) differs from that of the type specimen (Stephenson 1941, pl. 77, figs 1–3) in having a slightly higher Ci of 7—compared to 6—on the body chamber. Penultimate limb fragments assigned to the species from Mexico exhibit Ci values of 7 (Ifrim *et al.* 2004, 2010) while descriptions of material from Tennessee (e.g. Cobban & Kennedy 1994a; Larson 2016) have emphasized a consistent Ci of 6 throughout development. It is also unclear if conspecific variability in suture line expression can account for the degree of bilateral saddle symmetry present in the Hornby Island material as compared to that illustrated from the US Western Interior (Cobban & Kennedy 1994a, fig. 2).

2.7.3 Family Nostoceratidae Hyatt, 1894

Age. Range: early Turonian–late Maastrichtian (e.g. Kennedy & Cobban 1993a; Wright *et al.* 1996).

Remarks. This family encompasses heteromorph ammonites which possess a helicoid form and irregular mode of coiling at some point beyond the juvenile stage (Hyatt 1894; Arkell *et al.* 1957; Wright *et al.* 1996). The family is also noted for the frequent occurrence of sexual dimorphism which has been described by numerous authors (e.g. Kennedy *et al.* 2000b; Küchler & Odin 2001; Larson 2016). Many forms bear constrictions and raised costal projections in the form of tubercles, spines, and megastria, along with a complex and often florid suture line in maturity (Arkell *et al.* 1957; Wright *et al.* 1996). Nearly all specimens belonging to the taxa represented within the Hornby Island assemblage possess ventrolateral tubercles or spines at some stage.

The subjectivity of character value assignment has been a challenge confronted time and time again in Linnaean taxonomic proceedings (e.g. Laurin 2010) as expressed by ammonite researchers in their examination of nostoceratid classification schemes (e.g. Anderson 1958). Following the earliest systematic approaches (Hyatt 1894; Arkell *et al.* 1957), the correct taxonomic assignment of nostoceratid material in the absence of complete specimens is difficult and designations must often be declared tentative (Anderson 1958; Jones 1963). For this reason, open nomenclature (Matthews 1973; Bengtson 1988) has frequently been utilized in the study of this family for the purpose of conveying uncertainty in taxonomic placement in order to ensure the integrity of the methods employed by previous workers.

Lewy (1969) recounted the taxonomic “chaos” which enveloped the early literature on the Nostoceratidae, and Klinger & Kennedy (2003b) subsequently summarized the history of attempts to classify the nostoceratids. Howarth (1965), for instance, considered *Didymoceras* Hyatt, 1894 and *Eubostrychoceras* Matsumoto, 1967 to be synonymous, whereas Klinger (1976) initially considered most ancyloconic forms as belonging to a loosely defined *Didymoceras* genus group. Many authors have since opted to relegate such taxa to subgenera within a broad *Nostoceras* genus (e.g. Wright *et al.* 1996; Küchler 2000; Niebuhr 2004) while others have chosen to retain these distinctions at the generic level (e.g. Klinger *et al.* 2007; Misaki & Maeda 2010). The subgeneric placement of *Didymoceras* within a broad *Nostoceras* genus as introduced by Wright *et al.* (1996) is herein considered to be fundamentally sound and is used in this study.

Genus *Nostoceras* Hyatt, 1894

Type species. *Nostoceras stantoni* Hyatt, 1894 subsequently designated a junior synonym of *Ancyloceras? approximans*, Conrad, 1855 (Kennedy & Cobban 1993b).

Age. Range: early Campanian–late Maastrichtian (e.g. Kennedy & Cobban 1993a; Cobban & Kennedy 1994b).

Remarks. The Hornby Island nostoceratid assemblage is comprised of ancyloconic forms corresponding to the *Nostoceras* subgenera *N. (Nostoceras)* and possibly *N. (Didymoceras)*. The former subgenus has been distinguished from the latter chiefly by the predominance of contiguous helical whorls with discontinuity only at the earliest juvenile stage (Kennedy *et al.* 2000a). *N. (Didymoceras)* exhibits considerable irregularity in pre-helical juvenile coiling, often characterized by ellipsoidal or hamitonic limbs (e.g. Kennedy *et al.* 2000c). Seemingly intergrading forms (Jones 1963; Zaborski 1985) suggest that these nostoceratids are most likely subgenera within a variable plexus (Wright *et al.* 1996). With mode of coiling as a fundamental character, the degree of whorl separation should remain a principle diagnostic component of subgeneric differentiation with *N. (Nostoceras)* being distinguished from *N. (Didymoceras)* chiefly by the predominance of phragmacone contiguity. The acquisition of more complete material may reveal that *N. (Nostoceras)* forms share the common character of a small initial shaft in approximate alignment with the axis of subsequent helical coiling, as has been shown in *N. (N.) hornbyense* (Whiteaves, 1895).

The identification of similarities in early shell structure is crucial as they offer an ontogenetic baseline for consistency in the observation of diagnostic traits (Wiedmann 1969). In many cases, a lack of juvenile material combined with conspecific dimorphism and polymorphism has led to considerable variance in interpretation with all factors compounded by a rapid rate of evolutionary modification into the late Campanian (Klinger & Kennedy 2003b). Although some uncertainty remains surrounding the hierarchy of early coiling morphology as it relates to subgeneric differentiation (Klinger & Kennedy 2003b), the helical whorls of *Nostoceras* present a distinct series of qualitative and quantitative traits, the expression of which constitute a basis for specific differentiation (Table 2.2; Appendix III). As argued herein, body chambers of *Nostoceras* are inherently undiagnostic and can only be referred to a species with

confidence if specimens in association with helical whorls have been recovered from the same locality and horizon, in which case a positive association can be inferred.

Table 2.2. Qualitative and quantitative characters applicable to the description of helical whorls belonging to species within the genus *Nostoceras* Hyatt, 1894.

Qualitative Characters	
Whorl contiguity (if present)	<i>low</i> = whorls slightly touching or with trailing flank costal depression; <i>moderate</i> = trailing flank flattened or with slightly concave zone of impression; <i>high</i> = whorls tightly impressed with deep trailing flank furrow
Whorl cross-section	expressed as a combined function of Wb/Wh and overall shape
Costal expression	presence or absence of bifurcation, recombination or intercalation
Projected ornamentation	presence, degree of projection (spinosity) and orientation
Quantitative Characters	
Apical angle	<i>low</i> = $Ap < 45^\circ$; <i>moderate</i> = $45^\circ \leq Ap < 90^\circ$; <i>high</i> = $Ap \geq 90^\circ$
Total volutions	total count of 360° whorl rotations
Constrictions per volution	if present, total count over 360° whorl rotation
Umbilical breadth	expressed as a function of U/Cd
Costae per volution	counted along the trailing ventral margin; can be extrapolated from whorl curvature or expressed as per volution fraction

Some authors (e.g. Jones 1963; Zaborski 1985; Klinger & Kennedy 2003b) have suggested that *N. (Didymoceras)* be characterized by a tendency toward greater overall conch dimensions and complex costal ornamentation with higher occurrences of bifurcation and intercalation on the retroversal body chamber. However, the diagnostic application and prevalence of these structural traits should be constrained to the specific level due to the wide variation in these features. Previous authors have described species with emphasis on Ci values and ornamentation (e.g. Kennedy *et al.* 2000d), despite a wide range of variation within populations (e.g. Kennedy & Cobban 1993b). Hornby Island nostoceratid material demonstrates that the arrangement of costal ornamentation and spinosity varies considerably even within individual specimens.

Like all Late Cretaceous heteromorphs, members of the genus *Nostoceras* bear quadrilobate septal walls following the nepionic constriction (Wiedmann & Kakabadzé 1993). However, sutural asymmetry during the torticonic stage is reflected by a more deeply incised lateral lobe on the flank distal to the apex (Ward 1976a, 1979). As demonstrated in this study, this feature holds true in the case of *N. (N.) hornbyense*, with deeper lobe incisions being characteristic of helical whorls of higher Ap values. Whereas the suture lines of *N. (Nostoceras)* appear to have a tendency to exhibit broader saddle stems than those of *N. (Didymoceras)*, variability in *N. (N.) hornbyense* reveals that specific taxonomic distinctions among these ancylocones cannot be based solely on the presentation of sutural elements. Therefore, a lack of consistency precludes the application of quantifiable measurement schemes previously explored (e.g. Ward *et al.* 2015). Many authors (e.g. Makowski 1962) have contended that the septal elements of Mesozoic ammonites are questionable taxonomic indicators and among members of this genus, this caution is well grounded.

Subgenus *Nostoceras (Didymoceras)* Hyatt, 1894

Type species. *Ancyloceras? nebrascense* Meek & Hayden, 1856 by subsequent designation (Hyatt 1894).

Age. Range: middle to late Campanian (e.g. Cobban & Kennedy 1994b; Kennedy *et al.* 1999; Larson 2016).

Nostoceras (Didymoceras?) adrotans sp. nov.

(Pls 2.7A–J, 2.8A–K; Fig. 2.16)

v.1903 *Anisoceras cooperi* Whiteaves: 338.

(?)2009 *Nostoceras hornbyense* (Whiteaves); Haggart *et al.*: 944, figs 5C, D.

Types. The type series consists of the holotype RBCM.EH2016.009.0014.001 (RBCM.67), paratypes RBCM.68–75, and paratype CDM No. 2008.1.102 HUN from the lower part of the Northumberland Formation, Hornby Island, housed in the RBCM and CDM.

Diagnosis. An ancyloconic heteromorph ammonite with a helical phragmacone unravelled to such an extent as to form a major portion of the penultimate limb. The penultimate limb may be marked by occasional irregularity in whorl progression in the form of gradual or abrupt directional readjustment. Mature limbs circular to subcircular in cross-section. The penultimate limb costal index far exceeds that of the retroversal body chamber with comparative averages of 10 and 6, respectively. Intercalated and bifurcated costae may occur at any point and are most common in approach to the retroversal body chamber. The conch may exhibit two rows of ventrolateral spines or tubercles, one row of ventral spines or no spinous ornamentation on the body chamber.

Etymology. Latin, *adrotans*, turning, wavering.

Material. Thirty-four specimens—22 from which measurements could be obtained. The material ranges from fragmentary portions of phragmacone and body chamber to penultimate limbs and elbows of varying degrees of completion.

Occurrence. Apart from two possible occurrences in the upper Campanian Tarundl Formation of Haida Gwaii (Haggart *et al.* 2009, figs. 5C, D), *N. (D.?) adrotans* is known only from the lower part of the upper Campanian Northumberland Formation exposed along the south-eastern shore of Hornby Island.

Description. Phragmacone sections are discontinuous having no indication of a contact furrow or marginal costal depression and are circular to subcircular in cross-section. The earliest stages are unknown. The holotype RBCM.67 (Pl. 2.7A) and paratype CDM No. 2008.1.102 HUN (Pl. 2.7F–H) appear to indicate that the whorls conformed to a helical axis often marked by abrupt phases of reorientation prior to the development of the retroversal body chamber. Polymorphism is evident although there is no indication of sexual dimorphism; this may be the result of a small sample size. The dimensions of the holotype reflect those typical of the population, with an elbow axis Wh of 25 mm.

The most distinguishing characteristic is the tendency of the final whorls of phragmacone to abandon their adherence to an open helical axis, effectively unraveling to form the elongated penultimate limb of the mature shell. In extreme instances such as CDM No. 2008.1.102 HUN, nearly half of the phragmacone appears to have comprised the penultimate limb. In the cases of RBCM.67 and CDM No. 2008.1.102 HUN, phragmacone development is punctuated by directional readjustments in whorl progression within sinistral and dextral modes of coiling, respectively (Pl. 2.7A, F–H). In these examples, costal obliquity indicates points of helical torsion around an axis situated within the penultimate limb itself. In all specimens, the body chamber is subquadrate in cross-section and usually begins just prior to the curve of the elbow, occasionally at the site of a subtle plication; it is at or near this point that the dorsum begins to flatten.

Costae are densely crowded and vary in direction along the penultimate limb becoming prorsiradiate before the elbow and rectiradiate at the retroversal elbow axis. Of seven specimens, the average penultimate limb C_i is 11. Costal bifurcations and intercalations are common on or approaching the elbow before diminishing and disappearing on the straightening body chamber. Near the aperture, costae are broadly spaced, flexuous, sharper, and of higher relief in relation to those of the penultimate limb. Transverse costae are weakly sigmoidal beginning on the dorsum and becoming prorsiradiate or rectiradiate on the dorsolateral margin before abruptly transitioning to rursiradiate on the flank in continuation toward the ventrolateral margin. Of nine specimens, the average body chamber C_i is 6 with three to five fine lirae present in the furrows between each costa.

Spinous ornamentation is generally subdued with underdeveloped spines manifesting as small nodes or tubercles. These projections arise from transverse or intercalated costae, most commonly along the ventrolateral margins of the penultimate limb, occurring in two parallel or alternating rows in approach to the body chamber. Each tubercle is linked by two looped costae across the venter and tuberculate costae are separated by one or two costae on or approaching the elbow. Tubercles continuing around the retroversal elbow and onto the body chamber may extend into spines in approach to the aperture. If present, spines on the body chamber may occur in two ventrolateral rows or in a single ventral row. The mature suture line is complex and highly florid with narrow-stemmed saddles and third-order incision elements (Fig. 2.16).

Remarks. The absence of juvenile material lends credence to the notion that the early helical whorls of *N. (D.?) adrotans* were not in contact. Separated whorls would make for an inherently more delicate conch with greater susceptibility to post mortem breakage and dislocation (Klinger & Kennedy 2003b). It is considered likely that the early whorls were reduced, in keeping with the conservative ornamentation and dimensions of the terminal phragmacone. The major portion of a penultimate limb in *N. (D.?) adrotans* is best interpreted as a straightened coil equivalent to at least one unraveled volution on the basis of high phragmacone volume and marked whorl expansion. These indicators, coupled with a highly intricate suture line marked by narrow-stemmed saddles similar to that of *N. (Didymoceras)* forms from the US Western Interior (e.g. Kennedy *et al.* 2000b, figs 3, 5, 2000c, figs 4, 17, 31), sees the tentative placement of this species within the subgenus.

The penultimate limbs of *N. (D.?) adrotans* also resemble those of *Nostoceras (Nostoceras) approximans* (Conrad, 1855). Nostoceratid forms previously assigned to *N. (N.) approximans* are compact conches characterized by fine, dense ribbing and subdued ornamentation (Kennedy 1993). However, the penultimate limb of the species differs from *N. (D.?) adrotans* in that it is much less elongated, with the body chamber typically occupying a major portion of the penultimate limb. The suture line of *N. (N.) approximans* is also less complex with broad-stemmed saddles. The mature stage of *N. (D.?) adrotans* also bears a superficial similarity to that of *Nostoceras (Didymoceras?) kernense* (Anderson, 1958), although the penultimate limb C_i of the former species is generally twice that of its body chamber where intercalated costae are absent. These two species are likely close phylogenetic allies with Baja California specimens possibly corresponding to *N. (D.?) kernense* (e.g. Ward *et al.* 2012, fig. 11E).

The closed helical coils and retroversal body chambers of the nostoceratids *N. (N.) hornbyense* and *Nostoceras (Nostoceras) aff. pauper* (Whitfield, 1892) are ubiquitous in the upper part of the Northumberland Formation exposed along the western shore of Hornby Island. However, these species are absent from the fossil record of the island's southeastern shore. This absence of material is an indication that these stratigraphically younger species were unlikely to have coexisted with the smaller, poorly ornamented *N. (D.?) adrotans* in the basal depositional interval of the Northumberland Formation.

Material corresponding to *N. (D.?) adrotans* is known from previous works, with specimen GSC No. 5955 as the primary example. This specimen, described but never figured (Whiteaves, 1903, p. 338), was assigned to the *nomen dubium* *Anisoceras cooperi* (Gabb, 1864) and the exact locality from which it was recovered on Hornby Island has never been established. Two specimens lacking helical whorl material assigned to *N. (N.) hornbyense* from Haida Gwaii (Haggart *et al.* 2009) bear higher Ci values on their penultimate limbs than on their retroversal body chambers; while the specimens are poorly preserved, this is a characteristic of *N. (D.?) adrotans* not shared by *N. (N.) hornbyense*.

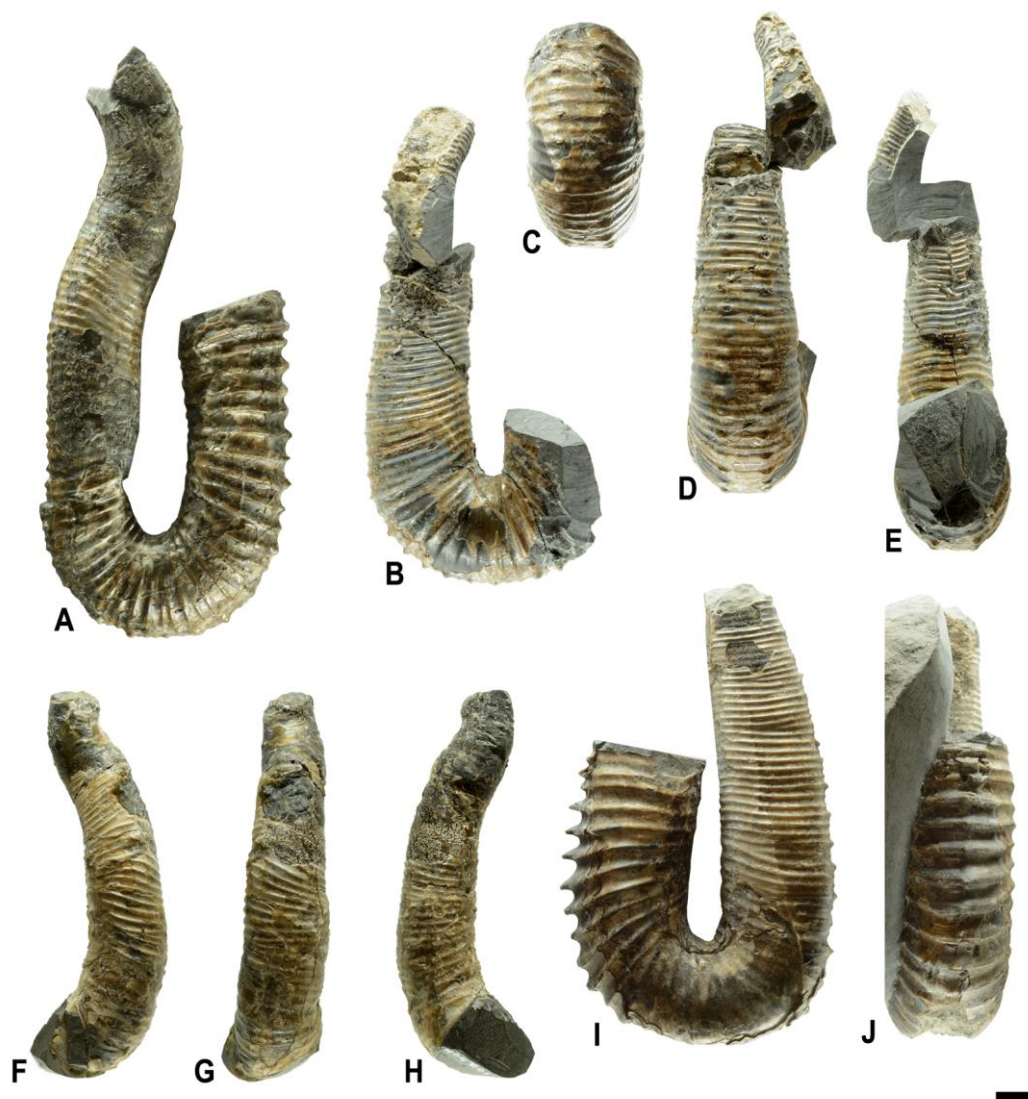


Plate 2.7. A–J, *Nostoceras (Didymoceras?) adrotans* sp. nov. A, torsional penultimate limb and body chamber, right F, holotype RBCM.67; B–E, penultimate limb and partial body chamber with two parallel

rows of spines, right F, two V sides and D, paratype RBCM.68; **F–H**, penultimate limb, torsional left F, V and right F, paratype CDM No. 2008.1.102 HUN; **I, J**, penultimate limb and body chamber with single row of spines, left F and V, paratype RBCM.69. Scale bar = 1 cm.

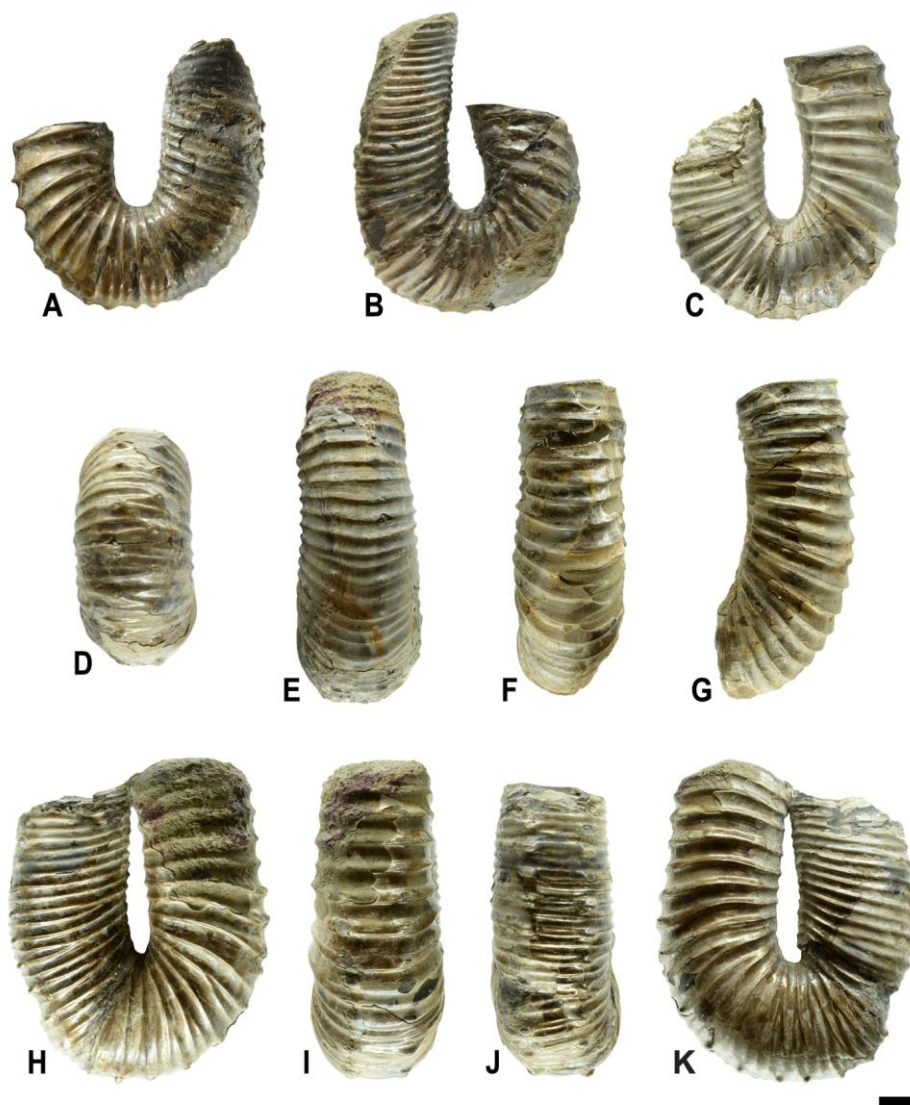


Plate 2.8. **A–K**, *Nostoceras (Didymoceras?) adrotans* sp. nov. **A**, penultimate limb and partial body chamber, left F, paratype RBCM.70; **B**, penultimate limb and partial body chamber, right F, paratype RBCM.71; **C, D**, penultimate limb and partial body chamber with two rows of alternating spines, right F and V, paratype RBCM.72; **E**, body chamber with two parallel rows of nodes, V, paratype RBCM.73; **F, G**, body chamber with no spinous protuberances, V and right F, paratype RBCM.74; **H–K**, penultimate limb and body chamber, right F, two V sides and left F, paratype RBCM.75. Scale bar = 1 cm.

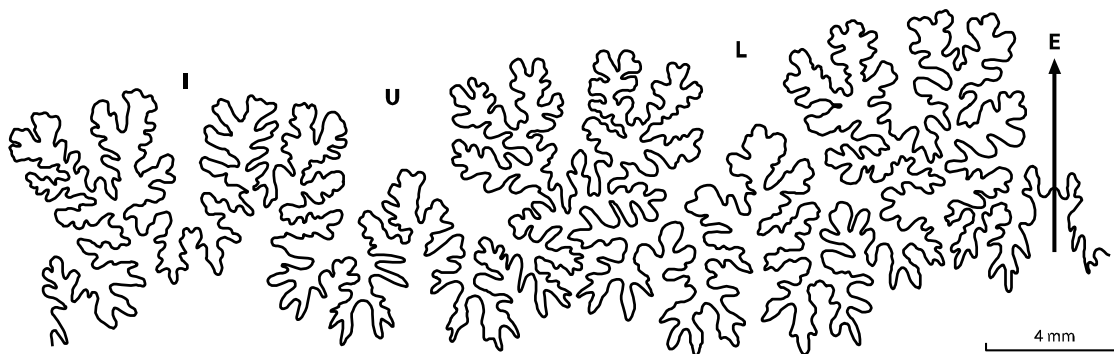


Figure 2.16. Suture line of *Nostoceras* (*Didymoceras*?) *adrotans* sp. nov., paratype CDM No. 2008.1.102 HUN, Wh = 18 mm.

Subgenus *Nostoceras* (*Nostoceras*) Hyatt, 1894

Type species. *Nostoceras stantoni* Hyatt, 1894, subsequently designated a junior synonym of *Ancyloceras? approximans* Conrad, 1855 (Kennedy & Cobban 1993c).

Age. Range: late Campanian–late Maastrichtian (e.g. Kennedy & Cobban 1993a; Kennedy *et al.* 2000d).

Nostoceras (*Nostoceras*) *hornbyense* (Whiteaves, 1895)

(Pls 2.9A–K, 2.10A–H, 2.11A–G, Figs 2.17A–C, 2.18A, 2.19)

- v*1895 *Heteroceras hornbyense* Whiteaves: 316.
- v*1903 *Heteroceras hornbyense* Whiteaves: 332, pl. 42, figs 1–4.
- v.1952 *Nostoceras hornbyense* (Whiteaves); Usher: 103, pl. 27, figs 1, 2, pl. 28, fig. 2, pl. 31, fig. 23 (*cum syn.*).
- v.1952 *Anisoceras cooperi* (Gabb); Usher: 107, pl. 29, fig. 1 (*cum syn.*).
- ?1954 *Didymoceras hornbyense* (Whiteaves); Reyment: 21.
- (?)1958 *Exiteloceras desertense* Anderson: 202, pl. 66, fig. 2a.
- (?)1958 *Exiteloceras bennisoni* Anderson: 201, pl. 72, fig. 7.
- 1958 *Nostoceras mexicanum* Anderson: 196, pl. 58, fig. 3.
- 1958 *Didymoceras californicum* Anderson: 197, pl. 72, fig. 6.

- 1963 *Didymoceras* aff. *D. hornbyense* (Whiteaves); Jones: 30, pl. 23, fig. 1 (*cum syn.*).
- 1965 *Didymoceras* cf. *hornbyense* (Whiteaves); Howarth: 377, pl. 8, figs 4a–c (*cum syn.*).
- 1965 *Nostoceras helicinum* (Shumard); Howarth: 383, pl. 8, figs 3, 5.
- (?)1965 *Nostoceras hyatti* (Stephenson); Howarth: 378, pl. 9, figs 2a, b.
- v.1970 *Nostoceras hornbyense* (Whiteaves); Jeletzky: pl. 28, fig. 6 (*redux* Usher 1952, pl. 28, fig. 2).
- (?)1985 *Didymoceras* aff. *hornbyense* (Whiteaves); Zaborski: 14, fig. 14a, b.
- v.1991 *Didymoceras hornbyense* (Whiteaves); Haggart: pl. 5, fig. 2 (*redux* Usher 1952, pl. 27, fig. 1).
- ?1994a *Didymoceras hornbyense* (Whiteaves); Cobban & Kennedy: B5, pl. 6, figs 1–3 (*cum syn.*).
- v.1994 *Nostoceras hornbyense* (Whiteaves); Ludvigsen & Beard: 110, fig. 80.
- v.1996 *Didymoceras hornbyense* (Whiteaves); Haggart: 174, fig. 14.4A (*redux* Usher 1952, pl. 28, fig. 2).
- v.1998 *Nostoceras hornbyense* (Whiteaves); Ludvigsen & Beard: 129, fig. 91 (*redux* Ludvigsen & Beard 1994, fig. 80).
- (?)2000 *Nostoceras (Nostoceras) hyatti* Stephenson; K uchler: 480, pl. 17, fig. 5.
- (?)2001 *Nostoceras (Nostoceras) hyatti* Stephenson; K uchler & Odin: 516, pl. 4, figs 11, 13.
- v.2003 *Nostoceras hornbyense* (Whiteaves); Mustard *et al.*: 109, fig. 7C, D (*redux* Usher 1952, pl. 27, figs 1, 2).
- (?)2012 *Didymoceras nebrascense* (Meek & Hayden); Ward *et al.*: figs 11G, H.
- (?)2012 *Nostoceras draconis* (Stephenson); Ward *et al.*: figs 11A–C.

Types. The lectotype is specimen GSC No. 5805, as designated, from the upper part of the upper Campanian Northumberland Formation exposed along the northwestern shore of Hornby Island (Usher 1952, p.104), in association with paratypes GSC Nos. 5805a, 5805b, 5805c, and 5827 of the original series (Whiteaves 1903) housed in the GSC national type collection.

Emended diagnosis. An ancyloconic heteromorph ammonite possessing a nearly straight shaft in approximate alignment with the axis of 6 to 7 sinistrally or dextrally coiled helical volutions of low to moderate contiguity. The apical angle ranges from 62–94° with 3–5 constrictions per

volution. The number of costae per volution ranges from 12–22 (45–85 a). The umbilical width-to-helical volution diameter averages 0.28. Inner whorl flanks are marked by depressed, flattened costae resulting from preceding whorl impression. Intercalated costae are common on the helical whorls and in later stages of maturity, on or approaching the penultimate limb. Mature limbs subcircular to squadrate in cross-section. Bifurcation of costae and recombination at the base of a tubercle or spine may occur throughout. Ornamentation marked by one or two rows of ventrolateral tubercles or spines occurring on alternating costae linked across the venter by one or two transverse costae or with a single spine borne on each costa in alternating fashion. The retroversal body chamber costal index ranges from 5–10 with sharp costae becoming blade-like and rursiradiate in approach to terminal apertural lirae.

Material. Three hundred sixty-nine specimens—207 from which measurements could be obtained. The material consists of independent helical whorls, retroversal limbs, body chambers, and 87 specimens either largely intact or with helical whorl and mature body chamber material in association.

Occurrence. *N. (N.) hornbyense* is recognized along the Pacific coast of North America from the upper Campanian of the Kaguyak and Matanuska formations of southern Alaska (Jones 1963), the Northumberland Formation on Hornby Island (Whiteaves 1895, 1903; Usher 1952), and the Rosario Formation of Baja California (Anderson 1958; Matsumoto 1959b). The species has also been described from the upper Campanian strata of Angola (e.g. Spath 1921; Howarth 1965) and Nigeria (Zaborski 1985). On Hornby Island, the species is restricted to exposures of the Northumberland Formation along the western shore from Shingle Spit north to Collishaw Point.

Description. The initial stage consists of a nearly straight shaft at least 14 mm in length in approximate alignment with the axis of subsequent helical coiling (Pl. 28A). The complete helical stage consists of 6 to 7 sinistral or dextral whorl volutions which are subcircular in cross-section of low to moderate contiguity (Fig. 2.18A). Of the 269 specimens for which coiling direction could be ascertained, 53.2 percent are sinistral and 46.8 percent are dextral. Whorls meet their subsequent volutions along the margin of the inner flank of the outer volution, marked by depressed costae resulting from preceding whorl impression (Fig. 2.18A). Of 36 specimens,

Ap values range from 62–94° averaging 77.8°. A ~ 1:1 ratio of septal wall separation to whorl breadth is constant throughout the helical stage. Of 48 specimens, the U/Cd ranges from 0.21–0.38, averaging 0.29. Occasional U/Cd ratio decreases and Ap value increases may occur but these are slight. Constrictions are present on the helical whorls, ranging from 3–5 per volution appearing shallower and more diminished on specimens with Cv values in excess of 17.

Transverse costae on the helical whorls are raised and sharp. All costae are prorsiradiate throughout the helical stage being weakly flexuous and deflected obliquely downward in the direction of coiling. Of 97 specimens, Cv values range from 12–22 (45–85 a), with an average of 15 (57 a). At all stages, costae are diminished on the dorsum. Costae become gradually more pronounced on the dorsolateral margin until fully raised along the flanks. Intercalated costae are common on the helical whorls and occur most frequently in later stages of maturity on or approaching the penultimate limb. The retroversal body chamber Ci ranges from 5–10, with costae becoming blade-like and folded such that they are posteriorly concave in approach to fine, terminal lirae which define the aperture (Pl. 2.9C).

Two rows of ventrolateral tubercles or spines of approximately the same size occur on the early coils, becoming proportionately longer with the maturity of the shell. These projections typically occur in two parallel rows of equal distance apart—or somewhat offset—from the venter on the outer helical whorl face. Two tubercles or spines typically occur on alternating costae linked across the venter by one or two transverse costae or with a single spine borne on each costa in alternating fashion. When present, alternating spines occur most commonly during the phase of transition from the last helical whorl to the penultimate limb. A single row of tubercles or spines may occur along the ventrolateral margin distal to the apex of the helical whorls. Such diminished ornamentation is rare and associated with increased costal densities where Cv values exceed 17. Bifurcation of costae and recombination at the base of a tubercle or spine may occur throughout.

Dimorphism is discernible and is attributed to gender differences within a broad range of polymorphism (Fig. 2.19). Microconch morphotypes are distinguished from their macroconch counterparts by their predominantly smaller size, subquadrate body chamber cross-section, and aperture located closer to the flank of the penultimate limb. Microconch Ci values average 5 and 6 on the penultimate limb and retroversal body chamber, respectively. Among microconchs, the ventrolateral apertural margins extend proportionately further than the dorsolateral margins in

comparison to those of macroconchs, being somewhat analogous to subdued lateral lappets (Pl. 2.9C). The fine lirae which define the aperture also tend to present greater sinuosity or arcuacy in the microconchs. The macroconch morphotype is characterized by a more inflated shell that is subcircular in cross-section with higher penultimate limb and retroversal body chamber C_i values averaging 7 and 8, respectively. In mature specimens, the body chamber comprises nearly the entire U-shaped portion of the conch suspended directly beneath the helical whorls. The phragmacone typically terminates early in the penultimate limb opposite to the aperture.

Of 18 specimens, H values range from 9° – 40° , illustrating variability in the orientation of the body chamber in relation to the helical whorls. The ratio between the F_1 – F_2 and D_3 – V_3 measurement transversals reveals subtle, dimorphic differences in growth following sexual maturity. Microconchs experience a marginally higher increase in shell diameter between the helical coiling and retroversal body chamber axes, averaging 11.6 percent in relation to macroconchs, which average 8.6 percent. Macroconch retroversal body chambers reached whorl heights in excess of 60 mm, often attaining a shell thickness of over 2.8 mm, nearly three times that of the average microconch. The suture line is complex, florid, and of variable geometry bearing third-order incision elements. Lobes and saddles are more elongate on the helical whorls before transitioning to the penultimate limb, where they become more quadrate following the release of whorl torsion (Fig. 2.17A–C).

Remarks. Contrary to subsequent description (Jones 1963) which has since been maintained (Shigeta *et al.* 2016), the whorls of *N. (N.) hornbyense* remain in contact throughout the helical stage. The whorls possess a region of costal depression on the trailing flank proximal to the apex of helical coiling. This depression can be subtle in some specimens or more pronounced in others but clearly denotes whorl contiguity. Also, indentations are common on the trailing flank where the growth of a subsequent volution accommodated the spines of the preceding whorl. Therefore, the absence of a pronounced furrow in a given specimen is an insufficient basis upon which to conclude that the whorls are not in contact when costal depression is evident. The presence of complete specimens aside (e.g. Case 1982, fig. 12-50), evidence that the volutions of *N. (N.) hornbyense* rested against one another is clear when their gradual angle of coiling and relative rate of expansion are considered. Close examination also reveals that open coiling previously

observed (Usher 1952, pl. 27, figs 1, 2, pl. 28, fig. 2) was the result of post mortem whorl dislocation.

Initially, the sinistral form of *N. (N.) hornbyense* was surmised to represent a separate species deemed *Heteroceras perversum* Whiteaves, 1895. This view was quickly abandoned in light of additional material demonstrating coiling in either direction (Whiteaves 1903). Although preference for the distinction did resurface (Anderson 1958), it was subsequently disregarded (Jones 1963). The ~ 1:1 ratio of coiling directionality in *N. (N.) hornbyense* is consistent with that observed in other members of the Nostoceratidae (e.g. Ward 1979; Okamoto 1989; Kennedy *et al.* 2000a). Even among the ancestral Turrilitidae Gill, 1871, conspecific dextrality and sinistrality in coiling is common. For example, a study of *Mariella worthensis* (Adkins & Winton, 1920) of the upper Albian Pawpaw Shale of Texas revealed an evenly divided population from one locality, in contrast with a population from another comprised of nearly all sinistral forms from which coil direction was inferred to be a trait determined by a single mutation (Clark 1965).

The assignment of gender morphotypes within the examined population sample of *N. (N.) hornbyense* is compatible with the criteria for establishing sexual dimorphism proposed by Makowski (1962) and expounded upon by subsequent authors (e.g. Callomon 1963; Davis 1972). Consistency in the degree of apertural projection, retroversal body chamber inflation and shell robustness reinforce an otherwise ambiguous mode of gender differentiation based on overall conch size. Such a size parameter alone fails to differentiate the antidimorphs between ~ 30–32 mm Wh at the V₃–D₃ transversal (Fig. 2.19). In *N. (N.) hornbyense*, the aforementioned gender-specific structural characteristics proposed herein are maintained across a spectrum of mature specimens, attributable to the expression of phenotypic plasticity within a continuum of polymorphic gender variance as explored by Matyja (1986).

Nostoceras mexicanum Anderson, 1958 from Baja California is herein considered a junior synonym of *N. (N.) hornbyense* with the holotype, specimen CAS No. 61815.01, corresponding to the morphology of a small macroconch (Anderson 1958, pl. 58, fig. 3). Body chamber specimens from California (Ward *et al.* 2012) figured as *Nostoceras nebrascense* (Meek & Hayden, 1856) are also consistent with the *N. mexicanum* holotype and by implication are potentially assignable to *N. (N.) hornbyense* should helical whorl material be recovered. Isolated body chambers attributed to *Nostoceras (Nostoceras) draconis* Stephenson, 1941 as of

late (Ward *et al.* 2012) could also just as easily conform to the *N. (N.) hornbyense* microconch. Numerous other North Pacific taxa described from fragments such as *Exiteloceras desertense* Anderson, 1958 and *Exiteloceras bennisoni* Anderson, 1958, are also likely assignable to the *N. (N.) hornbyense* macroconch morphotype.

Retroversal body chamber specimen C.83144, among the material described from Nigeria (Zaborski 1985, figs 14a, b), bears a striking similarity to *N. (N.) hornbyense* while other figured specimens (Zaborski 1985, figs 12, 13) are likely referable to another species with whorls resembling those of *Nostoceras (Nostoceras) splendidus* (Shumard, 1861). The remaining Nigerian specimens lack adequate description (Reyment 1954) and that subsequently figured (Reyment 1955, pl. 1, fig. 3) as *Nostoceras (Didymoceras) hornbyense* (Whiteaves, 1895) is likely synonymous with *Nostoceras (Nostoceras) magdadiae* Lefeld & Uberna, 1991, a species described from Libya and Mississippi (Cobban & Kennedy 1995) characterized by subquadrate whorls, coarse ornamentation, and a flattened venter. Other whorl fragments initially described as *Nostoceras (Didymoceras) hornbyense* (Whiteaves, 1895) from the Tennessee Valley (Cobban & Kennedy 1994a) were later reassigned to *N. (Didymoceras) cf. aurarium* Kennedy *et al.* 2000a following the acquisition of discontinuous specimens (Larson 2016).

Contemporaneous *N. (Nostoceras)* species from the North Pacific region bear numerous morphological similarities. *N. (Nostoceras) awajiense* (Yabe, 1901) from the Seidan Formation of Japan appears closely allied with *N. (N.) hornbyense*, from which it differs in possessing irregular helical whorl constrictions, a non-linear translation rate, a C-shaped body chamber with a pre-apertural constriction, and a proportionately larger phragmocone (Morozumi 1985). Although the Japanese species was originally assigned to *N. (Didymoceras)*, there is little uncertainty as to the contiguity and orientation of its earliest helical whorls (Morozumi 1985, pl. 10, figs 1–4). *N. (Nostoceras) hetonaiense* Matsumoto, 1977, another Japanese form with a body chamber corresponding to the *N. (N.) hornbyense* macroconch morphotype, lacks constrictions on the helical whorls altogether. Both *N. (N.) awajiense* and the stratigraphically younger *N. (N.) hetonaiense* exhibit some of the highest costal densities of any species in the subgenus.

Small microconchs of *N. (N.) hornbyense* such as RBCM.78 and RBCM.79 may resemble those of several index species characteristic of the late Campanian global *Nostoceras (Nostoceras) hyatti* Assemblage Zone, including *N. (N.) hyatti* Stephenson, 1941, *N. (N.) approximans*, and *Nostoceras (Nostoceras) helicinum* (Shumard, 1861). In general, the

retroversal body chamber of *N. (N.) hornbyense* is more elongated than those of the smaller index species, but this is not always the case. Typically, *N. (N.) hyatti* is characterized by coarse, uniform, broadly-spaced transverse costae which produce deeply incised plications on the internal mould of an equal Ci on both the penultimate limb and retroversal body chamber (e.g. Howarth 1965, pl. 9, figs 1, 2; Cobban 1974b, pl. 6, figs 1–12). *N. (N.) approximans* occupies the other end of the costal spectrum with body chambers exhibiting fine, dense ribbing throughout. It is notable that lateral apertural crests have also been observed in *N. (N.) approximans* (Hyatt 1894), features herein considered indicative of microconch morphology in *N. (N.) hornbyense*.

The interspecific overlap of mature body chamber morphology among *N. (N.) hornbyense* and the aforementioned species underscores the crucial importance of helical whorl traits in taxonomic diagnosis. In general, the volutions of *N. (N.) hyatti*, *N. (N.) approximans*, and *N. (N.) helicinum* number 4 to 5 for the former two species and 4 for the latter, with each bearing 3–5, 2–4, and 4 constrictions per volution, respectively (Kennedy & Cobban 1993c; Larson 2016). The helical stage of *N. (N.) hornbyense* exhibits 6 to 7 volutions with each bearing 3–5 constrictions, in contrast to those of members of the *hyatti* Assemblage Zone. The helical whorls of the *N. (N.) hyatti* holotype (Stephenson 1941, pl. 81, fig. 9) also stand apart from those typical of *N. (N.) hornbyense* in being dominated by transverse costae with markedly less obliquity across the venter. Comparison to *N. (N.) hyatti* material from the Atlantic Highlands (Cobban 1974b; Kennedy *et al.* 2000d) indicates a U/Cd ratio which exceeds that of the *N. (N.) hornbyense* population sample. Specimens of *N. (N.) hyatti* collected from the Tennessee Valley (Cobban & Kennedy 1994a; Larson 2016) also possess a translation rate which is markedly non-linear, transitioning from a lower to higher Ap value with development, in contrast to the typical uniformity of whorl progression in *N. (N.) hornbyense*.

Considering the lectotype of *N. (N.) approximans* (Stephenson 1941, pl. 80 figs 3–5), designated from the original suite (Kennedy & Cobban 1993c), the species possesses a high degree of whorl contiguity such that the ventrolateral margins of each volution are strongly impressed against one another, resulting in a smooth, conical appearance to the spire, in contrast to the broadly rounded flanks and often subtle whorl impression of *N. (N.) hornbyense*. The helical whorls of the *N. (N.) approximans* lectotype bear denser, simpler ribbing with infrequent intercalated costae as compared to *N. (N.) hornbyense*. Costal bifurcation and flexuosity along the venter is also much more prevalent on the helical whorls of *N. (N.) hornbyense*, in contrast to

those of *N. (N.) approximans*. CDM No. 2008.1.82 HUN (Pl. 2.8E–G) is one such example which links *N. (N.) hornbyense* helical whorls with a body chamber comparable to *N. (N.) approximans* through conventional interpretation.

The close association between the nostoceratids of the *hyatti* Assemblage Zone and *N. (N.) hornbyense* has been approached by previous authors in acknowledgment of their morphological affinity and stratigraphic co-occurrence (e.g. Howarth 1965). It has been suggested that size alone is essentially the only differentiating trait between *N. (N.) hornbyense* and *N. (N.) helicinum* (Usher 1952), while comparison of the former with the *N. (N.) helicinum* neotype (Stephenson 1941, pl. 80, figs 11–12) even lead to the suggestion of conspecificity (Haas 1943). These early interpretations did not take into account the fundamental differences in total helical whorl volutions and constriction frequency, although the observations of a markedly narrow whorl diameter in *N. (N.) helicinum* seem to provide differentiation enough (Kennedy & Cobban 1993c; Larson 2016). With its low apical angle and prevalence of bifurcating, intercalating, and zig-zagging costae, *N. (N.) helicinum* is undoubtedly one of the closest allied species to *N. (N.) hornbyense*.

Nostoceratid body chambers described from northern Spain (Küchler 2000, pl. 17, fig. 5) and southwestern France (Küchler & Odin 2001, pl. 4, figs 11, 13) approach the range of variation proposed herein for microconchs of *N. (N.) hornbyense* but lack helical whorl material. These European specimens have been recognized as possibly representing a larger subspecies of *N. (N.) hyatti* (Küchler & Odin 2001). The correct taxonomic placement of body chamber specimens from Angola assigned to *N. (N.) hyatti* (Howarth 1965, pl. 9, figs 2a, b) also cannot be resolved unless sufficient helical whorl material is examined.



Plate 2.9. A–K, *Nostoceras (Nostoceras) hornbyense* (Whiteaves, 1895). A, initial shaft and two whorl revolutions, V, GSC No. 139086, arrow denotes earliest constriction, scale bar = 5 mm; B, five and one-half whorl revolutions, V and right F umbilical, RBCM.76; C, one whorl revolution, right F umbilical, RBCM.77, scale bar = 1 cm; D–K, microconchs; D, four partial revolutions, penultimate limb and body chamber, left

F, RBCM.78; E–G, two and one-half slightly dislocated volutions, penultimate limb and body chamber, left F and two V sides, CDM No. 2008.1.82 HUN; H, penultimate limb and body chamber, left F, QBM No. P2015.171; I, penultimate limb and body chamber, right F, QBM No. P2015.172; J, K, penultimate limb and body chamber, right F and V, RBCM.79, scale bar = 1 cm.



Plate 2.10. A–H, *Nostoceras (Nostoceras) hornbyense* (Whiteaves, 1895) microconchs. C, D, *redux* Ludvigsen & Beard (1994, fig. 80, 1998, fig. 91). A, four partial whorl volutions, V, RBCM.80; B, penultimate limb and body chamber, left F, RBCM.81, arrow denotes encrusted anomiid bivalve on body chamber; C, three and one-half whorl volutions, penultimate limb and body chamber, left F, CDM No. 998.1.866 COP, arrow denotes forward-projected ventrolateral apertural margin and sinuous lirae; D, three and one-half whorl volutions, penultimate limb and body chamber, V, CDM No. 998.1.866 COP; E, impression of final whorl volution, penultimate limb and body chamber, left F, CDM No. 2008.1.17 HUN; F, G, penultimate limb and body chamber with two alternating rows of spines, right F and V, RBCM.82; H, penultimate limb and body chamber, right F, RBCM.83. Scale bar = 1 cm.

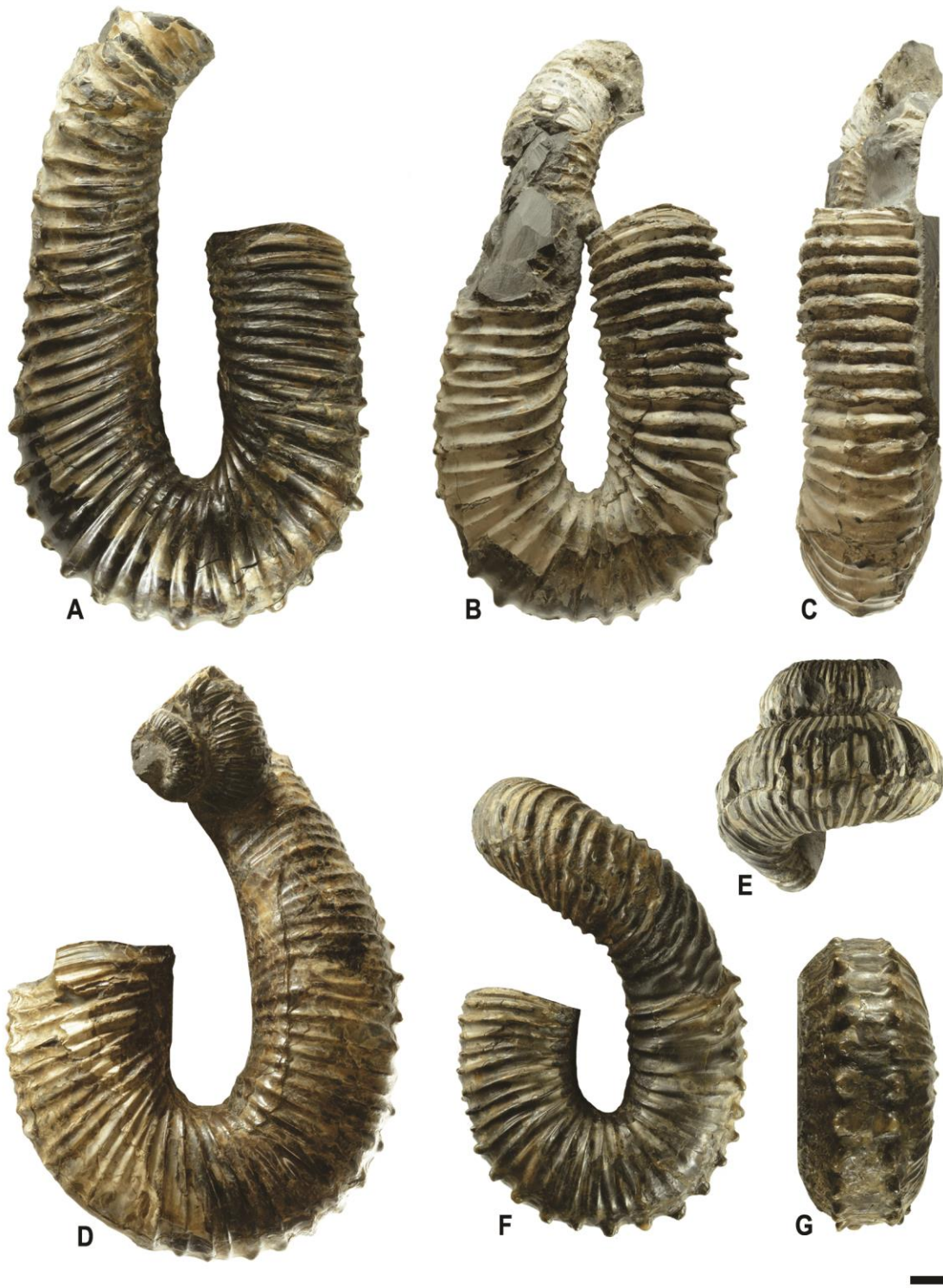


Plate 2.11. A–G, *Nostoceras (Nostoceras) hornbyense* (Whiteaves, 1895) macroconchs. **A**, penultimate limb and body chamber, right F, CDM No. 2008.1.1 HUN; **B**, **C**, penultimate limb and body chamber, right F and V, RBCM.84; **D**, two dislocated partial whorls, penultimate limb and body chamber, left F,

RBCM.85; E, two whorl volutions, V, QBM No. P2015.170; F, G, penultimate limb and body chamber, left F and V, CDM No. 2008.1.15 HUN. Scale bar = 1 cm.

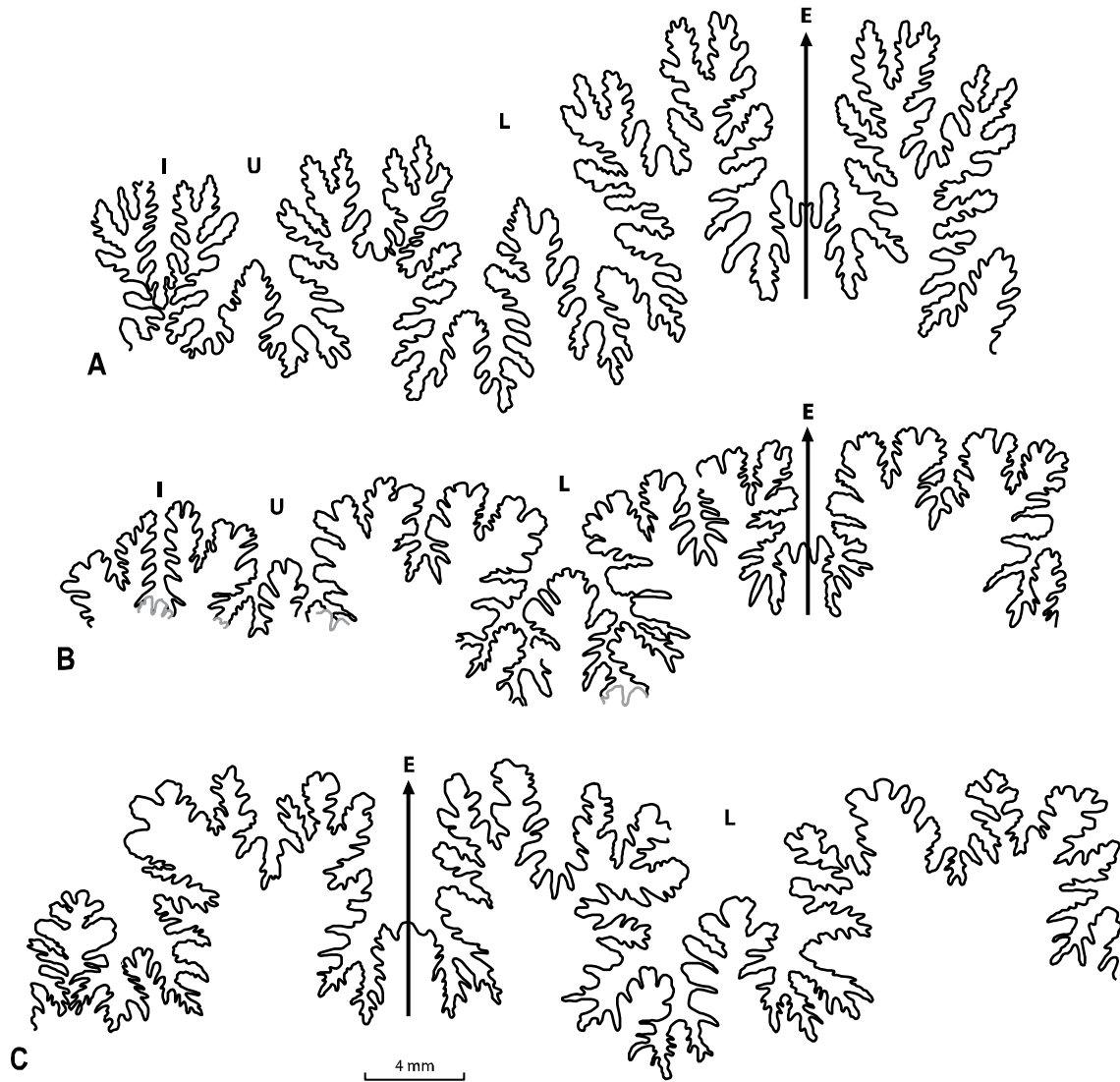


Figure 2.17. A–C, suture line of *Nostoceras (Nostoceras) hornbyense* (Whiteaves, 1895). A, RBCM.76, helical Wh = 17.9 mm; B, penultimate septum, RBCM.79, penultimate limb Wh = 20 mm, tips of preceding folioles (grey) illustrate septal approximation; C, penultimate septum, CDM No. 2008.1.17 HUN, penultimate limb Wh = 28 mm.

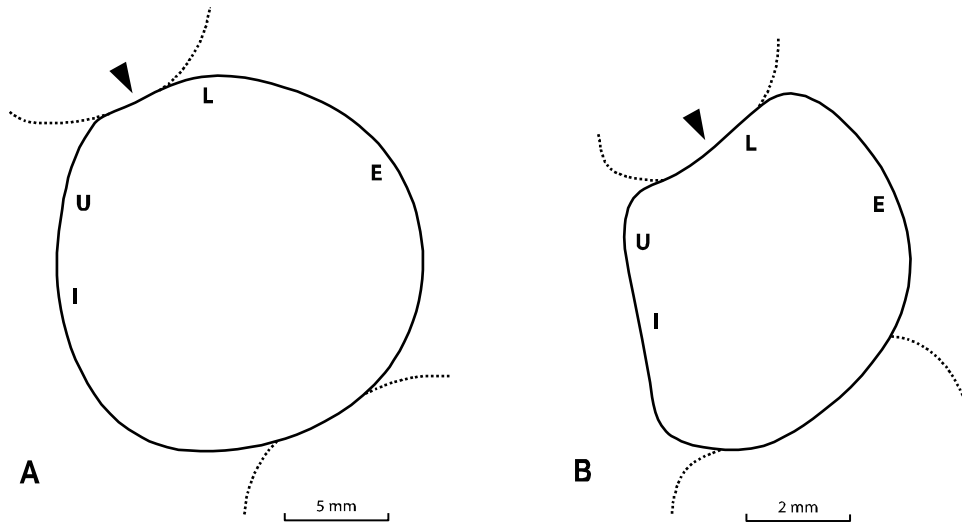


Figure 2.18. **A, B**, whorl cross-section and lobe positioning in *Nostoceras (Nostoceras) hornbyense* (Whiteaves, 1895) and *Nostoceras (Nostoceras) aff. pauper* (Whitfield, 1892). **A**, *N. (N.) hornbyense* (Whiteaves, 1895), RBCM.76, Wh = 18 mm; **B**, *N. (N.) aff. pauper* (Whitfield, 1892), RBCM.88, Wh = 5.7 mm. Dotted lines indicate adjacent whorl surfaces. Arrows indicate sites of preceding whorl impression.

Nostoceras (Nostoceras) aff. pauper (Whitfield, 1892)

(Pl. 2.12A–K; Figs 2.18B, 2.20A, B)

Compare:

1892 *Turrilites pauper* Whitfield: 268, pl. 45, figs 1–5.1974b *Nostoceras pauper* (Whitfield); Cobban: 12, pl. 9, figs 1–22, text-fig. 10 (*cum syn.*).1993 *Nostoceras (Nostoceras) cf. pauper* (Whitfield); Kennedy: 106, pl. 2, figs 4–6.v.1994 *Nostoceras* sp. Ludvigsen & Beard: 112, fig. 81.v.1998 *Nostoceras* sp. Ludvigsen & Beard: 129, fig. 92 (*redux* Ludvigsen & Beard 1994, fig. 81).2000d *Nostoceras (Nostoceras) pauper* (Whitfield); Kennedy *et al.*: 15, fig. 8A–H (*cum syn.*).

Type. The holotype is specimen NJSM No. 7659 as designated from the upper Campanian–lower Maastrichtian Navesink Formation of the Navesink Hills, New Jersey (Whitfield 1892, p. 268, pl. 45, figs 1–5).

Material. Twenty specimens—15 from which measurements could be obtained—consisting of helical whorls, retroversal limbs, and body chambers.

Occurrence. *N. (N.) pauper* has been described from the upper Campanian–lower Maastrichtian Nacatoch Sand of northeastern Texas (Stephenson 1941), Saratoga Chalk of central Arkansas (Kennedy & Cobban 1993c), and from the Navesink Formation of the Atlantic Highlands, New Jersey (Cobban 1974b; Kennedy *et al.* 2000d). Possible occurrences have also been recorded from the upper Campanian–lower Maastrichtian Barroso Formation of Columbia (Valencia-Giraldo *et al.* 2016) and the lower Maastrichtian phosphatic chalk of western Belgium (Kennedy 1993). On Hornby Island, *N. (N.) aff. pauper* occurs in the upper Campanian Northumberland Formation exposed along the western shore from Shingle Spit north to Collishaw Point.

Description. An ancyloconic heteromorph ammonite with sinistrally or dextrally coiled helical whorls of high contiguity which are rhomboidal in cross-section in early to intermediate stages

(Fig. 2.18B). Of the twenty specimens, 65 percent are sinistral and 35 percent are dextral in their direction of coiling. Of nine specimens, low to moderate A_p values ranging from 40° – 60° with a high translation rate are indicative of a total number of volutions approaching 6 or 7, if the A_p values obtained were to remain constant. The helical whorls possess a narrow umbilicus with W_b exceeding W_h at all stages. Among ten specimens, the U/C_d ratio averages 0.17. Three deep, flexuous, prorsiradiate constrictions are present per volution. The earliest preserved stage of whorl development in specimen RBCM.91 has a W_b/W_h ratio of 0.86 at a W_h of 6.5 mm. In all specimens, a deep contact furrow is present on the trailing flank of each subsequent whorl, reflecting accommodation of the bottom of the preceding volution.

Costae are typically raised and sharp with frequent intercalations. Of twelve specimens, C_v values range from 11–15 (41–57 a) with an average of 13 (52 a). Costae exhibit the highest relief along the outer margin of the contact furrow. Two rows of ventrolateral tubercles or spines of approximately the same size occur on the early coils, becoming proportionately longer with the maturity of the shell. These projections typically occur in two parallel rows of equal distance apart—or somewhat offset—from the venter on the outer helical whorl face. Two tubercles or spines typically occur on alternating costa linked across the venter by one or two transverse costae or with a single spine borne on each costa in alternating fashion. When present, alternating spines occur most commonly during the phase of transition from the last helical whorl to the penultimate limb. Bifurcation of costae and recombination at the base of a tubercle or spine may occur throughout.

The retroversal body chamber is hook-like, forming a compact C-shape, positioned directly beneath the helical whorls. Among five specimens, H values range from 11° – 18° . The suture line is only known from helical whorls, where it is marked by a broad external lobe and a small internal lobe with underdeveloped third-order incision elements (Fig. 2.20A, B).

Remarks. *N. (N.)* aff. *pauper* differs from *Nostoceras (Nostoceras) pauper* (Whitfield, 1892) only in exhibiting low to moderate A_p values ranging from 40° – 60° and possessing 3 constrictions per volution, whereas the latter species is characterized by generally lower A_p values ranging from 20° – 42° and at least 2 constrictions per volution. *Nostoceras (Nostoceras) colubriiformis* Stephenson, 1941, another similar species with a high translation rate, has also been distinguished from *N. (N.) pauper* by finer, denser costal ornamentation (Kennedy &

Cobban 1993c). The helical whorls of the *N. (N.) colubriformis* holotype (Stephenson 1941, pl. 81, figs 1–3) also appear to bear a much higher X_r and W_b/W_h ratio, underscoring a fundamental difference in whorl structure. *N. (N.)* aff. *pauper* shares its distinctive rhomboidal helical whorl cross-section with the early Maastrichtian *Nostoceras (Nostoceras) alternatum* (Tuomey, 1854) *sensu* Ifrim *et al.* (2004), although the latter species bears moderate to high A_p values ranging from 45° – 90° , coarser costae, and spines restricted to the leading whorl flank.

N. (N.) pauper has been distinguished from the similarly high-spired species *Nostoceras (Nostoceras) splendidus* (Shumard, 1861) on the grounds of looped and zig-zagging costae on the outer whorl face (Kennedy & Cobban 1993c), although the ornamentation of the latter is noted as variable (Stephenson 1941). *Turrilites excelsus* Anderson, 1958, described from the Maastrichtian of the Moreno Formation of California, has been interpreted (Matsumoto 1959b) as synonymous with *N. (N.) splendidus* as figured by Stephenson (1941), which appears reasonable given the high translation rate. With costal ornamentation being one of the most plastic traits in the genus *Nostoceras*, *N. (N.) splendidus* is likely a close ally to *N. (N.) pauper*, differing mainly in lower A_p values and a higher number of volutions.

Helical whorls of a low apical angle and an abruptly recurving C-shaped body chamber separate *N. (N.)* aff. *pauper* from the predominant nostoceratid population of *N. (N.) hornbyense* on Hornby Island. In comparison, *N. (N.) hornbyense* is characterized by an elongated U-shaped body chamber and helical whorls with moderate to high A_p values. Costae of *N. (N.)* aff. *pauper* transect the dorsum of the body chamber obliquely, reflecting a mode of development still subject to torsion following the helical whorls. Comparatively, *N. (N.) hornbyense* is typified by a penultimate limb and retroversal body chamber bearing costae which transect the dorsum more rectiradially. The helical whorls of *N. (N.)* aff. *pauper* are also easily distinguished from those of *N. (N.) hornbyense* by their rhomboidal cross-section, lower U/C_d ratio, and deeper contact furrow.



Plate 2.12. A–K, *Nostoceras* (*Nostoceras*) aff. *pauper* (Whitfield, 1892). A, B, one and one-half helical whorl volutions, right F umbilical and V, RBCM.86; C, D, one and one-half helical whorl volutions, right F umbilical and V, RBCM.87; E, five helical whorl volutions and partial body chamber, V, RBCM.88; F, two partial helical whorl volutions and body chamber, left F, RBCM.89; G, two partial helical whorl volutions and body chamber, left F, RBCM.90; H, two partial helical whorl volutions and weathered body chamber, right F, RBCM.91; I, J, two and one-half helical whorl volutions, right F umbilical and V, RBCM.92; K, partial final helical whorl volution and body chamber, left F, RBCM.93. Scale bar = 1 cm.

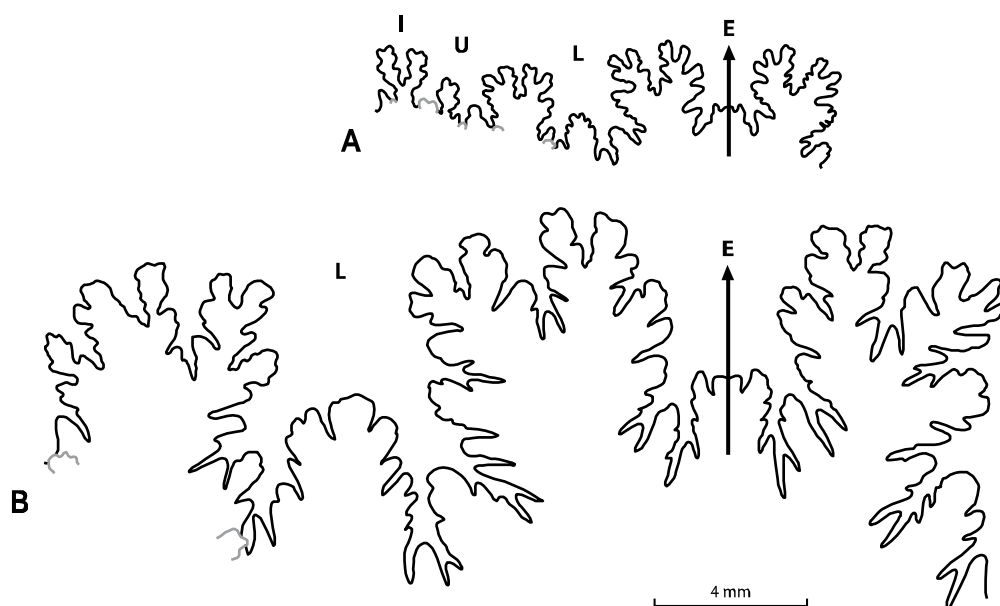


Figure 2.20. A, B, suture line of *Nostoceras* (*Nostoceras*) aff. *pauper* (Whitfield, 1892). A, RBCM.88, Wh = 5.8 mm; B, RBCM.92, Wh = 15 mm, tips of preceding folioles (grey) illustrate septal approximation.

2.8 Discussion

Building on the work of Cobban (1974b), Kennedy *et al.* (1992) established *N. (N.) hyatti* as but one taxon in association with thirteen other distinct heteromorph ammonite species in North America—*N. (N.) pauper* and *Solenoceras reesidei* among them—which characterize the latest Campanian interval. In Europe, *E. (Neancyloceras) bipunctatum* is also firmly associated with the *hyatti* Assemblage Zone (Kennedy *et al.* 1992), with only an isolated fragment having been recovered from Arkansas that is potentially referable to the species (Kennedy & Cobban 1993d). Odin *et al.* (1996) were the first to propose the occurrence of *N. (N.) hyatti* as one of the global markers for the Campanian-Maastrichtian boundary (CMB). The taxon was later defined as the sixth youngest among a sequence of nine faunal horizons indicative of the CMB transition with its last occurrence datum at the 72.5–71.0 Ma interval (Odin & Lamaurelle 2001).

The temporal extent of the *hyatti* Assemblage Zone in North America has come to be regarded as latest Campanian (Kennedy & Cobban 1993c; Kennedy *et al.* 2000d; Ifrim & Stinnesbeck 2010; Ifrim *et al.* 2015), with its last occurrence datum corresponding to that of the

US Western Interior *Baculites jenseni* Teilzone (Cobban 1962) placed at 72.74 Ma (Ogg *et al.* 2012). Biostratigraphic studies (McGugan 1962, 1979, 1982; Muller & Jeletzky 1970; Sliter 1973), magnetostratigraphy (Raub *et al.* 1998; Enkin *et al.* 2001; Ward *et al.* 2012), and carbon isotope stratigraphy (Hasegawa *et al.* 2015; Haggart *et al.* *in prep*) have all placed approximately the same age constraint on the herein proposed reference section for the regional *N. (N.) hornbyense* Zone (Haggart *et al.* 2009). The presence of *N. (N.)* aff. *pauper*, *Solenoceras* cf. *reesidei*, and *E. (N.)* aff. *bipunctatum* also supports *hornbyense* Zone equivalency with the *hyatti* Assemblage Zone in addition to the morphological affinity of the zonal namesakes. Likewise, the Hornby Island interval is further constrained by the emergence of *N. (N.) hornbyense* above the local *Nostoceras (Didymoceras?) adrotans* Assemblage Zone proposed in this study (Fig. 2.2). On the basis of nostoceratid morphological succession, the top of the Hornby Island *adrotans* Assemblage Zone is correlative with that of the *Nostoceras (Didymoceras) cheyennense* Teilzone of the US Western Interior with a last occurrence datum at 74.21 Ma (Ogg *et al.* 2012).

Faunal correlation between the Northumberland Formation of Hornby Island and Gulf Coast and Atlantic Seaboard localities is possible due to the spatiotemporal convergence of the *hornbyense* Zone and the *hyatti* Assemblage Zone by way of a Caribbean corridor during the latest Campanian (Fig. 2.21). The *hornbyense* Zone within the Northumberland Formation is also correlative with the US Western Interior, given *N. (N.) hyatti* has been documented as far inland as Colorado where it is known from the Pierre Shale (Kennedy & Cobban 1993c). However, the *adrotans* local Assemblage Zone of the basal Northumberland Formation shares greater affinity with the US Western Interior than the Gulf Coast due to the near absence of *D. (D.) cylindraceum* and the prevalence of *Solenoceras* and *Exiteloceras* taxa. By extension, these North American localities are correlative with coeval strata in western Europe (e.g. Kennedy & Cobban 1993c; Kennedy *et al.* 2000d; Summesberger *et al.* 2007).

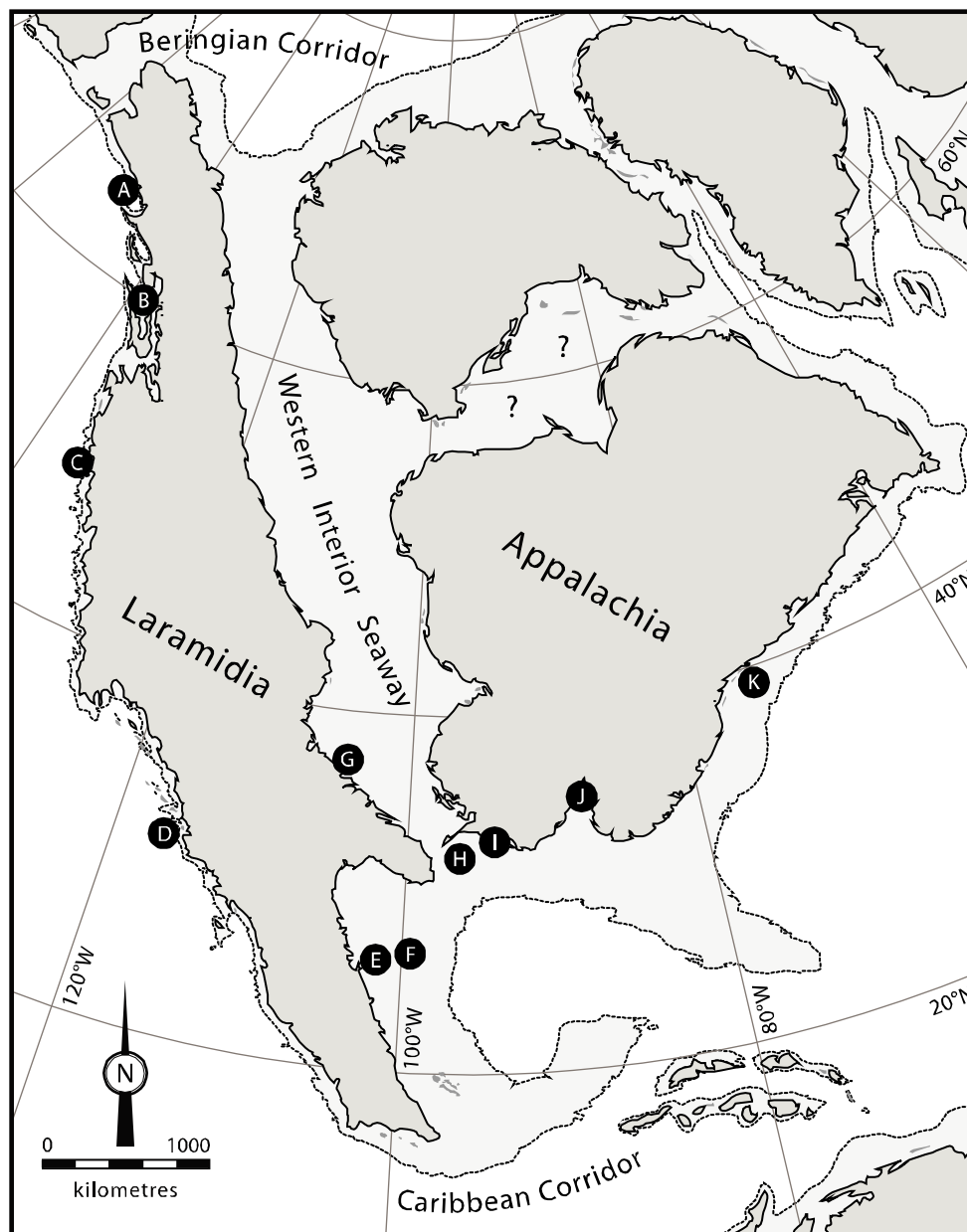


Figure 2.21. Palaeogeographic map of North America during the latest Campanian modified from Blakey (2014). A–I, inferred positions of regional localities correlative with the *Nostoceras* (*Nostoceras*) *hyatti* global Assemblage Zone. A, Kaguyak Formation, Alaska; B, Matanuska Formation, Alaska; C, Northumberland Formation, Hornby Island; D, Rosario Formation, Baja California; E, Perras Shale, Coahuila, Mexico; F, Méndez Formation, Nuevo León, Mexico; G, Pierre Shale, Colorado; H, Nacatoch Sand, Texas; I, Saratoga Chalk, Arkansas; J, Ripley Formation, Tennessee; K, Navesink Formation, New Jersey. Locations A–D are poorly constrained due to uncertainties in tectonic translation.

2.9 Summary

This study has attempted to place the rich heteromorph ammonite fauna from the Northumberland Formation on Hornby Island into the context of the Late Cretaceous for the North Pacific and a positive correlation with the latest Campanian global *Nostoceras* (*Nostoceras*) *hyatti* Assemblage Zone has been inferred. Taxa referable to the following species are now recognized from the locality: *Baculites occidentalis* Meek, 1862, *D. (Diplomoceras) cylindraceum* (Defrance, 1816), *E. (Exiteloceras) densicostatum* sp. nov., *E. (Neancyloceras) bipunctatum* (Schlüter, 1872), *Fresvillia constricta* Kennedy, 1986a, *N. (Didymoceras?) adrotans* sp. nov., *N. (Nostoceras) hornbyense* (Whiteaves, 1895), *N. (Nostoceras) pauper* (Whitfield, 1892), *Phylloptychoceras horitai* Shigeta & Nishimura, 2013, *Solenoceras exornatus* sp. nov., and *Solenoceras reesidei* Stephenson, 1941. This work has aimed to lay a foundation for greater reliability and scope in the utility of the Baculitidae, Diplomoceratidae, and Nostoceratidae through comparative synthesis of the present species and related taxa.

Significant collections with representation from these families have been amassed in recent decades enabling taxonomic framework revision and re-evaluation of the diagnostic trait hierarchy. We have demonstrated the feasibility of our systematic approach given optimal material preservation and preparation. Conch reconstructions have been rendered for the diplomoceratids *D. (D.) cylindraceum* and *P. horitai* based on this new material. Re-examination of members of the genus *Nostoceras* has bolstered the premise that body chambers and suture lines alone are an insufficient basis upon which to place specific assignment without conveying uncertainty. A substantial body of quantitative data derived from shell measurements has warranted the synonymization of numerous taxonomic entities. Frequency and consistency in the expression of shell geometry, ornamentation, and morphologic congruency have been assessed to better refine the parameters for defining genera, species, and antidimorphs represented within the Northumberland Formation. This enhanced understanding of character expression and combination holds the potential to further refine conceptualization of heteromorph ammonite taxonomy, re-adjusting the lens through which the global data set is perceived.

2.10 Acknowledgments

The authors would like to extend their gratitude to the following individuals: Dr. Richard Hebda of the Royal BC Museum, Dr. Marcin Machalski of the Polish Academy of Sciences, and an anonymous referee for providing editorial review; Dr. Herbert Klinger of the Iziko South African Museum for sharing his thoughts on heteromorph ammonite taxonomy; Marji Johns of the Royal BC Museum and the late Marjorie Thorpe of the Courtenay and District Museum for providing access to palaeontological materials while remaining tirelessly committed to collections management. This research was also supported by generous financial and anecdotal contributions from David Starr of Washington State. The presence of a vibrant amateur palaeontological community on Vancouver Island made the extent of this work possible. Graham Beard, Doug Carrick, Betty Franklin, Raymond Graham, Joe Haegert, Bob Hunt, Stevi Kittleson, Kurt Morrison, and Jean Sibbald are thanked for their correspondence and generosity in contributing many of the exquisite specimens featured in this study. Their diligence in the collection, preparation, and documentation of macrofossils is a reflection of the passion they have for palaeontology and their will to help shape the narrative of Earth history. It is with our affinity toward science that we are kindred spirits.

Chapter 3

General Discussion

3.1 Heteromorph ammonite taphonomy

Heteromorph ammonites in Nanaimo Group strata are rarely completely preserved and specimens known from the Northumberland Formation are no exception. However, the fine-grained mudstone of the Northumberland Formation allows for high-quality preservation of organic materials. The best preservation of heteromorph ammonites is generally observed in calcareous concretions where the cameral chambers are filled by calcite crystals which developed after the shell became waterlogged and sank to the sea floor (Maeda & Seilacher 1996). Sections of phragmacone are generally well preserved due to the buttressing of septal walls while shattered body chambers provide evidence that unsupported body chambers were more susceptible to implosion under deep sea water pressures. It is the observation of the author through field counts that ~ 3–5 % of all spherical to ellipsoidal concretions ranging from ~ 5–15 cm in diameter contain macrofossil remains of some kind.

In situ orientation indicates that the majority of specimens were not fully immersed in sediment with the portion preserved representing the side which came to rest on the sea floor. With heteromorph ammonites, this mode of preservation is most commonly observed in limb sections and is consistent with the remains of other molluscs collected from the same exposures. Following the eventual collapse and dissolution of the exposed upward-facing shell, the downward-facing side would have seen its cameral chambers only partially filled with sediment (Maeda & Seilacher 1996). In specimens with minimal deformation, the preserved portion usually ranges from one to two thirds of the inflated chamber. The earliest whorls of mature shells are generally among the portions not preserved presumably due to deficiencies in sediment transportation through the siphuncle to the juvenile cameral chambers (Nunnallee 1983).

Low-energy settings such as those at the outer reaches of a submarine fan (Mustard 1994; Katnick 2001) would have been conducive to the organic weathering of exposed shell material and dispersal by scavengers. Prior to any diagenetic compression or deformation, limited

bioturbation could account for instances of shell fragmentation beyond that attributable to necrolytic collapse provided adequate oxygen levels were maintained. Therefore, post-mortem burial would have been primarily contingent on the settling of sediments disturbed when the conch impacted the sea floor. Larger whorl diameters were less prone to complete preservation; a principle attributed to the insufficiency of force required upon descent to ensure full conch immersion in substrate sediments.

$\delta^{13}\text{C}$ isotope analysis suggests the presence of the Campanian-Maastrichtian Boundary (CMB) in either the overlying Geoffrey or Spray formations (Hasegawa *et al.* 2015; Haggart *et al.* in press). Assuming the CMB at 72.1 Ma (Ogg *et al.* 2016) and the first occurrence datum of *N. (N.) hornbyense* corresponding to that of the last occurrence datum of *Nostoceras (Didymoceras) cheyennense* (Meek & Hayden, 1856) at 74.21 Ma (Ogg *et al.* 2012) sees a projected sedimentation rate of at least ~ 159 m per Ma; a figure well within the established range for coeval forearc basins of Japan (Okada 1997). If this sedimentation rate were constant, the entire Northumberland Formation section would be representative of a ~ 2.49 Ma interval in line with the temporal range inferred from magnetostratigraphy (Raub *et al.* in Ward *et al.* 2012).

A curious phenomenon commonly observed within the Northumberland Formation mudstone is the tendency of juvenile heteromorph ammonites to occur in clusters within concretions as is typically the case with specimens of *Baculites occidentalis*, *D. (Diplomoceras) cylindraceum*, *Fresvillia constricta* and *Phylloptychoceras horitai*. Such concretions are densely fossiliferous containing an immense variety of micro- and macrofossils in a phenomenon observed at other localities (e.g. Tanabe *et al.* 1993; Mapes & Nützel 2009). The frequent presence of terrestrial botanical matter in these concretions—such as seeds, cones and wood—suggests the possibility that planktic juvenile ammonites became bound in drifting masses conducive to agglutination prior to their loss of buoyancy and deposition. The transport mediums in question may have been floating algal mats (Stinnesbeck *et al.* 2016) or the gelatinous egg masses or membranous brood sacs of these very ammonoids (Landman *et al.* 1996a). Alternatively, mass die-offs of planktic juveniles may have been triggered by breakdowns in ocean stratification and short-term mixing events (e.g. Stephens *et al.* 2012).

3.2 Heteromorph ammonite polymorphism

Polymorphism is perhaps one of the most dramatic traits to be observed in the Hornby Island heteromorph ammonite assemblage with members of the Nostoceratidae exhibiting some of the highest degrees of morphological variation. This reality is compounded by broad-ranging conspecific morphology which poses an array of challenges to the taxonomic classification and growth modeling of these organisms (Jones 1963; Tanabe *et al.* 1981; Okamoto 1996).

Additionally, nostoceratid populations such as that of *N. (N.) hornbyense* in the present study are a case in point for the principle of phenotypic plasticity (Scheiner 1993) and the concept sexual dimorphism (e.g. Makowski 1962; Callomon 1963; Davis 1972) within a continuum of polymorphic variance (e.g. Matyja 1986; Klug *et al.* 2015).

Beyond sexual dimorphism alone, a substantial range in whorl positioning and limb dimensions exists. When considering both the Diplomoceratidae and Nostoceratidae, deeper sutural lobe incision can be regarded as a function of increasing whorl discontinuity; a likely ontogenetic adaptation to provide structural stability in line with the premise of sutural buttressing (e.g. Packard 1972; Batt 1989). This hypothesis is supported by the presence of the highest sutural floridity occurring in heteromorph taxa such as *D. (Diplomoceras)* and *N. (Didymoceras)* where complete whorl discontinuity would result in water pressure distributed over the entire conch surface area. In the case of nostoceratid retroversal body chambers, the cause of dimensional variance between specimens is both a function of helical whorl diameter at the stage at which sexual maturity was triggered and gender predisposition to dimorphism to larger and smaller forms from early development.

Septal suture intricacy and lobe orientation are arguably more taxonomically significant characteristics in the Diplomoceratidae than they are in the Nostoceratidae. In the latter family, adherence to a general geometric arrangement of elements is consistent but with considerable ontogenetic variability in their proportions. This is apparently due to a series of physical controls acting on whorl expansion during the helical stage—chiefly, cameral chamber compression due to volution contiguity and torsion acting on the dorsal surface as a function of greater translation rate. This results in stretching of the external and lateral sutural elements and compression of the internal and umbilical sutural elements. However, following the advent of maturity and

development of the retroversal body chamber, the lobes and saddles exhibit unencumbered expression.

Correlation between warmer surface temperatures and early-onset maturity in modern squid resulting from seasonal differences in breeding has been observed (Matyja 1986). Similarly, if nostoceratid maturity was triggered by migration to higher levels in the water column resulting from exposure to less hydrospheric pressure, warmer temperatures and greater light intensity (Bucher *et al.* 1996), a much greater range in the number of helical whorl volutions would be expected. In *N. (N.) hornbyense*, the helical stage is constrained to 6–7 volutions making it more likely that maturity was determined by terminal countdown morphogenetics (Kaplan 2002) with rate of growth as a function of nutrient intake accounting for marginal variability in the total number of volutions and greater variability in costal density. While the helical whorls of *N. (D.?) adrotans* are not known, the extent of variability in the penultimate limb suggests that phragmacone orientation is of less importance than body chamber recurvature in the mature stage.

In both nostoceratids and diplomoceratids, variations in costal density may be presumed to indicate individual rates of growth based on environmental conditions relating to shelf position and nutrient access. Rate of shell construction is understood to decrease with depth due to water pressure and lower temperatures which act to slow metabolic and generative functions (Westermann 1996). This principle bolsters the hypothesis of pronounced ornamentation in association with shallow water environments (Batt 1989) and therefore implies conditions conducive to upwelling and greater shell modification. This assertion is plausible as an increased degree in the projection of spines is a clear function of lower costal density in all heteromorphs within the Hornby Island assemblage.

Assemblage differences indicate that some heteromorph ammonoid antidimorphs may have preferred differing environments (Davis *et al.* 1996). Although gender distribution among the population sample of *N. (N.) hornbyense* appears to be relatively balanced, the predisposition of macroconches to a higher Ci is suggestive of favouritism toward deeper waters with fewer nutrients promoting slower growth. Reduced macro- and microconches are therefore interpreted as representing less successful individuals with malnourishment accounting for condensed ribbing and reduced dimensions. Similarly, fluctuations in Ci and constriction frequency throughout development in *D. (D.) cylindraceum* may present a record of subsistence over

cyclical stages of shell growth akin to those observed in the Santonian diplomoceratid *Polyptychoceras pseudogaultinum* (Yokoyama, 1890) by Okamoto & Shibata (1997) in line with the concept of episodic growth (Arkell 1957; Bucher *et al.* 1996).

The scarcity of reduced forms of *N. (N.) hornbyense* in the Hornby Island assemblage may be indicative of a preference for more neritic environments among these smaller adults. This is conceivable given that foraminiferal bathymetric findings have placed the Northumberland Formation depositional environment at depths ranging from 150–400 m (Sliter 1973; Cameron 1988). These depth estimates are much greater than those proposed for neighbouring regions of the Gulf Coast (Puckett 1991) and Atlantic highlands (Olsson 1963; Cobban 1974) where palaeodepths have been placed at less than 100 m and smaller species such as *N. (N.) approximans* were well established (e.g. Kennedy *et al.* 2000d). While the comparatively smaller nostoceratid *N. (D.?) adrotans* is restricted to the lower Northumberland formation, a shallower water habitat alone cannot account for reduced dimensions given the success of larger members of the genus in the Western Interior (Gill & Cobban 1966).

With respect to ornamentation variability, intraspecific overlap among nostoceratids demands a conceptual re-evaluation of these organisms from an ecological standpoint and a loosening of the narrow parameters so often used in previous works to define species. The conclusions drawn from the recent reassessment of index baculitids (Ward *et al.* 2015) are potentially transferable in underscoring the taxonomic value of considering trait ratios as opposed to strict presence and absence as was generally employed in earlier studies. With spatial factors such as endemism and environmental controls considered, morphotype ratios could remain an important indicator demarcating degrees of transition between biotic provinces if traced through populations. Shared temporal constraints would also see the retention of biostratigraphic significance.

In the case of the highly variable *D. (D.) cylindraceum*, there remains the possibility that regional subspecies may have existed following the species' emergence in the late Campanian (Whiteaves 1903; Blaszkiewicz 1980; Matsumoto & Myauchi 1984). However, it could also be argued that this single species occurred with a flexible morphology reflective of its ecological resilience. Notable characteristics of Hornby Island specimens such as phragmaconic plications, abrupt angles of limb divergence and frequent constrictions are unusual in previously described collections from other localities but are not unknown (e.g. Henderson *et al.* 1992; Fatmi &

Kennedy 1999). The prevalence of these shell elements in the Hornby Island material could be interpreted as representing nothing more than regional endemism in a North Pacific population of *D. (D.) cylindraceum*.

3.3 Heteromorph ammonoid ontogeny and palaeoecology

Like other ammonoids, members of the Turrilitoidea likely began as epipelagic planktic hatchlings (Shigeta 1993). The often asymmetrical and elaborate shells these heteromorphs constructed has long brought into question their ecological role and mode of life (e.g. Westermann 1996). The absence of soft body fossils has led to much speculation regarding heteromorph locomotion and subsistence patterns with interpretations ranging from crawling foragers (e.g. Ebel 1992) to slow-swimming, mesopelagic zooplankton feeders (e.g. Ward & Westermann 1977; Ward 1979, 1986; Westermann 1996). Oxygen isotopes obtained from Nanaimo Group ammonites have denoted palaeotemperatures which suggest that planispiral pachydiscid and muniericeratid ammonoids developed their shells in benthic zones of shelf environments (Zakharov *et al.* 2013). It is widely accepted that heteromorph ammonoids were either nektobenthic predators, thriving in habitats largely similar to those of their planispiral contemporaries (e.g. Arkell 1957; Wiedmann 1969; Klinger 1980; Monks & Young 1998; Kruta *et al.* 2011) or planktic drifters (e.g. Westermann 1996; Lukeneder 2015).

Morphological analysis of large population samples enables more accurate taxonomic placement of aberrant forms given the greater window into the spectrum of conspecific diversity within a regional setting. The limitations of genetic determinism in shell development necessitate that heteromorph ammonite fossils preserve a detailed record of their life cycle, relationship to their surroundings and adaptive responses to environmental conditions (Ebel 1992; Okamoto & Shibata 1997). Early evolutionary thought surmised that new shell features supplanted ancestral traits in a gradual process bound by what was defined as the law of replacement (Hyatt 1894). However, simulated growth modelling of the *Eubostrychoceras* descendent *Nipponites* Yabe, 1904 suggests that changes in coiling may have occurred so suddenly that intermediate forms were virtually non-existent (Okamoto 1988b, 1989; Klinger & Kennedy 2003b; Klinger 2008). Similarly, immediate stratigraphic succession and close morphological affinity also bolsters the interpretation of abrupt phylogenetic transition between such forms as *N. (N.) awajiense* and

Pravitoceras sigmoidal (Yabe 1902) in Japan (Morozumi 1985; Klinger 2008); a notion in agreement with modern understanding of gene mutation and the evolutionary theory of punctuated equilibrium.

Hamitonic taxa such as *Diplomoceras* are generally accepted as having been planktic floaters and probably epipelagic (e.g. Klinger 1980; Westermann 1996). With their complex, multi-limbed shells, these ammonoids would have undergone numerous—and potentially abrupt—instances of reorientation as the organism rounded each point of recurvature (Ward 1976a; Monks & Young 1998). The smaller polyptychoceratids such as *Phylloptychoceras* were likely more agile swimmers due to their comparatively compact and streamlined limb orientation (Kakabadzé & Sharikadzé 1993). Largely gyroconic genera such as *Exiteloceras*, regarded to have been pelagic (Westermann 1990), would have been poorly hydrodynamic with sudden unidirectional movements hindered by conch propensity to pivot around the axis of coiling.

The shell structure of the nostoceratids is indicative of at least two distinct states of physical orientation probably coinciding with changes in habitat occupation (Okamoto 1988a; Westermann 1996). Inefficient propulsion marked the juvenile and intermediate stages as the helical conch was typically oriented with the venter on the exterior flank of the whorl—as opposed to the bottom—placing the camerae toward one side of the body chamber rather than directly above it (Westermann 1996). For this reason, bilaterally asymmetrical ammonoid shells have been conceived to be most suited to a benthic niche (Tanabe *et al.* 1981) although the locomotive limitations associated with a helical conch are evident, no loss in buoyancy potential has been noted (Ward 1976b). A smaller phragmocone proportionate to the body chamber in mature nostoceratids may denote reduced buoyancy potential and therefore life near the substrate (Klinger 1980) if high-volume occupation of the body chamber is presumed. However, evidence from prominent dorsal muscle scars near the front end of the body chamber in the Lower Cretaceous genus *Ancyloceras* d'Orbigny, 1842 suggest that a large portion of the ancyloconic ammonoid soft body was likely extended beyond the aperture (Dogudzhava & Mikhailova 1991).

Shells of *N. (Didymoceras)* from the Western Interior Seaway of North America have been found to have similar isotopic composition to those of inoceramid bivalves (He *et al.* 2005) reinforcing the notion of a benthic mode of life for ancyloconic heteromorphs. However, it has been argued that adult nostoceratids would have been largely unsuccessful at hunting and

scavenging on or near the ocean floor due to the constraints imposed by whorl buoyancy in relation to the post-helical upturned retroversal shell (e.g. Trueman 1941). These ammonoids may have been capable of reorientation through simultaneous action of protruding body parts, hyponomic water expulsion and cameral fluid exchange (Kakabadzé 2016). All avenues of locomotion considered, the upturned body chamber was perhaps most conducive to life higher in the water column where adults could utilize their lateral manoeuvrability to breed and live out their mature stage as microphagous zooplankton feeders (Ward 1976b; Nesis 1986; Lewy 1996; Okamoto 1996).

Helicoid shells of the Turrilitoidea were probably most adept to vertical migration in deep waters (e.g. Ward 1976b, 1979; Ward & Westermann 1977; Tanabe *et al.* 1981; Westermann 1990, 1996; Klinger 2008). This adaptation to vertical migration has been attributed to subsistence patterns in response to new trophic opportunities presented by the Early Cretaceous radiation of microorganisms such as calcareous nannoplankton and foraminifera (Nesis 1986; Cecca 1997). On Hornby Island, heteromorph ammonites present a clear association with a rich dinoflagellate assemblage which would have supported a prolific source of zooplankton as a potential food source. Lateral rotation around a helicoid axis may have been advantageous for suspension feeding in a mode of life similar to that postulated for spiral hemichordates of the order Graptoloidea (Pospelova pers. comm).

The development of a descended retroversal body chamber with the advent of sexual maturity likely afforded ancyloconic taxa greater lateral manoeuvrability (Kakabadzé 2016); a kinesthetic adaptation which would have benefited adult ammonoids assuming a predatory mode of life, pursuing macroorganisms. Additionally, such a shell modification could have supported the accommodation of reproductive organs and potentially brood pouches (e.g. Jacobs & Chamberlain 1996; Lewy 1996, 2002). The recent interpretation of ancylocones as stationary plankton feeders hooked on algal fronds (Arkhipin 2014) is problematic. The Hornby Island nostoceratid assemblage demonstrates that diminished ornament on the dorsum is an ontogenetically consistent trait not attributable to isolated abrasion of the retroversal body chamber. Additionally, a sessile mode of life raises the question as to why such organisms would require a means of regulating shell buoyancy. Moreover, if these ammonoids became stationary at maturity, any means of frond attachment during an otherwise highly awkward and impractical transitional growth phase would be entirely speculative.

3.4 Heteromorph ammonoid evolutionary progression

Based on their shell structure and mode of coiling, members of the Albian–middle Cenomanian Turrilidae are widely presumed to have given rise to the Diplomoceratidae and Nostoceratidae (Arkell *et al.* 1957a; Matsumoto 1967; Wright *et al.* 1996). During the Cenomanian, turrilitids enjoyed a cosmopolitan existence spanning the globe from Northeast Russia to the Western Interior Seaway of North America (Cobban & Scott 1972; Wright *et al.* 1996; Jagt-Yazykova 2011). The demise of the turrilitids and other ammonoid faunas near the Cenomanian-Turonian boundary is compelling evidence of a global extinction event (Jagt-Yazykova 2011, 2012). However, the chronologic sequence of ammonoid progression in the Late Cretaceous demands that populations of these heteromorph taxa survived this event and subsequently diverged into the emergent families of the Turonian.

The ancyloconic nostoceratid genus *Eubostriochoceras* has been surmised as the most likely common ancestor to both the diplomoceratids and nostoceratids of the Late Cretaceous (Matsumoto 1967). From a morphological standpoint, *Eubostriochoceras* appears to provide an adequate evolutionary conduit to account for the succeeding lineages of *N.* (*Nostoceras*) and *N.* (*Didymoceras*) which went on to flourish in the late Campanian (Matsumoto 1967, 1977; Jagt-Yazykova 2011). Early stage coiling irregularity observed in *Eubostriochoceras*, typified by a shaft enveloped by subsequent helical whorls (e.g. Tanabe *et al.* 1981), would be retained among its helicoid descendants and expressed through differing modes of early shaft orientation.

In the North Pacific, *Eubostriochoceras* became conspicuous well into the Santonian only to disappear with the advent of a period distinguished by the proliferation of the Diplomoceratidae and Nostoceratidae (Wright *et al.* 1996; Jagt-Yazykova 2011, 2012). The wide dispersal and ecological success of the genus following its emergence in the Turonian also supports its candidacy as an ancestor of both lineages. Matsumoto (1977) postulated the bi- to quadrituberculate *Hyphantoceras* Hyatt, 1900 as a possible *Eubostriochoceras* descendant which formed the root stock of the tuberculate nostoceratids belonging to the subgenus *N.* (*Didymoceras*). Recently, more immediate ancestors have been surmised in lower–middle Campanian forms assigned to *Eodidymoceras* Klinger & Kennedy, 2003b with the late Campanian *Bostrychoceras* Hyatt, 1900 representing likely variants of *N.* (*Didymoceras*) typified by the European index species *N.* (*Didymoceras*) *polyplocum* (Roemer, 1841).

Eubostriochoceras progeny in *Scalarites* Wright & Matsumoto, 1954 and its gyroconic descendants *Neoglyptoxoceras* Collignon, 1969 and *Glyptoxoceras* Spath, 1925 exemplify stages of a helicoid transition to a planispiral mode of coiling. These taxa have been conceived as precursors to the predominantly hamiticonic *Diplomoceras* (Matsumoto 1959; Matsumoto & Myauchi 1984; Klinger & Kennedy 2003a; Jagt-Yazycova 2011). As proposed in this work and in line with the reasoning of others (Wiedmann 1962; Klinger 1976), *Neoglyptoxoceras* and *Glyptoxoceras* can be confidently regarded as *Diplomoceras* subgenera. A more direct phylogenetic relationship between *Scalarites* and the hamiticone *Polyptychoceras* Yabe, 1927 has been hypothesized (Okamoto & Shibata 1997; Jagt-Yazycova 2011); a genus which would later be succeeded by *Phylloptychoceras* into the Maastrichtian (Ward 1976b; Shigeta & Nishimura 2013). Ultimately, *Exiteloceras* and *Solenoceras* likely arose through the polyptychoceratine *Pseudoxybeloceras* Wright & Matsumoto, 1954 in the middle to late Campanian (Klinger 1982).

In the North American Western Interior, the earliest records of *Eubostriochoceras* hail from the upper Turonian Frontier Formation of Wyoming, the Carlile Shale in northeastern Wyoming and southwestern South Dakota, and the Mancos Shale of southern New Mexico (Cobban 1987; Wahl 2011). The earliest material is indicative of a late Turonian movement of the genus through the seaway during a time of regression noted for the southerly migration of boreal ammonoid faunas (Batt 1989; Voight & Weise 2000). A lack of heteromorph material suggests that *Eubostriochoceras* may not have reached the Gulf Coast during the Turonian (Ifrim & Stinnesbeck 2007) although its movement would later progress across the Atlantic with numerous species establishing broad geographic ranges from Europe (e.g. Kaplan & Schmid 1988) to Madagascar (e.g. Collignon 1969; Klinger & Kennedy 1997). Aside from poorly preserved, fragmentary material collected from the Western Interior of North America (Cobban & Kennedy 1992; Kennedy & Cobban 2001), there is little indication that the genus persisted into the Campanian.

In approach to the Campanian, ancyloconic heteromorph populations in the Western Interior were likely to have found themselves sufficiently removed from the open ocean as to allow for the development of regional nostoceratid lineages distinct from those in other biotic provinces. Some endemic taxa would come to represent Campanian zonal index species such as *Nostoceras* (*Didymoceras*) *nebrascense*, *Nostoceras* (*Didymoceras*) *stevensoni* (Whitfield, 1877)

and *N. (D.) cheyennense* (e.g. Kennedy 1989; Kennedy *et al.* 2000c). The first two of these three index species are closer to *Eubostrychoceras* not only chronostratigraphically but morphologically in sharing a robust, C-shaped living chamber with the aperture at an oblique angle—or adjacent to—the final helical whorl (Kennedy *et al.* 2000c, fig. 21B).

While abrupt shifts in morphology may have transpired in some populations, *N. (D.) cheyennense* appears to represent a *N. (Didymoceras)* species in transition to a form more typical of *N. (Nostoceras)*. This is especially true in comparison with Hornby Island specimens given the degree of helical whorl reduction in relation to an elongated U-shaped retroversal body chamber with an upward-facing aperture positioned directly under the helical whorls. The *N. (Nostoceras)* taxa of the upper Northumberland Formation succeeded *N. (D.?) adrotans* toward the latest Campanian much in the same manner that *N. (Didymoceras)* index species gave way to those of the subgenus *N. (Nostoceras)* belonging to the more widely distributed *N. (N.) hyatti* assemblage zone fauna in the Western Interior (Kennedy & Cobban 1993c; Kennedy *et al.* 2000d). This does not necessarily imply a direct phylogenetic relationship, but rather illustrates increasing regional prevalence of *N. (Nostoceras)* over *N. (Didymoceras)* in approach to the CMB.

3.5 Heteromorph ammonoid palaeobiogeography

Tracking morphological changes over time is essential in developing models for the evolutionary progression of taxa. Isolating the factors that determine geographic range is equally important in an approach to understanding speciation and relationships between populations. Based on the small size of their embryonic shells, heteromorph ammonoids are presumed to have released vast numbers of eggs in a breeding cycle (e.g. Kennedy 1993) and therefore their egg masses and neanic individuals drifting high in the water column would have been greatly susceptible to dissemination by ocean currents (e.g. Arkell 1957; Tanabe *et al.* 1981; Sohl 1985; Westermann 1996; Lewy 2002). This reproductive strategy and central facet of ammonoid ecology would have been a major underlying factor accounting for the broad dispersal of taxa and the world-wide distribution of many forms.

The waters of the world's oceans stood removed from those of the Western Interior Seaway of North America during the late Campanian where diplomoceratid diversification was reduced and ammonoid speciation was comparatively low inland than it was in its southern

reaches (Tsujita & Westermann 1998). Studies considering ammonite assemblages from the Western Interior and Gulf Coast have concluded that regional differences in the representation of taxa were due to ecological segregation corresponding to palaeobathymetry (Batt 1989; Ifrim *et al.* 2004). The depth of the Western Interior Seaway, as interpreted from the Pierre Shale of Wyoming, was around 60 m where both *Exiteloceras* and *Solenoceras* occur (Gill & Cobban 1966). Outer shelf sediments of the Navesink Formation of New Jersey, representing the eastern extent of *Exiteloceras* in North America were deposited at depths perhaps no greater than 100 m (Olsson 1963; Cobban 1974).

Unlike members of *Exiteloceras* and *Solenoceras*, certain heteromorph taxa such as *D.* (*D.*) *cylindraceum* and *N.* (*N.*) *hornbyense* flourished in the North Pacific during the late Campanian yet remain entirely absent in the fossil record of the Western Interior Seaway. One explanation is that these species may have been among those which preferred deeper water habitats in shelf environments (Nesis 1986; Ward 1986) in turn favouring pelagic migratory routes which largely bypassed the seaway. For reasons previous outlined, septal suture complexity and shell morphology advocate the capacity of such forms to exploit benthic niches (e.g. Ward & Westermann 1977; Klinger 1980; Tanabe *et al.* 1981; Batt 1989; Westermann 1996; He *et al.* 2005). Even if drifting egg masses or neanic juveniles were to be carried inland, their development would have likely been hindered by differences in water temperature, salinity (Wright 1987; He *et al.* 2005), and increased predation (Ward 1996) in the shallow shelf environment.

A westward surface current along the southwest coast of North America during the Late Cretaceous has been postulated (Sliter 1973). This scenario would present conditions more favourable to exotic taxa—such as species of *Solenoceras*—entering the North Pacific province. However, the same could be argued for an East-flowing current around the Gulf of Mexico into the Atlantic in approach to the Maastrichtian allowing for the broader dissemination of taxa with probable origins in the North Pacific such as *Fresvillia* and *Phylloptychoceras*. While the directionality of such currents is speculative, what remains clear is the necessity of a Caribbean corridor during the late Campanian to account for interprovincial ammonoid migration (Ifrim *et al.* 2004). Indeed, the presence of *N.* (*Didymoceras*), *Exiteloceras*, and *Solenoceras* within the Hornby Island heteromorph assemblage—taxa well represented from the Gulf Coast and Western Interior—requires movement to have taken place between these biotic provinces.

Post-mortem shell drift has been perceived as an unlikely factor impacting heteromorph ammonoids in epicontinental seas (Batt 1989). In contrast, post-mortem drift in modern *Nautilus* has been recorded up to a distance of 10^3 km in the open ocean (Saunders & Spinosa 1979) although shell distribution is generally confined to latitudes within their original habitat (Tanabe 1979). The presence of *N. (N.) hornbyense* material in Angola (e.g. Spath 1921; Howarth 1965) and Nigeria (Zaborski 1985) is therefore supporting evidence for Caribbean passage and the likelihood that the species was predominantly subtropical. The cosmopolitan planispiral tetragonitid *Pseudophyllites indra* (Forbes, 1846), for instance, has been recorded from Hornby Island (e.g. Whiteaves 1903; Usher 1952) and observed from the Gulf Coast and Atlantic Highlands (Cobban & Kennedy 1995) to Far East Russia (Jagt-Yazycova 2011) demonstrating the permeability of the North Pacific province by either Arctic or Caribbean corridors during the late Campanian.

While the earliest records of taxa point to their locations of emergence, these occurrences constitute an insufficient basis upon which to draw firm conclusions as to the palaeogeographic origins of family lineages. It is important to note that isolating incidents of faunal migration and dispersal is inherently problematic given that these events are virtually instantaneous when perceived through the lens of the vast expanse of geologic time. Greater accuracy can be demonstrated in the mapping of phylogenetic relationships between groups based on their morphological characteristics. While such efforts can be complicated by regional endemism and potentially abrupt changes in shell modification (Okamoto 1988b, 1989), these structural adaptations offer insight into ammonoid ecology that must be considered within a broader context of climactic and environmental upheaval.

Chapter 4

Late Campanian (Late Cretaceous) dinoflagellate cysts from Hornby Island, British Columbia with implications for Nanaimo Group biostratigraphy and palaeoenvironmental reconstructions

4.1 Abstract

Thirty mudstone subsamples obtained from coastal exposures of the Northumberland Formation on Hornby Island have yielded diverse dinoflagellate cyst and terrestrial palynomorph assemblages. Dinoflagellate cyst taxa corresponding to eight families and 60 genera are well preserved. Specimens referable to 61 formally established species are identified. The areoligeracean *Canningia diezeugmenis* sp. nov. is proposed. The palynological record supports a late Campanian age for the Northumberland Formation. The assemblages suggest that sediment deposition occurred within an inner shelf environment marked by high nutrient influx and primary productivity.

4.2 Materials and methods

Twenty-five mudstone samples—and thirty subsamples—originating from a series of coastal exposures on Hornby Island were obtained through field work and the collections of the Royal BC Museum (Victoria, British Columbia, Canada). All processed subsamples were assigned catalogue numbers and are housed within the Palaeoenvironmental and Marine Palynology Laboratory, School of Earth and Ocean Sciences, University of Victoria (UVic; Victoria, British Columbia, Canada). Twenty-nine of the 30 matrix subsamples were extracted from carbonate mudstone concretions; 24 of which bore molluscan macrofossils. A non-concretionary sample (yielding subsample UVic 14-270) was taken from finely laminated, friable mudstone to serve as

a control since this lithology comprises the bulk of the section. Both the geographic location (Fig. 4.1) and inferred stratigraphic position (Fig. 4.2) of each concretionary sample was plotted.

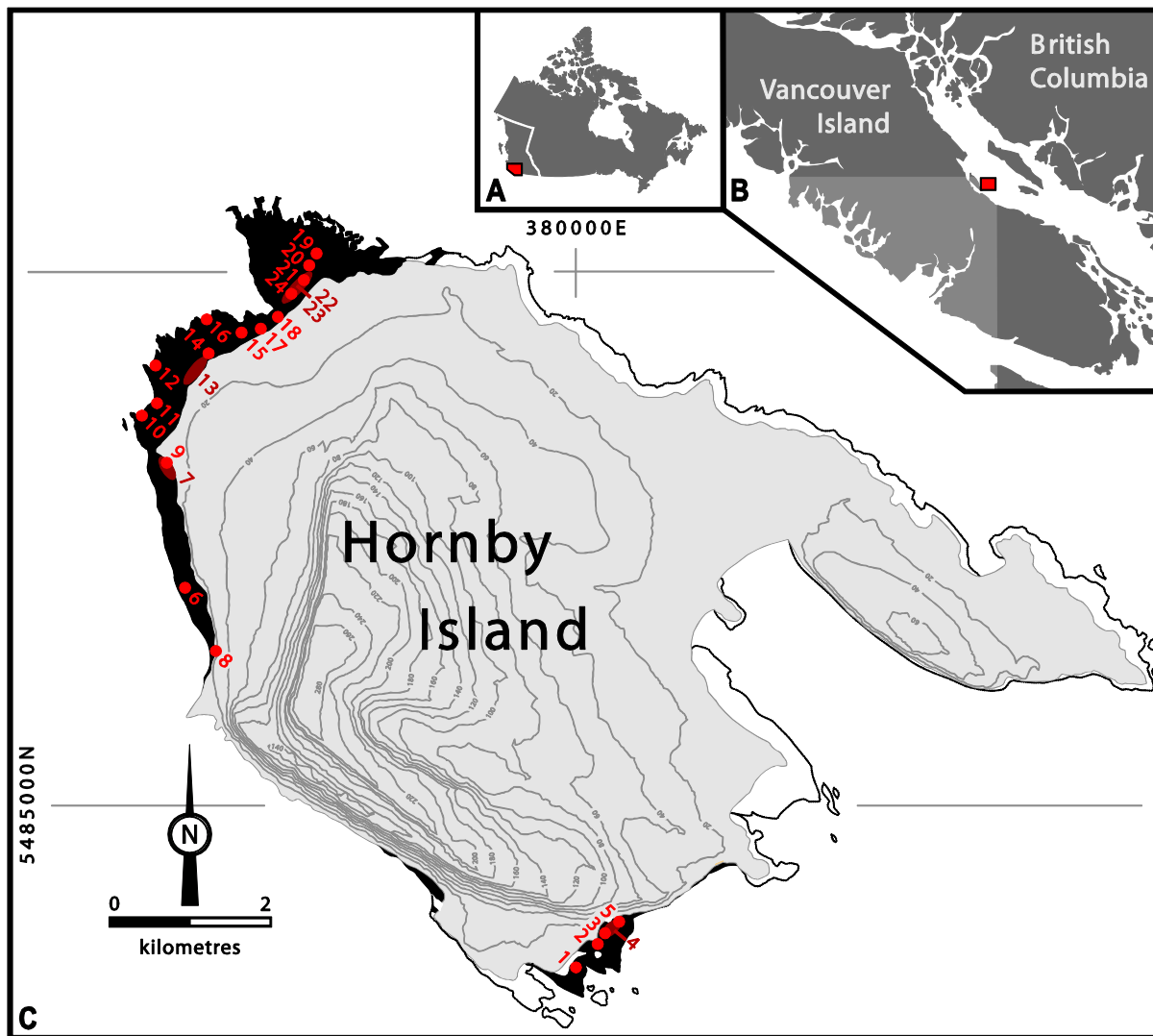


Figure 4.1. **A**, location of the Georgia Basin (red) within British Columbia. **B**, location of Hornby Island (red). **C**, geology and topography of Hornby Island adapted from Katnick & Mustard (2001, 2003) with locations of concretionary mudstone matrix samples (red points) marked across the extent of Northumberland Formation coastal outcrop (black). Dark red zones denote float sample localities. Solid points denote in situ samples.

Figure 4.2. Schematic framework of the Northumberland Formation on Hornby Island, modified from McLachlan & Haggart (accepted), with plotted stratigraphic positions of matrix samples and dinoflagellate cyst zonation. Grey denotes imprecision of float samples. Chronostratigraphy inferred from Haggart *et al.* (in prep). Magnetostratigraphy and chron assignments (C33n, C32n.2n) inferred from Raub *et al.* in Ward *et al.* (2012). DC = dinoflagellate cyst ecozones. F = foraminiferal zones of McGugan in Muller & Jeletzky (1970). M = molluscan zones of McLachlan & Haggart (accepted). Lithostratigraphy modified from Katnick (2001). ST = stratigraphic level above base of section. D = DeCourcy Formation. G = Geoffrey Formation.

Sediment samples were treated using a standard palynological method (e.g. Rochon *et al.* 1999; Pospelova *et al.* 2005, 2010; Mertens *et al.* 2009). For each sample, subsamples of ~ 2 cm³ of matrix were weighed and placed in 50 ml test tubes. The dry weight of the subsamples was recorded with an average of 7.6 g. Subsamples were treated repeatedly with 10 ml of 10 percent room-temperature hydrochloric acid (HCl) which was effective in dissolving a major portion of the carbonates. Concretionary subsamples reacted immediately due likely to higher carbonate concentration in relation to laminated mudstone subsample 14-270 which showed a delayed reaction time of 15–20 minutes. One 18,584-spore *Lycopodium clavatum* tablet of batch #177745 produced at the Earth and Ecosystem Sciences Department of Lund University (Lund, Sweden) was added to each subsample to enable the establishment of dinoflagellate cyst absolute abundances (e.g. Benninghoff 1962; Mertens *et al.* 2009, 2012). Following HCl, the subsamples were sieved through 15 µm nylon mesh to remove excess particles prior to being left to sit in 15 ml of 48 percent hydrofluoric acid (HF) for up to three weeks. Afterward, each subsample underwent one round of HCl and two rinses of reverse osmosis water to remove any remaining HF residue before final sieving through 120 µm and 15 µm mesh to remove particles with up to one minute of sonication.

Once sieving was completed, portions of the concentrated residue were mounted on glass slides in preparation for light microscopy. Mounting was conducted on a hot plate where the material from a pipette-transferred subsample drop was consolidated with a drop of glycerin jelly through toothpick stirring. Coverslips were applied and sealed with Rimmel Lasting Finish Pro nail polish. Once examined under a Nikon Eclipse 80i light microscope, photography was conducted under 600x or 1000x magnification—depending on specimen size—with a Nikon DS-

5M-L1 digital camera system. Epifluorescence analysis was conducted on selected dinoflagellate cysts using a Nikon Intensilight C-HGFI precentred fiber illuminator. Among the dinoflagellate cysts analysed for epifluorescence were examples of all peridiniinean taxa present; of those genera which illuminated, an epifluorescent image is provided.

Bright-field photo micrographs of specimens were arranged into bitmap plate images using Macromedia Fireworks 8 software. For clarity of presentation, extraneous particulate debris was removed from the field of view through use of the eraser, lasso, and marquee tool in the software. A neutral portion of the bitmap was then selected, expanded and subjected to the Gaussian blur function to create a neutral background over which the unaltered specimen image was then superimposed. The brightness and contrast were then balanced between both layers through black level adjustment. The Gaussian blur function was applied to a duplicate dinoflagellate cyst image layered above the neutral background and beneath the unaltered dinoflagellate cyst image; the eraser tool was then applied to create seamless pixilation between them. During the bitmap modification process, care was taken to retain a bright-field perimeter around each dinoflagellate cyst image layer so that pixel alteration through cropping or erasing was limited exclusively to the bright-field and any surrounding debris.

In approach to conducting palynomorph counts, a *principle of majority bodies* was applied wherein a single entity was recorded as such if the majority of its structure was intact, i.e. over one-half of a dinoflagellate cyst (operculum notwithstanding), bisaccate pollen central bodies in association with at least one bladder, and a trilete spore of at least two-thirds. Foraminiferal organic linings were counted as long as at least three adjoining chambers were present. Marine palynomorphs were counted as dinoflagellate cysts, acritarchs, and other palynomorphs; terrestrial palynomorphs were counted according to the categories of *Aquilapollenites* pollen, bisaccate pollen, Normapolles pollen, other pollen, monolete spores, and trilete spores. A minimum of at least 200 cysts were counted for each concretionary subsample, a figure deemed sufficient for statistical purposes in light of previous Mesozoic analytics (e.g. Harker *et al.* 1990). Beyond the counts, a minimum of at least two slides were scanned for each subsample to ensure observation of outlying taxa.

Terminology relating to classes of relative abundance follow the parameters of Pospelova *et al.* (2004): present (> 0–1%); rare (1–5%); common (5–30%); abundant (30–50%); dominant (>50%). Grouping of taxa (spp.) was conducted where generic affinity could be established but

identification to the specific level was difficult due to morphological gradation or a high frequency of unusual trait combinations. In total, 99 dinoflagellate cyst taxonomic entities were established and their stratigraphic distribution plotted throughout the studied section (Table 4.1) Absolute and relative abundances of dinoflagellate cysts and terrestrial palynomorphs were calculated based on counts data (Appendix V, VI) and presented using Tilia and Adobe Illustrator CS2 software.

Table 4.1. Stratigraphic distribution of dinoflagellate cyst taxa within the Northumberland Formation on Hornby Island in order of lowest stratigraphic occurrence. Dotted line denotes the 4.4 km separation along strike between northwestern and southeastern coastal exposures.

Sample No.	Subsample (UVic ID)	Slides Examined
24	15-767	2
24	15-766	2
23	16-369	2
23	14-274	2
22	16-368	5
22	14-273	2
21	16-366	2
20	16-365	2
19	15-768	2
18	15-765	2
17	16-364	2
16	15-764	2
15	16-363	2
14	16-377	2
13	14-272	2
12	15-763	2
11	15-762	2
10	15-761	2
9	15-760	2
8	15-758	2
7	16-367	2
7	14-271	2
6	15-759	2
5	16-362	2
4	14-269	2
3	15-757	2
2	15-756	2
1	16-361	3
1	15-755	3

●	<i>Dinogymnium avellana</i>
●	Cyst Type B
●	<i>Dapsilidinium cf. pseudocolligerum</i>
●	<i>Dinogymnium cretaceum</i>
●	<i>Alterbidinium ? spp.</i>
●	<i>Dinogymnium longicorne</i>
●	<i>Hystrichosphaeridium tubiferum</i>
●	<i>Dinogymnium acuminatum</i>
●	<i>Xenascus ceratioides</i>
●	<i>Hafniasphaera septata</i>
●	<i>Impagidinium rigidaseptatum</i>
●	<i>Polysphaeridium spp.</i>
●	<i>Spiniferites sp. A</i>
●	<i>Fibrocysta spp.</i>
●	<i>Hafniasphaera delicata</i>
●	<i>Hystrichodinium pulchrum</i>
●	Peridinioid Group B
●	<i>Areoligera spp.</i>
●	<i>Cladopyxidium paucireticulatum</i>
●	<i>Cyclonephellium spp.</i>
●	<i>Glyphanodinium facetum</i>
●	<i>Impagidinium cf. scabrosum</i>
●	<i>Phanerodinium belgicum</i>
●	<i>Spiniferites cornuta</i>
●	<i>Spiniferites spp.</i>
●	<i>Tanyosphaeridium xanthiopyxides</i>
●	<i>Xenicodinium delicatum</i>
●	Cyst? Type A
●	<i>Dinogymnium sp. A</i>
●	<i>Dinogymnium sp. B</i>
●	<i>Neoeurysphaeridium ? sp.</i>
●	<i>Phanerodinium sp.</i>
●	<i>Phanerodinium ? turnhoutensis</i>
●	<i>Cerodinium glabrum</i>
●	<i>Cerodinium diebelii</i>
●	<i>Hystrichosphaeridium recurvatum</i>
●	<i>Eisenackia ? sp.</i>
●	<i>Glaphyrocysta-Membranophoridium spp.</i>
●	<i>Laciniadinium rhombiforme</i>
●	<i>Lejeuniacysta cf. hyalina</i>
●	<i>Lejeuniacysta sp.</i>
●	<i>Bohaidina spp.</i>
●	Peridinioid Group A

Age. Previously constrained to the early–middle Eocene (Damassa 1979; de Coninck 1986).

Genus *Alterbidinium* (Lentin & Williams, 1985) Fensome *et al.*, 2016

Alterbidinium? spp.

(Pl. 4.2A–E)

Remarks. Specimens assigned to *Alterbidinium* spp. encompass forms akin to *Alterbidinium recticorne* (Vozzhennikova, 1967) Harker *et al.*, 1990 in being rhomboidal while others approach an ovoid profile. Cysts within this group possess either an isodeltaform hexa I_{2a} or I_{1–3a} archaeopyle; the latter running contrary to conventional interpretation of the genus (e.g. Fensome *et al.* 2009, 2016). Specimens of rhomboidal profile typically exhibit an I_{1–3a} archaeopyle although it is noteworthy that ovoid forms bearing an I_{2a} archaeopyle frequently present dehiscence along the sutural boundaries between the apical plates and intercalary plates 1a and 3a.

Genus *Areoligera* (Lejeune-Carpentier, 1938) Williams & Downie, 1966

Remarks. Specimens assigned to *Areoligera* are distinguished from all other areoligeracean genera within the Hornby Island section by the presence of disjunct, penitabular, taeniate process complexes with basal ridges arranged in annulate or arcuate fashion on the dorsal surface. In *Cyclonephelium* spp., process complexes are predominantly marginate and of unit type. In the *Glaphyrocysta–Membranophoridium* spp. plexus, marginate process complexes range from those with trabecular, distal connections to those forming an intricate lattice or perforate membrane.

Areoligera spp.

(Pl. 4.3C, D; Fig. 4.3D–F)

Remarks. Fensome *et al.* (2009) defined a series of subdivisions within the plexus of morphologies which comprise the genus *Areoligera*. Within the Hornby Island subsamples, areoligeracean cysts assignable to *Areoligera* spp. encompass forms corresponding to *Areoligera*

coronata (Wetzel, 1933) Lejeune-Carpentier, 1938, *Areoligera volata* Drugg, 1967, *Areoligera flandrensis* Slimani, 1994, *Areoligera medusettiformis* (Wetzel, 1933 ex Lejeune-Carpentier, 1938 *sensu* Schiøler & Wilson (2001), and *Areoligera senonensis* Lejeune-Carpentier, 1938. The vast majority of specimens fall within the parameters of *A. coronata* and *A. volata* but specific placement of these morphotypes has been withheld due to gradation between forms within the same subsamples.

In specimens approaching *A. coronata* morphology, the distal ends of lateral processes often recurve, touching the tips of adjacent processes. These recurving process tips are fused in other specimens, forming branched, trabecular connections within the linear, wing-like structures which characterize *A. volata*. The plexus exhibits variability in the length of processes, overall cyst size and pronunciation of antapical lobes.

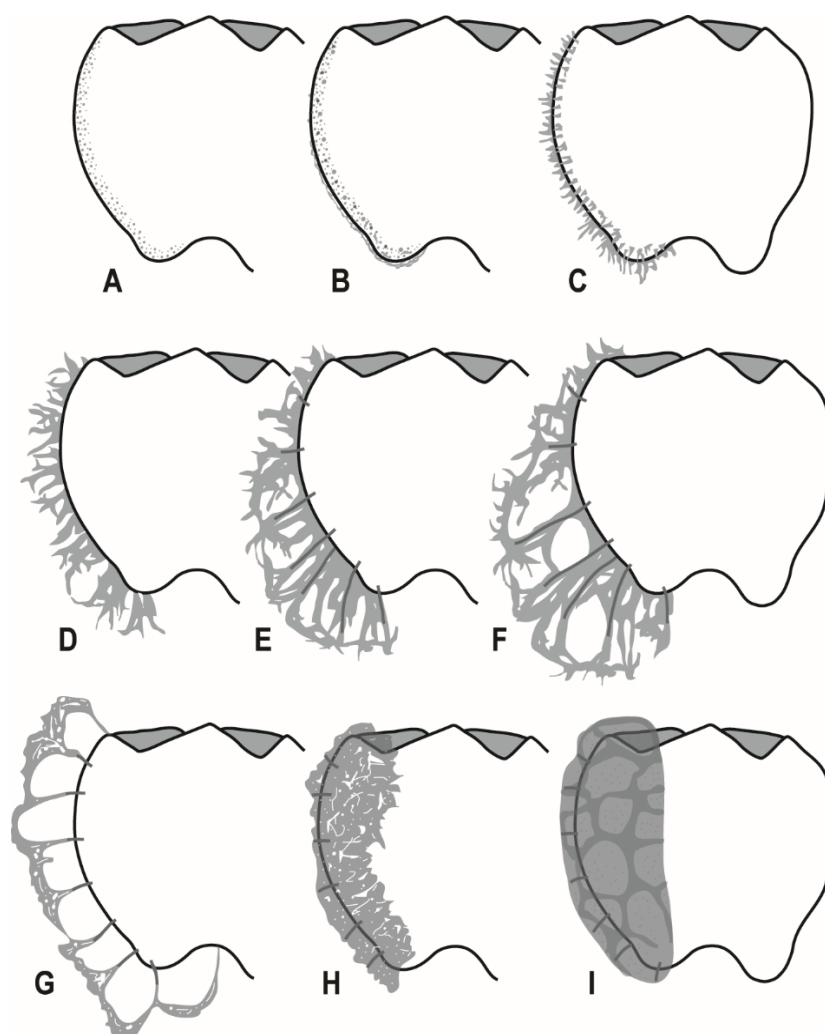


Figure 4.3. A–I, schematic diagrams illustrating the plexus of morphologies corresponding to various areoligeracean cyst taxa within the Hornby Island section as expressed through ventral margin ornamentation. **A**, *Circulodinium* cf. *colliveri*; **B**, *Circulodinium*? sp.; **C**, *Cyclonephelium* spp.; **D–F**, *Areoligera* spp.; **G, H**, *Glaphyrocysta–Membranophoridium* spp. plexus; **I**, *Renidinium* spp.

Genus *Areosphaeridium* (Eaton, 1971) Stover & Williams, 1995

Areosphaeridium? sp.

(Pl. 4.3E)

Remarks. Represented by a single specimen, this cyst is questionably assigned to *Areosphaeridium* due to the presence of what appears to be a single process centered in the antapical region—as opposed to two—which defines *Enneadocysta* (Stover & Williams 1995; Fensome *et al.* 2006). However, the ambiguous orientation of the archaeopyle in relation to this and adjacent fenestrate, clypeate processes sees its placement within this genus as uncertain.

Genus *Bohaidina* (Song Zhichen *et al.*, 1978) Sun Xeukun, 1994

Age. Previously constrained to the Paleogene (e.g. Chen *et al.* 1988; Sun Xeukun 1994).

Bohaidina spp.

(Pl. 4.2F–I)

Remarks. Specimens assigned to *Bohaidina* spp. encompass morphologies with hyaline to finely granulate surface texture corresponding to forms similar to *Bohaidina laevigata* (Song Zhichen *et al.*, 1978) Xu Jinli & Mao Shaozhi, 1989 and *Bohaidina retirugosa* (Song Zhichen *et al.*, 1978) Xu Jinli & Mao Shaozhi, 1989. There exists the hypothetical possibility of confusion between forms with a hyaline autophragm and the endophragm of cysts assigned to *Alterbidinium* spp. Although damage or alteration resulting in total periphragm disassociation is difficult to demonstrate, speculation on isolated endocysts of circumcavate peridiniaceans holds precedent (e.g. Edwards 2001).

Genus *Canningia* (Cookson & Eisenack, 1960b) Helby, 1987

Canningia diezeugmenis sp. nov.

(Pl. 4.4A–I; Fig. 4.4A, B)

Types. The type series is housed in the Palaeoenvironmental and Marine Palynology Laboratory, School of Earth and Ocean Sciences, University of Victoria and consists of the holotype (subsample 14-273, slide A, England Finder reference V38/3) and paratypes of the cyst body (subsample 16-368, slide E, England Finder reference W33/3) and operculum (subsample 16-368, slide E, England Finder reference S38/2).

Diagnosis. Proximochorate, subpentagonal to pentagonal cyst. Holocavate with the exception of closely appressed wall layers in mid-dorsal and mid-ventral areas. Archaeopyle apical, with formula $A_{(1-4)}$. Ectophragm comprised of a perforate membrane supported by membranous columnar to taeniate, ribbon-like processes largely constrained to the dorso- and ventrolateral margins. Apical, lateral and antapical horns well developed. Antapex asymmetrical with the left antapical horn longer than the right.

Etymology. Latin, *diezeugmenos*, meaning disjunct or separate in reference to the disparity in ornamentation and ectocoel separation between lateral and medial regions.

Description. Proximochorate, subpentagonal to pentagonal cyst. Holocavate with the exception of closely appressed wall layers in mid-dorsal and mid-ventral areas. Archaeopyle apical, with formula $A_{(1-4)}$, operculum detached leaving zigzag margin. Ectophragm comprised of a perforate, fenestrate membrane (Pl. 4.4D) supported by membranous columnar to taeniate, ribbon-like processes largely constrained to the dorso- and ventrolateral margins. Endophragm and ectophragm (both 0.5 μm thick in holotype) appressed on mid-dorsal and mid-ventral surfaces where processes sparse or absent. Surface marked by fine granulation. Apical, lateral and antapical horns well developed. Antapex asymmetrical with the left antapical horn longer than the right, the former often attaining twice the length of the latter. Tabulation indicated by bands of processes aligned along dorsolateral margins.

Dimensions (μm).

W:	75.31 (105.49) 132.97; N: 48.
Wi:	61.6 (90.44) 116.88; N: 50.
L:	64.02 (103.46) 80.24; N: 53.
Li:	53.38 (78.80) 93.1; N: 56.
L ₁ :	6.59 (15.75) 25.57; N: 56.
L ₂ :	2.49 (5.96) 15.95; N: 56.
O:	43.3 (50.42) 57.53; N: 2.
Oi:	42.18 (44.61) 47.04; N: 2.

Remarks. *C. diezeugmenis* bears closest affinity to *Canningia grandis* Helby, 1987 with which it shares a comparable ectophragm reticulum but differs in the restriction of this feature to the dorso- and ventrolateral margins where there is typically greater separation between the endo- and ectophragm. *Canningia bassensis* Marshall, 1990 is similar as well in exhibiting reduced ectophragm separation on the dorsal and ventral surfaces, although the species' ectophragm occurs in elevated patches in these regions resulting in a clearly discernable cingulum indicated by transverse sutural folds. *C. diezeugmenis* exhibits greater development and projection of the lateral and antapical horns than any other species belonging to the genus. It is possible that these taxa represent ecophenotypic variants but such an hypothesis, as may be applicable to other areoligeraceans, would require support from the observation of gradational morphotypes within an isolated assemblage.

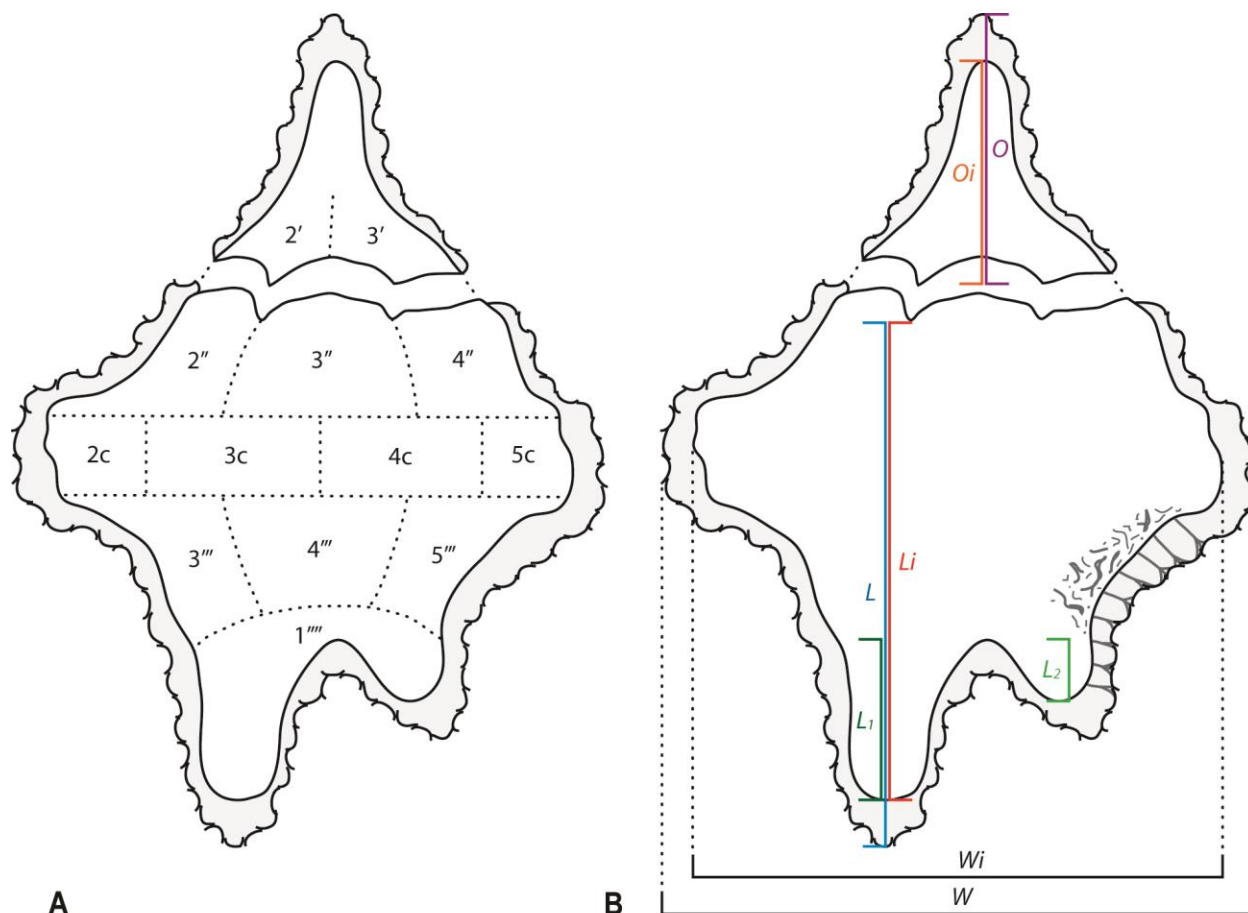


Figure 4.4. **A, B**, inferred tabulation and areoligeracean cyst measurement model modified from Clarke & Verdier (1967) applied to schematic diagrams of *Canningia diezeugmenis* sp. nov. **A**, inferred tabulation of dorsal surface; **B**, imposed measurement parameters on dorsal surface with ectophragm texture and support structure distribution indicated in posterolateral quadrant. Grey area denotes ectocoel.

Genus *Cerodinium* (Vozzhennikova, 1963) Lentin & Williams, 1987

Cerodinium diebelii (Alberti, 1959) Lentin & Williams, 1987

(Pl. 4.5B, C)

Remarks. One specimen from subsample 15-757 (Pl. 3.5B) appears to exhibit a latideltiform hexa archaeopyle which contravenes the isodeltaform to isothetaform archaeopyle parameters of the genus (*sensu* Fensome & Williams 2005; Fensome *et al.* 2009, 2016). However, it is possible that a small degree of periphragm folding could account for this seemingly aberrant geometry.

Cerodinium cf. leptodermum (Vozzhennikova, 1963) Lentin & Williams, 1987

(Pl. 4.5E)

Remarks. Represented by a single specimen, this cyst possesses the characteristic elongate body and longitudinal wrinkles of *C. leptodermum* but differs from the original description of the species in exhibiting a broader apical horn and thinner walls. In their expanded description of the taxon, Lentin & Vozzhennikova (1990) note dark brown colouration in their material. However, the specimen examined herein is nearly translucent as a function of its thin wall.

Genus *Circulodinium* Alberti, 1961

Remarks. Fensome & Williams (2005) informally proposed the genus “*Reculadinium*” to account for areoligeracean cysts bearing low-relief, granulate to denticulate ornamentation. While forms attributable to such a group have since been retained within *Circulodinium* (Williams *et al.* 2017), the basis upon which “*Reculadinium*” was founded is also reflected in specimens from the Hornby Island section with respect to variability in the degree of asymmetry and antapical lobe definition.

Circulodinium? sp.

(Pl. 4.6A–C; Fig. 4.3B)

Remarks. Cysts questionably assigned to *Circulodinium* given the presence of a periphragm clearly appressed in most areas while allowing for discreet cornucavation in the antapical region. Among members of the genus, this species is most similar in its cross-sectional profile to *Circulodinium assymmetricum* (Burger, 1980) He Chengquan & Sun Xuekun, 2000.

Genus *Cladopyxidium* (McLean, 1972) Below, 1987

Cladopyxidium sp.

(Pl. 4.7D, E)

Remarks. Represented by a single specimen, the vermiculate sutural ridges and elongated, ellipsoidal profile distinguish this cyst from prevalent examples of *Cladopyxidium*

paucireticulatum Slimani, 1994 within the Hornby Island section as well as and all other species recognized within the genus.

Genus *Cordosphaeridium* (Eisenack, 1963) Davey, 1969b

Cordosphaeridium callosum Morgenroth, 1966

(Pl. 4.1C, D)

Age. Previously constrained to the Eocene (e.g. de Coninck 1986).

Cordosphaeridium spp.

(Pl. 4.1E, F)

Remarks. Chorate cysts with variable degrees of surface granulation as well as proximal and distal width of mesotabular, fibrous processes. Archaeopyle presumed precingular; rarely observed.

Genus *Coronifera* (Cookson & Eisenack, 1958) Moa Shaozhi & Norris, 1988

Coronifera oceanica Cookson & Eisenack, 1958 *sensu* Schiøler & Wilson (2001)

(Pl. 4.8A–C)

Remarks. Represented by three specimens, these cysts bear a pronounced, elongated apical process not noted in the original description (Yun Hyesu 1981). This feature, coupled with a distinct antapical process, was essentially the basis of the informally proposed species *Coronifera “bipolare”* of Fensome & Williams (2005) figured by Schiøler & Wilson (2001, pl. 2, fig. 40). These forms are transitional between *C. oceanica sensu stricto* and *Coronifera hebospina* (Yun Hyesu, 1981) Peyrot, 2011 given occasional bifurcate distal process endings which characterize the former among those which are predominantly acuminate and diagnostic of the latter.

Genus *Cyclonephelium* Deflandre & Cookson, 1955 *sensu* Fensome *et al.* (2009)

Cyclonephelium spp.

(Pl. 4.6E, F; Fig. 4.3C)

Remarks. Specimens assigned to *Cyclonephelium* spp. possess dorsal and ventral surfaces devoid of process complexes. Only the lateral margins of the pre-, cingular, and postcingular plate series may be indicated by the alignment of low-relief, taeniate processes of unit type. This plexus encompasses forms most similar to *Cyclonephelium compactum* Deflandre & Cookson, 1955 and *Cyclonephelium vannophorum* Davey, 1969a.

Genus *Dapsilidinium* (Davey & Williams, 1966) Bujak *et al.*, 1980

Dapsilidinium cf. pseudocolligerum (Stover, 1977) Bujak *et al.*, 1980

(Pl. 4.10A, B)

Remarks. Specimens assigned to *D. cf. pseudocolligerum* are noted for possessing an apical boss, a feature not included in the original description of the species. Mertens *et al.* (2014) regarded *D. pseudocolligerum* to be a junior synonym of *Dapsilidinium pastielsii* (Davey & Williams, 1966) Bujak *et al.*, 1980. However, explicit identification for the Hornby Island morphotype is withheld due to lack of correspondence with the latter taxon *sensu stricto* and the morphological distinctions between forms noted by Fensome *et al.* (2009, 2016)

Genus *Dinogymnium* (Evitt *et al.*, 1967) Lentin & Vozzhennikova, 1990

Dinogymnium cf. aerlicum Londeix *et al.*, 1996

(Pl. 4.11E)

Remarks. Represented by a single specimen, this form is distinguished from others assignable to *D. longicorne* chiefly by its acutely acuminate antapical region.

Age. Previously constrained to the late Berriasian–Hauterivian (Londeix *et al.* 1996).

Dinogymnium avellana (Lejeune-Carpentier, 1951) Evitt *et al.*, 1967

(Pl. 4.11F)

Remarks. Represented by a single specimen.

Dinogymnium sp. A

(Pl. 4.11H)

Remarks. Represented by two specimens, this form is distinguished from others assignable to the genus within the Hornby Island section by its densely granulate surface.

Dinogymnium sp. B

(Pl. 4.11I)

Remarks. Represented by a single specimen, this form is distinguished from others assignable to the genus within the Hornby Island section by its small size, subovate profile, and what is presumed to be a reduced epitheca.

Genus *Diphyes* (Cookson, 1965a) Goodman & Witmer, 1985

Diphyes spp.?

(Pl. 4.12B–F)

Remarks. Represented by four specimens, these proximochorate cysts are referable to the genus *Diphyes* but differ from all other described species in bearing short, verrucate to acutely acuminate, nontabular processes and a broadly rounded, depressed to bulbous, antapical process. Endophragm is granulate and in contact with hyaline periphragm accept beneath processes. Distal process bifurcations are present in only one specimen (Pl. 4.12E) which also bears a somewhat reduced antapical process in comparison to the other three. Due to the small sample size and known variability in other species such as *Diphyes colligerum*, justification for the taxonomic distinction of this specimen on these grounds remains unresolved.

Genus *Druggidium* (Habib, 1973) Harding, 1986

Druggidium? cf. discretum Slimani & Louwye, 2011

(Pl. 4.9A–D)

Age. Previously constrained to the late Maastrichtian (Slimani & Louwye 2011; Slimani *et al.* 2011).

Remarks. Proximate cysts with a prominent P_{2a} archaeopyle questionably assigned to *Druggidium*, differing from forms characteristic of the genus by the presence of a small, distally open apical horn. These cysts are also tentatively referred to *D. discretum* from which they differ in possessing epi- and hypothecae of approximately equal size. A similar distally open apical horn-like feature also appears to be visible in the holotype (Slimani & Louwye, 2011, Pl.1 fig. 3) although it has been attributed to an operculum comprised of an apical and anterior intercalary plate series. It is with their spongy, tectate wall structure and presence of an—albeit reduced—apical horn that these cysts also resemble *Apteodinium granulatum* (Eisenack, 1958) Lucas-Clark, 1987 *sensu* Riding & Fensome (2002). Specimens epifluorescent.

***Druggidium?* sp.**

(Pl. 4.9E, F)

Remarks. Ovoid cysts questionably assigned to *Druggidium* in possessing epi- and hypothecae of approximately equal size. These cysts bear a finely granulate surface with tabulation clearly indicated by low, modestly vermiculate, sutural ridges and a well-defined cingulum. Beyond lacking an apical horn, these forms bear superficial affinity to *Cribroperidinium* taxonomic junior synonym *Millioudodinium* in lacking accessory ridges beyond those which demarcate plate boundaries (Stover & Evitt 1978; Duxbury 1980).

Genus ***Eisenackia*** (Deflandre & Cookson, 1955) Quattrocchio & Sarjeant, 2003

***Eisenackia?* sp.**

(Pl. 4.13A–C)

Remarks. Specimens assigned to *Eisenackia?* sp. bear closest affinity to *Eisenackia crassitabulata* (Deflandre & Cookson, 1955) McLean, 1973 but differ in expressing much less extensive connectivity between rugulate surficial elements in alignment along sutural

boundaries. The mode of contabular ornamentation is not unlike that of *Cerebrocysta* which differs from *Eisenackia* in possessing a precingular archaeopyle (Bujak *et al.* 1980).

Genus *Fibrocysta* Stover & Evitt, 1978

Fibrocysta spp.

(Pl. 4.14A–E)

Remarks. Specimens assigned to *Fibrocysta* spp. encompass a range of morphologies with variability in process width and their degree of basal connectivity. The plexus consists of forms similar to *Fibrocysta ovalis* (Hansen 1977) Lentin & Williams, 1981 *sensu* Machalski *et al.* (2016).

Genus *Geiselodinium* (Krutzsch, 1962) Chen *et al.*, 1988

Geiselodinium geiseltalense Krutzsch, 1962

(Pl. 4.15A, B)

Remarks. Represented by a single specimen.

Age. Previously constrained to the lower-middle Eocene (e.g. Krutzsch 1962).

Genus *Gonyaulacysta* (Deflandre, 1964) Helenes & Lucas-Clark, 1997

Gonyaulacysta? sp.

(Pl. 4.9G, H)

Remarks. Represented by a single specimen. A proximate cyst with periphragm comprising numerous vermiculate surficial folds and blunt, acuminate apical horn. Cingulum clearly demarcated. I_{2a} archaeopyle.

Genus Group *Glaphyrocysta* (Stover & Evitt, 1978) Fensome *et al.*, 2009

–*Membranophoridium* (Gerlach, 1961) Stover & Evitt, 1978

Remarks. Although members of both *Glaphyrocysta* and *Membranophoridium* are devoid of dorsal or ventral process complexes, they often present cingular indications predominantly restricted to the dorsolateral margins; such indications range from the sutural alignment of taeniate processes in *Glaphyrocysta* to “linear thickenings” in *Membranophoridium* (Stover & Hardenbol, 1994, p. 37). In some Hornby Island specimens, these features achieve transverse continuity across the dorsum. In principal, surficial folds or expressions of reduced granulation reflecting dorsal tabulation become increasingly more evident in plexus gradation from forms corresponding to *Glaphyrocysta* to those more akin to *Membranophoridium*.

Generic differentiation within this plexus has proven problematic with the challenge constrained to gradation between the intricate trabecular lattices of *Glaphyrocysta* and the perforate membranes supported by processes, which constitute the ectophragm of *Membranophoridium*. Despite the gradation between forms, the author acknowledges the merit in conceptual retention of *Membranophoridium* as proposed by Fensome & Williams (2005). Additional difficulty surrounds determination of the point at which the continuous membranes of *Membranophoridium* fully envelope the lateral margins of the endocyst effectively becoming maginocavate ectophragm structures approaching the diagnostic pericoels of *Renidinium*.

***Glaphyrocysta–Membranophoridium* spp.**

(Pl. 4.3F–H; Fig. 4.3G, H)

Remarks. This plexus of morphologies encompasses forms similar to species such as *Glaphyrocysta expansa* (Corradini, 1973) Roncaglia & Corradini, 1997, *Glaphyrocysta perforata* Hultberg & Malmgren, 1985, and *Membranophoridium bilobatum* Michoux, 1985.

Genus ***Hafniasphaera*** (Hansen, 1977) Fensome *et al.*, 2009

Remarks. There appears to be gradation between coarse granulation in *Spiniferites* and finely vesiculate forms attributable to *Hafniasphaera*. Generally, the presence of vesicles is clearly discernable and therefore generic differentiation has been maintained. However, it is entirely conceivable that vesiculate morphotypes traditionally assignable to *Hafniasphaera* represent outliers within the spectrum of the *Spiniferites* complex and that the eruption of vesicles could be

triggered by environmental stresses as would appear to be indicated in modern assemblages (Pospelova pers. comm.).

Hafniasphaera delicata Fensome *et al.*, 2009

(Pl. 4.16A–C)

Remarks. Spherical to subspherical cysts with a coarsely vesiculate body. Sutural boundaries at most faintly discernable and demarcated by the alignment of vesicles slightly larger than those which typically comprise the cyst wall.

Hafniasphaera cf. delicata Fensome *et al.*, 2009

(Pl. 4.16D, E)

Remarks. Cysts with a spherical body possessing thin, vesiculate processes and vesiculate, low-relief sutural ridges. *H. cf. delicata* differs from the original description of the species in bearing a nearly smooth to faintly granulate, non-vesiculate central body. This form occurs at its highest numbers in subsamples along side specimens of *H. delicata sensu stricto* and may represent a transitional form.

Genus *Impagidinium* Stover & Evitt, 1978 *sensu* Fensome & Williams (2005)

Remarks. The genus *Impagidinium* is regarded to encompass gonyaulacacean cysts on the basis of sutural crests in excess of seven percent of the maximum diameter of the central body which would otherwise be considered referable to *Pterodinium* Eisenack, 1958 (Fensome & Williams 2005).

Impagidinium cf. scabrosum Slimani, 1994

(Pl. 4.17B, C)

Remarks. Specimens assigned to *I. cf. scabrosum* are similar to *Impagidinium scabrosum* Slimani, 1994 in profile and overall serrated sutural crest structure but differ in possessing an

apical boss and an acuminate apical horn comprised of periphragm contrary to the species' original description (Slimani 1994).

Impagidinium cf. sphaericum Wall, 1967–*multiplex* Wall & Dale, 1968 of de Coninck (1968)
(Pl. 4.17D–F)

Age. *I. sphaericum* and *I. multiplex* are taxa recognized from the Cenozoic; the former species has been reported with a late Miocene–Holocene range (e.g. McMinn 1993; Voronina *et al.* 2001) and the later reported with an Oligocene–late Pleistocene range (e.g. Kuhlmann 2004; Mao *et al.* 2004). The cysts assigned to this plexus are most similar to the seemingly transitional middle to late Eocene form of de Coninck (1968, 1995; Iakovleva 2015).

Impagidinium spp.

(Pl. 4.17G)

Remarks. This plexus encompasses forms of variable size, extent of apical boss projection, sutural crest height and granulate surface texture. As occurrences of *Impagidinium* are rare throughout the Hornby Island section, the small specimen sample size within a given subsample impedes efforts to ascertain the range of variability within taxa of outlying morphologies.

Genus *Kleithriasphaeridium* (Davey, 1974) Fensome *et al.*, 2009
Kleithriasphaeridium perforatum (Firth, 1993) Fensome *et al.*, 2009
(Pl. 4.18E, F)

Remarks. Represented by a single specimen.

Genus *Lejeuniacysta* (Artzner & Dörhöfer, 1978) Lentin & Williams, 1976
Lejeuniacysta cf. hyalina (Gerlach, 1961) Artzner & Dörhöfer, 1978
(Pl. 4.5F)

Remarks. Represented by a single specimen, and partially obscured by debris, this cyst is tentatively assigned to *Lejeuniacysta* cf. *hyalina* due to shared proportions, a clearly delineated cingular furrow, and the presence of longitudinal folds on the epitheca and hypotheca.

***Lejeuniacysta* sp.**

(Pl. 4.5G)

Remarks. Represented by a single specimen, the most similar species, *Lejeuniacysta brassensis* Biffi & Grignani, 1983, differs from *Lejeuniacysta* sp. in having a small, distinct apical boss rather than an acuminate apical horn.

Genus ***Leptodinium*** (Klement, 1960) Sarjeant, 1982

***Leptodinium* sp.**

(Pl. 4.9H, I)

Remarks. Represented by a single specimen, this cyst bears similarities to *Leptodinium acneum* Snape, 1992 and *Leptodinium arcuatum* (Klement, 1960) Sarjeant, 1984 in profile being characterized by an elongate, tapering, subconical hypotheca although both species possess higher sutural crests and are significantly larger. The former species presents a reduced apical horn in contrast with the short, blunt protuberance of *L. sp.* while *L. arcuatum* lacks such a feature entirely. Of these species, only *L. acneum* shares a granulate surface comparable to that of *L. sp.*

Genus ***Litosphaeridium*** (Davey & Williams, 1966) Lucas-Clark, 1984

***Litosphaeridium* spp.**

(Pl. 4.14F–G)

Remarks. Forms assigned to *Litosphaeridium* spp. vary in their range of process morphology. Some specimens may bear indications of distal process openings but most are predominately closed, intratabular (one per plate), dome shaped to conical, and generally broader than long. Some specimens bear processes analogous to those typical of *Conosphaeridium* which differs

from *Litosphaeridium* in possessing a precingular rather than apical archaeopyle (e.g. Cookson & Eisenack 1969).

Genus *Minisphaeridium* Fensome *et al.*, 2009

***Minisphaeridium* sp.**

(Pl. 4.10F, G)

Remarks. Chorate cysts with broad, distally closed processes comprised of hyaline periphragm. Distal process ends are slightly broader than their bases. Process presumed to be mesotabular, with minimal interspaces, thus occupying nearly the entire surface area of their corresponding plates.

Genus *Nematosphaeropsis* (Deflandre & Cookson, 1955) Wrenn, 1988

***Nematosphaeropsis* sp.**

(Pl. 4.23I)

Remarks. Represented by two specimens, these cysts bear greatest similarity to *Nematosphaeropsis balcombiana* Deflandre & Cookson, 1955 and *Nematosphaeropsis philippotii* (Deflandre, 1947) de Coninck, 1969, the later of which has been recognized as constrained to the Late Cretaceous (Guédé *et al.* 2014). However, they differ from the *N. balcombiana* holotype—for which it has been recommended the name be restricted (Head & Wrenn 1992) due to literary ambiguity (Wrenn 1988; Head & Westphal 1999)—in possessing greater distal process connectivity and from *N. philippotii* in possessing more robust, membranaceous processes.

Genus *Neourysphaeridium* Slimani, 1994

***Neourysphaeridium?* sp.**

(Pl. 4.1G–I)

Remarks. Represented by two specimens, *Neoeurysphaeridium?* sp. differs from *Neoeurysphaeridium glabrum* Slimani, 1994, the only species recognized within the genus, by lacking taeniate processes and possessing a reduced tubular process on precingular plate 1".

Genus *Odontochitina* (Deflandre, 1937b) Núñez-Betelu & Hills, 1998

Odontochitina cf. *tabulata* El Mehdawi, 1998

(Pl. 4.19C, D)

Remarks. The two specimens assigned to *O.* cf. *tabulata* differ from the original description of the taxon only in lacking pronounced perforations along the medial and distal portions of the lateral and antapical horns.

Age. Previously constrained to the late Santonian–early Campanian (El Mehdawi 1998; Slimani *et al.* 2016).

Odontochitina cf. *nuda* (Gocht, 1957) Dörhöfer & Davies, 1980

(Pl. 4.19A, B)

Remarks. Nøhr-Hansen (1993) argued for placement of this species within the genus *Pseudoceratium* by challenging the assertion of cornucavation (Dörhöfer & Davies 1980), claiming ambiguity in the holotype (Gocht 1957), subsequent material (Brideaux 1977), and his own specimens. However, no such transfer of *O. nuda* to *Pseudoceratium* has been made in re-examinations of the genus (e.g. Helby 1987; Williams *et al.* 2017), albeit without comment. In the two Hornby Island specimens, a smooth periphragm and cornucavation is clearly discernable. The material differs from the species' description only by the presence of a transverse cingular periphragm fold and two minute longitudinal folds denoting the sulcal area.

Age. Previously constrained to the late Hauterivian–lower Aptian (e.g. Gocht, 1957; Wall & Evitt 1975; Nøhr-Hansen 1993).

Genus *Phanerodinium* (Deflandre, 1937a) Slimani, 1994

Phanerodinium belgicum Slimani & Louwye, 2011

(Pl. 4.20A–C)

Age. Previously constrained to the late Maastrichtian–early Danian (Slimani 1994; 1995; Slimani *et al.* 2011; Slimani & Louwye 2011) with a possible additional occurrence in the Paleocene (Groot & Groot 1962).

Phanerodinium cf. belgicum Slimani & Louwye, 2011

(Pl. 4.20D, E)

Remarks. Represented by a single specimen, *P. cf. belgicum* differs from the original description of the species only in possessing an unusually elongated epitheca and may represent an extremity of the spectrum of variability within *P. belgicum*.

Phanerodinium sp.

(Pl. 4.20F)

Remarks. Represented by a single specimen, *P. sp.* resembles *P. belgicum* in profile and granulate surface texture but differs in possessing serrate septal crests akin to those of *Phanerodinium fourmarieri* (Lejeune-Carpentier, 1951) Slimani & Louwye, 2011. Although the description of *P. belgicum* encompasses forms with septal membrane undulations, the character does not approach the level of angular incision exhibited in this specimen.

Polysphaeridium (Davey & Williams, 1966) Bujak *et al.*, 1980*Polysphaeridium spp.*

(Pl. 4.14H, I)

Remarks. *Polysphaeridium spp.* represents a plexus of morphologies in ornamentation constrained to variability in processes size, length, width, and number; elements often utilized as criteria for specific differentiation (e.g. Davey & Williams 1966). The presence of an apical archaeopyle sees assignment of these cysts to *Polysphaeridium* as opposed to the similarly

ornamented genera *Amphorosphaeridium* (Davey 1969 *sensu* Lejeune-Carpentier & Sarjeant 1981) and *Exochosphaeridium* (Davey *et al.* 1966 emend. Helenes 2000) which each bear a precingular archaeopyle. The polar processes of the Hornby Island specimens also in no way appear to be exceptional larger or more distinct from the others as is characteristic of *Exochosphaeridium*. *Polysphaeridium* differs from *Cordosphaeridium* due to its apical archaeopyle and higher number of processes with a tendency toward branching.

Genus *Protoperidinium* Bergh, 1881

***Protoperidinium* sp. A**

(Pl. 4.21A–C)

Remarks. Represented by six specimens. Proximate, pentagonal protoperidiniacean cysts comprised of smooth to faintly granulate autophragm only. Solid distal tip of apex formed by compound apical boss. Cysts assigned to *Protoperidinium* sp. A, due to affinity with the cysts of the living motile genus, bear resemblance to the fossil taxon *Pierceites pentagonus* (May, 1980) Habib & Drugg, 1987 in profile although members of said species differ from the Hornby Island entities in possessing an I_{1–3a}—as opposed to an I_{2a}—archaeopyle. It is also notable that Fensome *et al.* (2009) regarded *P. pentagonus* to be a deflandreoid peridiniacean despite its apparent lack of an endocyst.

***Protoperidinium* sp. B**

(Pl. 4.21D–F)

Remarks. Represented by a single specimen. A proximate, pentagonal protoperidiniacean cysts comprised of smooth autophragm only. Solid distal tip of conical apex. Plate 2a partially corroded as to indicate potential I_{2a} archaeopyle.

Genus *Pterodinium* Eisenack, 1958

Remarks. Placement of taxa within *Pterodinium* would be inconsistent with the interpretation of Fensome & Williams (2005) thus it has been maintained herein only in the context of the

occurrence of the taxon *Pterodinium cingulatum* (Wetzel, 1933) Below, 1981 *sensu* Antonescue *et al.* (2001a).

Pterodinium cingulatum (Wetzel, 1933) Below, 1981 *sensu* Antonescue *et al.* (2001a)
(Pl. 4.17H)

Remarks. Represented by a single specimen.

Genus *Renidinium* Morgenroth, 1968

Renidinium spp.

(Pl. 4.6G–I; Fig. 4.3I)

Remarks. This plexus consists of subovate to ovoid cysts with endophragm and ectophragm appressed on mid-dorsal and mid-ventral surfaces. Dorsal tabulation is often discernible through low-relief ectophragm folds. Some forms bear similarity to *Renidinium vitilare* (Cookson, 1965b) Stover & Evitt, 1978, but differ in greater elongation of the endophragm as well as marginate pericoel surficial reticulation and vermiculation (Pl. 4.6I, Fig. 4.3I).

Genus *Senegalinium* (Jain & Millepied, 1973) Stover & Evitt, 1978

Senegalinium? simplex Lucas-Clarke, 2006

(Pl. 4.22E)

Age. Previously constrained to the late Maastrichtian–Paleocene (e.g. Edwards 2001; Lucas-Clarke 2006; Dastas *et al.* 2014).

Remarks. The present author maintains the reservation originally expressed in assigning the species to *Senegalinium* due to the presence of communication between the ectophragm and periphragm in the apical region (Lucas-Clarke 2006).

Genus *Senoniasphaera* Clarke & Verdier, 1967

Senoniasphaera cf. protrusa (Clarke & Verdier, 1967) Prince *et al.*, 1999

(Pl. 4.3I)

Dimensions (μm).

B: 85.03 (89.75) 97.07; N: 4.

Bi: 71.93 (74.98) 77.66; N: 4.

L: 65.77 (72.41) 74.95; N: 4.

Li: 54.2 (62.69) 68.23; N: 4.

L₁: 6.76 (8.69) 9.91; N: 4.

Age. Previously recorded from the middle Santonian–late Campanian (e.g. Prince *et al.* 1999; Slimani *et al.* 2016) apart from a single questionable occurrence in the Paleogene (Mohamed *et al.* 2013).

Remarks. Specimens range from subspherical to elongate, contrary to the established description (Prince *et al.* 1999). All cysts assigned to *S. cf. protrusa* are inherently asymmetrical due to a right antapical horn reduced to the point of virtual absence and therefore cannot be placed with *S. rotundata*. These cysts comprise specimens with reduced to well developed, blunt, lateral horns comprised of periphragm only with the periphragm more closely appressed along the anterolateral margins. The only protrusion of the endophragm in any of these specimens is that observable in the well developed left antapical horn.

Conceptually, if the endophragm of *S. cf. protrusa* were to protrude into the lateral horns, forms within the plexus would achieve a pentagonal profile, in essence appearing transitional to *Canningia diezeugmenis* sp. nov. Marshall (1990) makes the comparison between members of *Senoniasphaera* and *Canningia* of the same ecological occurrence in *S. edenensis* and *C. bassensis* noting the shared presence of ectophragm support structures. While the later taxon is characterised by the predominance of support structures as opposed to the former (Marshall 1990), the observation none the less carries the implication that at least one form of *Senoniasphaera* may not be exclusively circumcavate and that gradation between both genera is a hypothetical possibility.

Genus *Spiniferella* Stover & Hardenbol, 1994

Spiniferella cornuta (Gerlach, 1961) Stover & Hardenbol, 1994

(Pl. 4.23A–C)

Age. Previously recorded from the early Maastrichtian–middle Miocene (e.g. Gerlach 1961; Slimani *et al.* 2012; Mohamed & Wagreich 2013; Slimani *et al.* 2016). While *S. cornuta* has been reported in several studies of Upper Cretaceous strata encompassing the CMB interval, several of these works neglected to include precise biostratigraphic data relating to this taxon (e.g. Roncaglia *et al.* 1999; Antonescue *et al.* 2001b; Brinkhuis *et al.* 2003). Therefore, it can only be stated with certainty that the species holds its first occurrence in at least the early Maastrichtian.

Genus *Spiniferites* (Mantell, 1850) Sarjeant, 1970

Spiniferites sp. A

(Pl. 4.16G–I)

Remarks. Subspherical to ovoid cysts with a finely granulate inretabular surface. Gonal and intergonal bifurcated processes present. Intergonal processes often arise entirely from the distal margins of sutural crest membranes. Apical boss present, bearing a short, acuminate apical horn.

Spiniferites spp.

(Pl. 4.23D–H)

Remarks. This plexus encompasses a wide range of morphologies including forms similar to *Spiniferites membranaceous* (Rossignol, 1964) Sarjeant, 1970, *Spiniferites mirabilis* (Rossignol, 1964) Sarjeant, 1970, *Spiniferites ramosus* (Ehrenberg, 1937) Mantell, 1854 and *Spiniferites ristingensis* Head, 2007. Forms vary from subcircular to subovate in profile, degree of basal process connectivity via sutural crests, and extent of distal bifurcation and trifurcation of gonal and intergonal processes. Aberrant specimens occur. One notable cyst, marked by reduced, simple, bifurcated processes otherwise unremarkable in the genus, bears a single, robust, lateral process which tapers gradually to distally trifurcated and bifurcated terminations (Pl. 4.23G–I).

Genus *Trichodinium* (Eisenack & Cookson, 1960) Clarke & Verdier, 1967

Trichodinium cf. erinaceoides Davies, 1983

(Pl. 4.8E, F)

Remarks. Represented by two specimens, *T. cf. erinaceoides* differs from the original description provided by Davies (1983) only in lacking the faintly expressed alignment of hair-like spines which delineates the cingulum.

Age. Previously recorded from the Kimmeridgian?–early Valenginian (e.g. Davies 1983; Courtenat 2000).

Genus *Trithyrodinium* Drugg, 1967*Trithyrodinium evittii* Drugg, 1967

(Pl. 4.22G–I)

Remarks. Represented by a single specimen.

Age. Previously recorded from the early Maastrichtian–early Selandian (e.g. Brinkhuis *et al.* 1998; Williams *et al.* 2004).

Genus *Unipontidinium* Wrenn, 1988*Unipontidinium aquaeductus* (Piasecki, 1980) Wrenn, 1988

(Pl. 4.17I)

Remarks. Represented by a single specimen.

Age. Previously constrained to the middle Miocene (e.g. Piasecki 1980; Williams *et al.* 2004).

Genus *Xenascus* Cookson & Eisenack, 1969 *sensu* Fensome *et al.*, (2009)

Remarks. The original description of the genus was not explicit about the parameters of lateral horn expression (Cookson & Eisenack 1969) with subsequent workers favouring diagnoses

involving either a single well-developed (Stover & Helby 1987) or two unequally developed (Stover & Evitt 1978; Fensome & Williams 2005; Fensome *et al.* 2009) lateral horns.

Xenascus ceratioides (Deflandre, 1937b) Lentin & Williams, 1973

(Pl. 4.19F, G)

Remarks. Beyond cornucavation, Fensome & Williams (2005) and Fensome *et al.* (2009) proposed specific diagnosis of *Xenascus ceratioides* based on a single, well developed lateral horn which is not distinctly perforate. In the original description of the species, it is noted that “several spines and horns are arranged around the equator” (translation: Deflandre 1937b, p. 19). In the absence of endocyst equatorial protrusions, this statement illustrates that there is room for subjectivity in what constitutes a large process in comparison to a horn. Authors may be left to classify horns based on greater dimensions in comparison to those of neighbouring processes.

Specimens assigned to *X. ceratioides* in the Hornby Island assemblage typically exhibit one well developed and one undeveloped lateral horn. The presence of the secondary lateral horn is substantiated on the grounds of a broad-based pericoel and consistent diametric opposition to the well-developed primary lateral horn.

Genus *Xenicodinium* Klement, 1960

Xenicodinium delicatum Hultberg, 1985 *sensu* Slimani *et al.* 2011

(Pl. 4.24A)

Age. Previously constrained to the early Maastrichtian–late Selandian (Hultberg 1985; Slimani *et al.* 2011; Slimani *et al.* 2016; Tabără & Slimani 2017; Tabără *et al.* 2017).

Remarks. Proximate, spherical to subspherical, translucent cyst bodies with finely granulate surface texture. Archaeopyle visible in rare instances; tabulation otherwise indiscernible. Of other dinoflagellate cyst taxa, these forms are also comparable to those of *Batiacasphaera* (Drugg, 1970) Dörhöfer & Davies, 1980 with dimensions and simplistic ornamentation specifically akin to that observed in the *Batiacasphaera micropapillata* Stover, 1977 plexus (Schreck & Matthiessen 2013). Specimens epifluorescent.

Peridiniacean Group A

(Pl. 4.21G, H)

Remarks. Proximate, subpentagonal to ellipsoidal, cornucavate cysts which vary in size, possessing a smooth surface texture. Transverse cingulum clearly delineated. Archaeopyle indiscernible. Apical horn present or absent. Antapical horns present and of equal or unequal size. Thin-walled and semi-translucent with colouration ranging from light-brown to rosey-brown. These forms correspond most closely to *Geiselodinium* and *Subtilisphaera* Morgenroth, 1968; two genera in need of taxonomic resolution (e.g. Stover & Evitt 1978; Chen *et al.* 1988).

Peridiniacean Group B

(Pl. 4.21I)

Remarks. Proximate, subpentagonal to rhomboidal cysts of variable size, and surface texture. Colouration generally dark-brown in specimens with a robust autophragm.

incertae sedis

Cyst Type A

(Pl. 4.24B, C)

Remarks. Represented by four specimens. Proximochorate cysts with smooth to granulate periphragm. Processes potentially meso-, ob-, or contabular, distally closed, blunt, conical to globular or verrucate.

Cyst Type B

(Pl. 4.24D–F)

Remarks. Represented by a single specimen presenting gonyaulacoid tabulation. An unusual pattern at plate boundaries resembles growth bands on a motile dinoflagellate. Therefore, this could be a preserved theca and not an actual cyst (Pospelova pers. comm.).

Cyst Type C

(Pl. 4.24G, H)

Remarks. Chorate cysts with hyaline, elongate, ovoid, bodies. Processes broad, densely fibrous, distally expanded and comprised of periphragm only. Tabulation indicated only by the presence of an apical archaeopyle. The processes are analogous to those of *Turbiosphaera* Archangelsky, 1969, a genus which bears a precingular archaeopyle, two-layered central body, and clearly demarcated cingular processes. These cysts also bear a superficial similarity to members of the heterotrophic genus *Polykrikos* Bütschli, 1873 but epifluorescence of these specimens precludes this affinity.

Cyst? Type A

(Pl. 4.24I)

Remarks. Spherical to subspherical bodies comprised of a hyaline autophragm enveloped by an apparent kalyptra. A lack of diagnostic characters sees questionable placement of this entity among the dinoflagellate cysts. Archaeopyle not definitively observed. Occasional endocyst breakage may demarcate points of plate dehiscion but tabulation, if present, is otherwise indiscernible.

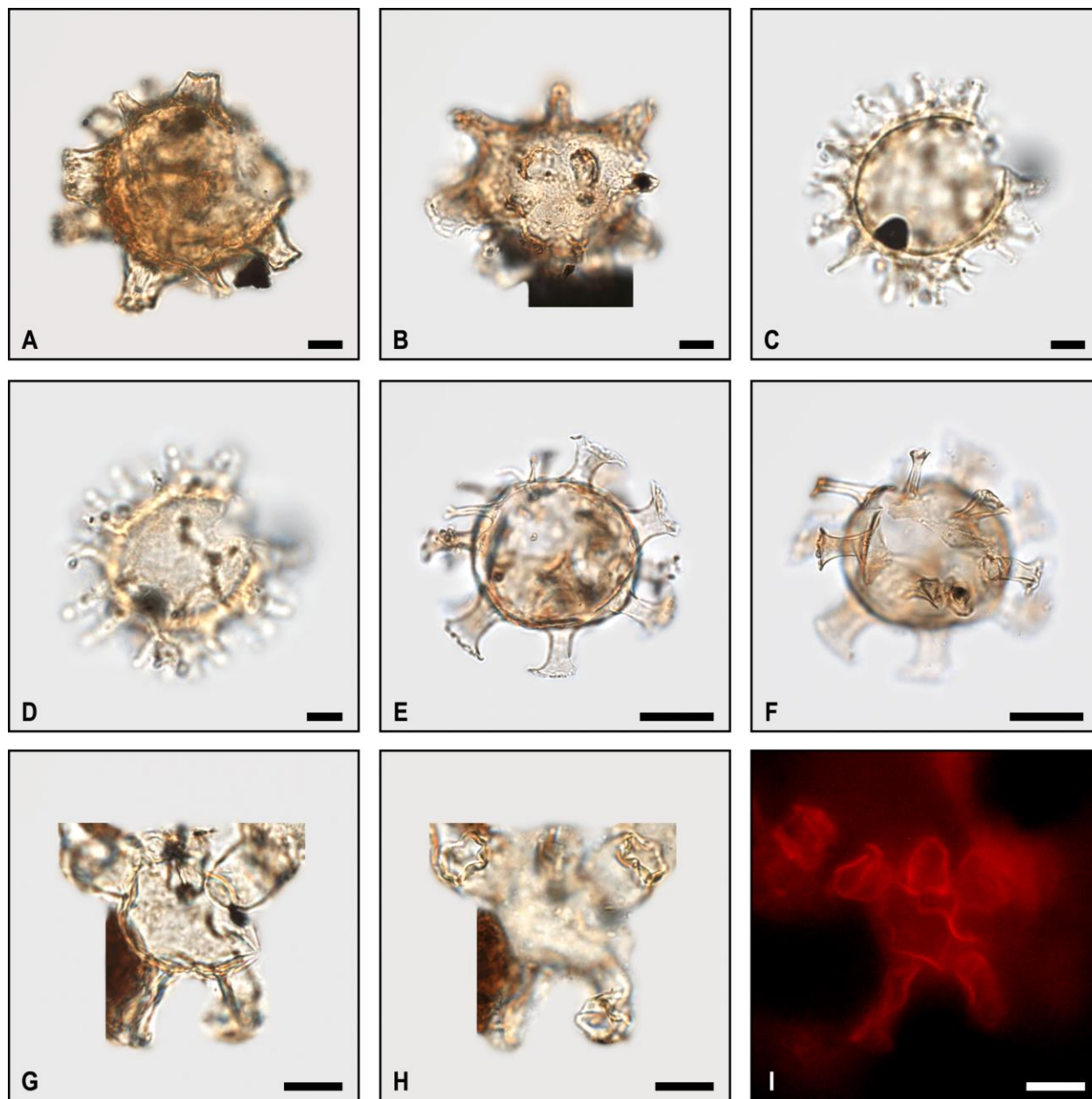


Plate 4.1. Bright-field photomicrographs and epifluorescence imaging of selected gonyaulacacean dinoflagellate cysts. **A, B**, *Aireiana salicta*. **A**, subsample 15-766, slide A, surficial focus; **B**, subsample 16-368, slide C, surficial focus. **C, D**, *Cordosphaeridium callosum*, subsample 16-366, slide A. **C**, mid-focus; **D**, surficial focus. **E, F**, *Cordosphaeridium* spp., subsample 15-766, slide C. **E**, mid-focus; **F**, archaeopyle in focus. **G–I**, *Neoeurysphaeridium?* sp., subsample 15-756, slide A. **G**, mid-focus; **H**, distal process openings in focus; **I**, epifluorescence. Scale bars = 10 μm .

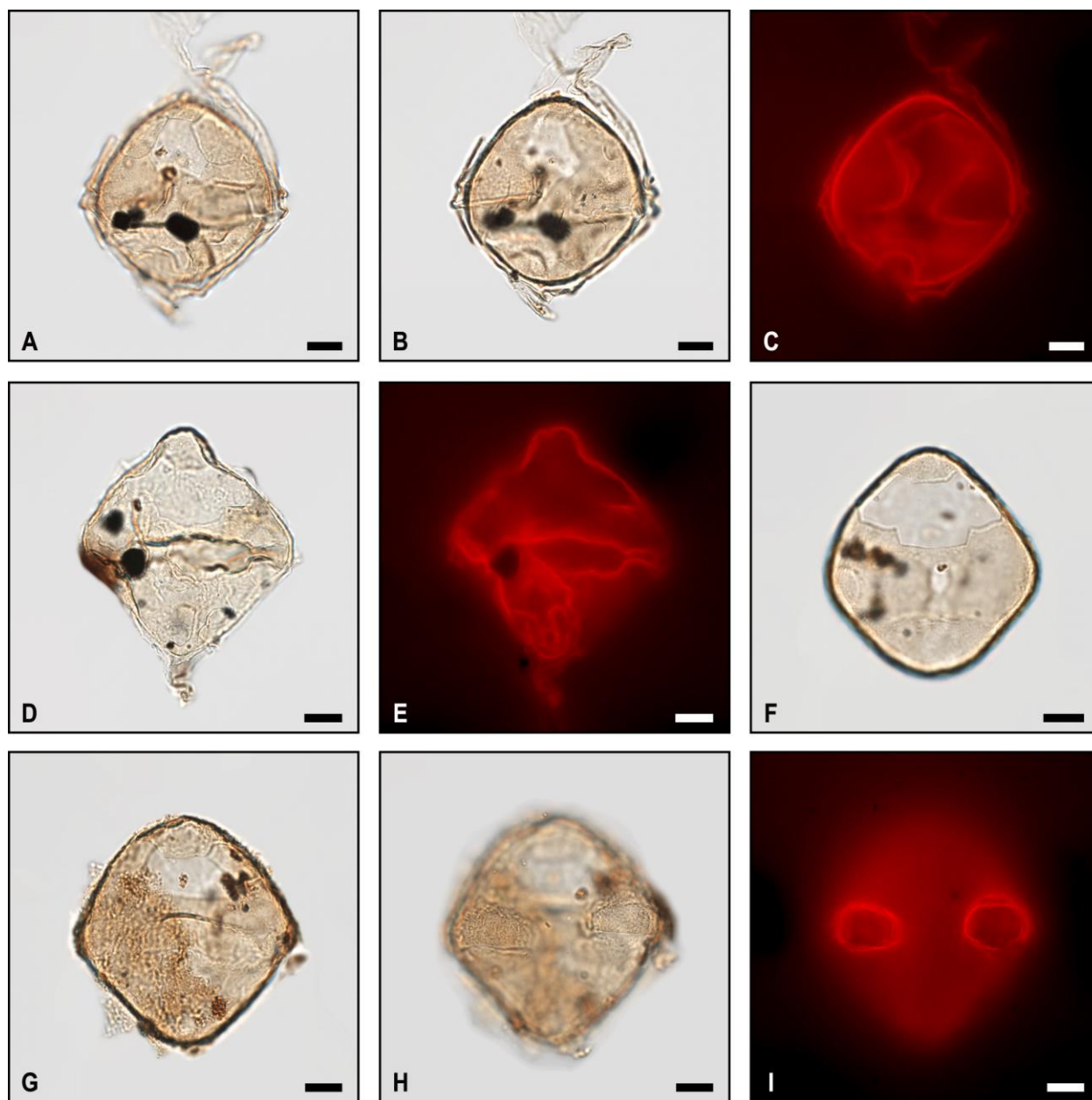


Plate 4.2. Bright-field photomicrographs and epifluorescence imaging of selected peridiniacean dinoflagellate cysts. **A–E**, *Alterbidinium?* spp. **A–C**, subsample 14-269, slide B; **A**, I_{2a} archaeopyle; **B**, mid-focus; **C**, epifluorescence; **D, E**, subsample 14-269, slide A; **D**, I_{1-3a} archaeopyle; **E**, epifluorescence. **F–I**, *Bohaidina* spp. **F**, I_{1-3a} archaeopyle, subsample 14-269, slide B; **G–I**, subsample 14-269, slide A; **G**, dorsal view; **H**, ventral view; **I**, ventral view, epifluorescence. Scale bars = 10 μm .

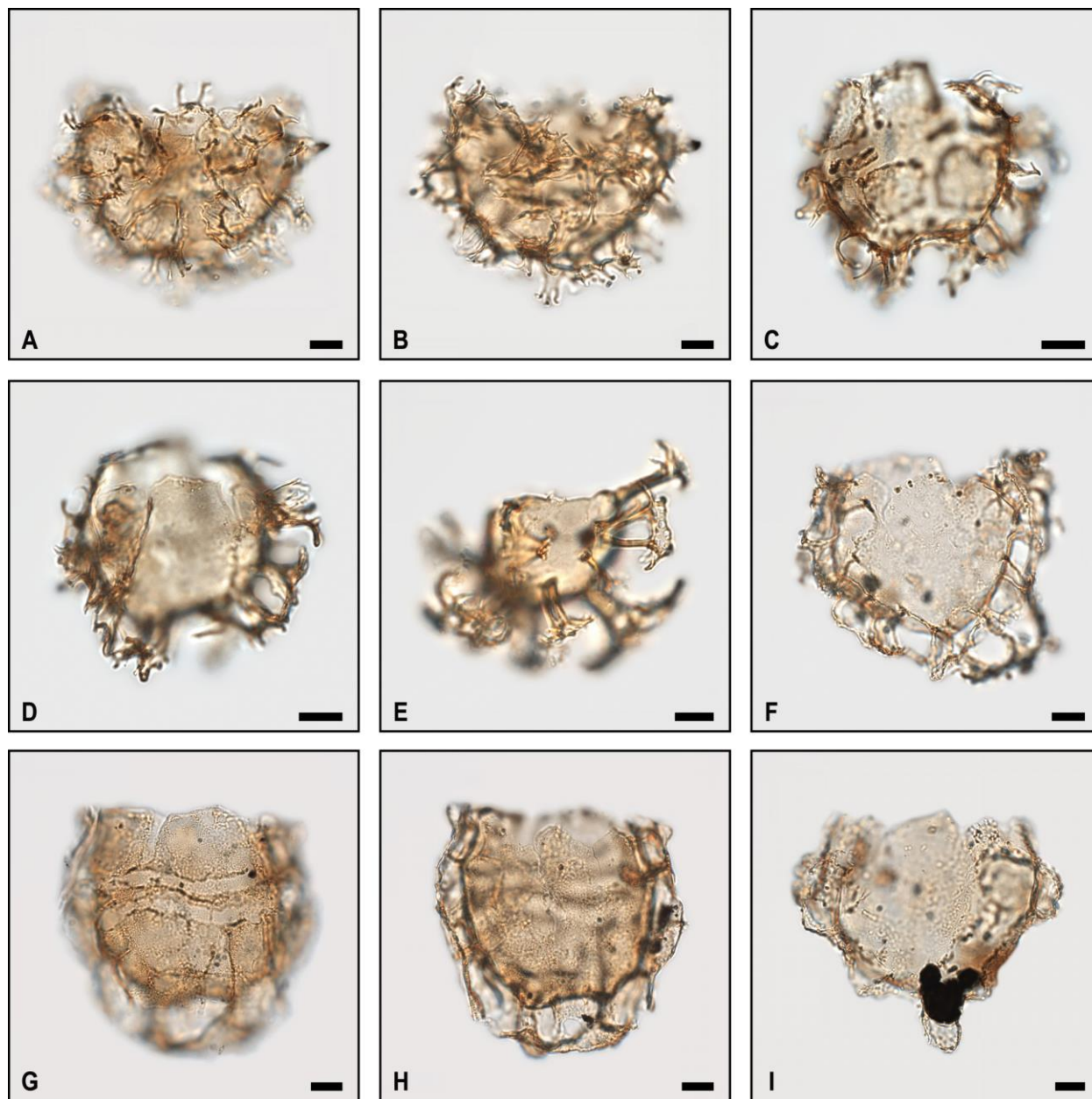


Plate 4.3. Bright-field photomicrographs of selected areoligeracean dinoflagellate cysts. **A, B**, *Areoligera* “*circumcoronata*”, subsample 14-271, slide B. **A**, dorsal view; **B**, ventral view. **C, D**, *Areoligera* spp., subsample 16-367, slide A. **C**, dorsal view; **D**, ventral view. **E**, *Areosphaeridium?* sp., subsample 14-271, slide B. **F**, *Glaphyrocysta-Membranophoridium* spp., subsample 14-274, slide A, ventral view. **G, H**, *Glaphyrocysta-Membranophoridium* spp., subsample 15-765, slide D; **G**, dorsal view; **H**, mid-focus. **I**, *Senoniasphaera* cf. *protrusa*, subsample 14-273, slide A, mid-focus. Scale bars = 10 μ m.

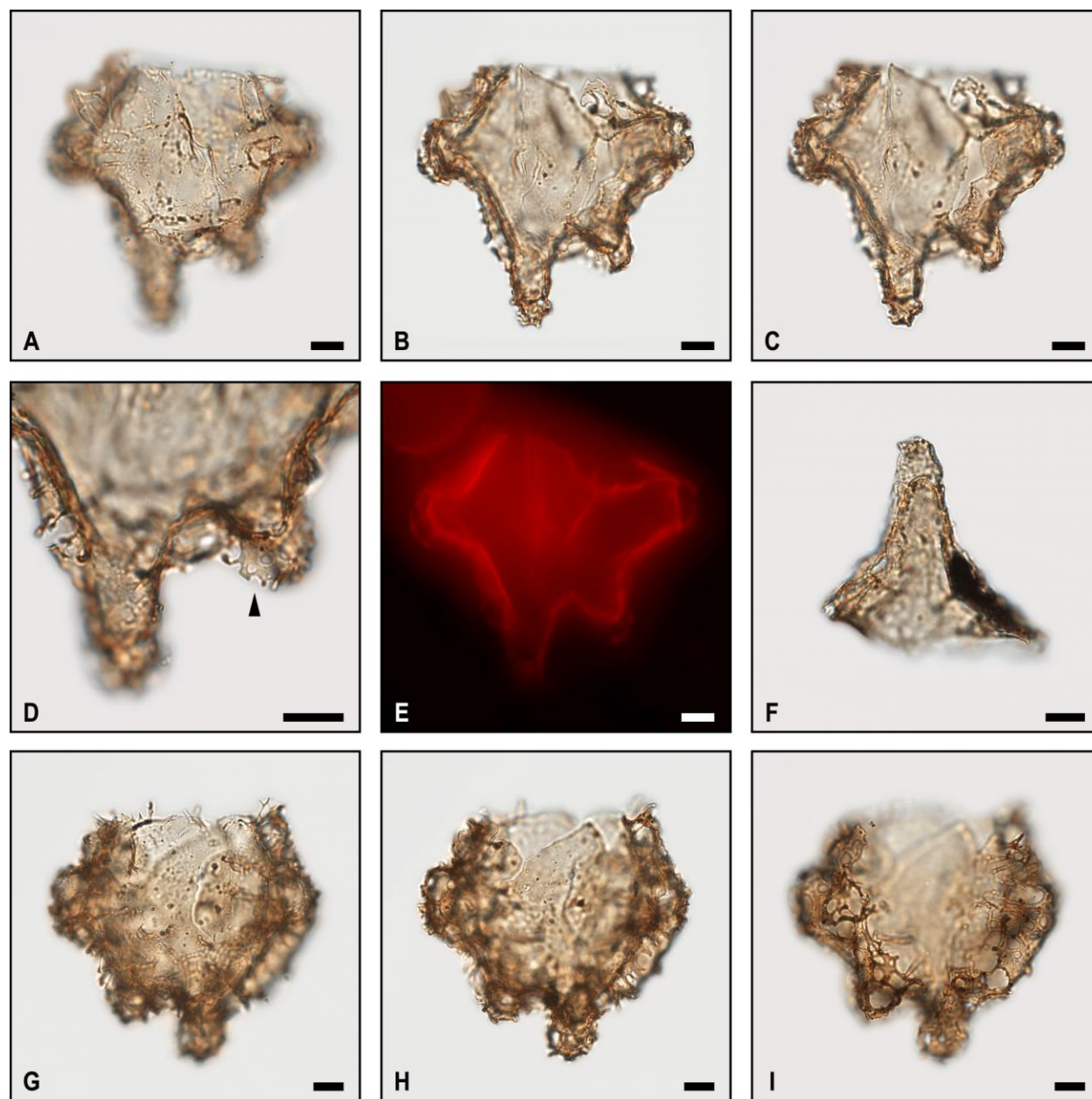


Plate 4.4. Bright-field photomicrographs and epifluorescence imaging of the areoligeracean dinoflagellate cyst *Canningia diezeugmenis* sp. nov. **A–E**, holotype, subsample 14-273, slide A, England Finder reference V38/3. **A**, dorsal view; **B**, mid-focus; **C**, ventral view; **D**, closeup of antapical region, arrow denotes ectophragm perforations; **E**, mid-focus, epifluorescence. **F**, paratype, subsample 16-368, slide E, England Finder reference S38/2, mid-focus, operculum. **G–I**, paratype, subsample 16-368, slide E, England Finder reference W33/3. **G**, dorsal view; **H**, mid-focus; **I**, ventral view. Scale bars = 10 μm .

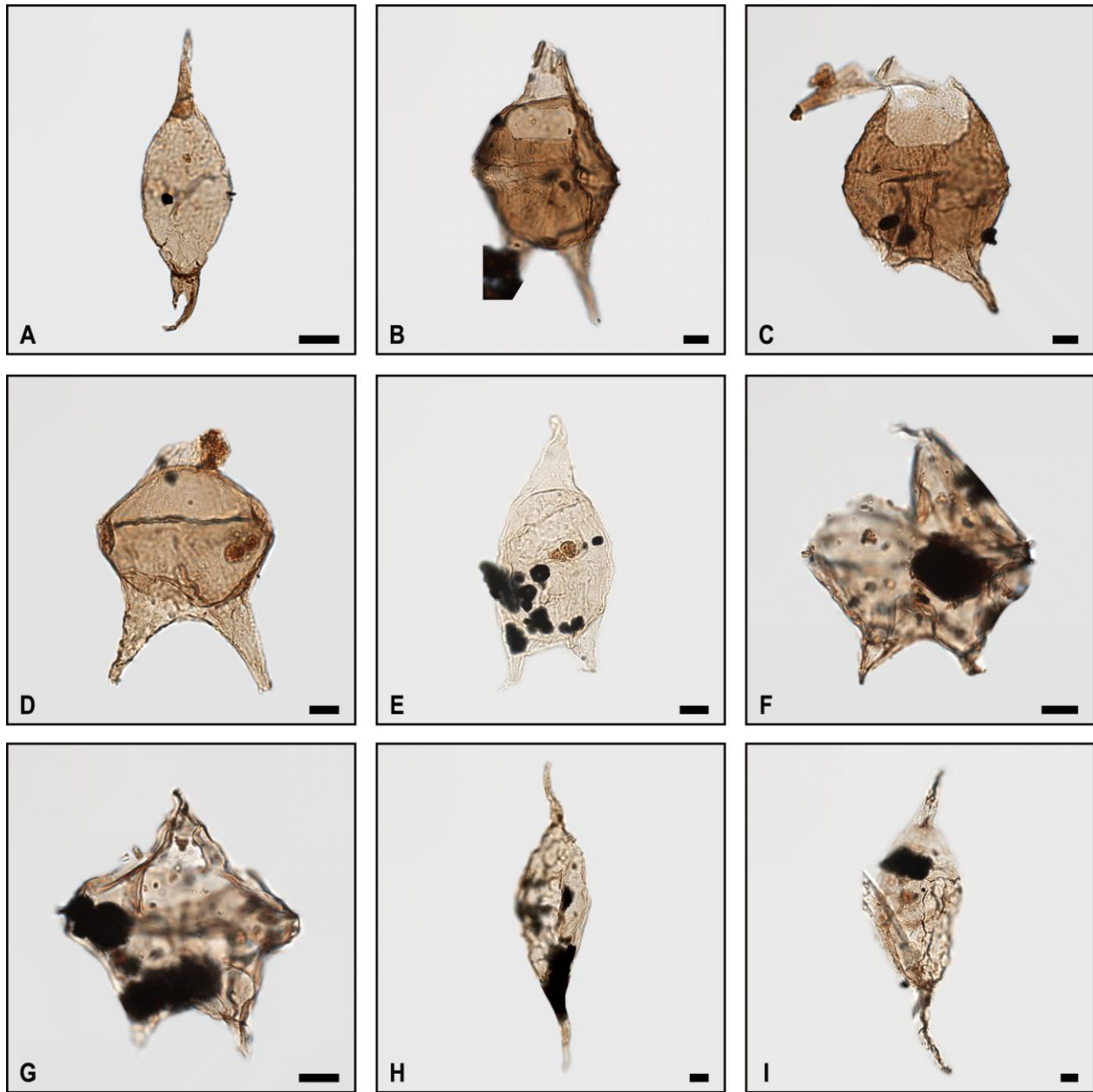


Plate 4.5. Bright-field photomicrographs of selected peridiniacean dinoflagellate cysts. **A**, *Andalusiella gabonensis*, subsample 15-766, slide C. **B**, **C**, *Cerodinium diebelii*; **B**, subsample 15-757, slide C; **C**, subsample 14-269, slide B. **D**, *Cerodinium glabrum*, subsample 15-759, slide A. **E**, *Cerodinium* cf. *leptodermum*, subsample 14-271, slide A. **F**, *Lejeuniacysta* cf. *hyalina*, subsample 15-757, slide C. **G**, *Lejeuniacysta* sp., subsample 15-757, slide C. **H**, **I**, *Palaeocystodinium golzowense*. **H**, subsample 15-767, slide A; **I**, subsample 14-274, slide A. Scale bars = 10 μ m.

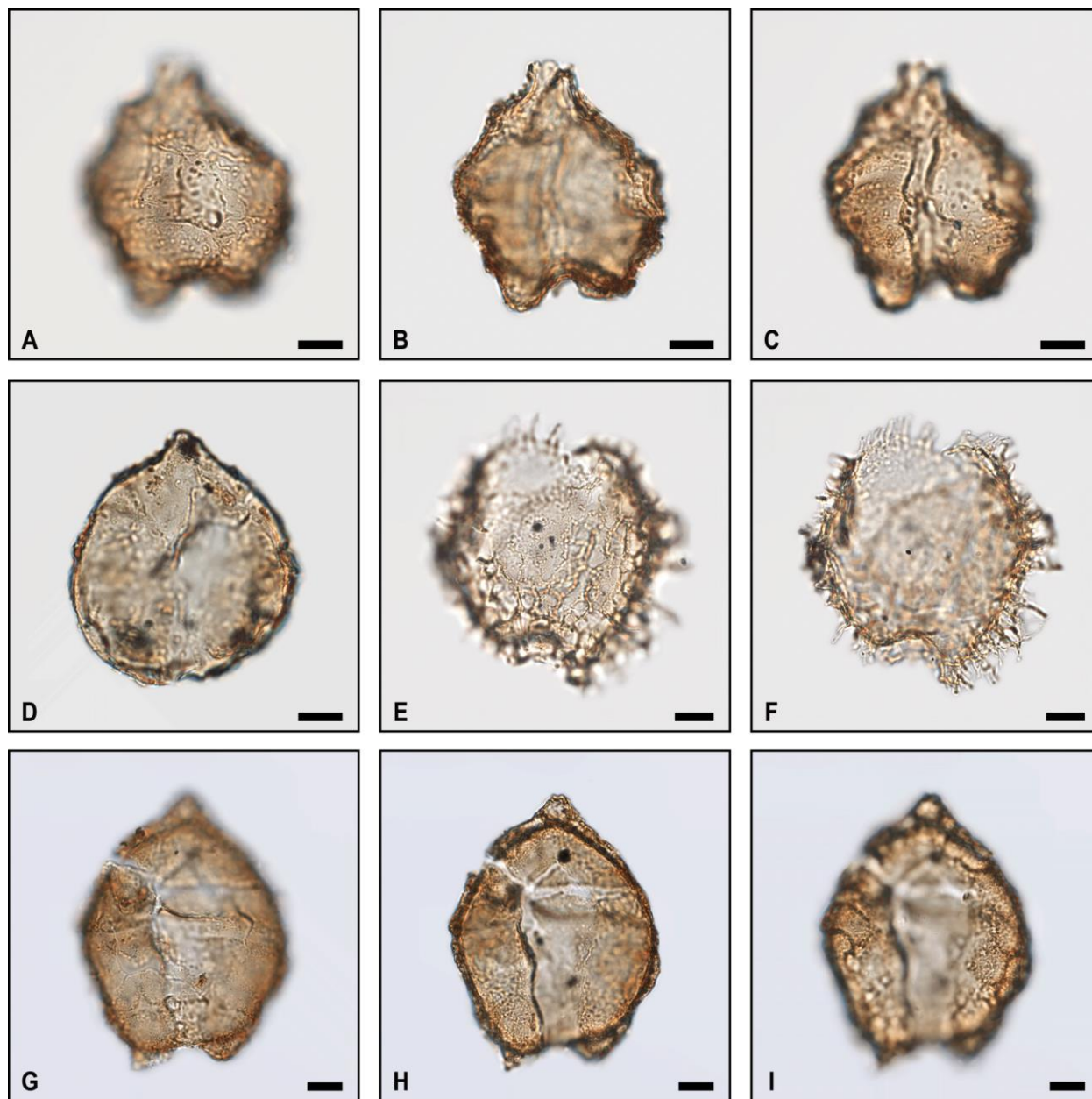


Plate 4.6. Bright-field photomicrographs of selected areoligeracean dinoflagellate cysts. **A–C**, *Circulodinium?* sp., subsample 16-368, slide E. **A**, dorsal view; **B**, mid-focus; **C**, ventral view. **D**, *Circulodinium colliveri*, subsample 16-368, slide E. **E, F**, *Cyclonephelium* spp., subsample 16-364, slide B. **E**, dorsal view; **F**, ventral view. **G–I**, *Renidinium* spp., subsample 15-766, slide C. **G**, dorsal view; **H**, mid-focus; **I**, ventral view. Scale bars = 10 μm .

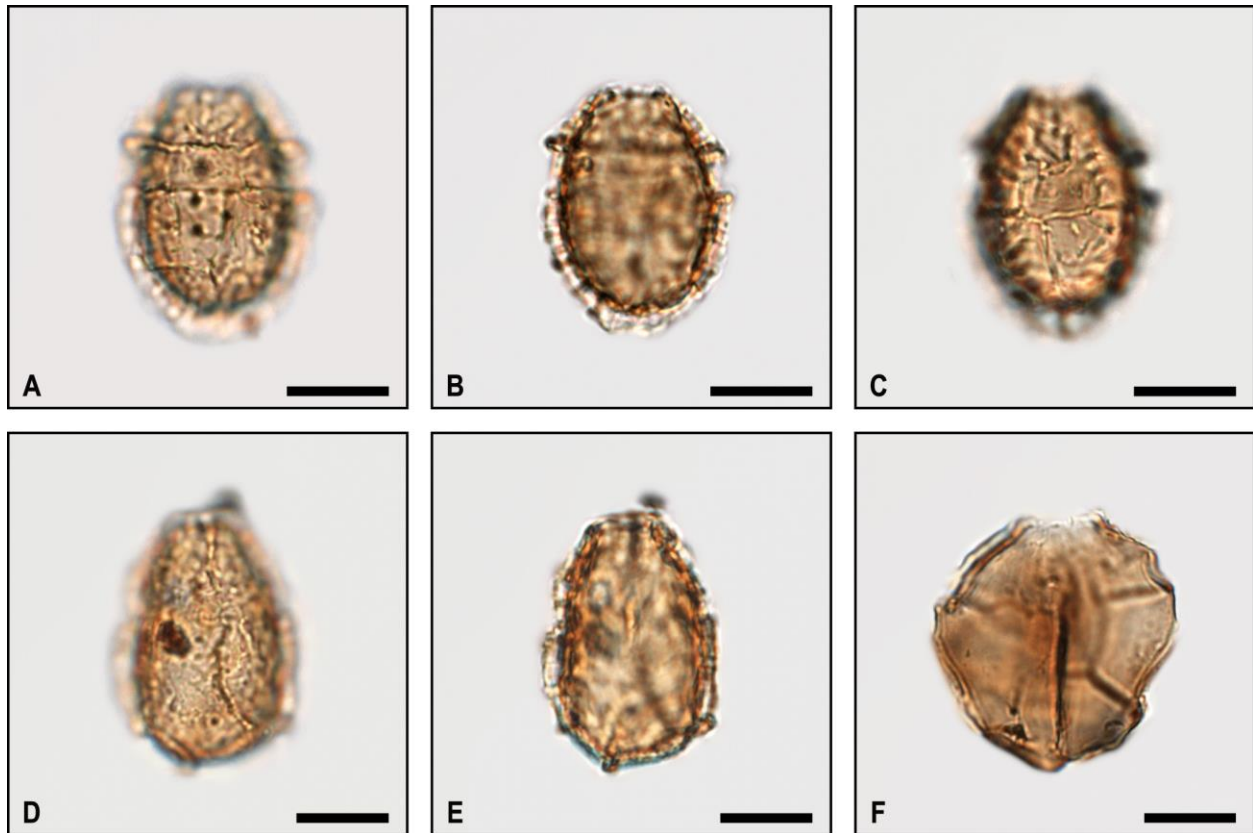


Plate 4.7. Bright-field photomicrographs of selected cladopyxiinean dinoflagellate cysts. **A–C**, *Cladopyxidium paucireticulatum*, subsample 14-272, slide A. **A**, dorsal view; **B**, mid-focus; **C**, ventral view. **D, E**, *Cladopyxidium* sp., subsample 14-271, slide B. **D**, dorsal view; **E**, mid-focus. **F**, *Glyphanodinium facetum*, subsample 14-274, slide B, mid-focus. Scale bars = 10 μm .

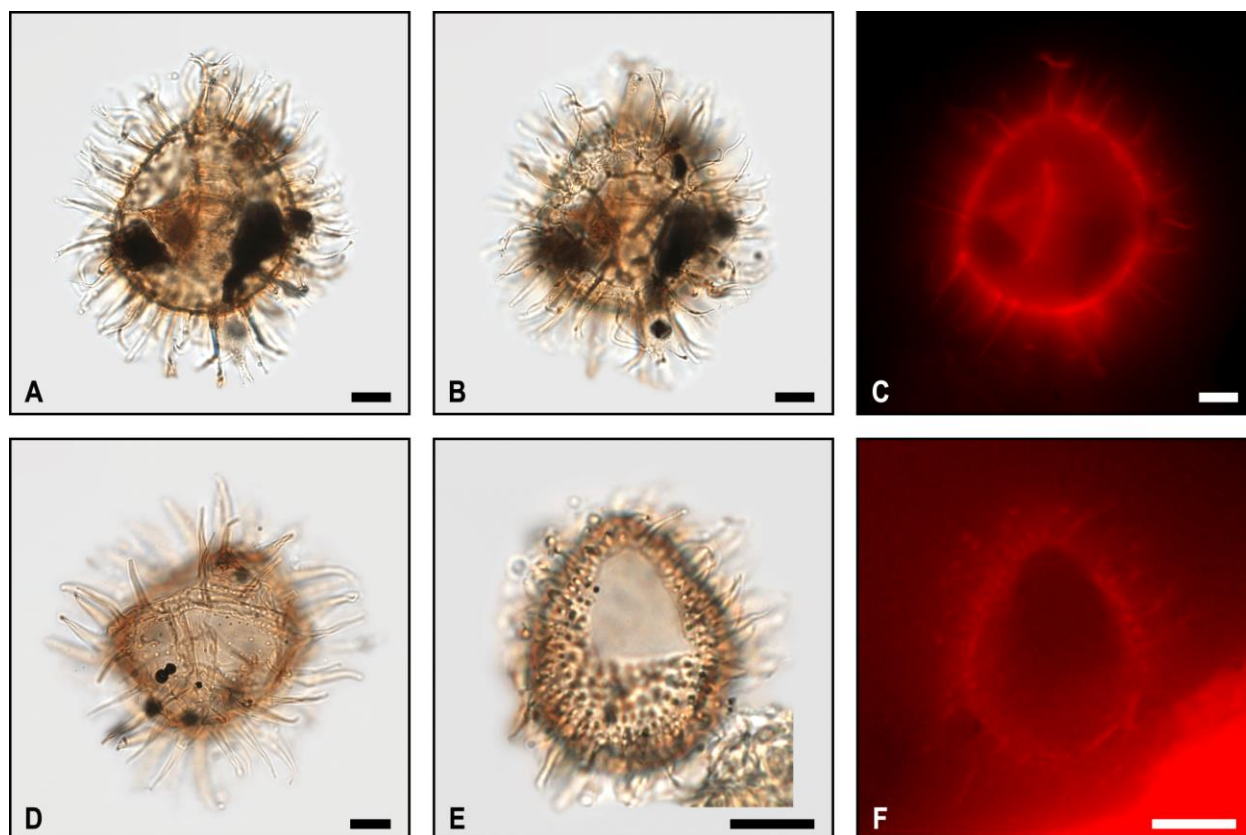


Plate 4.8. Bright-field photomicrographs and epifluorescence imaging of selected gonyaulacacean dinoflagellate cysts. **A–C**, *Coronifera oceanica sensu Schiøler & Wilson (2001)*, subsample 16-368, slide E. **A**, mid-focus; **B**, basal process periphragm in focus; **C**, mid-focus, epifluorescence. **D**, *Hystrichodinium pulchrum*, subsample 14-273, slide B. **E, F**, *Trichodinium cf. erinaceoides*, subsample 14-273, slide B. **E**, dorsal view; **F**, dorsal view, epifluorescence. Scale bars = 10 μm .

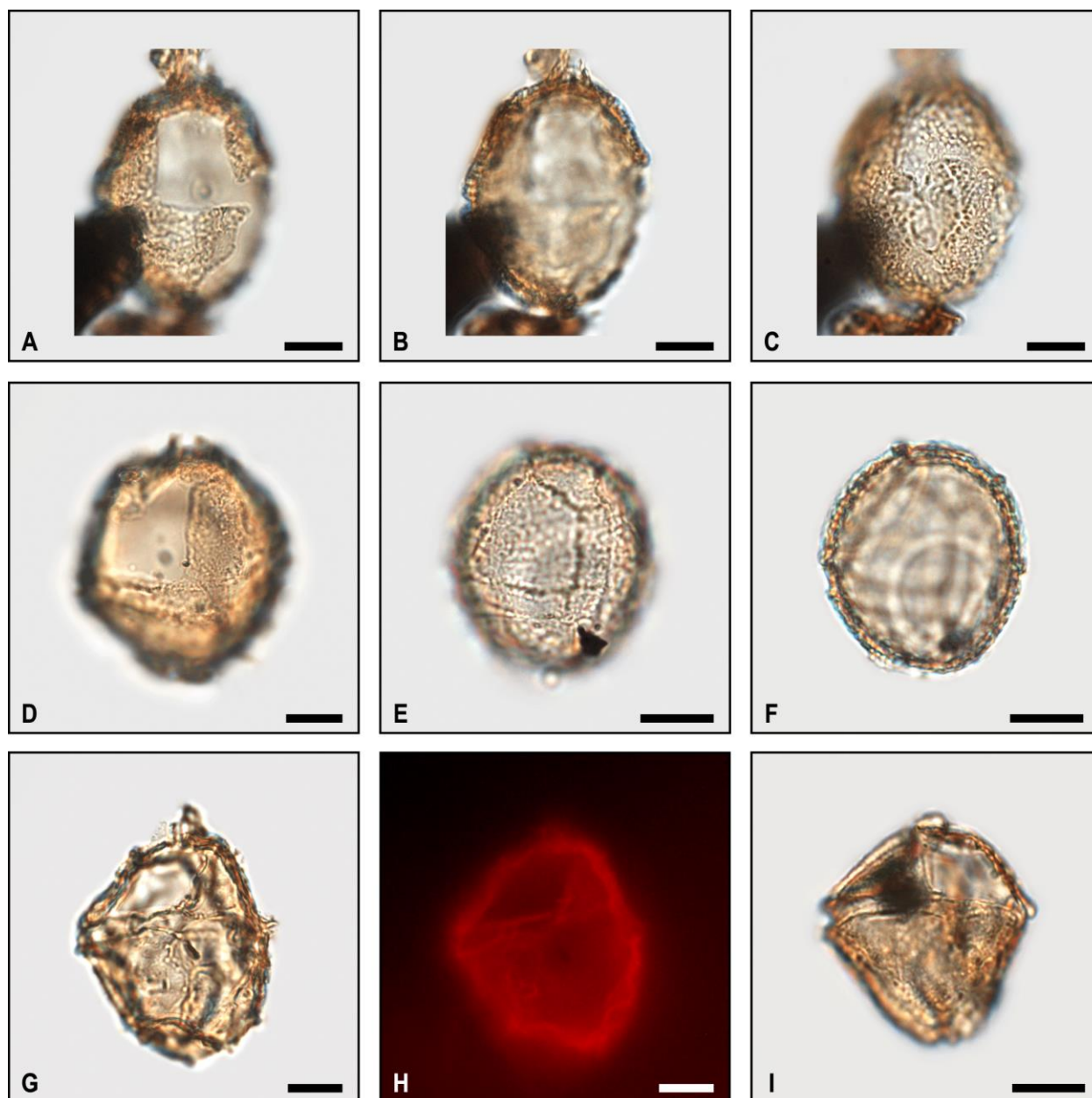


Plate 4.9. Bright-field photomicrographs and epifluorescence imaging of selected cladopyxiinean and gonyaulacacean dinoflagellate cysts. **A–D**, *Druggidium?* cf. *discretum*, subsample 14-271, slide A. **A**, dorsal view; **B**, mid-focus; **C**, ventral view; **D**, dorsolateral view, subsample 14-273, slide A. **E**, **F**, *Druggidium?* sp., subsample 16-363, slide B. **E**, dorsolateral? view; **F**, mid-focus. **G**, **H**, *Gonyaulacysta?* sp., subsample 15-758, slide C. **G**, dorsolateral view; **H**, dorsolateral view, epifluorescence. **I**, *Leptodinium* sp., dorsolateral view, subsample 15-761, slide C. Scale bars = 10 μ m.

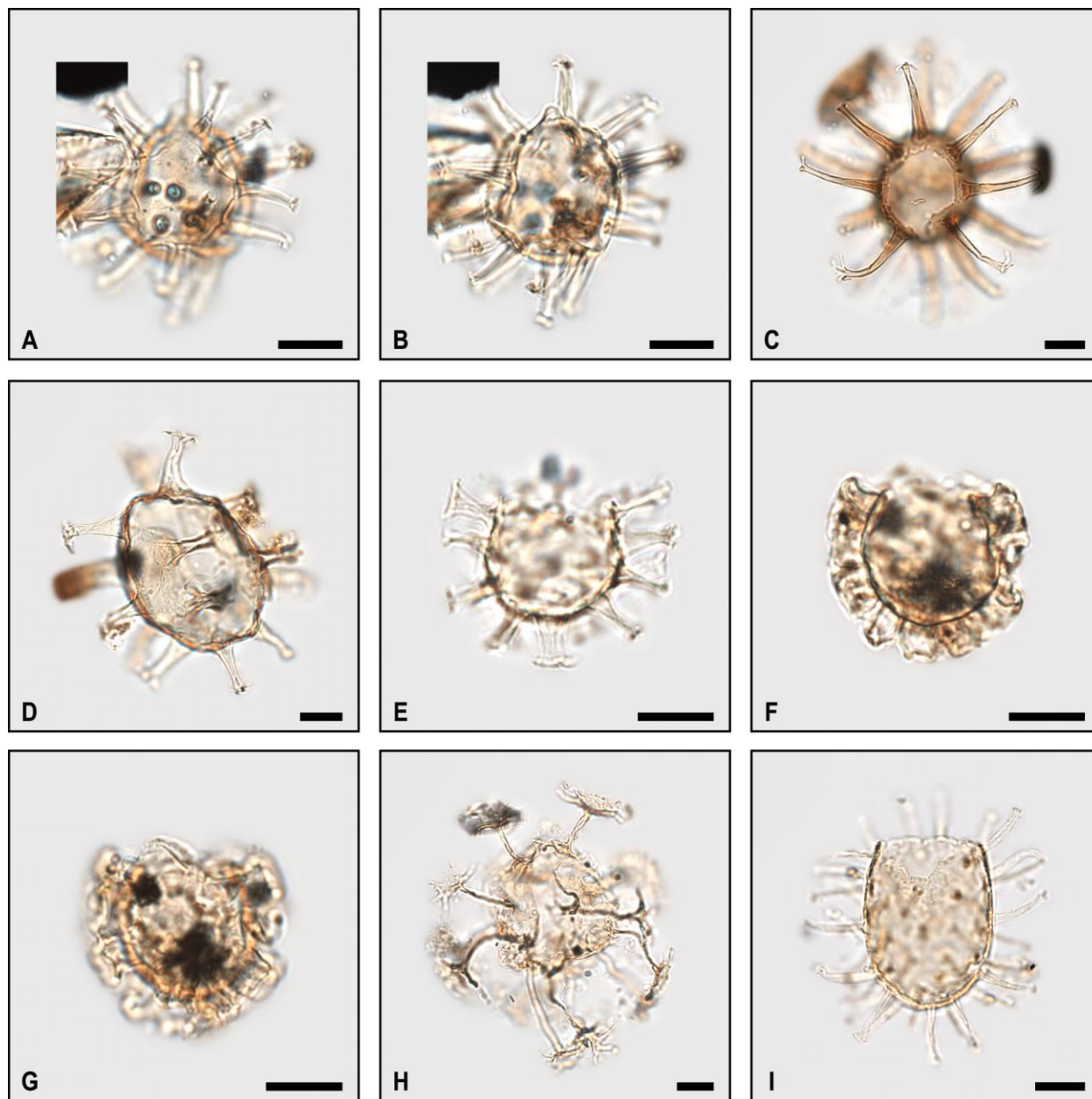


Plate 4.10. Bright-field photomicrographs of selected gonyaulacacean and goniodomacean dinoflagellate cysts. **A, B**, *Dapsilidinium* cf. *pseudocolligerum*, subsample 15-755, slide D; **A**, surficial view; **B**, mid-focus. **C**, *Hystrichosphaeridium recurvatum*, subsample 14-273, slide B, apical view. **D**, *Hystrichosphaeridium tubiferum*, subsample 14-269, slide A, apical view. **E**, *Minisphaeridium latiricum*, subsample 14-272, slide B, mid-focus. **F, G**, *Minisphaeridium* sp., subsample 15-766, slide C. **F**, mid-focus; **G**, surficial view. **H**, *Oligosphaeridium complex*, apical view, subsample 15-767, slide A. **I**, *Tanyosphaeridium xanthiopyxides*, subsample 14-272, slide A, precingular plate margin of apical archaeopyle in focus. Scale bars = 10 μ m.

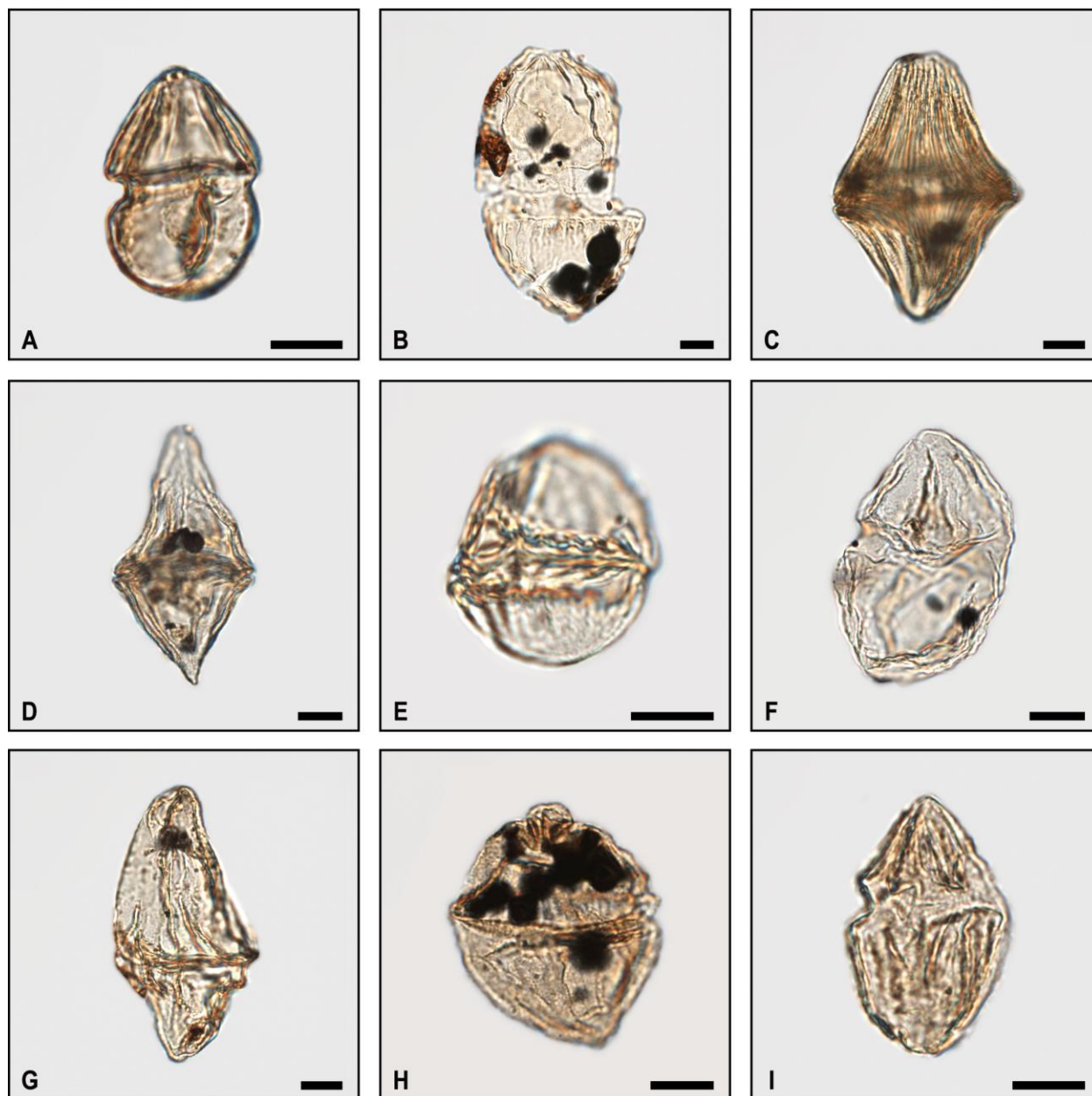


Plate 4.11. Bright-field photomicrographs of selected ptychodiscacean dinoflagellate cysts. **A**, *Alisogymnium euclaense*, subsample 15-766, slide C. **B**, *Amphigymnium cooksoniae*, subsample 14-269, slide B. **C**, *Dinogymnium acuminatum*, subsample 14-271, slide A. **D**, *Dinogymnium* cf. *aerlicum*, subsample 16-362, slide B. **E**, *Dinogymnium avellana*, subsample 15-755, slide D. **F**, *Dinogymnium cretaceum*, subsample 15-755, slide D. **G**, *Dinogymnium longicorne*, subsample 14-269, slide B. **H**, *Dinogymnium* sp. A, subsample 15-756, slide A. **I**, *Dinogymnium* sp. B, subsample 15-756, slide A. Scale bars = 10 μ m.

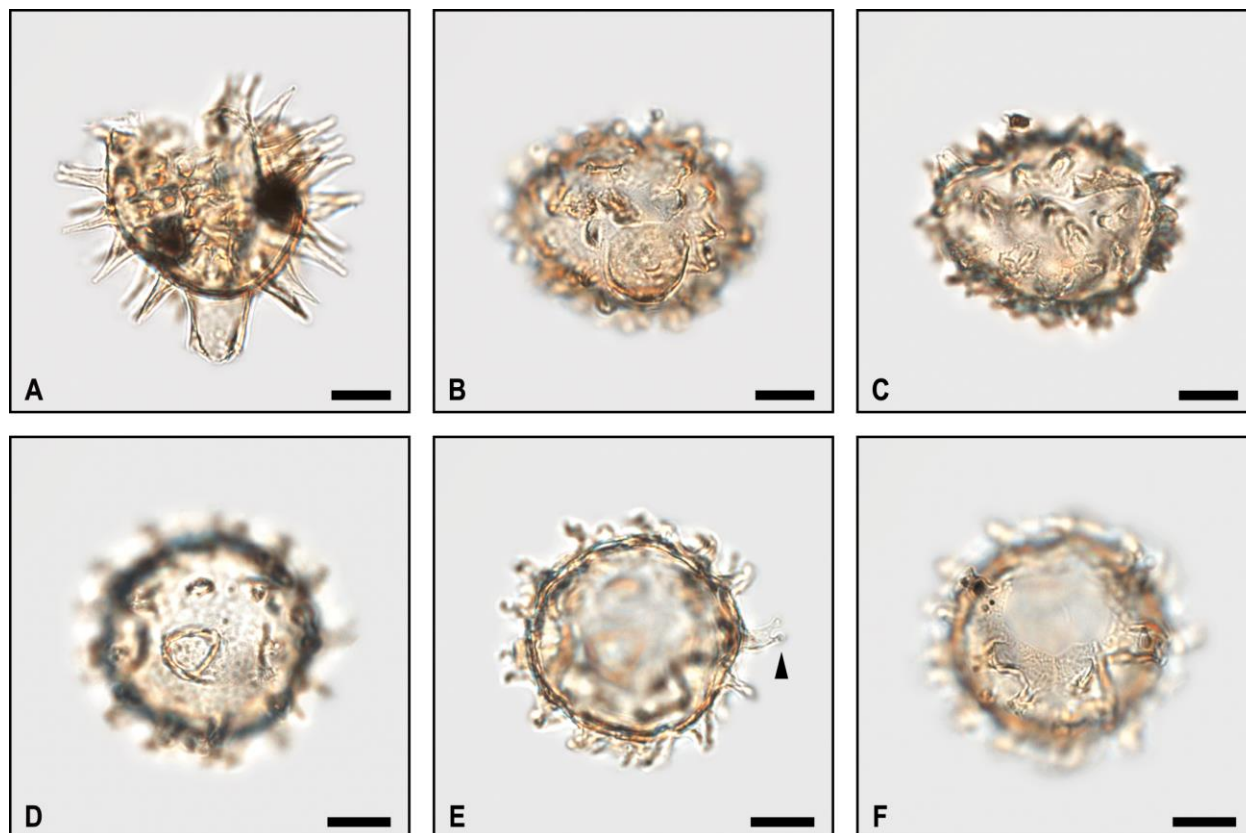


Plate 4.12. Bright-field photomicrographs of selected gonyaulacacean dinoflagellate cysts. **A**, *Diphyes colligerum*, subsample 14-271, slide A. **B–F**, *Diphyes* spp.? **B**, **C**, subsample 15-766, slide C; **B**, antapical view; **C**, apical view; **D–F**, subsample 14-272, slide B; **D**, antapical view; **E**, mid-focus; **F**, apical view. Scale bars = 10 μm .

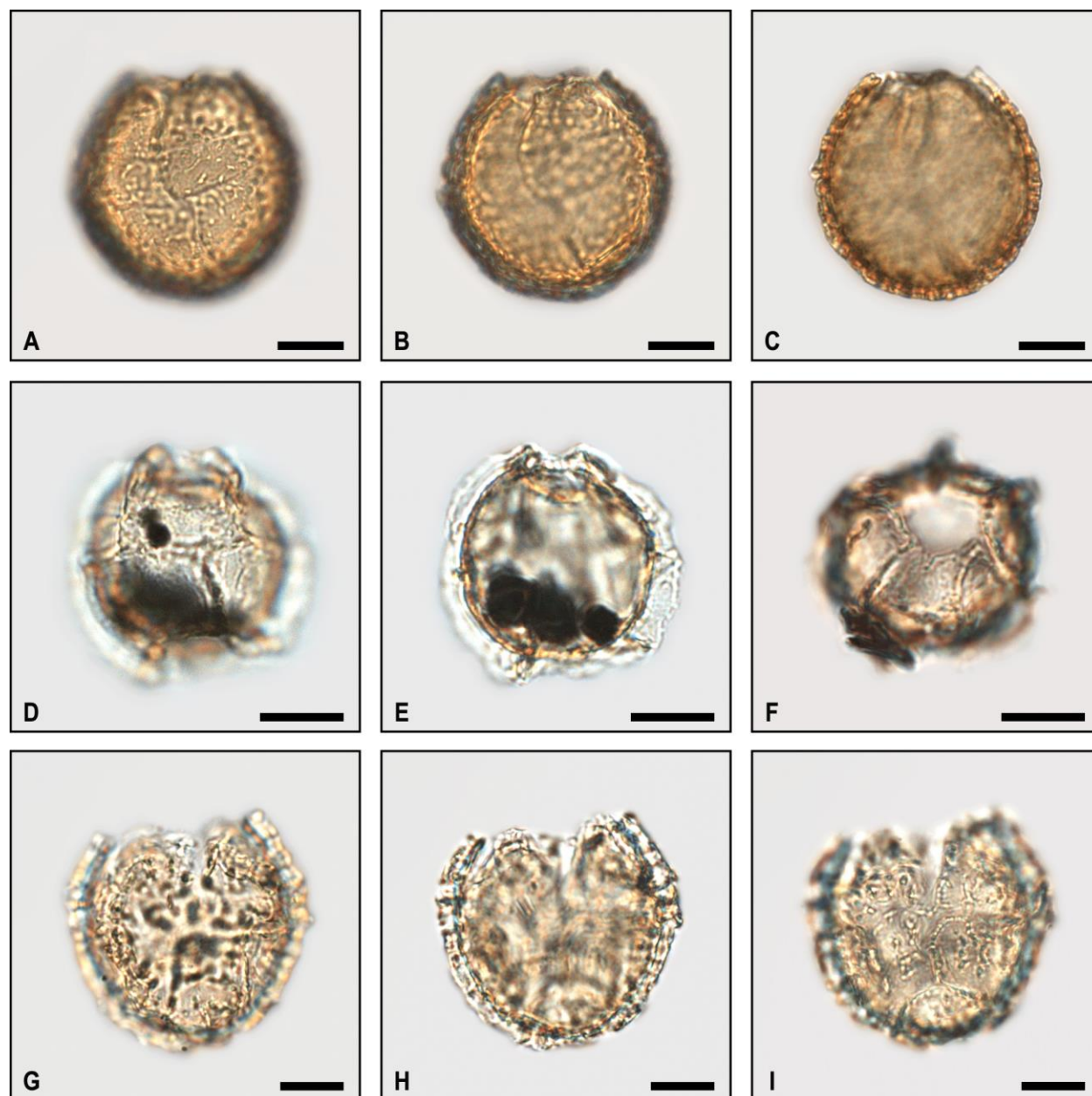


Plate 4.13. Bright-field photomicrographs of selected cladopyxiinean and goniodomacean dinoflagellate cysts. **A–C**, *Eisenackia?* sp., subsample 14-271, slide A. **A**, surficial view; **B**, one-quarter focus; **C**, mid-focus. **D–F**, *Microdinium carpentierae*. **D**, **E**, subsample 15-768, slide A; **D**, dorsal view; **E**, mid-focus; **F**, subsample 15-760, slide D apical view. **G–I**, *Microdinium mariae*, subsample 14-272, slide B. **G**, dorsal view, one-quarter focus; **H**, mid-focus; **I**, ventral view. Scale bars = 10 μm .

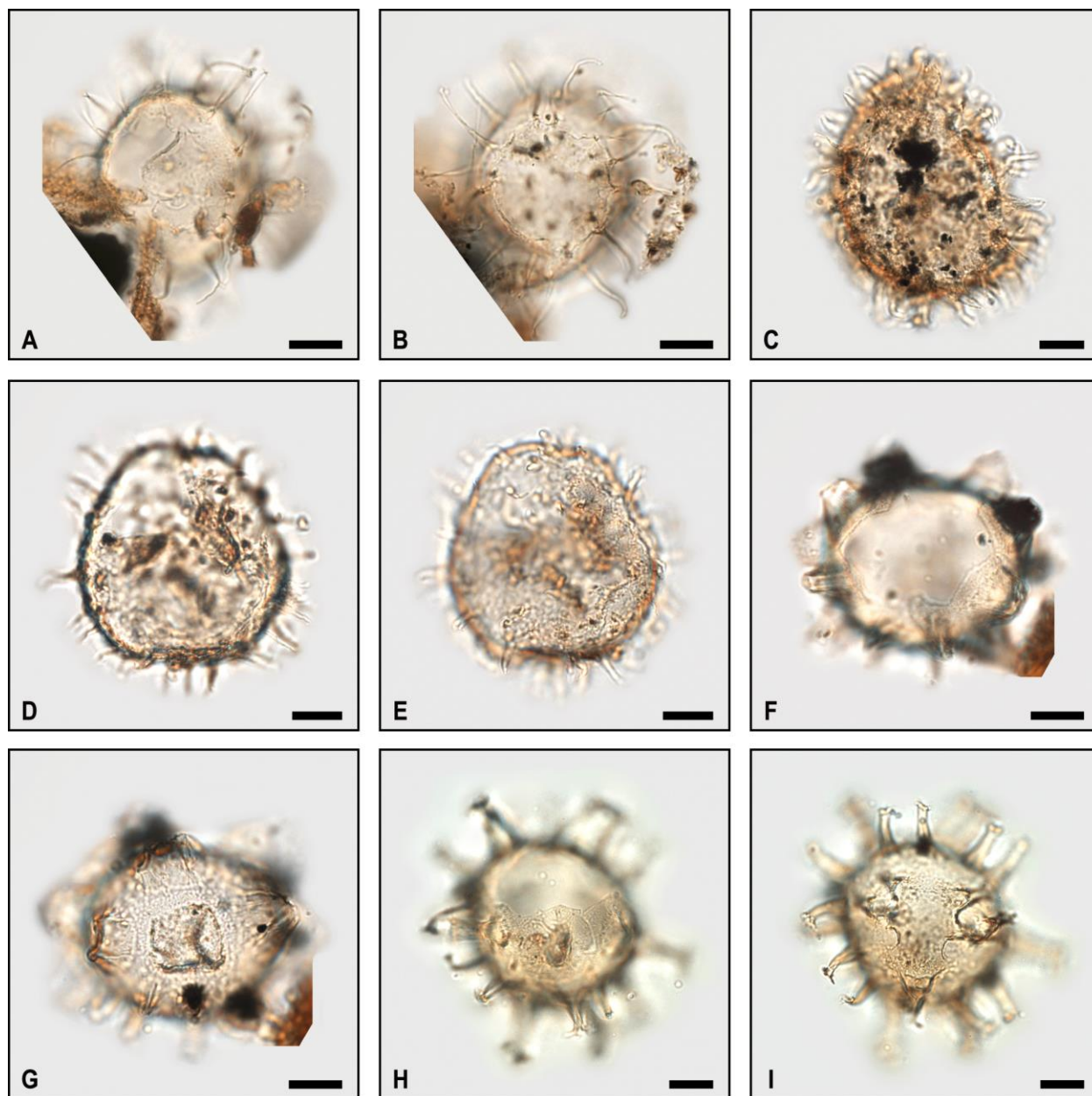


Plate 4.14. Bright-field photomicrographs of selected goniodomacean and gonyaulacacean dinoflagellate cysts. **A–E**, *Fibrocysta* spp.. **A**, **B**, subsample 14-274, slide B; **A**, dorsolateral view; **B**, ventrolateral view; **C**, subsample 14-269, slide B surficial view; **D**, **E**, subsample 14-269, slide B; **D**, dorsolateral view; **E**, ventrolateral view. **F**, **G**, *Litosphaeridium* spp., subsample 14-273, slide B. **F**, apical view; **G**, surficial view. **H**, **I**, *Polysphaeridium* spp. subsample 16-367, slide B. **H**, precingular plate margin of apical archaeopyle in focus; **I**, surficial view. Scale bars = 10 μm .

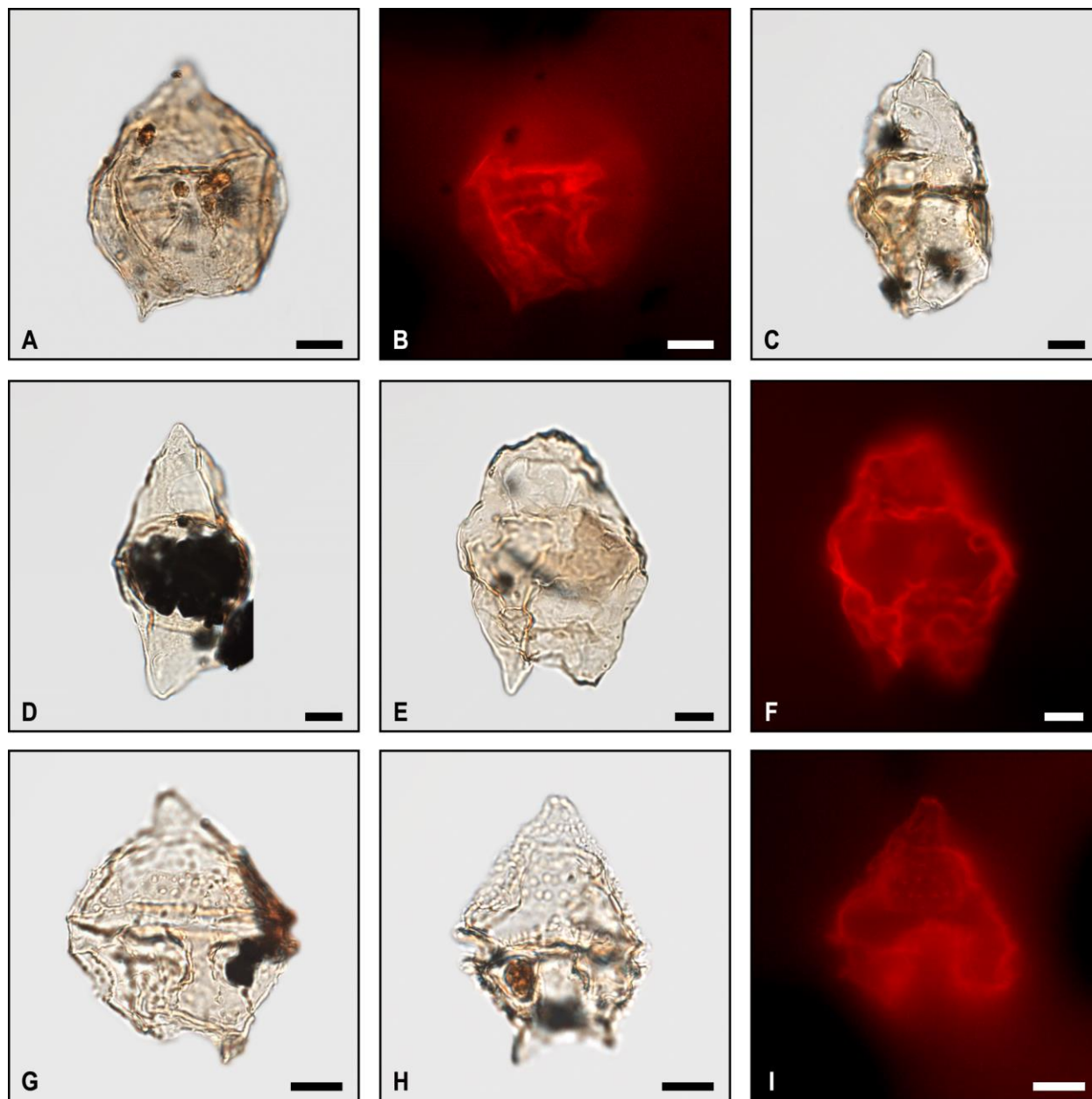


Plate 4.15. Bright-field photomicrographs and epifluorescence imaging of selected peridiniacean dinoflagellate cysts. **A, B**, *Geiselodinium geiseltense*, subsample 15-760, slide D. **A**, dorsal view; **B**, dorsal view, epifluorescence. **C, D**, *Isabelidinium bakeri*. **C**, subsample 15-764, slide A dorsolateral view; **D**, subsample 14-272, slide B, dorsolateral view. **E, F**, *Isabelidinium weidichii*, subsample 15-758, slide C. **E**, dorsal view; **F**, mid-focus, epifluorescence. **G**, *Spinidinium densispinatum*, subsample 14-272, slide A, dorsal view. **H, I**, *Spinidinium echinoideum*, subsample 14-272, slide A. **H**, mid-focus; **I**, mid-focus, epifluorescence. Scale bars = 10 μm .

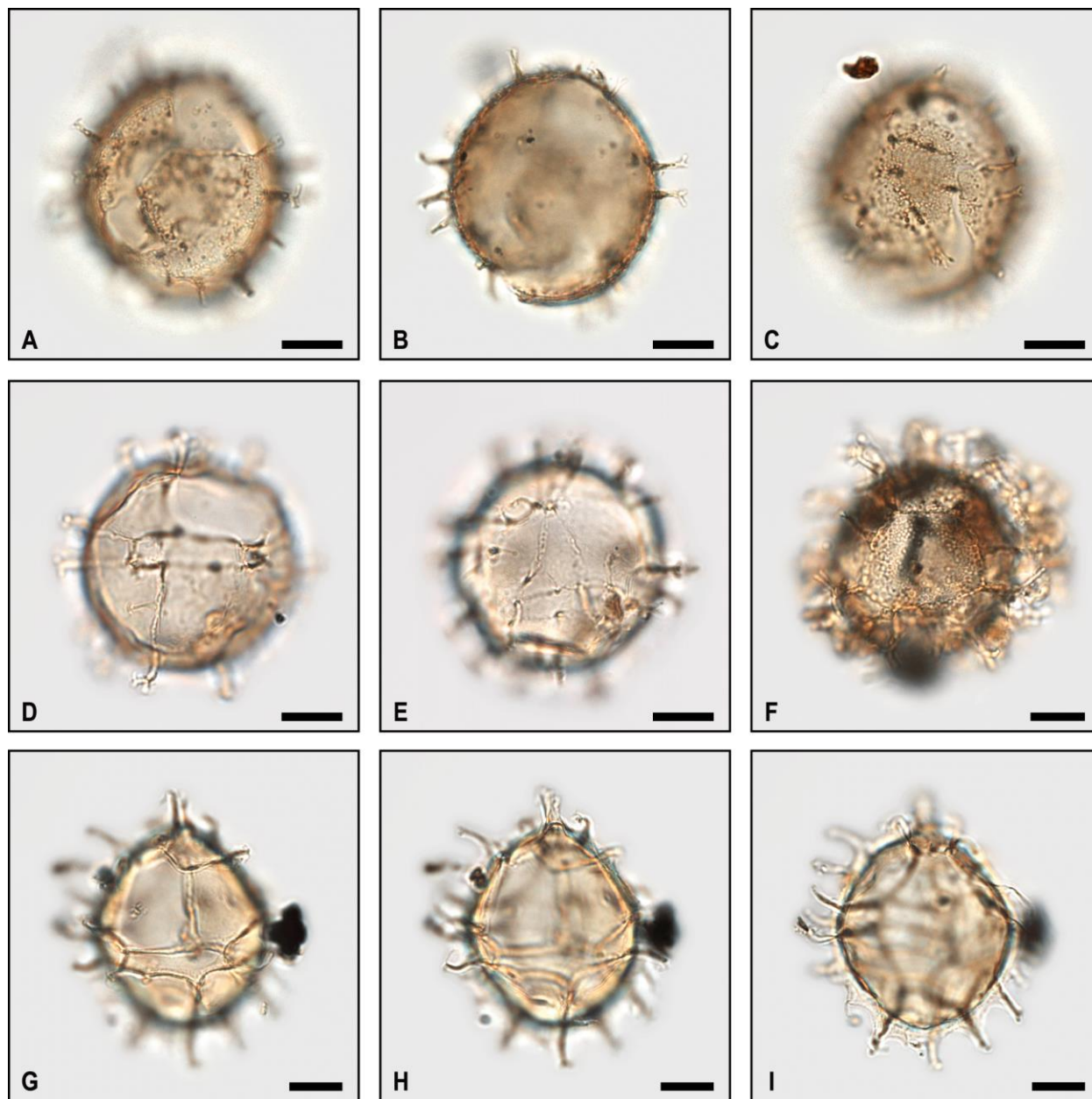


Plate 4.16. Bright-field photomicrographs of selected gonyaulacacean dinoflagellate cysts. **A–C**, *Hafniasphaera delicata*, subsample 16-366, slide B. **A**, dorsolateral view; **B**, mid-focus; **C**, ventral view. **D, E**, *Hafniasphaera cf. delicata*, subsample 14-272, slide A. **D**, dorsolateral view; **E**, ventral view. **F**, *Hafniasphaera septata*, subsample 14-269, slide B, dorsolateral view. **G–I**, *Spiniferites* sp. A, subsample 14-269, slide A. **G**, dorsolateral view; **H**, mid-focus; **I**, ventral view, one-quarter focus. Scale bars = 10 μm .

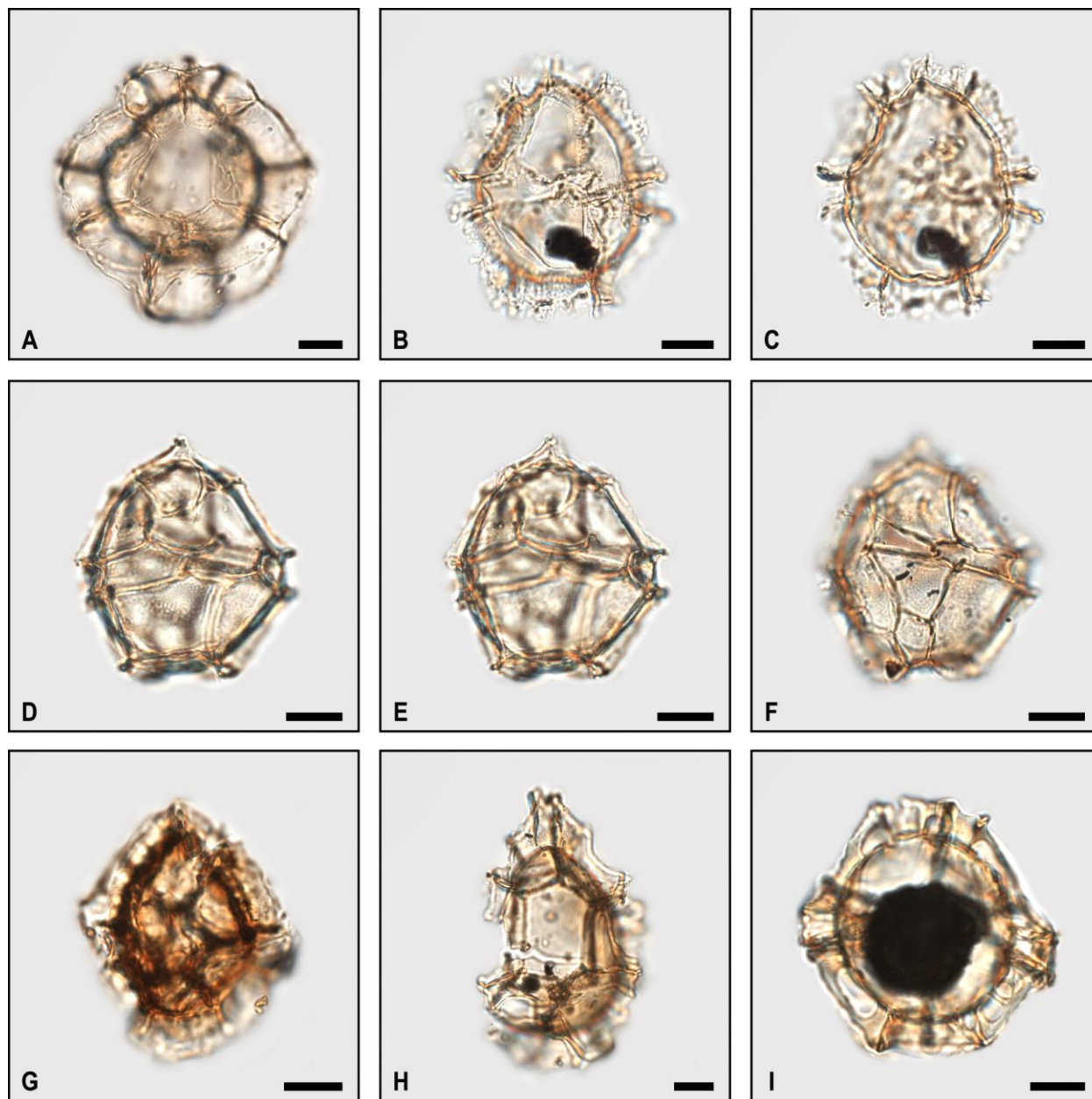


Plate 4.17. Bright-field photomicrographs of selected gonyaulacacean dinoflagellate cysts. **A**, *Impagidinium rigidaseptatum*, subsample 14-273, slide B dorsal view. **B**, **C**, *Impagidinium* cf. *scabrosum*, subsample 14-272, slide A. **B**, dorsolateral view; **C**, mid-focus. **D–F**, *Impagidinium* cf. *sphaericum–multiplex* of de Coninck (1968), subsample 15-760, slide A. **D**, dorsolateral view; **E**, mid-focus; **F**, ventrolateral view. **G**, *Impagidinium* spp., subsample 15-755, slide C, one-quarter focus, dorsal view. **H**, *Pterodinium cingulatum sensu Antonescue et al.* (2001a), subsample 15-759, slide C, dorsal view. **I**, *Unipontidinium aquaeductus*, subsample 14-272, slide B, dorsolateral view. Scale bars = 10 μ m.

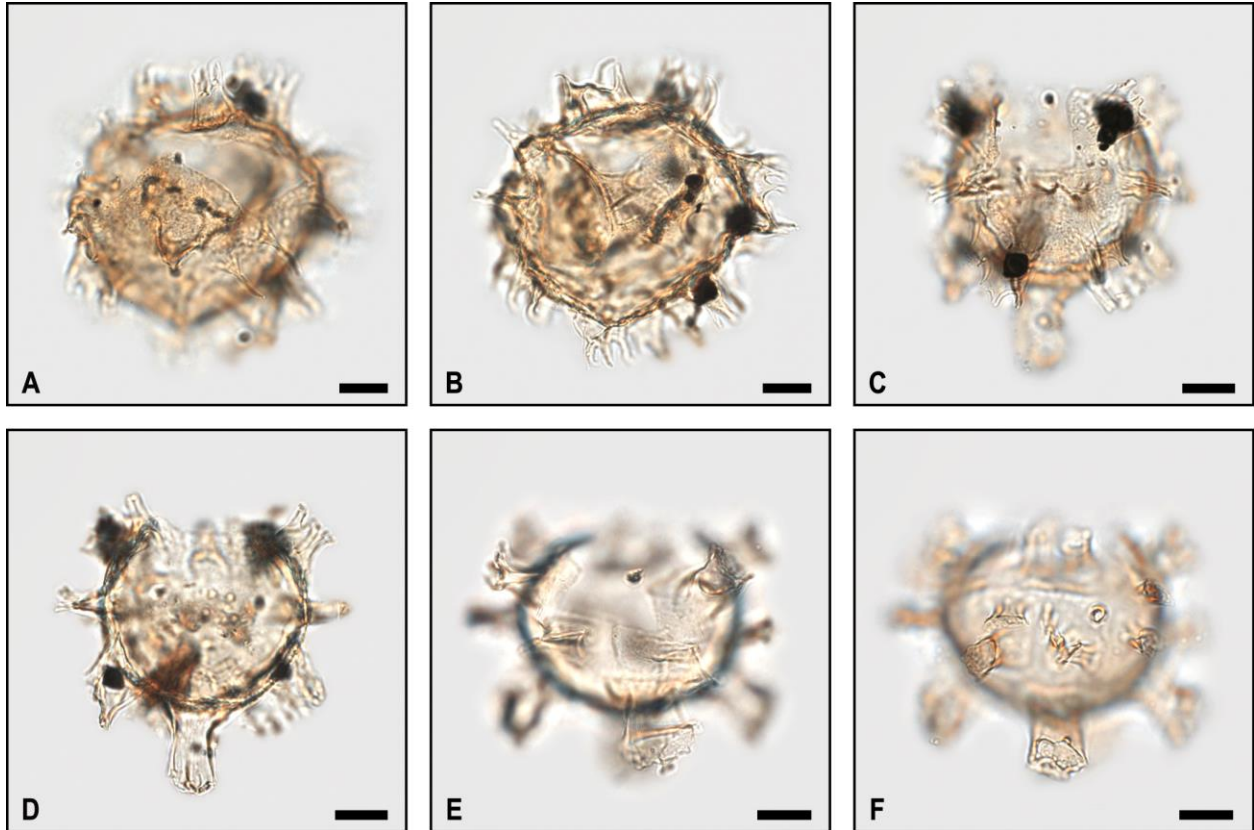


Plate 4.18. Bright-field photomicrographs of selected gonyaulacacean dinoflagellate cysts. **A, B**, *Florentinia ferox*, subsample 14-272, slide B. **A**, surficial view with precingular plate margin of apical archaeopyle in focus; **B**, mid-focus. **C, D**, *Florentinia laciniata*, subsample 15-763, slide A. **C**, dorsal view; **D**, mid-focus. **E, F**, *Kleithriasphaeridium perforatum*, subsample 14-272, slide A. **E**, dorsolateral view; **F**, ventral view. Scale bars = 10 µm.

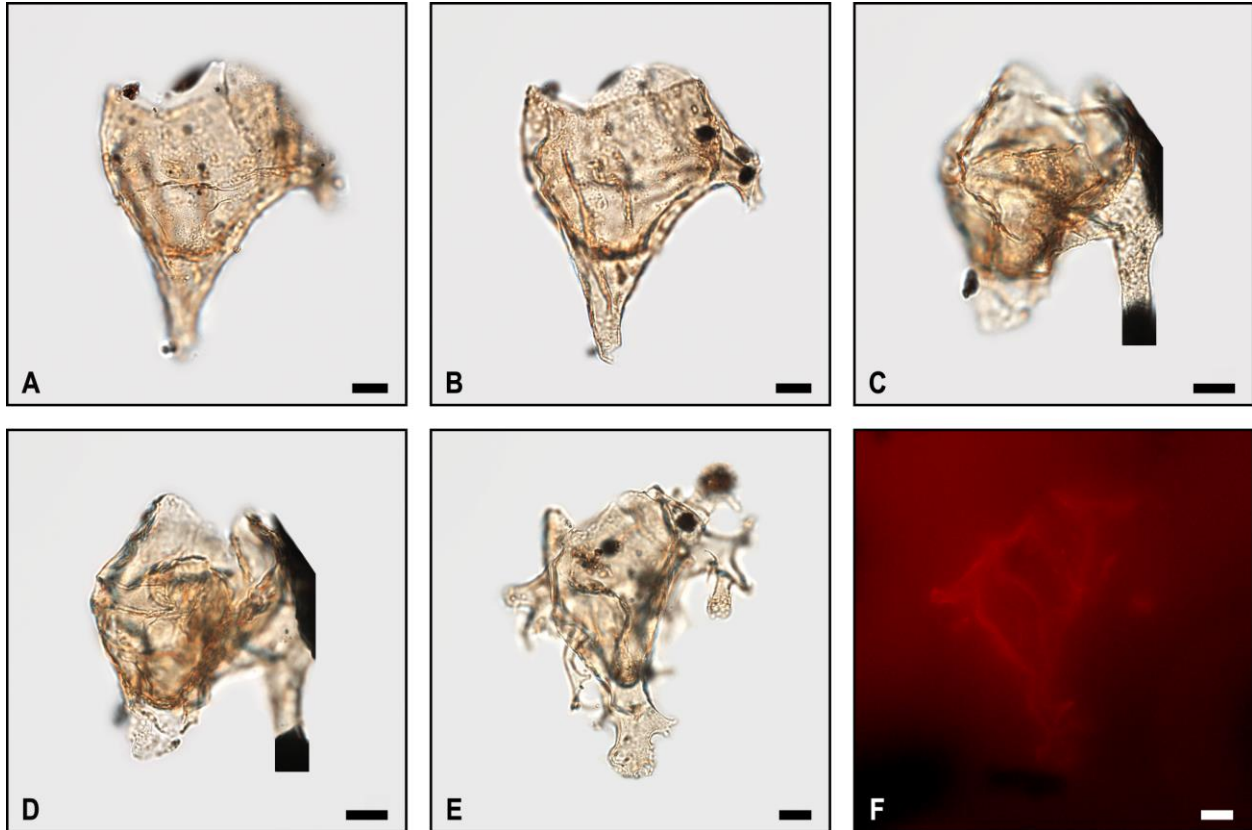


Plate 4.19. Bright-field photomicrographs and epifluorescence imaging of selected ceratiacean dinoflagellate cysts. **A, B**, *Odontochitina cf. nuda*, subsample 16-368, slide C. **A**, dorsal view; **B**, ventral view. **C, D**, *Odontochitina cf. tabulata*, subsample 14-269, slide B. **C**, dorsolateral view, one-quarter focus; **D**, ventrolateral view. **E, F**, *Xenascus ceratioides*, subsample 14-269, slide B. **E**, mid-focus; **F**, mid-focus, epifluorescence. Scale bars = 10 µm.

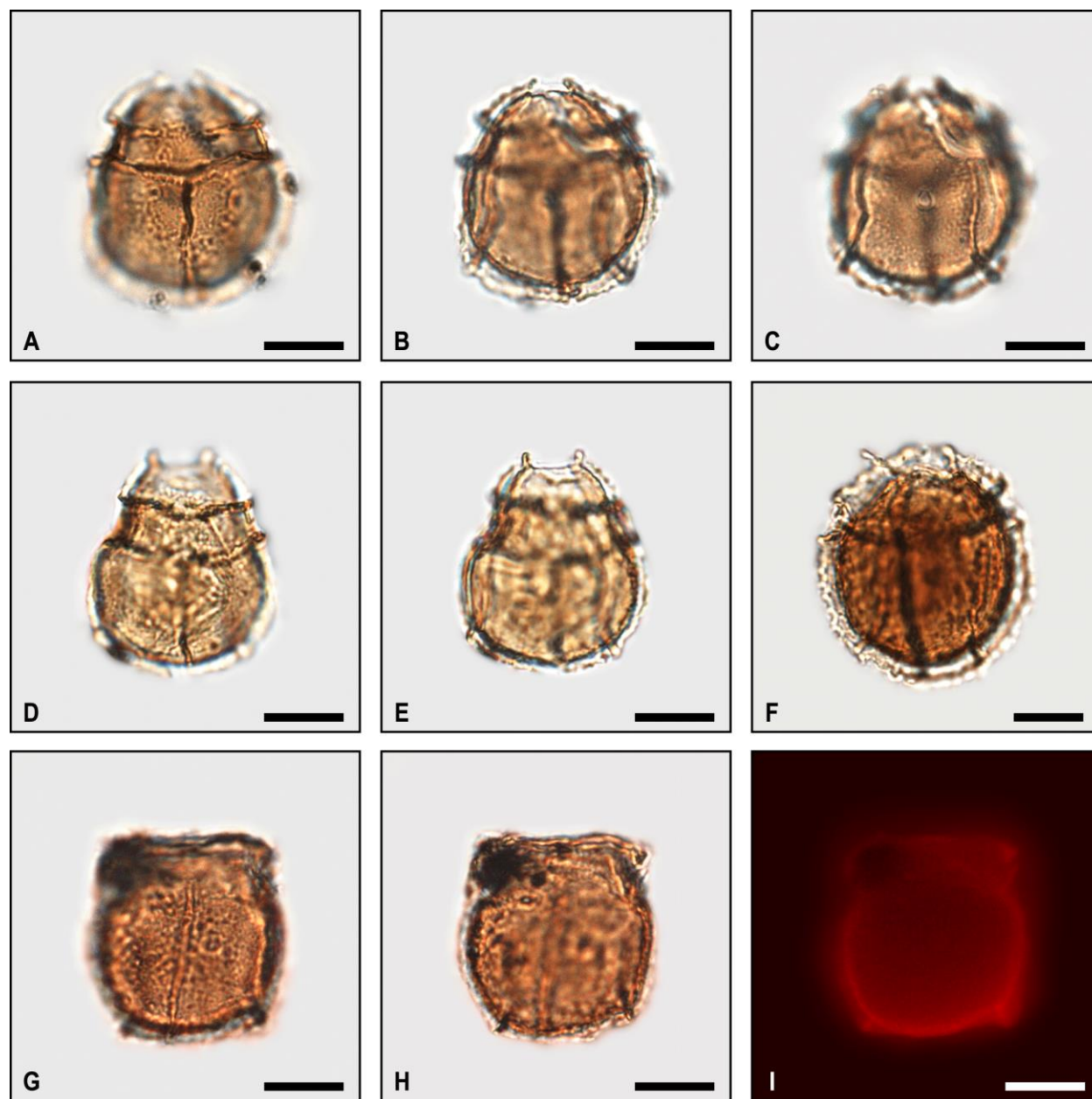


Plate 4.20. Bright-field photomicrographs and epifluorescence imaging of selected gonyaulacacean dinoflagellate cysts. **A–C**, *Phanterodinium belgicum*, sample 15-767, slide B. **A**, dorsal view; **B**, mid-focus; **C**, ventral view. **D, E**, *Phanterodinium cf. belgicum*, sample 15-768, slide A. **D**, dorsal view; **E**, mid-focus. **F**, *Phanterodinium* sp., dorsolateral view, sample 15-756, slide A. **G–I**, *Phanterodinium?* *turnhoutensis*, sample 15-756, slide A. **G**, dorsal view; **H**, dorsal view, one quarter focus; **I**, mid-focus, epifluorescence. Scale bars = 10 μm .

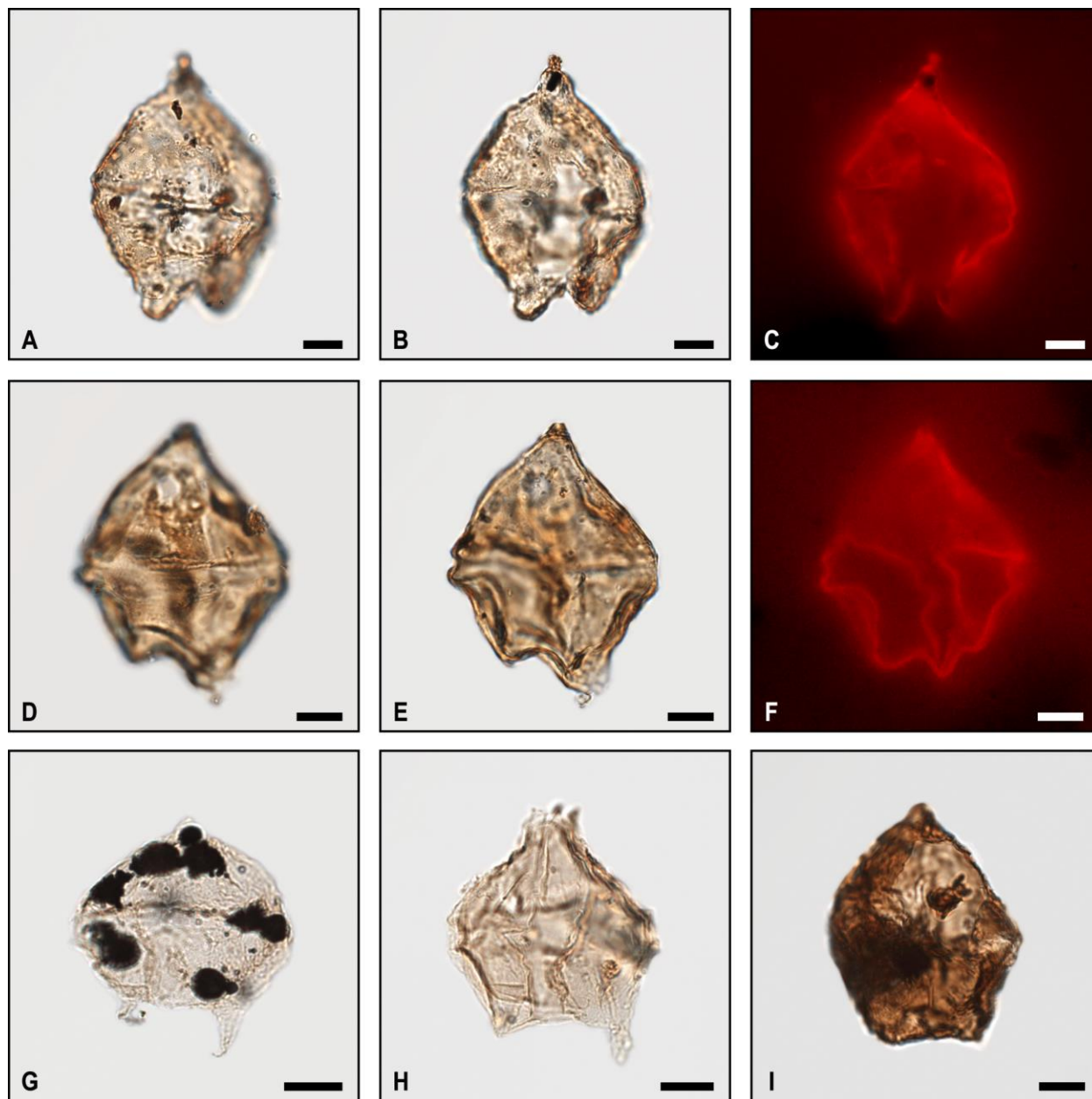


Plate 4.21. Bright-field photomicrographs and epifluorescence imaging of selected protoperidiniacean and peridiniacean dinoflagellate cysts. **A–C**, *Protoperidinium* sp. *A*, sample 15-759, slide C. **A**, dorsal view; **B**, ventral view; **C**, ventral view, epifluorescence. **D–F**, *Protoperidinium* sp. *B*, sample 16-365, slide B. **D**, dorsal view; **E**, mid-focus; **F**, ventral view, epifluorescence. **G**, **H**, Peridiniacean Group A. **G**, sample 16-362, slide A, dorsal view; **H**, sample 14-269, slide B, ventral view. **I**, Peridiniacean Group B, sample 15-755, slide D, dorsolateral view. Scale bars = 10 μm .

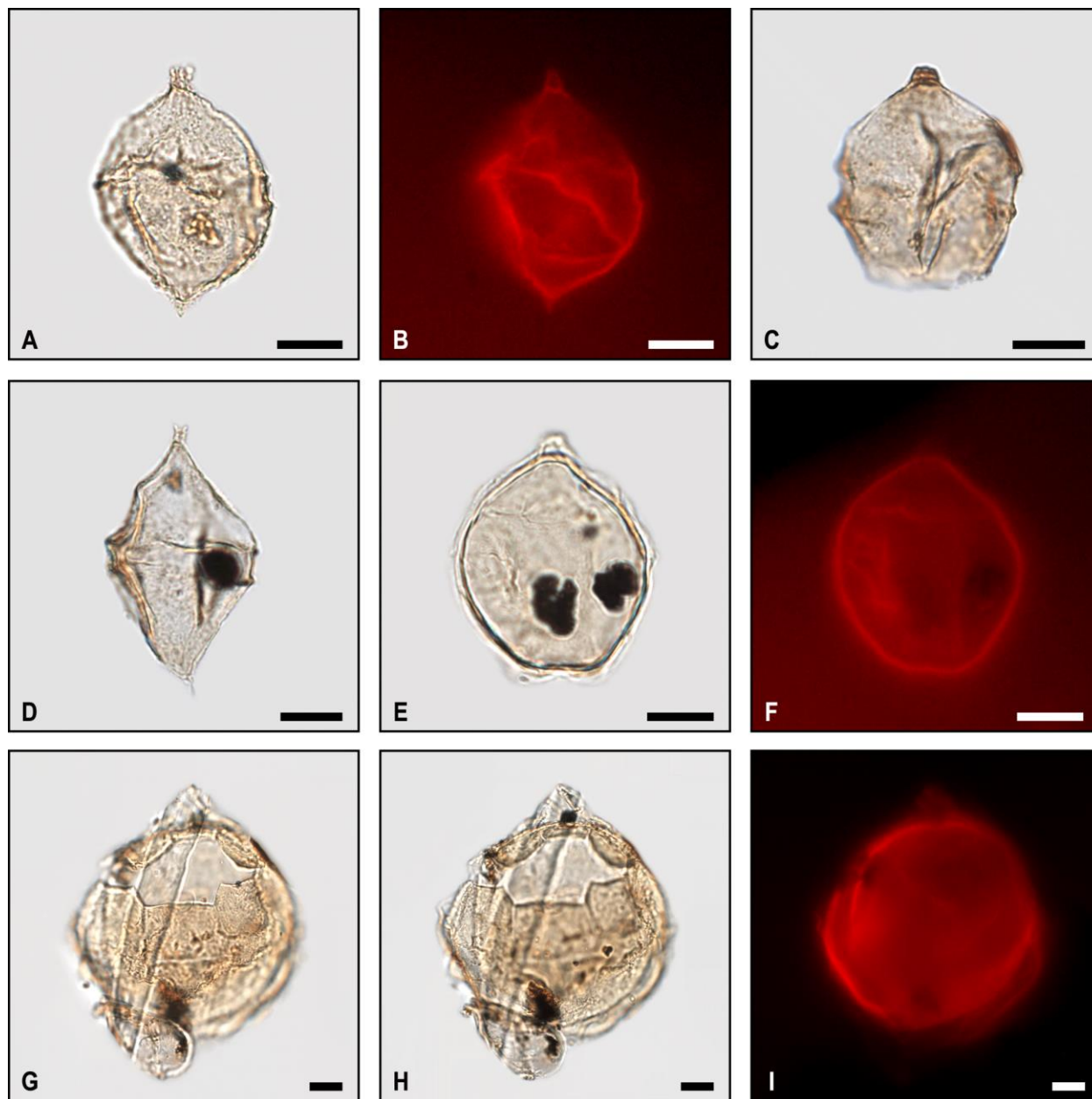


Plate 4.22. Bright-field photomicrographs and epifluorescence imaging of selected peridiniacean dinoflagellate cysts. **A, B**, *Laciniadinium arcticum*, sample 14-272, slide B. **A**, surficial view; **B**, surficial view, epifluorescence. **C**, *Laciniadinium firmum*, sample 15-766, slide C, ventral view. **D**, *Laciniadinium rhombiforme*, sample 15-766, slide C, surficial view. **E, F**, *Senegalinium? simplex*, sample 14-271, slide A. **E**, dorsal view; **F**, dorsal view, epifluorescence. **G–I**, *Trithyrodinium evittii*, sample 14-274, slide A. **G**, dorsal view; **H**, mid-focus; **I**, mid-focus, epifluorescence. Scale bars = 10 μm .

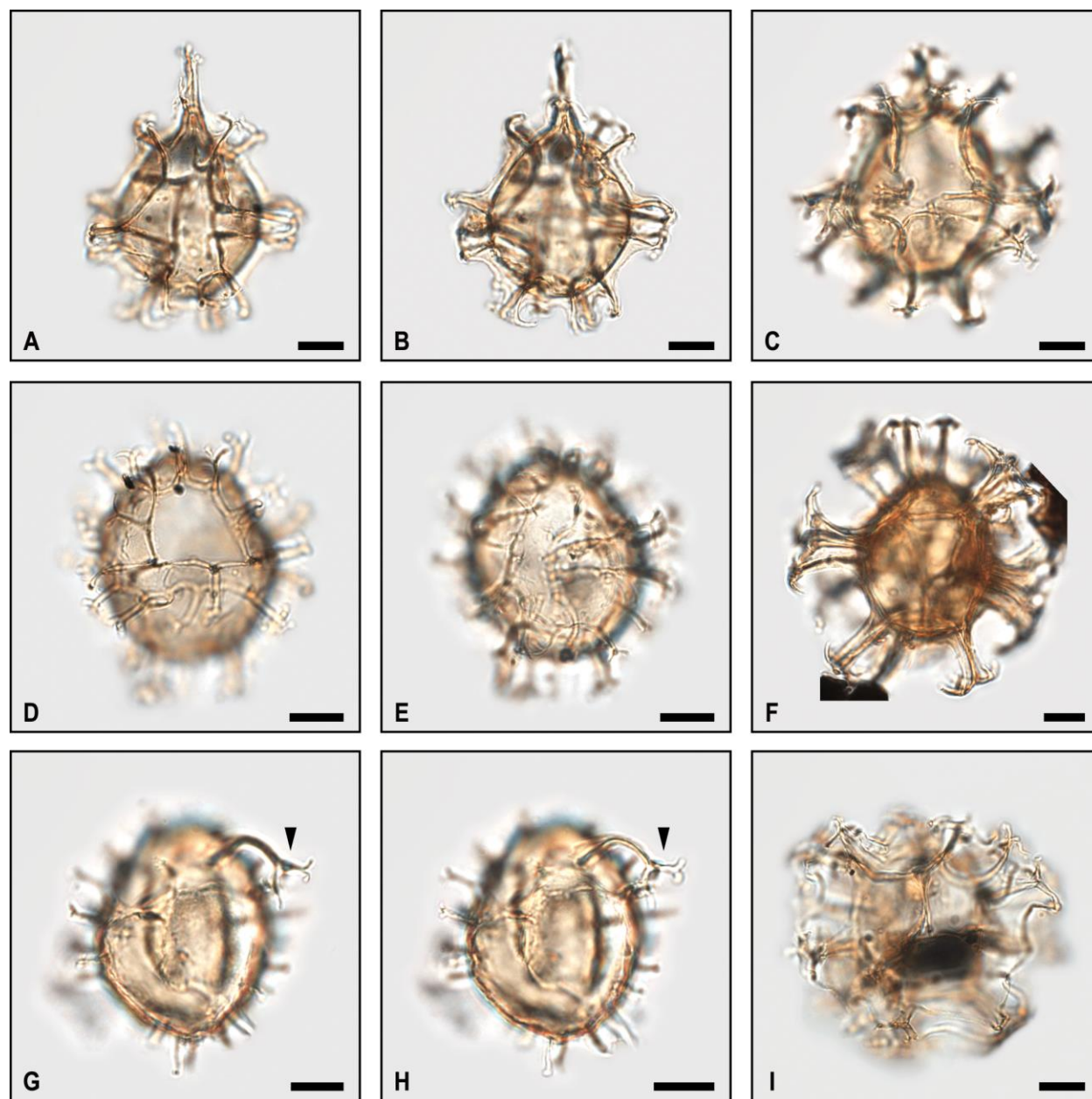


Plate 4.23. Bright-field photomicrographs of selected gonyaulacacean dinoflagellate cysts. **A–C**, *Spiniferella cornuta*. **A**, **B**, sample 15-765, slide C; **A**, ventral view; **B**, mid-focus; **C**, sample 14-272, slide A, dorsal view. **D–H**, *Spiniferites* spp. **D–F**, sample 16-368, slide E, form with gonal and intergonal processes; **D**, dorsal view; **E**, ventral view; **F**, mid-focus, form with robust gonal processes; **G**, **H**, sample 14-274, slide A, aberrant form, arrow denotes a single, large, distally trifurcated and bifurcated process; **G**, surficial view; **H**, one-quarter focus. **I**, *Nemosphaeropsis* sp., sample 16-368, slide E. Scale bars = 10 μm .

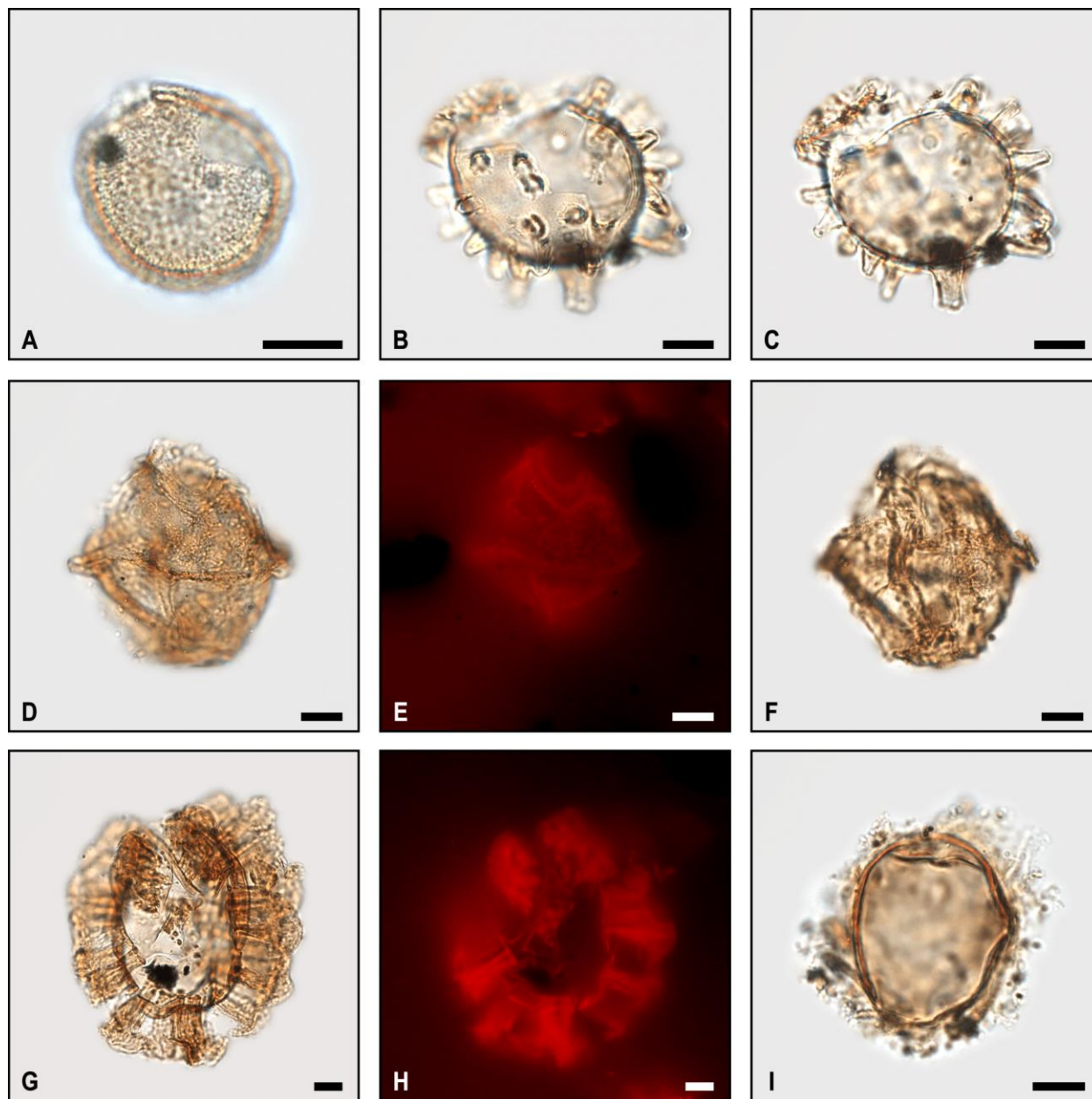


Plate 4.24. Bright-field photomicrographs and epifluorescence imaging of selected gonyaulaccean, indeterminate, and possible dinoflagellate cysts. **A**, *Xenicodinium delicatum sensu Slimani et al.* 2011, sample 15-762, slide A, dorsolateral view. **B**, **C**, Cyst Type A, sample 14-273, slide B. **B**, precingular plate margin of apical archaeopyle in focus; **C**, mid-focus. **D–F**, Cyst Type B, sample 15-755, slide A. **D**, dorsal view; **E**, dorsal view, epifluorescence; **F**, ventral view. **G**, **H**, Cyst Type C, 15-766, slide C. **G**, surficial view; **H**, surficial view, epifluorescence. **I**, Cyst? Type A, sample 16-368, slide E, mid-focus. Scale bars = 10 μm .

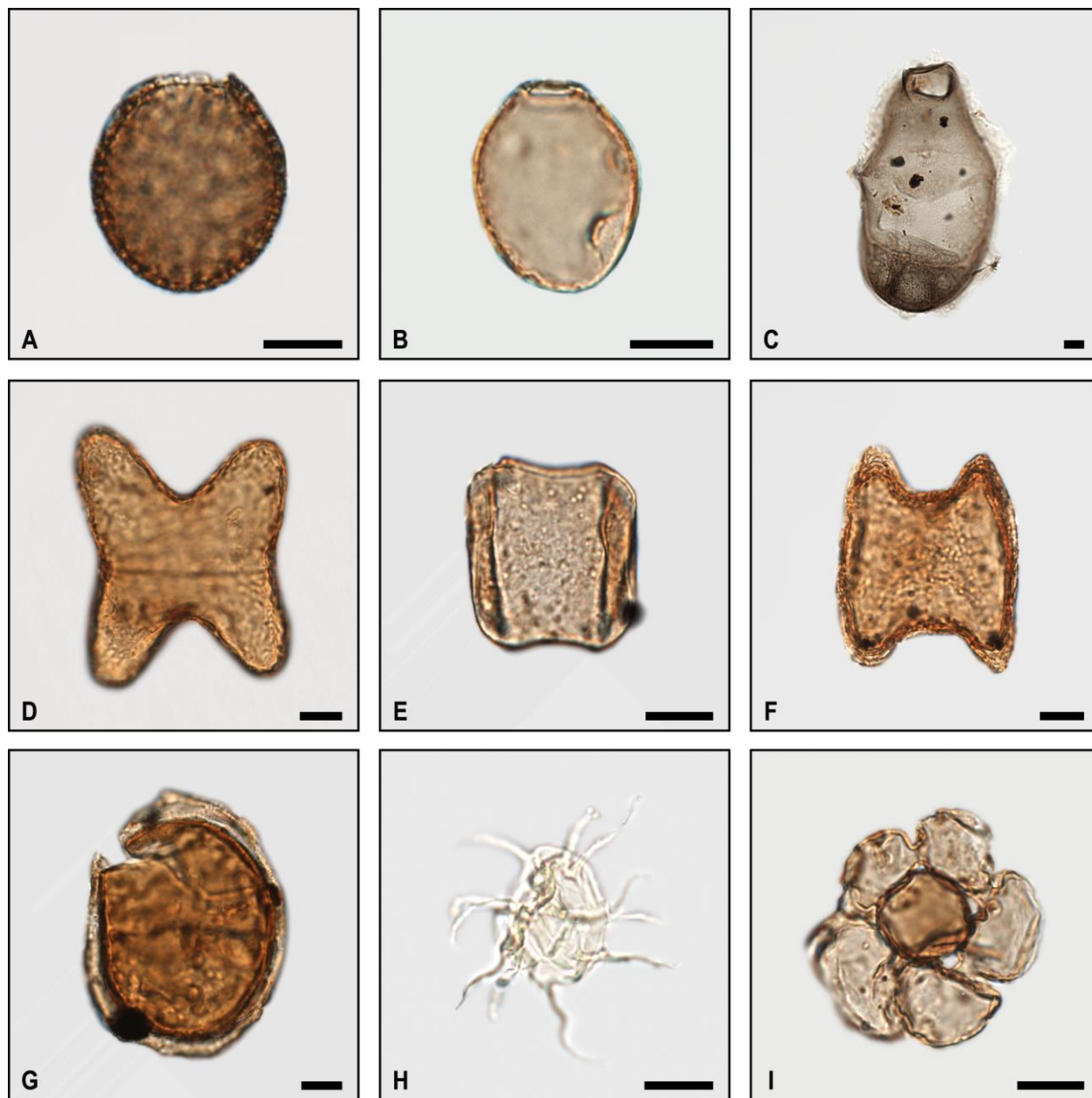


Plate 4.25. Bright-field photomicrographs of selected marine acritarchs and other palynomorphs. **A**, *Palaeostomocystis reticulata*, subsample 15-767, slide B. **B**, *Fromea chytra*, subsample 14-272, slide A. **C**, *Fromea* sp., subsample 14-269, slide A. **D**, *Schizocysta rugosa*, 15-756, slide A. **E**, *Tetrachacysta* sp., subsample 15-766, slide C; **F**, *Horolonginella?* sp., subsample 14-272, slide B. **G**, *Paralecaniella indentata*, subsample 15-766, slide C. **H**, *Micrhystridium* sp., subsample 14-270, slide A. **I**, Foraminifera organic lining, subsample 15-756, slide A. Scale bars = 10 μ m.

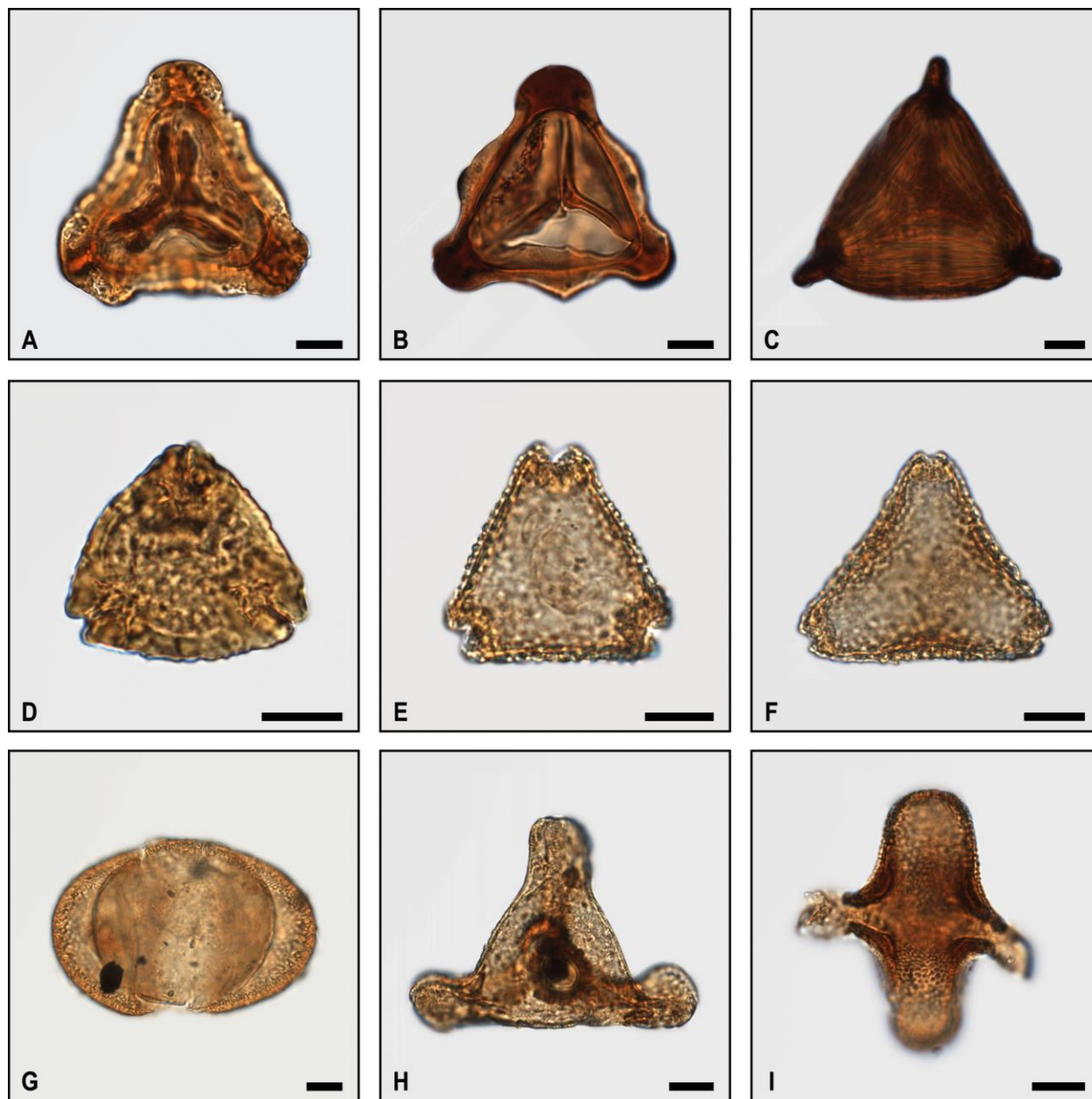


Plate 4.26. Bright-field photomicrographs of selected terrestrial miospores and pollen grains. **A**, *Trilobosporites* cf. *humilis*, subsample 14-269, slide B. **B**, *Trilobosporites* sp., subsample 15-767, slide B. **C**, *Appendicisporites* sp., subsample 15-766, slide C. **D**, *Trudopollis* sp., subsample 16-361, slide A. **E**, *Proteacidies* sp., subsample 14-269, slide B. **F**, *Atlantopolis* sp., subsample 16-363, slide A. **G**, *Picea* sp., subsample 15-766, slide C. **H**, *Aquilapollenites* cf. *pseudoaucellatus*, subsample 15-766, slide C. **I**, *Aquilapollenites* sp., subsample 15-755, slide D. Scale bars = 10 μm .

4.5 Discussion

4.5.1 Age interpretation

Dinoflagellates achieved some of their greatest levels of diversity in the Late Cretaceous (e.g. Bujak & Williams 1979; Stover *et al.* 1996; Matthiessen & Schreck 2015) and were largely unaffected by the K-Pg extinction event (e.g. Hansen 1977; Brinkhuis & Zachariasse 1988; Slimani *et al.* 2010). Many dinoflagellate cyst taxa present a record of long-ranging, highly successful organisms with those known to have chronostratigraphic ranges of less than 10 Ma being most useful for biostratigraphic studies (e.g. Williams *et al.* 2004; Pearce *unpub.*). Twenty-four dinoflagellate cyst forms have been identified from the Hornby Island samples that are referable to species which provide age constraints within the Late Cretaceous–Paleocene (Figure 4.5). Taken as an suite, the following taxa have enabled the determination of a late Campanian–early Maastrichtian age for the Northumberland Formation: the areoligeracean *S. protrusa* (e.g. Prince *et al.* 1999; Slimani *et al.* 2016); ceratiaceans *X. ceratioides* (e.g. Hoek *et al.* 1996; Williams *et al.* 2004; Fensome *et al.* 2008) and *O. tabulata* (El Mehdawi 1998; Slimani *et al.* 2016); cladopyxiineans *C. paucireticulatum* (Slimani 1994, 2000, 2003; Riding & Kyffen-Hughes 2004; Slimani *et al.* 2011; Surlyk *et al.* 2013; Guzhikova 2016), *D.?* *discretum* (Slimani & Louwye 2011; Slimani *et al.* 2011), *M. carpentierae* (Wilson 1971, 1974?; Marheinecke 1992; Slimani 1994; Schiøler & Wilson 2001; Antonescue *et al.* 2001b; Odin 2001), and *M. mariae* (Slimani 1994; Slimani *et al.* 2011); gonyaulacaceans *I. rigidaseptatum* (e.g. Slimani 1994; Brinkhuis & Schiøler 1996; Antonescue *et al.* 2001b; Schiøler & Wilson 2001; Slimani *et al.* 2011), *I. scabrosum* (Slimani 1994), *K. perforatum* (e.g. Firth 1993; Fensome *et al.* 2008), *P. belgicum* (Slimani 1994, 1995; Slimani & Louwye 2011; Slimani *et al.* 2011), *P.?* *turnhoutensis* (Lejeune-Carpentier, 1951?; Marheinecke 1992?; Slimani 1994), *S. cornuta* (e.g. Gerlach 1961; Mohamed & Wagreich 2013; Slimani *et al.* 2016), and *X. delicata sensu* Slimani *et al.* 2011 (Hultberg 1985; Slimani *et al.* 2011, 2016; Slimani & Tabără 2017; Tabără *et al.* 2017); ptychodiscaceans *A. euclaense* (e.g. Pearce *unpub.*), *D. acuminatum* (e.g. Pearce *unpub.*), *D. longicorne* (e.g. Moradian & Allameh 2010; Pearce *unpub.*; Allameh & Nejad 2016), *D. avellana* (e.g. Evitt *et al.* 1967; Boltenhagen 1977; Oloto 1989), and *D. cretaceum* (e.g. Boltenhagen 1977; Rauscher & Doubinger 1982; M’Hamid *et al.* 2015; Tabără *et al.* 2017); peridiniaceans *C. diebelii* (e.g. Pearce *unpub.*), *C. glabrum* (e.g. Kurita *et al.* 1994; Fensome *et*

al. 2009), *C. leptodermum* (e.g. Jaramillo & Amezquita 1994; Oboh-Ikuenobe *et al.* 1998; McIntyre 1999; Aleksandrova *et al.* 2012), *L. rhombiforme* (e.g. Lentin & Vozzhenikova 1990; Schiøler *et al.* 1997; Lebedeva 2006, 2017), *S.?* *simplex* (e.g. Lucas-Clarke 2006; Dastas *et al.* 2014), *S. echinoideum* (e.g. Williams *et al.* 2004; Pearce unpub.), *T. evittii* (e.g. Williams *et al.* 2004), and *I. weidichii* (Kirsch 1991; Núñez-Betelu *et al.* 1994).

It is noteworthy that most records of *C. glabrum* hail from strata of late Paleocene–early Eocene age (Gocht 1969; Fensome *et al.* 2009). However, *C. glabrum* was originally regarded as a subspecies of *Cerodinium speciosum* (Alberti, 1959) Lentin & Williams, 1987 prior to recent re-examination (Fensome *et al.* 2009). Without subspecific distinction, *C. speciosum* has its earliest occurrence in the late Campanian (e.g. Harker *et al.* 1990; Smith 1992?)–early Maastrichtian (e.g. Pavlishina 1995; Roncaglia & Corradini 1997) interval with the first occurrence of *C. glabrum* having only been reported with confidence from exposures of the upper Campanian Bearpaw Formation in southern Alberta (Kurita *et al.* 1994).

Figure 4.5. Known chronostratigraphic ranges of selected dinoflagellate cysts referable to forms present within the Hornby Island assemblage as plotted over 30 Ma spanning the Late Cretaceous–Paleocene. Yellow band denotes inferred age interval of the Northumberland Formation on Hornby Island. Solid bar terminations denote absolute range horizons.

4.5.2 Dinoflagellate cyst zones

Zone 1. The lower boundary is undefined below the contact with the underlying DeCourcy Formation. The upper boundary is defined by the range-tops of *Alterbidinium?* spp., *Bohaidina* spp., *Dinogymnium longicorne*, and *Hystrichosphaeridium tubiferum*. Specimens of *Alterbidinium?* spp. are present in every sample from the southeastern coast and absent from all samples up-section obtained from exposures along the west coast. Precedent exists for the utility of members of *Alterbidinium* in Late Cretaceous biozonation schemes within the northern hemisphere (e.g. Oloto 1989; Kirsch 1991; Harker *et al.* 1990; Schiøler & Wilson 1993; Ilyina *et al.* 1994; Slimani 2001; Lebedeva 2006) as with species of *Dinogymnium* (e.g. Clarke & Verdier 1967; Zaitzeff & Cross 1970; Jain & Millepied 1975; Benson 1976; Aurisano 1989; Harker *et al.* 1990; Stover *et al.* 1996) and *H. tubiferum* (e.g. Wilson 1974; Marheinecke 1992; Lebedeva 2006). Peridiniaceans belonging to *Bohaidina*, notably associated with lacustrine to brackish conditions (e.g. Jianyu Chen *et al.* 1996, 1998; Guangli Wang *et al.* 2008, 2010), are likely endemic to the North Pacific with their presence in the Hornby Island section marking the first geographic occurrence of the genus beyond the coastal basins of eastern China (e.g. Song Zhichen *et al.* 1978; Sun Xeukun 1994).

Zone 2. The lower boundary is defined by the first occurrences of *Aireiana salicta*, *Druggidium?* cf. *discretum*, and *Spinidinium densispinatum* above 60 m in the section marking the ecological turnover following the 4.4 km offset along strike. The latter two taxa are absent in the two samples obtained from the uppermost 10 m of the 255 m exposed along the western coast while *A. salicta* is still present. Therefore, the upper boundary remains undefined, potentially above the contact with the overlying Geoffrey Formation. The cladopyxiinean *Druggidium discretum* has been shown to be narrowly constrained within the uppermost Cretaceous succession of Belgium (Slimani & Louwye 2011; Slimani *et al.* 2011) and its occurrence within the Northumberland

Formation represents a probable 6–7 Ma range extension into older sedimentary rocks. Species belonging to the deflandroid genus *Spinidinium* have proven application in numerous Late Cretaceous biostratigraphic studies as well (e.g. Clarke & Verdier 1967; Aurisano 1989; Harker *et al.* 1990; Stover *et al.* 1996; Lebedeva 2006). The interval is also characterized by increased species diversity and prevalence of areoligeraceans and heterotrophic peridiniaceans.

4.5.3 Palaeoenvironmental and palaeolatitudinal reconstructions

Dinoflagellate cyst concentrations range from 263 cysts g^{-1} in subsample 15-755 to 112,841 cysts g^{-1} in subsample 16-368 with higher values occurring up-section (Fig. 4.6). Dinoflagellate cyst abundance on the scale of thousands per gram coupled with high species diversity is indicative of elevated palaeoproductivity likely associated with a continental margin or shelf setting (e.g. Dale 1996; Pospelova *et al.* 2008; de Vernal 2009).

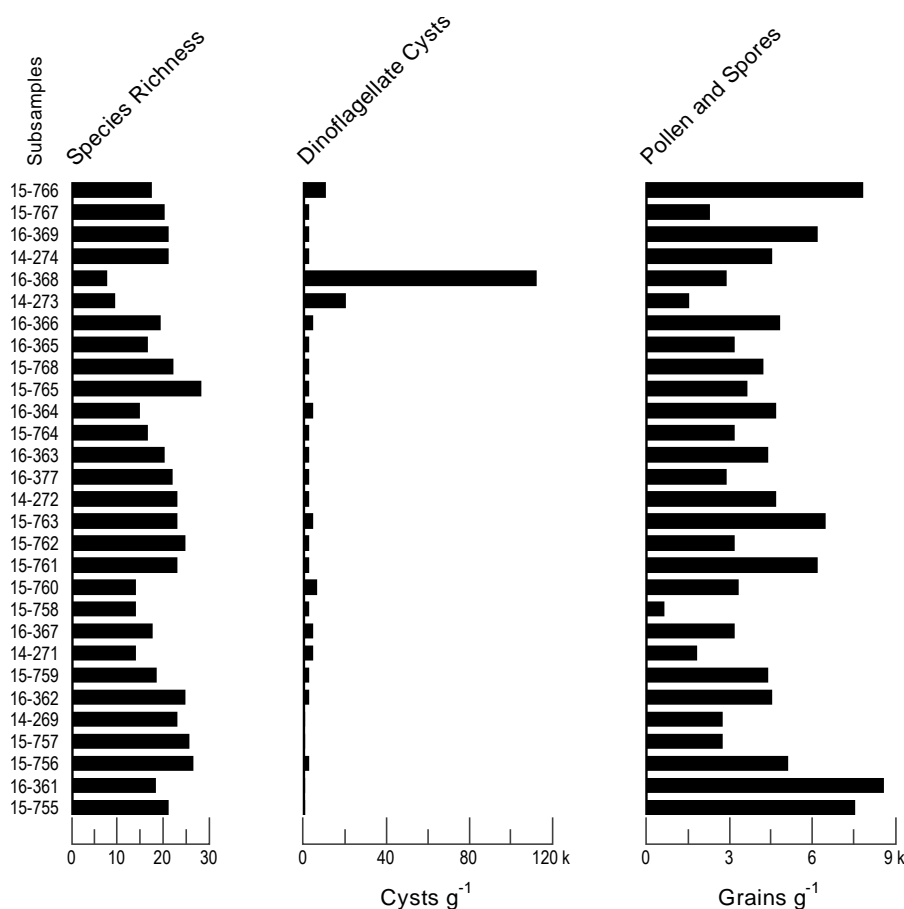


Figure 4.6. Absolute abundance of dinoflagellate cysts and terrestrial palynomorphs within the Hornby Island subsample suite based on counts data. Subsamples ascending in order of stratigraphic succession.

Areoligeraceans are abundant to dominant in eight of the 29 Hornby Island subsamples (Fig. 4.7). In their examination of Eocene sediments, Downie *et al.* (1971) suggested that *Spiniferites* and *Areoligera* dominance denotes open-sea conditions (noted in Sarjeant 1974, p. 121). Following more recent work, the *Areoligera* complex *sensu* Evitt (1985) has come to be considered indicative of high energy, inner neritic settings in studies of early Cenozoic assemblages (e.g. Brinkhuis 1994; Powell *et al.* 1996; Schiøler *et al.* 1997; Pross & Brinkhuis 2005; Sluijs *et al.* 2008; Sluijs & Brinkhuis 2009; Wade *et al.* 2012) along with the goniodomacean genus *Hystrichosphaeridium* (e.g. Brinkhuis 1994; Schiøler *et al.* 1997; Crouch & Brinkhuis 2005). The areoligeracean genus *Glaphyrocysta* has also received attention as an indicator of shallow, nearshore environments in examinations of the K–Pg interval (e.g. Brinkhuis & Zachariasse 1988; Eshet *et al.* 1992; Slimani *et al.* 2010) being positively correlated with *Cordosphaeridium* (Crouch & Brinkhuis 2005), a genus known from neritic sediments (e.g. Wilpshaar & Leereveld 1994; Leereveld 1995; Schiøler *et al.* 1997).

Gonyaulacaceans are abundant to dominant in 17 of the 29 Hornby Island subsamples (Fig. 4.7). The genera *Hafniasphaera*, *Spiniferella*, and *Spiniferites*, associated with outer neritic conditions (e.g. Brinkhuis 1994; Sluijs *et al.* 2008; Sluijs & Brinkhuis 2009; Shcherbinina *et al.* 2016), are well represented being abundant to dominant in 10 of the 29 subsamples. Comparatively rarer occurrences of *Impagidinium* and *Nematosphaeropsis*—genera regarded to be outermost neritic to pelagic (e.g. Wall *et al.* 1977; Edwards & Andrieu 1992; Brinkhuis 1994; Dale 1996; van Mourik *et al.* 2001; Pross & Brinkhuis 2005; Shcherbinina *et al.* 2016)—are also present throughout the section but are scarce, peaking at a mere 4.1% of all dinoflagellate cysts in subsample 15-765.

Peridiniineans are generally rare in the Hornby Island material with the exception of *Spinidinium* spp. abundance in subsamples 15-760, 15-768, and 16-365 (Fig. 4.7). Beyond *Spinidinium*, peridiniaceans attributable to deflandreoid genera such as *Alterbidinium*, *Isabelidinium*, *Senegalinium*, and *Trithyrodinium* have been shown to respond to ultraviolet light providing ample evidence of autotrophic capability with implications for familial ratio inferences carried forward from early studies (e.g. Schiller 1937; Harland 1973). These taxa are common in only in a few samples while members of exclusively heterotrophic genera within the *Deflandrea* complex *sensu* Evitt (1985) such as *Andalusiella*, *Cerodinium*, *Lejeuniacysta*, and *Palaeocystodinium* never exceed 2% of any subsample assemblage. Heterotrophic peridiniaceans

of deflandreoid affinity have been surmised as indicators of shallow, coastal, potentially brackish waters with high nutrient availability in Cenozoic studies (e.g. Brinkhuis *et al.* 1992; Powell *et al.* 1992, 1996; Brinkhuis 1994; Firth 1996; Sluijs *et al.* 2005).

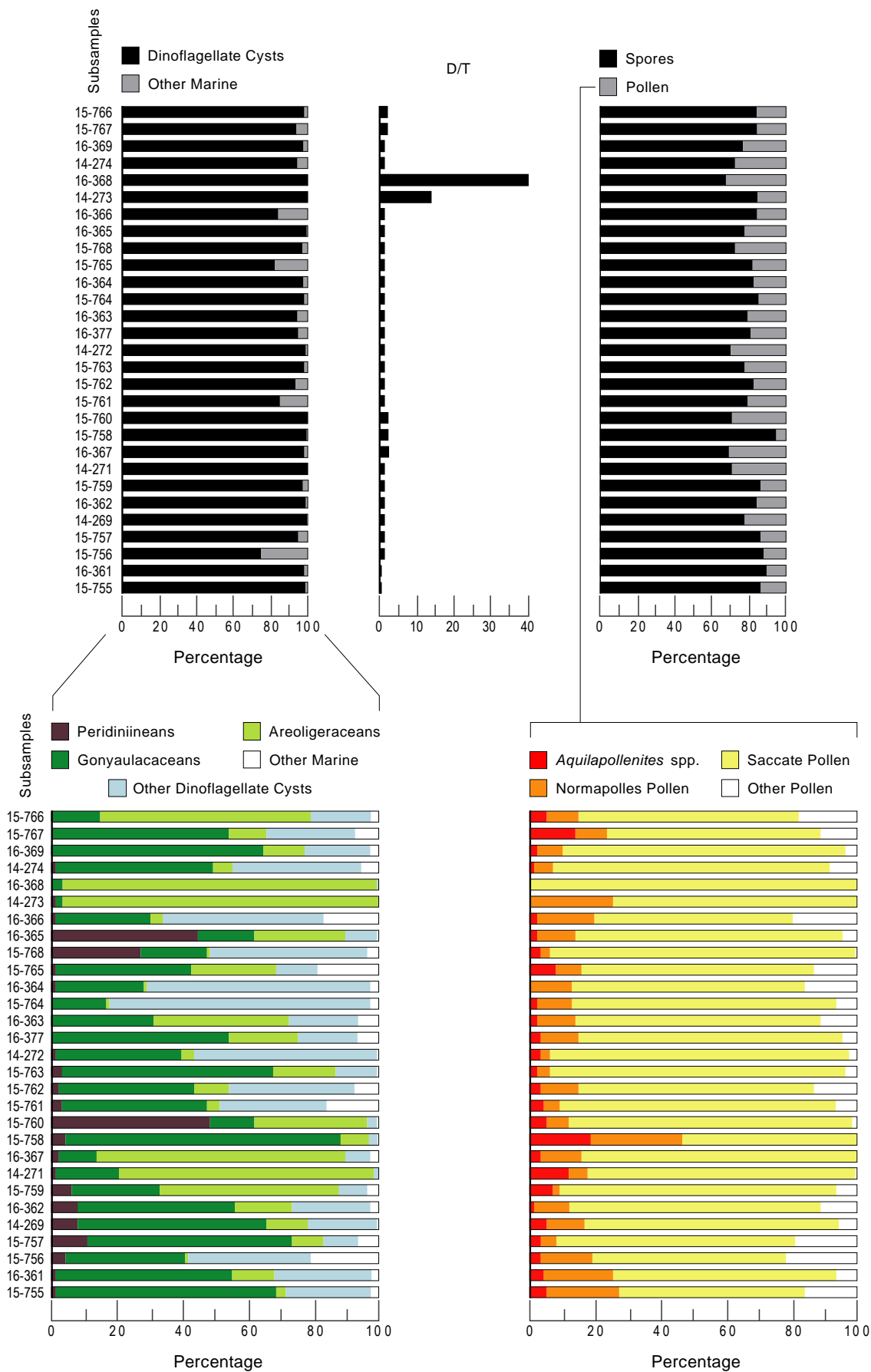


Figure 4.7. Relative abundance of dinoflagellate cysts and terrestrial palynomorph constituents within the Hornby Island subsample suite based on counts data. Subsamples ascending in order of stratigraphic succession. D/T = dinoflagellate cysts to terrestrial palynomorph ratio.

In addition to dinoflagellate cysts, there exists a wide range of marine (e.g. Pl. 4.25) and terrestrial (e.g. Pl. 4.26) microfossils and palynomorphs with 21 of the 29 subsamples containing higher concentrations of terrestrial as compared to marine palynomorphs (Fig. 4.6). Of the marine palynomorph constituents, *Paralecaniella* (Pl. 4.25G), an algal cyst genus with its highest relative abundance in samples 14-269 and 16-377, is regarded as an indicator of shallow marginal or restricted marine conditions (Elsik 1977; Brinkhuis & Schiøler 1996; Schiøler *et al.* 1997; Fensome *et al.* 2009, 2016). As a group, spores are denser and less susceptible to aeolian transportation than saccate pollen grains (e.g. Schwendemann *et al.* 2007; Grega *et al.* 2013) and are present in far higher proportions than would be expected from sediments deposited in an outer shelf or oceanic setting. Of the terrestrial palynomorph constituents, trilete and monolete spores occur on average in a 4:1 ratio with pollen grains throughout the Northumberland formation section (Fig. 4.7). The notable predominance of spores is probably due to factors such as terrestrial outflow and current transport within a neritic environment. Variability in the marine to terrestrial palynomorph ratios likely reflects conditions subject to fluctuation in coastal runoff affecting sedimentation rates, transport of detrital plant material, and changes in local vegetation density (e.g. Muller 1959; Cross *et al.* 1967; Zaitzeff & Cross 1970).

A number of entities within the palynological assemblage hold implications for palaeolatitudinal projection. Among the dinoflagellate cysts, a low-latitude preference has been documented for members of the genera *Andalusiella*, *Impagidinium*, *Lejeuniacysta*, and *Palaeocystodinium* along with the species *Areoligera volata* and *Trithyrodinium evittii* (e.g. Brinkhuis *et al.* 1998; M'Hamid *et al.* 2015; Vellekoop *et al.* 2015). Conversely, taxa belonging to *Laciniadinium* and species such as *Cerodinium diebelii* and *Hystrichodinium tubiferum* are regarded to be high-latitude (e.g. Lentin & Williams 1980; Brinkhuis *et al.* 1998).

Among the terrestrial palynomorphs are members of the angiosperm Normapolles (Pl. 4.26D–F) and *Aquilapollenites* (Pl. 4.26H, I) pollen groups long considered markers of subtropical and boreal phytogeoprovinces respectively within the Late Cretaceous (e.g. Srivastava 1994; Herngreen *et al.* 1996; Daly & Jolley 2015). Normapolles specimens are rare in

Western North America (e.g. Wolf 1975; Tschudy 1981) and their co-occurrence in higher proportions with *Aquilapollenites* may be attributable to transport from coastal runoff reflecting ecological preference across an elevation gradient. As a whole, the palynomorph assemblage seems to represent an ecology transitional between boreal and subtropical realms and intermixing of these floras prior to the late Maastrichtian (e.g. Srivastava 1981, 1994). This interpretation is entirely consistent with recent palaeobiogeographic (Carter & Haggart 2006) and detrital zircon provenance studies (Mahoney *et al.* 1999, 2014, 2016) which support Nanaimo Basin situation at approximately the current terrain latitude contrary to findings derived from palaeomagnetism (e.g. Ward *et al.* 1997; Kodama & Ward 2001; Kim & Kodama 2004; Krijgsman & Tauxe 2006).

While the sampling resolution of this study is too limited to enable any conclusive projection of palaeoenvironmental trends in eustasy or primary productivity within the Northumberland Formation sequence, the palynological assemblage examined is clearly indicative of an inner neritic setting. These findings reaffirm a shelf depositional environment as accommodated within the interpretations of previous works in biostratigraphy (Sliter 1973; Cameron 1988) and lithostratigraphy (e.g. Mustard 1994; Katnick & Mustard 2003; Mustard *et al.* 2003). The setting seems likely to have been situated more toward an inner shelf position where nutrient influences from offshore upwelling likely met with coastal runoff-related mixing. Terrigenous input through outflow currents also stands as a probable factor impacting both dinoflagellate cyst eco-group representation (e.g. Pross & Brinkhuis 2005) and terrestrial palynomorph assemblages (e.g. Zaitzeff & Cross 1970).

4.6 Acknowledgments

The author wishes to extend his gratitude to Dr. Vera Pospelova for providing access and introduction to lab equipment, literature, procedural methodology, and assistance with subsample processing. Dr. Richard Hebda for lending his insights in the identification and taxonomic treatment of the terrestrial palynomorphs.

4.7 Taxonomic entities

Aireiana salicta Damassa, 1979

Alisogymnium euclaense (Cookson & Eisenack, 1970a) Lentin & Vozzhennikova, 1990

Alterbidinium? spp.
Amphigymnium cooksoniae (Boltenhagen, 1977) Lentin & Vozzhennikova, 1990
Andalusiella gabonensis (Stover & Evitt, 1978) Wrenn & Hart, 1988
Areoligera “*circumcoronata*” (Eaton, 1976) of Fensome *et al.* (2009)
Areoligera spp.
Areosphaeridium? sp.
Bohaidina spp.
Canningia diezeugmenis sp. nov.
Cerodinium diebelii (Alberti, 1959) Lentin & Williams, 1987
Cerodinium glabrum (Gocht, 1969) Fensome *et al.*, 2009
Cerodinium cf. *leptodermum* (Vozzhennikova, 1963) Lentin & Williams, 1987
Circulodinium colliveri (Cookson & Eisenack, 1960b) Helby, 1987
Circulodinium? sp.
Cladopyxidium paucireticulatum Slimani, 1994
Cladopyxidium sp.
Cordosphaeridium callosum Morgenroth, 1966
Cordosphaeridium spp.
Coronifera oceanica Cookson & Eisenack, 1958 *sensu* Schiøler & Wilson (2001)
Cyclonephelium spp.
Dapsilidinium cf. *pseudocolligerum* (Stover, 1977) Bujak *et al.*, 1980
Dinogymnium acuminatum (Evitt *et al.*, 1967) Lentin & Vozzhennikova, 1990
Dinogymnium cf. *aerlicum* Londeix *et al.*, 1996
Dinogymnium avellana (Lejeune-Carpentier, 1951) Evitt *et al.*, 1967
Dinogymnium cretaceum (Deflandre, 1936) Evitt *et al.*, 1967
Dinogymnium longicorne (Vozzhennikova, 1967) Lentin & Vozzhennikova, 1990
Dinogymnium sp. A
Dinogymnium sp. B
Diphyes colligerum (Deflandre & Cookson, 1955) Goodman & Witmer, 1985
Diphyes spp.?
Druggidium? cf. *discretum* Slimani & Louwye, 2011
Druggidium? sp.

Eisenackia? sp.
Fibrocysta spp.
Florentinia ferox (Deflandre, 1937b) Duxbury, 1980
Florentinia laciniata Davey & Verdier, 1973
Glaphyrocysta–Membranophoridium spp.
Geiselodinium geiseltalense Krutzsch, 1962
Glyphanodinium facetum Drugg, 1964
Gonyaulacysta? sp.
Hafniasphaera delicata Fensome *et al.*, 2009
Hafniasphaera cf. *delicata* Fensome *et al.*, 2009
Hafniasphaera septata (Cookson & Eisenack, 1967) Hansen, 1977
Hystrichodinium pulchrum Deflandre, 1935
Hystrichosphaeridium recurvatum (White, 1842) Lejeune-Carpentier, 1940
Hystrichosphaeridium tubiferum (Ehrenberg, 1937) Davey & Williams, 1966
Impagidinium rigidaseptatum Slimani, 1994
Impagidinium cf. *scabrosum* Slimani, 1994
Impagidinium cf. *sphaericum* Wall, 1967–*multiplex* Wall & Dale, 1968 of de Coninck (1968)
Impagidinium spp.
Isabelidinium bakeri (Deflandre & Cookson, 1955) Lentin & Williams, 1977
Isabelidinium weidichii Kirsch, 1991
Kleithriasphaeridium perforatum (Firth, 1993) Fensome *et al.*, 2009
Laciniadinium arcticum (Manum & Cookson, 1964) Lentin & Williams, 1980
Laciniadinium firmum (Harland, 1973) Morgan, 1977
Laciniadinium rhombiforme (Vozzhennikova, 1967) Lentin & Vozzhennikova, 1990
Lejeuniacysta cf. *hyalina* (Gerlach, 1961) Artzner & Dörhöfer, 1978
Lejeuniacysta sp.
Leptodinium sp.
Litosphaeridium spp.
Microdinium carpentierae Slimani, 1994
Microdinium mariae Slimani, 1994
Minisphaeridium latiricum (Davey & Williams, 1966) Fensome *et al.*, 2009

Minisphaeridium sp.
Nematosphaeropsis sp.
Neoeurysphaeridium? sp.
Odontochitina cf. *nuda* (Gocht, 1957) Dörhöfer & Davies, 1980
Odontochitina cf. *tabulata* El Mehdawi, 1998
Oligosphaeridium complex (White, 1842) Davey & Williams, 1966
Palaeocystodinium golzowense Alberti, 1961
Phanerodinium belgicum Slimani & Louwye, 2011
Phanerodinium cf. *belgicum* Slimani & Louwye, 2011
Phanerodinium sp.
Phanerodinium? *turnhoutensis* Slimani, 1994
Polysphaeridium spp.
Protoperidinium sp. A
Protoperidinium sp. B
Pterodinium cingulatum (Wetzel, 1933) Below, 1981 *sensu* Antonescue *et al.* (2001a)
Renidinium spp.
Senegalinium? *simplex* Lucas-Clarke, 2006
Senoniasphaera cf. *protrusa* (Clarke & Verdier, 1967) Prince *et al.*, 1999
Spinidinium densispinatum Stanley, 1965
Spinidinium echinoideum (Cookson & Eisenack, 1960a) Lentin & Williams, 1981
Spiniferella cornuta (Gerlach, 1961) Stover & Hardenbol, 1994
Spiniferites sp. A
Spiniferites spp.
Tanyosphaeridium xanthiopyxides (Wetzel, 1933 *ex* Deflandre, 1937b) Sarjeant, 1985
Trichodinium cf. *erinaceoides* Davies, 1983
Trithyrodinium evittii Drugg, 1967
Unipontidinium aquaeductus (Piasecki, 1980) Wrenn, 1988
Xenascus ceratioides (Deflandre, 1937b) Lentin & Williams, 1973
Xenicodinium delicatum Hultberg, 1985 *sensu* Slimani *et al.* 2011
Peridiniacean Group A
Peridiniacean Group B

Cyst Type A

Cyst Type B

Cyst Type C

Cyst? Type A

Fromea chytra Drugg, 1967

Fromea sp.

Horolonginella? sp.

Micrhystridium sp.

Palaeostomocystis reticulata Deflandre, 1937b

Paralecaniella indentata (Deflandre & Cookson, 1955) Cookson & Eisenack, 1970b

Schizocysta rugosa (Cookson & Eisenack, 1962) Elsik, 1968

Tetrachacysta sp.

Appendicisporites sp.

Aquilapollenites cf. *pseudoaucellatus* Takahashi & Shimono, 1982

Aquilapollenites sp.

Atlantopolis sp.

Pinus sp.

Proteacidies sp.

Trilobosporites cf. *humilis* Delcourt & Sprumont, 1959

Trilobosporites sp.

Trudopollis sp.

Chapter 5

Conclusion

5.1 Summary of research

Numerous Mesozoic ammonite taxa erected in works of the 19th and early 20th century have since been amalgamated on the grounds of synonymy, through natural course, in light of the recovery of more complete material. This work further substantiates the validity of such conservative groupings, in demonstrating the variability of a multitude of heteromorph ammonite forms—specifically among the Nostoceratidae—during a period of accelerated diversification near the end of the Cretaceous. Building from the material amassed over decades through the diligent collecting of dedicated palaeontological enthusiasts, the rich heteromorph ammonite fauna of Hornby Island has found its place within a renewed taxonomic framework. This effort has been but one step in the ongoing process toward further refinement of an objective classificatory approach based on quantitative and qualitative trait hierarchies to enable clarity of taxonomic distinction between these perplexing entities.

The enclosed microfossil study has aimed to open the door for the exploration of a palaeoecological dimension never before examined within the Late Cretaceous of the North Pacific and suggests an inner neritic habitat preference for the heteromorph ammonoid taxa present. The Northumberland Formation has offered a snapshot of a highly diverse invertebrate and palynological fossil record with far-reaching implications for continued revision of the temporal progression, geophysical processes, and palaeoenvironmental circumstances which contributed to the evolution of the Nanaimo Group succession. A wealth of dinoflagellate cyst material holds promise from the confirmation of index taxa to gradational plexes which present grounds for possible re-evaluation of fossil species concepts and the utility of potential ecophenotypes—namely among the Areoligeraceae—in palaeoenvironmental reconstruction. Both micro- and macrofossil frontiers will serve to elucidate a region of the globe which remains encouraging for Cretaceous research.

References

- Adkins, W. S. & Winton, W. M.** 1920. Paleontological correlation of the Fredricksburg and Washita formations in north Texas. *University of Texas Bulletin*, **1945**, 128 pp.
- Alberti, G.** 1959. Zur Kenntnis der Gattung *Deflandrea* Eisenack (Dinoflag.) in der Kreide und im Alttertiär Nord-und Mitteldeutschlands. *Mitteilungen aus dem Geologischen Staatsinstitut in Hamburg*, **28**, 93–105, pls 8–9.
- Alberti, G.** 1961. Zur Kenntnis mesozoischer und alttertiärer Dinoflagellaten und Hystrichosphaerideen von Nord-und Mitteldeutschland sowie einigen anderen europäischen Gebieten. *Palaeontographica, Abteilung A*, **116**, 1–58, pls 1–12.
- Aleksandrova, G. N., Oreshkina, T. V., Iakovleva, A. I. & Radionova, E. P.** 2012. Late Paleocene–early Eocene diatoms and dinocysts from biosiliceous facies of the Middle Trans-Urals region. *Stratigraphy and Geological Correlation*, **20**(4), 380–404.
- Allameh, M. & Nejad, E. G.** 2016. Palynology and palynofacies of Santonian–Maastrichtian strata (Abtalkh Fm.) in eastern Koppeh-Dagh Basin, NE of Iran. *Arabian Journal of Geoscience*, **9**(3), 207.
- Anderson, F. M.** 1958. Upper Cretaceous of the Pacific coast. *Geological Society of America Memoir*, **71**, 378 pp., 75 pls.
- Antonescuc, E., Foucher, J. -C. & Odin, G. S.** 2001a. Dinoflagellate cysts from the transition at Tercis les Bains (Landes, France). Pp. 235–252 in G. S. Odin (ed.) The Campanian–Maastrichtian stage boundary, characterization at Tercis les Bain (France) and correlation with Europe and other continents. *Developments in Palaeontology and Stratigraphy*, **19**.
- Antonescuc, E., Foucher, J. -C. & Odin, G. S., Schiøler, P., Siegl-Farkas & Wilson, G. J.** 2001b. Dinoflagellate cysts in the Campanian–Maastrichtian succession of Tercis les Bains (Landes, France), a synthesis. Pp. 253–264 in G. S. Odin (ed.) The Campanian–Maastrichtian stage boundary, characterization at Tercis les Bain (France) and correlation with Europe and other continents. *Developments in Palaeontology and Stratigraphy*, **19**.
- Archangelsky, S.** 1969. Sobre el paleomicroplancton del Terciario inferior de Río Turbio, Provincia de Santa Cruz. *Ameghiniana*, **5**(10), 406–416.
- Arkadiev, V. V., Atabekian, A. A., Baraboshkin, E. Yu. & Bodganova, T. N.** 2000. Stratigraphy of ammonites of the Cretaceous deposits of south-west Crimea. *Palaeontographica*, **255**(4–6), 85–128.

- Arkell, W. J.** 1957. Introduction to Mesozoic Ammonoidea. Pp. L81–L129 in R. C. Moore (ed.) *Treatise on Invertebrate Paleontology, Part L, Mollusca 4, Cephalopoda, Ammonoidea*. Geological Society of America, Boulder & University of Kansas Press, Lawrence.
- Arkell, W. J., Kummel, B. & Wright, C. W.** 1957a. Systematic descriptions. Pp. L129–L437 in R. C. Moore (ed.) *Treatise on Invertebrate Paleontology, Part L, Mollusca 4, Cephalopoda, Ammonoidea*. Geological Society of America, Boulder & University of Kansas Press, Lawrence.
- Arkell, W. J., Kummel, B., Miller, A. K. & Wright, C. W.** 1957b. Morphological Terms Applied to Ammonoidea. Pp. L2–L6 in R. C. Moore (ed.) *Treatise on Invertebrate Paleontology, Part L, Mollusca 4, Cephalopoda, Ammonoidea*. Geological Society of America, Boulder & University of Kansas Press, Lawrence.
- Arkhipkin, A.** 2014. Getting hooked: the role of a U-shaped body chamber in the shell of adult heteromorph ammonites. *Journal of Molluscan Studies*, **80**, 354–364.
- Artzner, D. G. & Dörhöfer, G.** 1978. Taxonomic note: *Lejeunecysta* nom. nov. pro *Lejeunia* Gerlach 1961 emend. Lentin and Williams 1976 - dinoflagellate cyst genus. *Canadian Journal of Botany*, **56**(11), 1381–1382.
- Aurisano, R. W.** 1989. Upper Cretaceous dinoflagellate biostratigraphy of the subsurface Atlantic Coastal Plain of New Jersey and Delaware, U.S.A. *Palynology*, **13**, 143–179.
- Batt, R. J.** 1989. Ammonoid shell morphotype distributions in the Western Interior Greenhorn Sea and some paleoecological implications. *Palaios*, **4**(1), 32–42.
- Below, R.** 1981. Dinoflagellaten-Zysten aus dem oberen Hauterive bis unteren Cenoman Süd-West-Marokkos. *Palaeontographica, Abteilung B*, **176**, 1–145, pls 1–15.
- Below, R.** 1987. Evolution und systematik von dinoflagellaten-zysten aus der Ordnung Peridinales. II. Cladopyxiaceae und Valvaeodiniaceae. *Palaeontographica, Abteilung B*, **206**, 1–115, pls 1–29.
- Bengtson, P.** 1988. Open nomenclature. *Palaeontology*, **31**(1), 223–227.
- Benninghoff, W. S.** 1962. Calculation of pollen and spores density in sediments by addition of exotic pollen in known quantities. *Pollen et Spores*, **6**, 332–333.
- Benson, D. G.** 1976. Dinoflagellate taxonomy and biostratigraphy at the Cretaceous-Tertiary boundary, Round Bay, Maryland. *Tulane Studies in Geology and Paleontology*, **12**(4), 169–233.
- Bergh, R. S.** 1881. Der organismus der Cilioflagellaten. Eine phylogenetische studie. *Morphologisches Jahrbuch*, **7**, 177–288, pls 12–16.

- Biffi, U. & Grignani, D.** 1983. Peridinioid dinoflagellate cysts from the Oligocene of the Niger Delta, Nigeria. *Micropaleontology*, **29**(2), 126–145, pls 1–7.
- Birkelund, T.** 1993. Ammonites from the Maastrichtian White Chalk of Denmark. *Bulletin of the Geological Society of Denmark*, **40**, 33–81.
- Blakey, R. C.** 2014. Paleogeography and paleotectonics of the Western Interior Seaway, Jurassic-Cretaceous of North America. *AAPG Search and Discovery, Article*, **30392**, 1–72.
- Błaszkiwicz, A.** 1980. Campanian and Maastrichtian ammonites of the middle Vistula River valley, Poland: a stratigraphic-paleontological study. *Prace Instytutu Geologicznego*, **92**, 1–63, 56 pls.
- Boltenhagen, E.** 1977. Microplankton du Crétacé Supérieur du Gabon. *Cahiers de Paléontologie*, 1–151, pls 1–25.
- Brideaux, W. W.** 1977. Taxonomy of Upper Jurassic–Lower Cretaceous microplankton from the Richardson Mountains, District of Mackenzie, Canada. *Geological Survey of Canada, Bulletin*, **281**, 1–89.
- Brinkhuis, H.** 1994. Late Eocene to Early Oligocene dinoflagellate cysts from the Priabonian type-area (Northeast Italy): biostratigraphy and paleoenvironmental interpretation. *Palaeogeography, Palaeoclimatology, Palaeoecology*, **107**, 121–163.
- Brinkhuis H. & Zachariasse W. J.** 1988. Dinoflagellate cysts, sea level changes and planktonic foraminifers across the Cretaceous-Tertiary boundary at El Haria, northwest Tunisia. *Marine Micropaleontology*, **13**(2), 153–191.
- Brinkhuis, H. & Schiøler, P.** 1996. Palynology of the Geulhemmerberg Cretaceous/Tertiary boundary section (Limburg, SE Netherlands). Pp. 193–213 in H. Brinkhuis & J. Smit (eds), *The Geulhemmerberg Cretaceous/Tertiary Boundary Section (Maastrichtian type area, SE Netherlands)*. *Geologie en Mijnbouw*, **75**.
- Brinkhuis, H., Powell, A. J. & Zevenboom, D.** 1992. High-resolution dinoflagellate cyst stratigraphy of the Oligocene/Miocene transition interval in north-west and central Italy. Pp. 219–258 in M. J. Head & J. H. Wrenn (eds) *Neogene and Quaternary Dinoflagellate Cysts and Acritarchs*. American Association of Stratigraphic Palynologists Foundation, Dallas.
- Brinkhuis, H., Bujak, J. P., Smit, J., Versteegh, G. J. M. & Visscher, H.** 1998. Dinoflagellate-based sea surface temperature reconstructions across the Cretaceous–Tertiary boundary. *Palaeogeography, Palaeoclimatology, Palaeoecology*, **141**(1–2), 67–83.
- Brinkhuis, H., Sengers, S., Sluijs, A., Warnaar, J. & Williams, G. L.** 2003. Southern Ocean and global dinoflagellate cyst events compared: index events for the Late Cretaceous–

- Neogene. In N. F. Exon, J. P. Kenneth & M. J. Malone (eds) *Proceedings of the Ocean Drilling Program, Scientific Results*, **189**, 1–48.
- Brunnschweiler, R. O.** 1966. Upper Cretaceous ammonites from the Carnarvon Basin of Western Australia. I. The Heteromorph Lytoceratina. *Bureau of Mineral Resources, Geology and Geophysics, Bulletin*, **58**, 58 pp, 8 pls.
- Bucher, H. Landman, N., Kiofak, S. M. & Guex, J.** 1996. Mode and rate of growth in ammonoids. Pp. 408–53 in N. H. Landman, K. Tanabe R. A. & Davis (eds) *Ammonoid Paleobiology, Topics in Geobiology*, **13**. Plenum Press, New York.
- Bujak, J. P. & Davies, E. H.** 1983. Modern and fossil Peridiniinae. *American Association of Stratigraphic Palynologists, Contributions Series*, **13**, 203 pp.
- Bujak, J. P. & Mudge, D. C.** 1994. A high-resolution North Sea Eocene dinocyst zonation. *Journal of the Geological Society of London*, **151**(3), 449–462.
- Bujak, J. B. & Williams, G. L.** 1979. Dinoflagellate diversity through time. *Marine Micropaleontology*, **4**, 1–12.
- Bujak, J. P., Downie, C., Eaton, G. L. & Williams, G. L.** 1980. Dinoflagellate cysts and acritarchs from the Eocene of southern England. *Special Papers in Palaeontology*, **24**, 1–100.
- Burger, D.** 1980. Early Cretaceous (Neocomian) microplankton from the Carpentaria Basin northern Queensland. *Alcheringa*, **4**(4), 263–279.
- Bütschli, O.** 1873. Einiger über Infusorien. *Archiv für Mikroskopie und Anatomie*, **9**, 657–678, pls 25–26.
- Bütschli, O.** 1885. Erster Band. Protozoa. Pp. 865–1088 in *Dr. H. G. Bronn's Klassen und Ordnungen des Thier-Reichs, wissenschaftlich dargestellt in Wort und Bild*. C. F. Winter'sche Verlagsbuchhandlung, Leipzig and Heidelberg.
- Callomon, J. H.** 1963. Sexual dimorphism in Jurassic ammonites. *Transactions of the Leicester Literary and Philosophical Society*, **57**, 21–56.
- Cameron, B. E. B.** 1988. Paleoenvironmental analysis of 61 samples from the Upper Cretaceous Nanaimo Group, from Vancouver Island and adjacent Gulf Islands. *Geological Survey of Canada, unpublished report*, **BEB C-1988-4**, 26 pp.
- Carter, E. S. & Haggart, J. W.** 2006. Radiolarian biogeography of the Pacific region indicates a mid- to high-latitude (>30°) position for the Insular superterrane since the late Early Jurassic. Pp. 109–132 in J. W. Haggart, R. J. Enkin & J. W. H. Monger (eds) *Paleogeography of the North American Cordillera: evidence for and against large-scale displacements*. Geological Association of Canada, Special Paper, **46**.

- Case, G. R.** 1982. *A Pictorial Guide to Fossils*. Van Nostrand, New York, 514 pp.
- Cecca, F.** 1997. Late Jurassic and early Cretaceous uncoiled ammonites: trophism-related evolutionary processes. *Comptes Rendus de l'Académie des Sciences-Series IIA-Earth and Planetary Science*, **325**(8), 629–634.
- Chen, Y. -Y., Harland, R., Stover, L. E. & Williams, G. L.** 1988. Fossil dinoflagellate taxa by Chinese authors, 1978–1984. *Canadian Technical Reports of Hydrography and Ocean Sciences*, **103**, 1–40.
- Clark, D. L.** 1965. Heteromorph ammonoids from the Albian and Cenomanian of Texas and adjacent areas. *Geological Society of America Memoir*, **95**, 99 pp.
- Clarke, R. F. A & Verdier, J.-P.** 1967. An investigation of microplankton assemblages from the chalk of the Isle of Wight, England. *Verhandelingen der Koninklijke Nederlandse Akademie van Wetenschappen, Afdeling Natuurkunde, Eerste Reeks*, **24**(3), 1–96, pls. 1–17.
- Cobban, W. A.** 1962. New *Baculites* from the Bearpaw Shale and equivalent rocks of the Western Interior. *Journal of Paleontology*, **36**(1), 126–135.
- Cobban, W. A.** 1970. Occurrence of the Late Cretaceous ammonites *Didymoceras stevensoni* (Whitfield) and *Exiteloceras jenneyi* (Whitfield) in Delaware. *U.S. Geological Survey, Professional Paper*, **700-D**, D71–D76.
- Cobban, W. A.** 1974a. Some ammonites from the Ripley Formation of Mississippi, Alabama, and Georgia. *Journal of Research of the U.S. Geological Survey*, **2**(1), 81–88.
- Cobban, W. A.** 1974b. Ammonites from the Navesink Formation at Atlantic Highlands, New Jersey. *U.S. Geological Survey, Professional Paper*, **845**, 21 pp., 11 pls.
- Cobban, W. A.** 1987. The Upper Cretaceous ammonoid *Eubostrychoceras* Matsumoto in the Western Interior of the United States. *U.S. Geological Survey, Bulletin*, **1690**, A1–A5, 1 pl.
- Cobban, W. A. & Kennedy, W. J.** 1991. Some Upper Cretaceous ammonites from the Nacatoch Sand of Hempstead County, Arkansas. Pp. C1–C5 in W. J. Sando (ed.) *Shorter contributions to paleontology and stratigraphy*, *U.S. Geological Survey, Bulletin*, **1985**, 1 pl.
- Cobban, W. A. & Kennedy, W. J.** 1992. Campanian ammonites from the Upper Cretaceous Gober Chalk of Lamar County, Texas. *Journal of Paleontology*, **66**(3), 440–454.
- Cobban, W. A. & Kennedy, W. J.** 1994a. Upper Cretaceous ammonites from the Coon Creek Tongue of the Ripley Formation at its type locality in McNairy County, Tennessee. Pp.

- B1–B12 in W. J. Sando (ed.) *Shorter contributions to paleontology and stratigraphy 1993, U.S. Geological Survey, Bulletin*, **2073**, 11 pls.
- Cobban, W. A. & Kennedy, W. J.** 1994b. Middle Campanian (Upper Cretaceous) ammonites from the Pecan Gap Chalk of central and northeastern Texas. Pp. D1–D9 in W. J. Sando (ed.) *Shorter contributions to paleontology and stratigraphy 1993, U.S. Geological Survey, Bulletin*, **2073**, 5 pls.
- Cobban, W. A. & Kennedy, W. J.** 1995. Maastrichtian ammonites chiefly from the Prairie Bluff Chalk in Alabama and Mississippi. *Memoir 44, Supplement to the Journal of Paleontology*, **69**(Supplement to No. 5), 1–40.
- Cobban, W. A. & Scott, G. R.** 1972. Stratigraphy and ammonite fauna of the Graneros Shale and Greenhorn Limestone near Pueblo, Colorado. *U.S. Geological Survey, Professional Paper*, **645**, 1–108, pls 1–39.
- Cobban, W. A., Kennedy, W. J. & Scott, G. R.** 1992. Upper Cretaceous ammonites from the *Baculites compressus* zone of the Pierre Shale in north-central Colorado. Pp. A1–A11 in W. J. Sando (ed.) *Shorter contributions to paleontology and stratigraphy, 1992, U.S. Geological Survey, Bulletin*, **2024**, 3 pls.
- Collignon, M.** 1969. Atlas des fossiles caractéristiques de Madagascar (ammonites), Fascicule XV (Campanien inférieur). *Ministère de l'Industrie et des Mines, Service Géologique Tananarive*, **15**, 216 pp.
- Collignon, M.** 1971. Atlas des fossiles caractéristiques de Madagascar (ammonites). Fascicule XVII (Maestrichtien). *Ministère de l'Industrie et des Mines, Service Géologique Tananarive*, **17**, 44 pp.
- Conrad, T. A.** 1855. Descriptions of eighteen new Cretaceous and Tertiary fossils, etc. *Proceedings of the Academy of Natural Sciences of Philadelphia*, **7**, 265–268.
- Conrad, T. A.** 1860. Descriptions of new species of Cretaceous and Eocene fossils of Mississippi and Alabama. *Journal of the Academy of Natural Sciences of Philadelphia*, 2nd Series, **4**, 275–298, pls 46–47.
- Cookson, I. C.** 1965a. Cretaceous and Tertiary microplankton from south-eastern Australia. *Proceedings of the Royal Society of Victoria*, **78**, 85–93, pls 9–11.
- Cookson, I. C.** 1965b. Microplankton from the Paleocene Pebble Point Formation, southwestern Victoria. *Proceedings of the Royal Society of Victoria*, **78**, 137–141, pls 24–25.
- Cookson, I. C. & Eisenack, A.** 1958. Microplankton from Australian and New Guinea Upper Mesozoic sediments. *Proceedings of the Royal Society of Victoria*, **70**(1), 19–78, pls 1–12.

- Cookson, I. C. & Eisenack, A.** 1960a. Microplankton from Australian Cretaceous sediments. *Micropaleontology*, **6**(1), 1–18, pls 1–3.
- Cookson, I. C. & Eisenack, A.** 1960b. Upper Mesozoic microplankton from Australia and New Guinea. *Palaeontology*, **2**(2), 243–261, pls 37–39.
- Cookson, I. C. & Eisenack, A.** 1962. Some Cretaceous and Tertiary microfossils from western Australia. *Proceedings of the Royal Society of Victoria*, **75**, 269–273, pl. 37.
- Cookson, I. C. & Eisenack, A.** 1965. Microplankton from the Browns Creek Clays, sw. Victoria. *Proceedings of the Royal Society of Victoria*, **79**, 119–131, pls 11–15.
- Cookson, I. C. & Eisenack, A.** 1967. Some microplankton from the Paleocene Rivernook Bed, Victoria. *Proceedings of the Royal Society of Victoria*, **80**(2), 247–257, pls 39–42.
- Cookson, I. C. & Eisenack, A.** 1969. Some microplankton from two bores at Balcatta, Western Australia. *Journal of the Royal Society of Western Australia*, **52**, 3–8.
- Cookson, I. C. & Eisenack, A.** 1970a. Cretaceous microplankton from the Eucla Basin, Western Australia. *Proceedings of the Royal Society of Victoria*, **83**(2), 137–157, pls 10–14.
- Cookson, I. C. & Eisenack, A.** 1970b. Die familie der Lecaniellaceae n. fam. - fossile Chlorophyta, Volvocales? *Neues Jahrbuch für Geologie und Paläontologie, Monatshefte*, **6**, 321–325.
- Cooper, M. R.** 1994. Towards a phylogenetic classification of the Cretaceous ammonites. IV. Phlycticriocerataceae. *Neues Jahrbuch für Geologie und Paläontologie, Abhandlungen*, **194**(2–3), 361–378.
- Corradini, D.** 1973. Non-calcareous microplankton from the Upper Cretaceous of the northern Apennines. *Bollettino della Societa paleontologica a italiana*, **11**, 119–197.
- Crouch, E. M. & Brinkhuis, H.** 2005. Environmental change across the Paleocene–Eocene transition from eastern New Zealand: A marine palynological approach. *Marine Micropaleontology*, **56**(3–4), 138–160.
- Courtenat, B.** 2000. Review of the dinoflagellate cyst *Subtilisphaera? inaffecta* (Drugg, 1978) Bujak & Davies, 1983 and *S.? paeminosa* (Drugg, 1978) Bujak & Davies, 1983. *Journal of Micropalaeontology*, **19**(2), 165–175.
- Cross, A. T., Thompson, G. G. & Zaitzeff, J. B.** 1967. Source and distribution of palynomorphs in bottom sediments, southern part of Gulf of California. *Marine Geology*, **4**(6), 467–524.
- d'Orbigny, A. C. V.** 1842. Paléontologie française: terrains crétacées. I. Pp. 431–662, pls 113–148 in *Céphalopodes*. Masson, Paris.

- Dale, B.** 1996. Dinoflagellate cyst ecology: Modeling and geological applications. Pp: 1249–1276 in J. Jansonius & D. C. McGregor (eds) *Palynology: Principles and Applications*, American Association of Stratigraphic Palynologists Foundation, Dallas.
- Daly, R. J. & Jolley, D. W.** 2015. What was the nature and role of Normapolles angiosperms? A case study from the earliest Cenozoic of Eastern Europe. *Palaeogeography, Palaeoclimatology, Palaeoecology*, **418**, 141–149.
- Damassa, S. P.** 1979. Eocene dinoflagellates from the Coastal Belt of the Franciscan Complex, northern California. *Journal of Paleontology*, **53**(4), 815–840, pls 1–8.
- Dastas, N. R., Chamberlain Jr., J. A. & Garb, M. P.** 2014. Cretaceous-Paleogene dinoflagellate biostratigraphy and the age of the Clayton Formation, southeastern Missouri, USA. *Geosciences*, **4**(1), 1–29.
- Davey, R. J.** 1974. Dinoflagellate cysts from the Barremian of the Speeton Clay, England. Pp. 41–75, pls 1–9 in *Symposium on Stratigraphic Palynology, Birbal Sahni Institute of Palaeobotany, Special Publication*, **3**.
- Davey, R. J.** 1969a. Non-calcareous microplankton from the Cenomanian of England, northern France and North America. I. *British Museum (Natural History) Geology, Bulletin*, **17**(3), 103–180, pls 1–11.
- Davey, R. J.** 1969b. The evolution of certain Upper Cretaceous hystrichospheres from South Africa. *Palaeontologia Africana*, **12**, 25–51, pls 1–4.
- Davey, R. J., Downie, C., Sarjeant, W. A. S. & Williams, G. L.** 1966. VII. Fossil dinoflagellate cysts attributed to *Baltisphaeridium*. Pp. 157–175, pls 2, 3, 8–11 in R. J. Davey, C. Downie, W. A. S. Sarjeant & G. L. Williams (eds) *Studies on Mesozoic and Cainozoic dinoflagellate cysts. British Museum (Natural History) Geology, Bulletin, Supplement 3*.
- Davey, R. J. & Verdier, J.-P.** 1973. An investigation of microplankton assemblages from latest Albian (Vraconian) sediments. *Revista espanola de micropaleontologia*, **5**, 173–212, pls 1–5.
- Davey, R. J. & Williams, G. L.** 1966. V. The genus *Hystrichosphaeridium* and its allies. Pp. 53–106, pls 3–12 in R. J. Davey, C. Downie, W. A. S. Sarjeant & G. L. Williams (eds) *Studies on Mesozoic and Cainozoic dinoflagellate cysts. British Museum (Natural History) Geology, Bulletin, Supplement 3*.
- Davey, R. J. & Williams, G. L.** 1969. Generic reallocations. Pp. 4–7 in R. J. Davey, C. Downie, W. A. S. Sarjeant & G. L. Williams (eds) Appendix to '*Studies on Mesozoic and Cainozoic dinoflagellate cysts*'. *British Museum (Natural History) Geology, Bulletin, Appendix to Supplement 3*.

- Davies, E. H.** 1983. The dinoflagellate Ooppel-zonation of the Jurassic-Lower Cretaceous sequences in the Sverdrup Basin, arctic Canada. *Geological Survey of Canada, Bulletin*, **359**, 1–59.
- Davis, R. A.** 1972. Mature modification and dimorphism in selected Late Paleozoic ammonoids. *Bulletins of American Paleontology*, **62**(242), 23–130, 22 pls.
- Davis, R. A., Landman, N. H., Dommergues, J., Marchand, D. & Bucher, H.** 1996. Mature Modifications and Dimorphism in Ammonoid Cephalopods. Pp. 464–529 in N. H. Landman, K. Tanabe & R. A. Davis (eds) *Ammonoid Paleobiology, Topics in Geobiology*, **13**. Plenum Press, New York.
- de Coninck, J.** 1968. Organic walled phytoplankton from the Bartonian and Eo-Oligocene transitional deposits of the Woensdrecht Borehole, southern Netherlands. *Mededelingen Rijks Geologische Dienst*, **40**(2), 1–49.
- de Coninck, J.** 1969. Dinophyceae et Acritarcha de l'Yprésien du sondage de Kallo. *Mémoires de l'Institut Royal des Sciences Naturelles de Belgique*, **161**, 1–67, pls 1–17.
- de Coninck, J.** 1995. Microfossiles à paroi organique du Bartonien, Priabonien et Rupélien inférieur dans le sondage de Kallo; espèces significatives dans les sondages de Woensdrecht, Kallo et Mol. *Mededelingen Rijks Geologische Dienst*, **53**, 65–105.
- de Vernal, A.** 2009. Marine palynology and its use for studying nearshore environments. *IOP Conference Series: Earth and Environmental Science*, **5**(1), 012002.
- Deflandre, G.** 1935. Considérations biologiques sur les microorganismes d'origine planctonique conservés dans les silex de la craie. *Bulletin Biologique de la France et de la Belgique*, **69**, 213–244, pls 5–9.
- Deflandre, G.** 1936. Microfossiles des silex crétacés. Première partie. Généralités. Flagellés. *Annales de Paléontologie*, **25**, 151–191, pls 1–10.
- Deflandre, G.** 1937a. *Phanerodinium*, genre nouveau de dinoflagelle fossile des silex. *La Société française de microscopie, Bulletin*, **6**, 109–115.
- Deflandre, G.** 1937b. Microfossiles des silex crétacés. Deuxième partie. Flagellés incertae sedis. Hystrichosphaeridés. Sarcodinés. Organismes divers. *Annales de Paléontologie*, **26**, 51–103 (al. 3–55), pls 11–18 (also labelled pls 8–15).
- Deflandre, G.** 1947. Sur une nouvelle hystrichosphère des silex crétacés et sur les affinités du genre *Cannosphaeropsis* O. We. *Comptes rendus Hebdomadaires des Séances de l'Académie des Sciences*, **224**, 1574–1576.

- Deflandre, G.** 1964. Remarques sur la classification des dinoflagellés fossiles, à propos d'*Evittodinium*, nouveau genre créacé de la famille des Deflandreaceae. *Comptes rendus hebdomadaires des séances de l'Académie des sciences*, **258**, 5027–5030.
- Deflandre, G. & Cookson, I. C.** 1955. Fossil microplankton from Australian Late Mesozoic and Tertiary sediments. *Australian Journal of Marine and Freshwater Research*, **6**(2), 242–313, pls 1–9.
- Defrance, M. J. L.** 1816. *Dictionnaire des Sciences naturelles, dans lequel on traite méthodiquement des différents Etres de la nature 3*. Levrault, Paris & Strasbourg. 492 pp.
- Delcourt, A. & Sprumont, G.** 1959. Spores, grains de pollen, Hystrichospheres et Peridiniens dans le Wealdien de Feron-Glageon. *Annales de la Société Géologique du Nord*, **79**, 29–64.
- Diener, C.** 1925. Ammonoidea neocretacea. *Fossilium catalogus* (1: Animalia), **29**, 244 pp.
- Dogudzhaeva, L. A. & Mikhailova, I. A.** 1991. New data on muscle system of heteromorph ammonites. *Doklady Akademii Nauk USSR*, **318**(4), 981–985.
- Dörhöfer, G. & Davies, E. H.** 1980. Evolution of archeopyle and tabulation in rhaetogonyaulacinean dinoflagellate cysts. *Miscellaneous Publication of the Royal Ontario Museum, Life Sciences Division*. Toronto, Canada, 91 pp.
- Douvillé, H.** 1928. Les ammonites de la Craie supérieure en Égypte et au Sinaï. *Mémoires de l'Académie des sciences de l'Institut de France*, **60**(1), 44 pp., 7 pls.
- Downie, C., Hussain, M. A. & Williams, G. L.** 1971. Dinoflagellate cyst and acritarch associations in the Paleogene of South-east England. *Geoscience and Man*, **3**, 29–35, pls.
- Drugg, W. S.** 1964. *Glyphanodinium*, a new dinoflagellate genus from the Paleocene of California. *Proceedings of the Biological Society of Washington*, **77**, 237–240.
- Drugg, W. S.** 1967. Palynology of the Upper Moreno Formation (Late Cretaceous–Paleocene) Escarpado Canyon, California. *Palaeontographica, Abteilung B*, **120**(1–4), 1–71, pls 1–9.
- Drugg, W. S.** 1970. Some new genera, species, and combinations of phytoplankton from the Lower Tertiary of the Gulf Coast, U.S.A. *Proceedings of the North American Paleontological Convention, Chicago, September 1969*, **G**, 809–843.
- Duxbury, S.** 1980. Barremian phytoplankton from Speeton, east Yorkshire. *Palaeontographica, Abteilung B*, **173**(4–6), 107–146, pls 1–13.
- Eaton, G. L.** 1971. A morphogenetic series of dinoflagellate cysts from the Bracklesham Beds of the Isle of Wight, Hampshire, England. Pp. 355–379 in A. Farinacci (ed.) *Proceedings of the 2nd Planktonic Conference, Rome, 1970*. Edizioni Tecnoscienza, Rome.

- Eaton, G. L.** 1976. Dinoflagellate cysts from the Bracklesham Beds (Eocene) of the Isle of Wight, southern England. *British Museum (Natural History) Geology, Bulletin*, **26**, 227–332, pls 1–21.
- Ebel, K.** 1992. Mode of life and soft body shape of heteromorph ammonites. *Lethaia*, **25**, 179–193.
- Edwards, L. E.** 2001. Dinocyst biostratigraphy of Tertiary sediments from five cores from Screven and Burke Counties, Georgia. Pp. G1–G25 in L. E. Edwards (ed.) *Geology and paleontology of five cores from Screven and Burke counties, eastern Georgia*. *US Geological Survey, Professional Paper*, **1603–G**.
- Edwards, L. E. & Andrie, V. A. S.** 1992. Distribution of selected dinoflagellate cysts in modern marine sediments. Pp. 259–288 in M. J. Head & J. H. Wrenn (eds) *Neogene and Quaternary Dinoflagellate Cysts and Acritarchs*. American Association of Stratigraphic Palynologists Foundation, Dallas.
- Ehrenberg, C. G.** 1837. Über das Massenverhältniss der jetzt lebenden Kiesel-Infusorien und über ein neues Infusorien-Conglomerat als Polierschiefer von Jastraba in Ungarn. *Königlich Akademie der Wissenschaften zu Berlin, Abhandlungen*, 1836, **1**, 109–135, pls 1–2.
- Eisenack, A.** 1958. Mikroplankton aus dem norddeutschen Apt, nebst einigen Bemerkungen über fossile Dinoflagellaten. *Neues Jahrbuch für Geologie und Paläontologie, Abhandlungen*, **106**(3), 383–422, pls 21–27.
- Eisenack, A.** 1963. *Cordosphaeridium* n.g., ex *Hystrichosphaeridium*, Hystrichosphaeridea. *Neues Jahrbuch für Geologie und Paläontologie, Abhandlungen*, **118**, 260–265.
- Eisenack, A. & Cookson, I. C.** 1960. Microplankton from Australian Lower Cretaceous sediments. *Proceedings of the Royal Society of Victoria*, **72**(1), 1–11.
- El Mehdawi, A. D.** 1998. *Odontochitina tabulata* sp. nov. A late Santonian–early Campanian dinoflagellate cyst from SE Sirte Basin, Libya. *Journal of Micropaleontology*, **17**(2), 173–178.
- Elsik, W. C.** 1968. Palynology of a Paleocene Rockdale lignite, Milam County, Texas. I. Morphology and taxonomy. *Pollen et Spores*, **10**(2), 263–314.
- Elsik, W. C.** 1977. *Paralecaniella indentata* (Defl. & Cooks. 1955) Cookson & Eisenack 1970 and Allied Dinocysts. *Palynology*, **1**, 95–102.
- England, T. D. J.** 1989. Lithostratigraphy of the Nanaimo Group, Georgia Basin, southwestern British Columbia. Pp. 197–206 in *Current Research, Part E, Geological Survey of Canada Paper*, **89-1E**.

- Enkin, R. J., Baker, J. & Mustard, P. S.** 2001. Paleomagnetism of the Upper Cretaceous Nanaimo Group, southwestern Canadian Cordillera. *Canadian Journal of Earth Sciences*, **38**(10), 1403–1422.
- Eshet, Y., Moshkovitz, S., Habib, D., Benjamini, C. & Margaretz, M.** 1992. Calcareous nannofossil and dinoflagellate stratigraphy across the Cretaceous/Tertiary boundary at Hor Hahar, Israel. *Marine Micropaleontology*, **18**, 199–228.
- Everhart, M. J. & Maltese, A.** 2010. First report of a heteromorph ammonite, cf. *Glyptoxoceras*, from the Smoky Hill Chalk (Santonian) of western Kansas, and a brief review of Niobrara Chalk cephalopods. *Transactions of the Kansas Academy of Science*, **113**(1/2), 64–70.
- Evitt, W. R.** 1985. *Sporopollenin and dinoflagellate cysts: their morphology and interpretation*. American Association of Stratigraphic Palynologists Foundation, Dallas, 333 pp.
- Evitt, W. R., Clarke, R. F. A. & Verdier, J.-P.** 1967. Dinoflagellate studies III. *Dinogymnium acuminatum* n. gen., n. sp. (Maastrichtian) and other fossils formerly referable to *Gymnodinium* Stein. *Stanford University Publications, Geological Sciences*, **10-4**, 1–27, pls 1–3.
- Fatmi, A. N. & Kennedy, W. J.** 1999. Maastrichtian ammonites from Balochistan, Pakistan. *Journal of Paleontology*, **73**(4), 641–662.
- Fensome, R. A. & Williams, G. L.** 2005. Scotian Margin PalyAtlas, Version 1. *Geological Survey of Canada, Open File*, **4677**. [Distributed as CD only.]
- Fensome, R. A., Taylor, F. J. R., Norris, G., Sarjeant, W. A. S., Wharton, D. I. & Williams, G. L.** 1993. A classification of fossil and living dinoflagellates. *Micropaleontology Press Special Paper*, **7**, 1–351.
- Fensome, R. A., Guerstein, G. R. & Williams, G. L.** 2006. New insights on the Paleogene dinoflagellate cyst genera *Enneadocysta* and *Licracysta* gen. nov. based on material from offshore eastern Canada and southern Argentina. *Micropaleontology*, **52**(5), 385–410.
- Fensome, R. A., Crux, J. A., Gard, I. G., MacRae, R. A., Williams, G. L., Thomas, F. C., Fiorini, F. & Wach, G.** 2008. The last 100 million years on the Scotian Margin, offshore eastern Canada: an event–stratigraphic scheme emphasizing biostratigraphic data. *Atlantic Geology*, **44**, 93–126.
- Fensome, R. A., Williams, G. L. & MacRae, R. A.** 2009. Late Cretaceous and Cenozoic fossil dinoflagellates and other palynomorphs from the Scotian Margin, offshore eastern Canada. *Journal of Systematic Palaeontology*, **7**(1), 1–79.

- Fensome, R. A., Nøhr-Hansen, H. & Williams, G. L.** 2016. Cretaceous and Cenozoic dinoflagellate cysts and other palynomorphs from the western and eastern margins of the Labrador–Baffin Seaway. *Geological Survey of Denmark and Greenland Bulletin*, **36**, 143 pp.
- Firth, J. V.** 1993. Dinoflagellate assemblages and sea-level fluctuations in the Maastrichtian of southwest Georgia. *Review of Palaeobotany and Palynology*, **79**, 179–204.
- Firth, J. V.** 1996. Upper middle Eocene to Oligocene dinoflagellate biostratigraphy and assemblage variations in hole 913B, Greenland Sea. Pp. 203–242 in J. Thiede, A. M. Myrhe, J. V. Firth, G. L. Johnson & W. F. Ruddiman (eds) *Proceedings of the Ocean Drilling Program, Scientific Results*, **151**.
- Föllmi, K. B., Garrison, R. E., Ramirez, P. C., Zambrano-Ortiz, F., Kennedy, W. J. & Lehner, B. L.** 1992. Cyclic phosphate-rich successions in the Upper Cretaceous of Colombia. *Palaeogeography, Palaeoclimatology, Palaeoecology*, **93**, 151–182.
- Forbes, E.** 1846. Report on the fossil Invertebrata from southern India, collected by Mr. Kay and Mr. Cunliffe. *Transactions of the Geological Society of London, Series 2*, **7**(3), 97–174, pls 7–19.
- Gabb, W. M.** 1864. Description of the Cretaceous fossils. Pp. 55–243, pls 9–32 in *Geological Survey of California, Palaeontology*, **1**(4), 1–243, pls 1–32.
- Gerlach, E.** 1961. Mikrofossilien aus dem Oligozän und Miozän Nordwestdeutschlands, unter besonderer Berücksichtigung der Hystrichosphaeren und Dinoflagellaten. *Neues Jahrbuch für Geologie und Paläontologie, Abhandlungen*, **112**(2), 143–228.
- Gill, T.** 1871. Arrangement of the families of mollusks. *Smithsonian Miscellaneous Collections*, **227**, 1–49.
- Gill, J. R. & Cobban, W. A.** 1966. The Red Bird Section of the Upper Cretaceous Pierre Shale in Wyoming. *U.S. Geological Survey, Professional Paper 393-A*, 1A–75A, 12 pls.
- Giudici, P. & Pallini, G.** 1993. Nostoceratidae (Ammonoidea) del Campaniano superiore nel Salento (Lecca-Italia meridionale). *Paleopelagos*, **3**, 315–324.
- Gocht, H.** 1957. Mikroplankton aus dem nordwestdeutschen Neokom. Teil I. *Paläontologische Zeitschrift*, **31**, 163–185.
- Gocht, H.** 1969. Formengemeinschaften alttertiären Mikroplanktons aus Bohrproben des Erdölfeldes Meckelfeld bei Hamburg. *Palaeontographica, Abteilung B*, **126**, 1–100, pl. 1–11.

- Goodman, D. K. & Witmer, R. J.** 1985. Archeopyle variation and paratabulation in the dinoflagellate *Diphyes colligerum* (Deflandre & Cookson 1955) Cookson 1965. *Palynology*, **9**, 61–84.
- Goolaerts, S., Kennedy, W. J., Dupuis, C. & Steurbaut, E.** 2004. Terminal Maastrichtian ammonites from the Cretaceous–Paleogene global stratotype section and point, El Kelf, Tunisia. *Cretaceous Research*, **25**(3), 313–328.
- Goolaerts, S.** 2010. *Late Cretaceous ammonites from Tunisia: chronology and causes of their extinction and extrapolation to other areas*. Ph.D. thesis, Arenberg Doctoral School, Katholieke Universiteit Leuven, Belgium, 537 pp.
- Grega, L., Anderson, S., Cheetham, M., Clemente, M., Colletti, A., Moy, W., Talarico, D., Thatcher, S. L. & Osborn, J. M.** 2013. Aerodynamic Characteristics of Saccate Pollen Grains. *International Journal of Plant Sciences*, **174**(3), 499–510.
- Groot, J. J. & Groot, C. R.** 1962. Some plant microfossils from the Brightseat Formation (Paleocene) of Maryland. *Palaeontographica, Abteilung B*, **111**, 161–171, pls 29–31.
- Guangli Wang, Wang, T.-G., Simoneit, B. R. T., Zhilin Chen, Linye Zhang & Jinli Xu.** 2008. The distribution of molecular fossils derived from dinoflagellates in Paleogene lacustrine sediments (Bohai Bay Basin, China). *Organic Geochemistry*, **39**(11), 1512–1521.
- Guangli Wang, Shu Li, Tieguan Wang & Linye Zhang.** 2010. Applications of molecular fossils in lacustrine stratigraphy. *Chinese Journal of Geochemistry*, **29**(1), 15–20.
- Guédé, K. É., Slimani, H., Louwye, S., Asebriy, L., Toufiq, A., Ahmamoub, M., El Hassani, I & Digbehi, Z. B.** 2014. Organic-walled dinoflagellate cysts from the Upper Cretaceous–lower Paleocene succession in the western External Rif, Morocco: new species and new biostratigraphic results. *Geobios*, **47**, 291–304.
- Guzhikova, A. A.** 2016. *Magnetostratigraphy Anichnogo Campanian–Maastrichtian interval of southeastern Russian plate*. Unpublished Ph.D. thesis, Saratov Chernyshevsky State University, Saratov, Russia, 177 pp.
- Haas, O.** 1943. Some abnormally coiled ammonites from the Upper Cretaceous of Angola. *American Museum Novitates*, **1222**, 1–17, 1 pl.
- Habib, D.** 1973. Taxonomy, morphology and suggested phylogeny of the dinoflagellate genus *Druggidium*. *Geoscience and Man*, **7**, 47–55, pls 1–3.
- Habib, D. & Drugg, W. S.** 1987. Palynology of sites 603 and 605, Leg 93, Deep Sea Drilling Project. Pp. 751–775 in J. H. Blakeslee & E. Whalen (eds) *Deep Sea Drilling Project, Washington, Initial Reports*, **93**.

- Haggart, J. W.** 1991. Biostratigraphy of the Upper Cretaceous Nanaimo Group, Gulf Islands, British Columbia. Pp. 222–257 in P. L. Smith (ed.) *A Field Guide to the Paleontology of Southwestern Canada. The First Canadian Paleontology Conference*. University of British Columbia, Vancouver.
- Haggart, J. W.** 1994. Turonian (Upper Cretaceous) strata and biochronology of southern Gulf Islands, British Columbia. Pp. 159–164 in *Current Research 1994-A, Geological Survey of Canada*.
- Haggart, J. W.** 1996. Mollusks: exotic shells from Cretaceous seas. Pp. 167–186 in R. Ludvigsen (ed.) *Life in Stone: A Natural History of British Columbia's Fossils*. UBC Press, Vancouver.
- Haggart, J. W. & Graham, R.** The crinoid *Marsupites* in the Upper Cretaceous Nanaimo Group, British Columbia: resolution of the Santonian-Campanian boundary in the North Pacific province. In press.
- Haggart, J. W., Ward, P. D. & Orr, W.** 2005. Turonian (Upper Cretaceous) lithostratigraphy and biochronology, southern Gulf Islands, British Columbia, and northern San Juan Islands, Washington State. *Canadian Journal of Earth Sciences*, **42**, 2001–2020.
- Haggart, J. W., Ward, P. D., Raub, T. D., Carter, E. S. & Kirschvink, J. L.** 2009. Molluscan biostratigraphy and paleomagnetism of Campanian strata, Queen Charlotte Islands, British Columbia: implications for Pacific coast North America biochronology. *Cretaceous Research*, **30**, 939–951.
- Haggart, J. W., Graham, R. & Beard, G.** 2011. Field Trip 2. The Upper Cretaceous of the Nanaimo–Courtenay region of Vancouver Island. Pp. 31–62 in J. W. Haggart & P. L. Smith (eds) *Field Trips to Harrison Lake and Vancouver Island, British Columbia*. 21st Canadian Paleontology Conference, Field Trip Guidebook, **16**.
- Haggart, J. W., Carter, E. S., McLachlan, S. M. S., Ross, R., Ward, P. D., Schröder-Adams, C. J., Cook, T., Starr, D. W., Nunnallee, D. & Beard, G.** Lithostratigraphy, fossil assemblages, and depositional setting of the Upper Cretaceous Nanaimo Group at Hornby Island, British Columbia, Canada: cornerstone of upper Campanian biochronology of the North Pacific Province. In prep.
- Hancock, J.** 1961. The Cretaceous system of Northern Ireland. *Quarterly Journal of the Geological Society of London*, **117**, 11–36.
- Hansen, J. M.** 1977. Dinoflagellate stratigraphy and echinoid distribution in Upper Maastrichtian and Danian deposits from Denmark. *Bulletin of the Geological Society of Denmark*, **26**, 1–26.
- Harding, I. C.** 1986. Archaeopyle variability in Early Cretaceous dinocysts of the partiform gonyaulacoid genus *Druggidium* Habib. *Journal of Micropalaeontology*, **5**(2), 17–26.

- Harker, S. D., Sarjeant, W. A. S. & Caldwell, W. G. E.** 1990. Late Cretaceous (Campanian) organic-walled microplankton from the interior plains of Canada, Wyoming and Texas: biostratigraphy, palaeontology and palaeoenvironmental interpretation. *Palaeontographica, Abteilung B*, **219**, 243 pp., pls 1–13.
- Harland, R.** 1973. Dinoflagellate cysts and acritarchs from the Bearpaw Formation (Upper Campanian) of southern Alberta, Canada. *Palaeontology*, **16**, 665–706, pls 84–88.
- Hasegawa, T., Moriya, K. & Haggart, J. W.** 2015. Campanian–Maastrichtian clay-rich sequences along the North Pacific margin: early cooling history of Cretaceous greenhouse Earth. *Geological Society of America, Abstracts with Programs*, **45**(7), 517.
- Haughton, S. H.** 1925. Notes on some Cretaceous fossils from Angola (Cephalopoda and Echinoidea). *Annals of the South African Museum*, **22**(4), 263–288, pls 11–14.
- He, S., Kyserb, T. K. & Caldwell, W. G. E.** 2005. Paleoenvironment of the Western Interior Seaway inferred from $\delta^{18}\text{O}$ and $\delta^{13}\text{C}$ values of molluscs from the Cretaceous Bearpaw marine cyclothem. *Palaeogeography, Palaeoclimatology, Palaeoecology*, **217**, 67–85.
- He Chengquan & Sun Xuekun.** 2000. Late Hauterivian dinoflagellates from the lower part of the Chengzihe Formation in Jixi Basin, eastern Heilongjiang, NE China. *Acta Palaeontologica Sinica*, **39**(1), 46–62.
- Head, M. J.** 2007. Last Interglacial (Eemian) hydrographic conditions in the southwestern Baltic Sea based on dinoflagellate cysts from Ristinge Klint, Denmark. *Geological Magazine*, **144**(6), 987–1013.
- Head, M. J. & Wrenn, J. H.** 1992. A forum on Neogene and Quaternary dinoflagellate cysts. Pp. 1–31 in M. J. Head & J. H. Wrenn (eds) *Neogene and Quaternary Dinoflagellate Cysts and Acritarchs*. American Association of Stratigraphic Palynologists Foundation, Dallas.
- Head, M. J. & Westphal, H.** 1999. Palynology and paleoenvironments of a Pliocene carbonate platform: the Clino core, Bahamas. *Journal of Paleontology*, **73**(1), 1–25.
- Helby, R.** 1987. *Muderongia* and related dinoflagellates of the latest Jurassic to Early Cretaceous of Australasia. Pp. 297–336 in P. A. Jell (ed.) *Studies in Australian Mesozoic palynology. Memoir of the Association of Australasian Palaeontologists*, **4**.
- Helenes, J.** 2000. *Exochosphaeridium alisitosenense* n. sp., a new gonyaulacoid dinoflagellate from the Albian of Baja California, Mexico. *Micropaleontology*, **46**(2), 135–142.
- Helenes, J. & Lucas-Clark, J.** 1997. Morphological variations among species of the fossil dinoflagellate genus *Gonyaulacysta*. *Palynology*, **21**, 173–196.

- Henderson, I. F. & Henderson, W. D.** 1920. A dictionary of scientific terms: pronunciation, derivation, and definition of terms in biology, botany, zoology, anatomy, cytology, embryology, physiology. Oliver & Boyd, Edinburgh, 376 pp.
- Henderson, R. A.** 1970. Ammonoidea from the Mata Series (Santonian-Maastrichtian) of New Zealand. *Special Papers in Palaeontology*, **6**, 82 pp., 15 pls.
- Henderson, R. A., Kennedy, W. J. & McNamara, K. J.** 1992. Maastrichtian heteromorph ammonites from the Carnarvon Basin, Western Australia. *Alcheringa: An Australasian Journal of Palaeontology*, **16**(2), 133–170.
- Herngreen, G. F. W., Kedves, M., Rovnina, L. V. & Smirnova, S. B.** 1996. Cretaceous palynofloral provinces: a review. Pp. 1157–1188 in J. Jansonius & D. C. McGregor (eds) *Palynology: principles and applications*. American Association of Stratigraphic Palynologists Foundation, Dallas.
- Hoek, P. H., Yoram, E. & Almogi-Labin, A.** 1996. Dinoflagellate Cyst Zonation of Campanian–Maastrichtian Sequences in Israel. *Micropaleontology*, **42**(2), 125–150.
- Howarth, M. K.** 1965. Cretaceous ammonites and nautiloids from Angola. *Bulletin of the British Museum (Natural History), Geology*, **10**(10), 335–412, 13 pls.
- Hultberg, S. U.** 1985. Systematic paleontology. Pp. 104–189 in Hultberg, S.U. *Dinoflagellate Studies of the Upper Maastrichtian and Danian in Southern Scandinavia*. Published Ph.D. thesis. Department of Geology, University of Stockholm, Stockholm, Sweden.
- Hultberg, S. U. & Malmgren, B. A.** 1985. Quantitative biostratigraphy based on upper Maastrichtian dinoflagellates and planktonic foraminifera from southern Scandinavia. Pp. 33–55 in S. U. Hultberg *Dinoflagellate Studies of the upper Maastrichtian and Danian in Southern Scandinavia*. Published Ph.D. thesis. Department of Geology, University of Stockholm, Stockholm, Sweden.
- Hyatt, A.** 1894. Phylogeny of an acquired characteristic. *Proceedings of the American Philosophical Society*, **32**, 349–647, 14 pls.
- Hyatt, A.** 1900. Cephalopoda. Pp. 502–604 in K. A. von Zittel (ed.) *Text-book of Palaeontology I*. MacMillan, London.
- Iakovleva, A. I.** 2015. Middle-late Eocene dinoflagellate cysts from NE Ukraine (Borehole No. 230, Dnepr-Donets Depression): stratigraphic and palaeoenvironmental approach. *Acta Palaeobotanica*, **55**(1), 19–51.
- Ifrim, C. & Stinnesbeck, W.** 2007. Early Turonian ammonites from Vallecillo, north-eastern Mexico: taxonomy, biostratigraphy and palaeobiogeographical significance. *Cretaceous Research*, **28**, 642–664.

- Ifrim, C. & Stinnesbeck, W.** 2010. Migration pathways of the late Campanian and Maastrichtian shallow facies ammonite *Sphenodiscus* in North America. *Palaeogeography, Palaeoclimatology, Palaeoecology*, **292**, 96–102.
- Ifrim, C. & Stinnesbeck, W.** 2013. Ammonoids from the Maastrichtian (Late Cretaceous) at El Zancudo, Nuevo Laredo, Tamaulipas, Mexico. *Boletín de la Sociedad Geológica Mexicana*, **65**(1), 189–200.
- Ifrim, C., Stinnesbeck, W. & López-Oliva, J. G.** 2004. Maastrichtian cephalopods from Cerralvo, north-eastern Mexico. *Palaeontology*, **47**(6), 1575–1627.
- Ifrim, C., Stinnesbeck, W., Garza, R. R. & Ventura, J. F.** 2010. Hemipelagic cephalopods from the Maastrichtian (late Cretaceous) Parras Basin at La Parra, Coahuila, Mexico, and their implications for the correlation of the lower Difunta Group. *Journal of South American Earth Sciences*, **29**, 597–618.
- Ifrim, C., Stinnesbeck, W., Espinosa, B. & Ventura, J. F.** 2015. Upper Campanian (Upper Cretaceous) cephalopods from the Parras Shale near Saucedas, Coahuila, Mexico. *Journal of South American Earth Sciences*, **64**, 229–257.
- Ifrim, C., Lara de la Cerda, J. E., Peña Ponce, V. H. & Stinnesbeck, W.** 2017. The upper Campanian–lower Maastrichtian cephalopod fauna of Botellos, Nuevo León: a key to understand faunal turnover across the Campanian–Maastrichtian boundary in NE Mexico. *Acta Geologica Polonica*, **67**(1), 145–162.
- Ikuno, K. & Hirano, H.** 2015. Nomenclatural review of *Polyptychoceras* and 18 related taxa (Ammonoidea: Diplomoceratidae). *Swiss Journal of Palaeontology*, **134**(2), 227–232.
- Ilyina, V. I., Kulkova, I. A. & Lebedeva, N. K.** 1994. Mikrofitofossilii i detalnaya stratigrafiya morskogo i kainozoya Sibiri. *Transactions of the United Institute of Geology, Geophysics and Mineralogy*, **818**, 192 pp.
- Jacobs, D. K. & Chamberlain, A. Jr.** 1996. Buoyancy and hydrodynamics in ammonoids. Pp. 170–220 in Landman, N. H., Tanabe, K. & Davis, R. A. (eds) *Ammonoid Paleobiology, Topics of Geobiology*, **13**. Plenum Press, New York.
- Jagt, J. W. M.** 1998. Ammonieten. *Grondboor & Hamer*, **52**(4/5), 114, 1 pl.
- Jagt, J. W. M.** 2012. Ammonites from the Late Cretaceous and early Paleogene Limburg. *Staringia*, **13**, 154–183.
- Jagt, J. W. M., Goolaerts, S., Jagt-Yazykova, E. A., Cremers, G. & Verhesen, W.** 2006. First record of *Phylloptychoceras* (Ammonoidea) from the Maastrichtian type area, The Netherlands. *Bulletin de l'Institut Royal des Sciences Naturelles de Belgique, Sciences de la Terre*, **76**, 97–103.

- Jagt-Yazykova, E. A.** 2011. Palaeobiogeographical and palaeobiological aspects of mid- and Late Cretaceous ammonoid evolution and bio-events in the Russian Pacific. *Scripta Geologica*, **143**, 15–121.
- Jagt-Yazykova, E. A.** 2012. Ammonoid faunal dynamics across bio-events during the mid-and Late Cretaceous along the Russian Pacific coast. *Acta Palaeontologica Polonica*, **57**(4), 737–748.
- Jaramillo, C. & Amezquita, O. Y.** 1994. Palinoestratigrafía del Grupo Olini (Coniaciano-Campaniano), Valle Superior del Magdalena, Colombia. *Estudios Geológicos del Valle Superior del Magdalena*, **17**, 1–18.
- Jain, K. P. & Millepied, P.** 1973. Cretaceous microplankton from Senegal Basin, NW Africa. 1. Some new genera, species and combinations of dinoflagellates. *The Palaeobotanist*, **20**, 22–32.
- Jain, K. P. & Millepied, P.** 1975. Cretaceous microplankton from Senegal Basin, W. Africa. II. Systematics and biostratigraphy. *Geophytology*, **5**(2), 126–171.
- Jeletzky, J. A.** 1970. Cretaceous macrofaunas. Pp. 649–662, pls 23–28 in E.W. Bamber (ed.) *Biochronology: Standard of Phanerozoic Time. Geological Survey of Canada, Economic Geology Report No. 1, Part B*.
- Jianyu Chen, Yanpong Bi, Jigou Zhang & Shuafu Li.** 1996. Oil–source correlation in the Fulin basin, Shengli petroleum province, East China. *Organic Geochemistry*, **24**(8–9), 931–940.
- Jianyu Chen, Shuafu Li, Ying Xiong, & Yanpong Bi.** 1998. Multiple petroleum systems in Tertiary extensional basins, East China: a case study of the Gunan-Fulin basin. *Journal of Petroleum Geology*, **21**(1), 105–118.
- Jones, D. L.** 1963. Upper Cretaceous (Campanian and Maestrichtian) ammonites from southern Alaska. *U.S. Geological Survey Professional Paper*, **432**, 1–53, 41 pls.
- Kakabadzé, M. V.** 2016. Speculations on the ethology of some heteromorph ammonites. *Swiss Journal of Palaeontology*, **135**, 63–68.
- Kakabadzé, M. V. & Sharikadzé, M. Z.** 1993. On the mode of life of heteromorph ammonites (heterocone, ancylocone, ptychocone). *Geobios*, **15**, 209–15.
- Kaplan, P.** 2002. Biomechanics as a test of functional plausibility: testing the adaptive value of terminal-countdown heteromorphy in Cretaceous ammonoids. Pp. 181–197 in H. Summesberger, K. Histon & A. Daurer, (eds) *Cephalopods Present and Past*, **57**. Abhandlungen der Geologischen Bundesanstalt.

- Kaplan U. & Schmid, F.** 1988. The heteromorph ammonite genera *Eubostrychoceras* and *Hyphantoceras* from the Turonian of northwestern Germany. *Geologie und Paläontologie in Westfalen*, **12**, 47–61, 13 pls.
- Katnick, D. C.** 2001. *Sedimentology, stratigraphy and provenance of the Upper Cretaceous Nanaimo Group, Denman and Hornby islands, British Columbia*. Unpublished M.Sc. thesis, Simon Fraser University, Burnaby, British Columbia, 265 pp.
- Katnick, D. C. & Mustard, P. S.** 2001. Geology of Denman and Hornby islands, British Columbia, NTS 92F/7E; 92F/10. *British Columbia Geological Survey, Geoscience Map 2001-3*, 1:50,000 scale.
- Katnick, D. C. & Mustard, P. S.** 2003. Geology of Denman and Hornby islands, British Columbia: implications for Nanaimo Basin evolution and formal definition of the Geoffrey and Spray formations, Upper Cretaceous Nanaimo Group. *Canadian Journal of Earth Sciences*, **40**, 375–393.
- Kennedy, W. J.** 1986a. The ammonite fauna of the Calcaire à *Baculites* (upper Maastrichtian) of the Cotentin Peninsula (Manche, France). *Palaeontology*, **29**(1), 25–83.
- Kennedy, W. J.** 1986b. The ammonite fauna of the type Maastrichtian with a revision of *Ammonites colligatus* Binkhorst, 1861. *Bulletin de l'Institut Royal des Sciences Naturelles de Belgique, Sciences de la Terre*, **56**, 151–267.
- Kennedy, W. J.** 1986c. Campanian and Maastrichtian ammonites from northern Aquitaine, France. *Special Papers in Palaeontology*, **36**, 1–145.
- Kennedy, W. J.** 1989. Thoughts on the evolution and extinction of Cretaceous ammonites. *Proceedings of the Geological Association*, **100**(3), 251–279.
- Kennedy, W. J.** 1993. Campanian and Maastrichtian ammonites from the Mons Basin and adjacent areas (Belgium). *Bulletin de l'Institut Royal des Sciences Naturelles de Belgique, Sciences de la Terre*, **63**, 99–131.
- Kennedy, W. J. & Cobban, W. A.** 1993a. Maastrichtian ammonites from the Corsicana Formation in northeast Texas. *Geological Magazine*, **130**(1), 57–67.
- Kennedy, W. J. & Cobban, W. A.** 1993b. Campanian ammonites from the Annona Chalk near Yancy, Arkansas. *Journal of Paleontology*, **67**(1), 83–97.
- Kennedy, W. J. & Cobban, W. A.** 1993c. Ammonites from the Saratoga Chalk (Upper Cretaceous), Arkansas. *Journal of Paleontology*, **67**(3), 404–434; **67**(5), 907.
- Kennedy, W. J. & Cobban, W. A.** 1993d. Upper Campanian ammonites from the Ozan-Annona formation boundary in southwestern Arkansas. *Bulletin of the Geological Society of Denmark*, **40**, 115–148.

- Kennedy, W. J. & Cobban, W. A.** 1999. Campanian (Late Cretaceous) ammonites from the Bergstrom Formation in central Texas: *Acta Geologica Polonica*, **49**(1), 67–80, 7 pls.
- Kennedy, W. J. & Cobban, W. A.** 2001. Campanian (Late Cretaceous) ammonites from the upper part of the Anacacho limestone in South-Central Texas. *Acta geologica Polonica*, **51**(1), 15–30.
- Kennedy, W. J., Cobban, W. A. & Scott, G. R.** 1992. Ammonite correlation of the uppermost Campanian of western Europe, the U.S. Gulf Coast, Atlantic Seaboard and Western Interior, and the numerical age of the base of the Maastrichtian. *Geological Magazine*, **129**(4), 497–500.
- Kennedy, W. J., Cobban, W. A. & Landman, N. H.** 1999. The heteromorph ammonite *Didymoceras cochleatum* (Meek and Hayden, 1858), from the Pierre Shale of South Dakota and Wyoming. *American Museum Novitates*, **3268**, 1–8.
- Kennedy, W. J., Cobban, W. A. & Scott, G. R.** 2000a. Heteromorph ammonites from the upper Campanian (Upper Cretaceous) *Baculites cuneatus* and *Baculites reesidei* zones of the Pierre Shale in Colorado, USA. *Acta Geologica Polonica*, **50**(1), 1–20.
- Kennedy, W. J., Cobban, W. A. & Scott, G. R.** 2000b. Heteromorph ammonites from the middle Campanian *Baculites scotti* Zone in the U.S. Western Interior. *Acta Geologica Polonica*, **50**(2), 223–241, 15 pls.
- Kennedy, W. J., Landman, N. H., Cobban, W. A. & Scott, G. R.** 2000c. Late Campanian (Cretaceous) heteromorph ammonites from the Western Interior of the United States. *Bulletin of the American Museum of Natural History*, **251**, 1–88.
- Kennedy, W. J., Landman, N. H., Cobban, W. A. & Johnson, R. O.** 2000d. Additions to the ammonite fauna of the Upper Cretaceous Navesink Formation of New Jersey. *American Museum Novitates*, **3306**, 1–30.
- Kennedy, W. J. & Lunn, G.** 2000. Upper Campanian (Cretaceous) ammonites from the Shinarish Formation, Djebel Sinjar, northwest Iraq. *Journal of Paleontology*, **74**(3), 464–473.
- Kennedy, W. J. & Henderson, R. A.** 1992. Heteromorph ammonites from the upper Maastrichtian of Pondicherry, South India. *Palaeontology*, **35**(3), 693–731.
- Kennedy, W. J. & Summesberger, H.** 1986. Lower Maastrichtian ammonites from Neuberg, Steiermark, Austria. *Beiträge zur Paläontologie von Österreich*, **12**, 181–242.
- Kennedy, W. J. & Summesberger, H.** 1987. Lower Maastrichtian ammonites from Nagoryanŷ (Ukrainian SSR). *Beiträge zur Paläontologie von Österreich*, **13**, 25–78.

- Kennedy, W. J. & Summesberger, H.** 1999. New late Campanian ammonites from the Gschlifgraben near Gmunden (Ultrahelvetic, Austria). *Beiträge zur Paläontologie*, **24**, 23–39.
- Kennedy, W. J. & Summesberger, H.** 2001. Additional ammonites from the upper Campanian (Upper Cretaceous) of the Gschlifgraben (Ultrahelvetic; Austria). *Annalen des Naturhistorischen Museums in Wien*, **102A**, 85–107.
- Kim, B. & Kodama, K. P.** 2004. A compaction correction for the paleomagnetism of the Nanaimo Group sedimentary rocks: implications for the Baja British Columbia hypothesis. *Journal of Geophysical Research*, **109**(B02102), 1–17.
- Kirsch, K.-H.** 1991. Dinoflagellatenzysten aus der Oberkreide des Helvetikums und Nordultrahelvetikums von Oberbayern. *Münchener Geowissenschaftliche Abhandlungen, Reihe A, Geologie und Paläontologie*, **22**, 1–306.
- Klement, K. W.** 1960. Dinoflagellaten und Hystrichosphaerideen aus dem unteren und mittleren Malm Südwestdeutschlands. *Palaeontographica, Abteilung A*, **114**(1–4), 1–104, pls 1–10.
- Klinger, H. C.** 1976. Cretaceous heteromorph ammonites from Zululand. *Memoirs of the Geological Survey of South Africa*, **69**, 142 pp., 43 pls.
- Klinger, H. C.** 1980. Speculations on buoyancy control and ecology in some heteromorph ammonoids. Pp. 337–355 in M. R. House & J. R. Senior (eds) *The Ammonoidea. Systematics Association, Special Volume*, **18**. Academic Press, London.
- Klinger, H. C.** 1982. Revision of *Ancyloceras bipunctatum* Schlüter, 1872 (Cephalopoda, Ammonoidea) and discussion of the validity, phylogeny and limits of the genus *Neancyloceras* Spath, 1926. *Annals of the South African Museum*, **90**(5), 219–239.
- Klinger, H. C.** 2008. *Genera and Species Referred to the Families Nostoceratidae Hyatt, 1894 and Diplomoceratidae Spath, 1926*. Unpublished manuscript, 538 pp.
- Klinger, H. C. & Kennedy, W. J.** 1997. On the affinities of *Madagascarites andimakensis* Collignon, 1966, and allied Upper Cretaceous heteromorph ammonites. *Annals of the South African Museum*, **105**, 227–247.
- Klinger, H. C., Kennedy, W. J., Lees, J. A. & Kitto, S.** 2001. Upper Maastrichtian ammonites and nannofossils and a Palaeocene nautiloid from Richards Bay, Kwa Zulu, South Africa. *Acta Geologica Polonica*, **51**(3), 273–291.
- Klinger, H. C. & Kennedy, W. J.** 2003a. Observations on the systematics, geographic and stratigraphic distribution and origin of *Diplomoceras cylindraceum* (Defrance, 1816) (Cephalopoda: Ammonoidea). *Annals of the South African Museum*, **110**(4), 171–198.

- Klinger, H. C. & Kennedy, W. J.** 2003b. Cretaceous faunas from Zululand and Natal, South Africa. The ammonite families Nostoceratidae Hyatt, 1894 and Diplomoceratidae Spath, 1926. *Annals of the South African Museum*, **110**(6), 219–336.
- Klinger, H. C., Kennedy, W. J & Grulke, W. E.** 2007. New and little-known Nostoceratidae and Diplomoceratidae (Cephalopoda: Ammonoidea) from Madagascar. *African Natural History*, **3**, 89–115.
- Klug, C., Zatoń, M., Parent, H., Hostettler, B. & Tajika, A.** 2015. Mature Modifications and Sexual Dimorphism. Pp. 253–320 in C. Klug, D. Korn, K. De Baets, I. Kruta, R. H. Mapes (eds) *Ammonoid Paleobiology: From anatomy to ecology, Topics in Geobiology*, **43**. Springer, Dordrecht.
- Kodama, K.P. & Ward, P. D.** 2001. Compaction-corrected paleomagnetic paleolatitudes for Late Cretaceous rudists along the Cretaceous California margin: evidence for less than 1500 km of post-Late Cretaceous offset for Baja British Columbia. *Geological Society of America Bulletin*, **113**, 1171–1178.
- Kofoed, C. A.** 1907a. Dinoflagellata of the San Diego region. III. Descriptions of new species. *University of California Publications in Zoology*, **3**(13), 299–340, pls 22–33.
- Kofoed, C. A.** 1907b. The plates of *Ceratium* with a note on the unity of the genus. *Zoologischer Anzeiger*, **32**(7), 177–183.
- Kofoed, C. A.** 1909. On *Peridinium steini* Jörgensen, with a note on the nomenclature of the skeleton of the Peridinidae. *Archiv für Protistenkunde*, **16**, 25–47, 1 pl.
- Kofoed, C. A.** 1911. Dinoflagellata of the San Diego region. IV. The genus *Gonyaulax*, with notes on its skeletal morphology and a discussion of its generic and specific characters. *University of California Publications in Zoology*, **8**(4), 187–286, pls 9–17.
- Krijgsman, W. & Tauxe, L.** 2006. E/I corrected paleolatitudes for the sedimentary rocks of the Baja British Columbia hypothesis. *Earth and Planetary Science Letters*, **242**(1–2), 205–216.
- Krupp, R.** 2015. *Diplomoceras cylindraceum* aus dem Obercampan von Misburg. *Arbeitskreis Paläontologie Hannover*, **43**(3), 76–80.
- Krutzsch, W.** 1962. Die Mikroflora der Geiseltalbraunkohle. Teil III. Stisswasserdinoflagellaten aus subaquatisch gebildeten Blatterkohlenlagen des mittleren Geiseltales. *Hallesches Jahrbuch für Mitteldeutsche Erdgeschichte*, **4**, 40–45, pls 10–11.
- Kruta, I., Landman, N., Rouget, I., Cecca, F. & Tafforeau, P.** 2011. The role of ammonites in the Mesozoic marine food web revealed by jaw preservation. *Science*, **331**(6013), 70–72.

- Küchler, T.** 2000. Upper Cretaceous of the Barranca (Navarra, northern Spain); integrated litho-, bio- and event stratigraphy. Part II: Campanian and Maastrichtian. *Acta Geologica Polonica*, **50**(4), 441–499, 18 pls.
- Küchler, T. & Odin, G. S.** 2001. Upper Campanian–Maastrichtian ammonites (Nostoceratidae, Diplomoceratidae) from Tercis les Bains (Landes, France). Pp. 500–528 in G.S. Odin (ed.) *The Campanian-Maastrichtian Boundary. Characterisation at Tercis les Bains (France) and Correlation with Europe and other Continents. Developments in Palaeontology and Stratigraphy 19*. Elsevier, Amsterdam.
- Kuhlmann, G.** 2004. High resolution stratigraphy and paleoenvironmental changes in the southern North Sea during the Neogene. An integrated study of Late Cenozoic marine deposits from the northern part of the Dutch offshore area. *Geologica Ultraiectina, Mededelingen van de Faculteit Geowetenschappen Universiteit Utrecht*, **245**, 1- 205.
- Kullmann, J. & Wiedmann, J.** 1970. Significance of sutures in phylogeny of Ammonoidea. *University of Kansas, Paleontological Contributions*, **47**, 1–32.
- Kurihara, K., Kano, M., Sawamura, H. & Sato, Y.** 2016. The last surviving ammonoid at the end of the Cretaceous in the North Pacific Region. *Paleontological Research*, **20**(2), 116–120.
- Kurita, H. & McIntyre, D. J.** 1994. Dinoflagellate assemblages and depositional environments of the Campanian Bearpaw Formation, Alberta. Pp. 67–83 in T. E. Bolton, B. S. Norford, S. Desbiens, H. Kurita, D. J. McIntyre, J. M. White, L. Marinovich Jr. & R. Higgs (eds) *Contributions to Canadian Paleontology. Geological Survey of Canada, Bulletin*, **479**.
- de Lamarck, J. B. P. A. M.** 1799. Prodrome d'une nouvelle classification des coquilles, comprenant une rédaction appropriée des caractères génériques, et l'établissement d'un grand nombre de genres nouveaux. *Mémoires de la Société d'Histoire Naturelle de Paris*, 63–91.
- de Lamarck, J. B. P. A. M.** 1801. Système des Animaux sans vertèbres. Deterville, Paris. 432 pp.
- Landman, N. H., Tanabe, K. & Shigeta, Y.** 1996a. Ammonoid embryonic development. Pp. 344–405 in N. H. Landman, K. Tanabe & R. A. Davis (eds) *Ammonoid Paleobiology, Topics in Geobiology*, **13**. Plenum Press, New York.
- Landman, N. H., Tanabe, K. & Davis, R. A.** 1996b. Glossary. Pp. 825–843 in N. H. Landman, K. Tanabe & R. A. Davis (eds) *Ammonoid Paleobiology, Topics of Geobiology*, **13**. Plenum Press, New York.
- Landman, N. H., Garb, M. P., Rovelli, R., Ebel, D. S. & Edwards, L. E.** 2012. Short-term survival of ammonites in New Jersey after the end-Cretaceous bolide impact. *Acta Palaeontologica Polonica*, **57**, 703–715.

- Landman, N. H., Goolaerts, S., Jagt, J. W. M., Jagt-Yazykova, E. A., Machalski, M. & Yacobucci, M. M.** 2014. Ammonite extinction and nautilid survival at the end of the Cretaceous. *Geology*, **42**(8), 707–710.
- Landman, N. H., Goolaerts, S., Jagt, J. W. M., Jagt-Yazykova, E. A. & Machalski, M.** 2015. Ammonites on the brink of extinction: diversity, abundance, and ecology of the Order Ammonoidea at the Cretaceous/Paleogene (K/Pg) boundary. Pp. 497–533 in C. Klug, D. Korn, K. De Baets, I. Kruta & R. H. Mapes (eds) *Ammonoid Paleobiology: from Macroevolution to Paleogeography, Topics in Geobiology*, **44**. Springer, Dordrecht.
- Larson, N. L.** 2012. The late Campanian (Upper Cretaceous) cephalopod fauna of the Coon Creek Formation at the type locality. *Journal of Paleontological Sciences*, H.2012.01, 1–68, 13 pls.
- Larson, N. L.** 2016. The Late Cretaceous (upper Campanian) cephalopod fauna from the Coon Creek Science Center, McNairy County, Tennessee. *Bulletin of the Alabama Museum of Natural History*, **33**(2), 21–58.
- Laurin, M.** 2010. The subjective nature of Linnaean categories and its impact in evolutionary biology and biodiversity studies. *Contributions to Zoology*, **79**(4), 131–146.
- Lebedeva, N. K.** 2006. Dinocyst Biostratigraphy of the Upper Cretaceous of Northern Siberia. *Paleontological Journal*, **40**, Supplement 5, S604–S621.
- Lebedeva, N. K., Kuzmina, O. B., Soboleva, E. S. & Khazina, I. V.** 2017. Stratigraphy of Upper Cretaceous and Cenozoic deposits of the Bakchar iron ore deposit (southwestern Siberia): new data. 2017. *Stratigraphy and Geological Correlation*, **25**(1), 76–98.
- Leereveld, H.** 1995. Dinoflagellate cysts from the Lower Cretaceous Rio Argos succession (SE Spain). *LPP Contribution Series*, **2**, 175 pp.
- Lefeld, J. & Uberna, J.** 1991. A new species of *Nostoceras* (Ammonites: Nostoceratidae) in northern Libya and its affinities with other global finds. Pp. 1383–1388 in M. J. Salem (ed.) *The Geology of Libya*, 4. Elsevier, Amsterdam.
- Lejeune-Carpentier, M.** 1938. L'étude microscopique des silex. *Areoligera*: nouveau genre d'Hystrichosphaeridée. (Sixième note.) *Annales de la Société géologique de Belgique*, **62**, B163–B174.
- Lejeune-Carpentier, M.** 1940. L'étude microscopique des silex. Systématique et morphologie des "tubifères". (Huitième note.) *Annales de la Société géologique de Belgique*, **63**, B216–B236.

- Lejeune-Carpentier, M.** 1951. L'étude microscopique des silex. *Gymnodinium* et *Phanerodinium* (Dinoflagellates) de Belgique. (Treizième note.) *Annales de la Société géologique de Belgique*, **74**, B307–B315.
- Lejeune-Carpentier, M. & Sarjeant, W. A. S.** 1981: Restudy of some larger dinoflagellate cysts and an acritarch from the Upper Cretaceous of Belgium and Germany. *Annales de la Société Géologique de Belgique*, **104**, 1–39, pls 1–6.
- Lentin, J. K. & Williams, G. L.** 1973. Fossil dinoflagellates: index to genera and species. *Geological Survey of Canada, Paper*, **73–42**, 1–176.
- Lentin, J. K. & Williams, G. L.** 1976. A monograph of fossil peridinioid dinoflagellate cysts. *Bedford Institute of Oceanography, Report Series*, **BI-R-75-16**, 237 pp.
- Lentin, J. K. & Williams, G. L.** 1977. Fossil dinoflagellate genus *Isabelidinium* nom. nov. *Palynology*, **1**, 167–168.
- Lentin, J. K. & Williams, G. L.** 1980. Dinoflagellate provincialism with emphasis on Campanian peridiniaceans. *American Association of Stratigraphic Palynologists, Contributions Series*, **7**, 47 pp.
- Lentin, J. K. & Williams, G. L.** 1981. Fossil dinoflagellates: index to genera and species, 1981 edition. *Bedford Institute of Oceanography, Report Series*, **BI-R-81-12**, 345 pp.
- Lentin, J. K. & Williams, G. L.** 1985. Fossil dinoflagellates: index to genera and species, 1985 edition. *Canadian Technical Reports of Hydrography and Ocean Sciences*, **60**, 451 pp.
- Lentin, J. K. & Williams, G. L.** 1987. Status of the fossil dinoflagellate genera *Ceratiopsis* Vozzhennikova 1963 and *Cerodinium* Vozzhennikova 1963 emend. *Palynology*, **11**, 113–116.
- Lentin, J. K. & Vozzhennikova, T. F.** 1990. Fossil dinoflagellates from the Jurassic, Cretaceous and Paleogene deposits of the USSR—a re-study. *American Association of Stratigraphic Palynologists, Contributions Series*, **23**, 221 pp.
- Lewy, Z.** 1967. Some late Campanian nostoceratid ammonites from southern Israel. *Israel Journal of Earth-Sciences*, **16**, 165–173.
- Lewy, Z.** 1969. Late Campanian heteromorph ammonites from southern Israel. *Israel Journal of Earth-Sciences*, **18**, 109–135, 4 pls.
- Lewy, Z.** 1996. Octopods: nude ammonoids that survived the Cretaceous-Tertiary boundary mass extinction. *Geology*, **24**, 627–630.
- Lewy, Z.** 2002. New aspects in ammonoid mode of life and their distribution. *Geobios*, **35**, Mémoire Spécial, 24, 130–139.

- Lommerzheim, A. J.** 1995. Stratigraphie und ammonitenfaunen des Santons und Campans im Münsterländer Becken (NW-Deutschland). *Geologie und Paläontologie in Westfalen*, **40**, 1–97.
- Londeix, L., Pourtoy, D. & Fenton, J. P. G.** 1996. The presence of *Dinogymnium* (Dinophyceae) in Lower Cretaceous sediments from the northwest Tethys (southeast France and western Switzerland) and Gulf of Mexico areas: stratigraphic and systematic consequences. *Review of Palaeobotany and Palynology*, **92**, 367–382.
- Lucas-Clark, J.** 1984. Morphology of species of *Litosphaeridium* (Cretaceous, Dinophyceae). *Palynology*, **8**, 165–193.
- Lucas-Clark, J.** 1987. *Wigginsella* n. gen., *Spongodinium*, and *Apteodinium* as members of the Aptiana-Ventriosum complex (fossil Dinophyceae). *Palynology*, **11**, 155–184.
- Lucas-Clark, J.** 2006. Small peridinioid dinoflagellate cysts from the Paleocene of South Carolina, U.S.A. *Palynology*, **30**, 183–210.
- Ludvigsen, R. & Beard, G.** 1994. West Coast fossils: A guide to the ancient life of Vancouver Island. Whitecap Books, Vancouver, 194 pp.
- Ludvigsen, R. & Beard, G.** 1998. West Coast fossils: A guide to the ancient life of Vancouver Island. 2nd edition. Harbour Publishing, Madeira Park, 216 pp.
- Lukeneder, A.** 2015. Ammonoid habitats and life history. Pp. 689–791 in C. Klug, D. Korn, K. De Baets, I. Kruta & R. H. Mapes (eds) *Ammonoid Paleobiology: From anatomy to ecology*, *Topics in Geobiology*, **43**. Springer, Dordrecht.
- Luger, P. & Gröschke, M.** 1989. Late Cretaceous ammonites from the Wadi Qena area in the Egyptian Eastern Desert. *Palaeontology*, **32**(2), 355–407.
- Macellari, C. E.** 1986. Late Campanian–Maastrichtian ammonite fauna from Seymour Island (Antarctic Peninsula). *Memoirs of the Paleontological Society*, **18**, 1–55.
- Machalski, M.** 2012. Stratigraphically important ammonites from the Campanian–Maastrichtian boundary interval of the Middle Vistula River section, central Poland. *Acta Geologica Polonica*, **62**(1), 91–116, 8 pls.
- Machalski, M. & Heinberg, C.** 2005. Evidence for ammonite survival into the Danian (Paleogene) from the Cerithium Limestone at Stevns Klint, Denmark. *Geological Society of Denmark, Bulletin*, **52**, 97–111.
- Machalski, M., Vellekoop, J., Dubicka, Z., Peryt, D. & Harasimiuk, M.** 2016. Late Maastrichtian cephalopods, dinoflagellate cysts and foraminifera from the Cretaceous–

- Paleogene succession at Lechówka, southeast Poland: Stratigraphic and environmental implications. *Cretaceous Research*, **57**, 208–227.
- Maeda, H. & Seilacher, A.** 1996. Ammonoid Taphonomy. Pp. 544–566 in Landman, N. H., Tanabe, K. & Davis, R. A. (eds) *Ammonoid Paleobiology, Topics in Geobiology*, **13**. Plenum Press, New York.
- Magalashvili, G. I.** 1978. On some Late Cretaceous ammonites of south and south-east periphery of the Dzirula Massif (Georgian SSR). *Gruzinskogo Polytekhnicheskogo Instituta im. V. I. Lenina, Trudy*, **1/202**, 83–101.
- Mahoney, J. B., Mustard, P. S., Haggart, J. W., Friedman, R. M., Fanning, M. & McNicoll, V. J.** 1999. Archean zircons in Cretaceous strata of the western Canadian Cordillera: the “Baja BC” hypothesis fails a “crucial test”. *Geology*, **27**, 195–198.
- Mahoney, J. B., Haggart, J. W., Link, P. K., Fanning, C. M. & Kimbrough, D. L.** 2014. Late Cretaceous basin evolution along the western margin of the Insular Superterrane: the Nanaimo Group, British Columbia. *Geological Society of America, Abstracts with Programs*, **46(6)**, 34.
- Mahoney, J. B., Haggart, J. W., Kimbrough, D. L., Link, P. K., Fanning, C. M. & Grove, M.** 2016. Late Cretaceous evolution and sediment provenance of the Nanaimo Basin: Definitive linkage to northern latitudes. *Geological Society of America, Abstracts with Programs*, **203-12**.
- Makowski, H.** 1962. Problem of sexual dimorphism in ammonites. *Palaeontologia Polonica*, **12**, 1–92, 20 pls.
- Mantell, G. A.** 1850. *A pictorial atlas of fossil remains consisting of coloured illustrations selected from Parkinson's 'Organic remains of a former world', and Artis's 'Antediluvian phytology'*. Henry G. Bohn, London, xii+207 pp., 74 pls.
- Mantell, G. A.** 1854. *The medals of creation; or, first lessons in geology and the study of organic remains*. 2nd ed. Henry G. Bohn, London, 930 pp., pls 1–6 (in two volumes).
- Manum, S. B. & Cookson, I. C.** 1964. Cretaceous microplankton in a sample from Graham Island, arctic Canada, collected during the second ‘Fram’ expedition (1898–1902). With notes on microplankton from the Hassel Formation, Ellef Ringnes Island. *Norske Videnskaps-Akademi i Oslo, I. Matematisk-Naturvidenskapelig Klasse, Skrifter, Ny Serie*, **17**, 1–36, pls 1–7.
- Mao Shaozhi, Wu Guoxuan & Li Jie.** 2004. Oligocene–early Miocene dinoflagellate stratigraphy, Site 1148, ODP Leg 184, South China Sea. W. L. Prell, P. Wang, P. Blum, D. K. Rea & S. C. Clemens (eds) *Proceedings of the Ocean Drilling Program, Scientific Results*, **184**, 1–29.

- Mapes, R. H. & Nützel, A.** 2009. Late Palaeozoic mollusk reproduction: Cephalopod egg-laying behavior and gastropod larval palaeobiology. *Lethaia*, **42**(3), 341–356.
- Marheinecke, U.** Monographie der Dinozysten, Acritarcha und Chlorophyta des Maastrichtium von Hemmoor (Niedersachsen). *Palaeontographica, Abteilung B*, **227**(1–6), 1–173, 1–30.
- Marshall, N. G.** 1990. Campanian dinoflagellates from southeastern Australia. *Alcheringa*, **14**, 1–38.
- Marshall, P.** 1926. The Upper Cretaceous ammonites of New Zealand. *Transactions and Proceedings of the New Zealand Institute*, **56**, 129–210, 19–47 pls.
- Martinioni, D. R., Olivero, E. B., Medina, F. A. & Palamarczuk, S.** 2013. Cretaceous stratigraphy of Sierra de Beauvoir, Fuegian Andes, Argentina. *Revista de la Asociación Geológica Argentina*, **70**(1), 70–95.
- Matsumoto, T.** 1938. A biostratigraphic study on the Cretaceous deposits of the Naibuti Valley, South Karahuto. *Proceedings of the Imperial Academy*, **14**, 190–194.
- Matsumoto, T.** 1959a. Upper Cretaceous ammonites of California. Part I. *Memoirs of the Faculty of Science, Kyushu University, Series D, Geology*, **8**(4), 91–171, pls 30–45.
- Matsumoto, T.** 1959b. Upper Cretaceous ammonites of California. Part II. *Memoirs of the Faculty of Science, Kyushu University, Series D, Geology, Special Volume I*, 172 pp., 41 pls.
- Matsumoto, T.** 1960. Upper Cretaceous ammonites of California. Part III. With notes on stratigraphy of the Redding area and the Santa Ana Mountains by T. Matsumoto and W. P. Popenoe. *Kyushu University, Memoirs of the Faculty of Science, Series D, Geology, Special Volume II*, 204 pp., 1 pl.
- Matsumoto, T.** 1967. Evolution of the Nostoceratidae (Cretaceous heteromorph ammonoids). *Memoirs of the Faculty of Science, Kyushu University, Series D, Geology*, **18**(2), 331–347, 18–19 pls.
- Matsumoto, T.** 1977. Some heteromorph ammonites from the Cretaceous of Hokkaido (Studies of the Cretaceous ammonites from Hokkaido and Saghalien-XXXI). *Memoirs of the Faculty of Science, Kyushu University, Series D, Geology*, **23**(3), 303–366, pls 43–61.
- Matsumoto, T.** 1984. Ammonites from the upper Campanian of the Teshio Mountains. *Palaeontological Society of Japan, Special Papers*, **27**, 5–32, pls 1–9.
- Matsumoto, T. & Miyauchi, T.** 1984. Some ammonites from the Campanian (Upper Cretaceous) of northern Hokkaido. *Palaeontological Society of Japan, Special Papers*, **27**, 33–76, pls 10–31.

- Matthews, S. C.** 1973. Notes on open nomenclature and on synonymy lists. *Palaeontology*, **16**(4), 713–719.
- Matthissen, J. & Schreck, M.** 2015. Dinoflagellates. Pp. 189–193 in J. Harff, M. Meschede, S. Petersen & J. Thiede (eds) *Encyclopedia of Marine Geosciences*. Springer, Dordrecht.
- Matyja, B. A.** 1986. Developmental polymorphism in Oxfordian ammonoids. *Acta Geologica Polonica*, **36**(1–3), 37–67.
- May, F. E.** 1980. Dinoflagellate cysts of the Gymnodiniaceae, Peridiniaceae, and Gonyaulacaceae from the Upper Cretaceous Monmouth Group, Atlantic Highlands, New Jersey. *Palaeontographica, Abteilung B*, **172**, 10–116, 1–23.
- McGugan, A.** 1962. Upper Cretaceous foraminiferal zones, Vancouver Island, British Columbia, Canada. *Journal of the Alberta Society of Petroleum Geologists*, **10**(11), 585–592.
- McGugan, A.** 1964. Upper Cretaceous zone Foraminifera, Vancouver Island, British Columbia, Canada. *Journal of Paleontology*, **38**(5), 933–951, pls 150–152.
- McGugan, A.** 1979. Biostratigraphy and paleoecology of Upper Cretaceous (Campanian and Maestrichtian) Foraminifera from the upper Lambert, Northumberland, and Spray formations, Gulf Islands, British Columbia, Canada. *Canadian Journal of Earth Sciences*, **16**, 2263–2274.
- McGugan, A.** 1982. Upper Cretaceous (Campanian and Maestrichtian) foraminifera from the upper Lambert and Northumberland formations, Gulf Islands, British Columbia, Canada. *Micropaleontology*, **28**(4), 399–430.
- McIntyre, D. J.** 1999. Campanian to Paleocene dinoflagellate assemblages from the Turtle Mountain core hole, Manitoba, western Canada. *Canadian Journal of Earth Sciences*, **36**, 769–774.
- McLean, D. M.** 1972. *Cladopyxidium septatum*, n. gen., n. sp., possible Tertiary ancestor of the modern dinoflagellate *Cladopyxis hemibrachiata* Balech, 1964. *Journal of Paleontology*, **46**, 861–863, 1 pl.
- McLean, D. M.** 1973. Emendation and transfer of *Eisenackia* (Pyrrhophyta) from the Microdiniaceae to the Gonyaulacaceae. *Geologiska Föreningens i Stockholm Förhandlingar*, **95**, 261–265.
- McLachlan, S. M. S. & Haggart, J. W.** Reassessment of the late Campanian (Late Cretaceous) heteromorph ammonite fauna from Hornby Island, British Columbia, with implications for the taxonomy of the Diplomoceratidae and Nostoceratidae. *Journal of Systematic Palaeontology*. Accepted.

- McMinn, A.** 1993. Neogene dinoflagellate cyst biostratigraphy from Sites 815 and 823, Leg 133, Northeastern Australian Margin. Pp. 97–105 in J. A. McKenzie, P. J. Davies, A. A. Palmer-Julson, & J. F. Sarg (eds) *Proceedings of the Ocean Drilling Program, Scientific Results*, **133**.
- Meek, F. B.** 1862. Descriptions of new Cretaceous fossils collected by the North-Western Boundary Commission, on Vancouver and Sucia islands. *Proceedings of the Academy of Natural Sciences of Philadelphia*, **13**, 314–318.
- Meek, F. B.** 1876. A report on the Invertebrate Cretaceous and Tertiary fossils of the Upper Missouri Country. *United States Geological Survey of the Territories*, **9**, 629 pp., 45 pls.
- Meek, F. B. & Hayden, F. V.** 1856. Descriptions of new species of Gasteropoda and Cephalopoda from the Cretaceous formations of Nebraska Territory. *Proceedings of the Academy of Natural Sciences of Philadelphia*, **8**, 70–72.
- Meek, F. B. & Hayden, F. V.** 1857. Descriptions of new species and genera of fossils, collected by Dr. F. V. Hayden in Nebraska Territory, under the direction of Lieut. GK Warren, U. S. Topographical Engineer, with some remarks on the Tertiary and Cretaceous formations of the North-West, and the parallelism of the latter with those of other portions of the United States and Territories. *Proceedings of the Academy of Natural Sciences of Philadelphia*, **9**, 117–148.
- Mertens, K. N., Verhoeven, K., Verleye, T., Louwye, S., Amorim, A., Ribeiro, S., Deaf, A. S., Harding, I. C., De Schepper, S., González, C., Kodrans-Nsiah, M., De Vernal, A., Henry, M., Radi, T., Dybkjaer, K., Poulsen, N. E., Feist-Burkhardt, S., Chitolie, J., Heilmann-Clausen, C., Londeix, L., Turon, J.-L., Marret, F., Matthiessen, J., McCarthy, F. M. G., Prasad, V., Pospelova, V., Kyffin-Hughes, J. E., Riding, J. B., Rochon, A., Sangiorgi, F., Welters, N., Sinclair, N., Thun, C., Soliman, A., Van Nieuwenhove, N., Vink, A. & Young, M.** 2009. Determining the absolute abundance of dinoflagellate cysts in recent marine sediments: The *Lycopodium* marker-grain method put to the test. *Review of Palaeobotany and Palynology*, **157**, 238–252.
- Mertens, K. M., Price, A. M. & Pospelova, V.** 2012. Determining the absolute abundance of dinoflagellate cysts in recent marine sediments II: Further tests of the *Lycopodium* marker-grain method. *Review of Palaeobotany and Palynology*, **184**, 74–81.
- Mertens, K. M., Takano, Y., Head, M. J. & Matsuoka, K.** 2014. Living fossils in the Indo-Pacific warm pool: a refuge for thermophilic dinoflagellates during glaciations. *Geology*, **42**, 531–534.
- M’Hamdi, A., Slimani, H., Louwye, S., Soussia, M., Ismail-Lattrachea, K. B. & Ali, W. B.** 2015. Les kystes de dinoflagelles et palynofacies de la transition Maastrichtien–Danien du stratotype El kef (Tunisie). *Comptes Rendus Palevol*, **14**, 167–180.

- Michoux, D.** 1985. Palynostratigraphie de l'Éocène de Montfort-en-Chalosse (Landes, France). *Revue de Micropaléontologie*, **28**, 138–153.
- Mikhailov, N. P.** 1951. The Upper Cretaceous ammonites from the southern European part of the USSR and their importance for zonal stratigraphy (Campanian, Maastrichtian). *Trudy Instituta Geologicheskikh Nauk, Akademya Nauk SSSR*, **129**, Geology Series 50, 143 pp., 19 pls.
- Misaki, A. & Maeda, H.** 2010. Two Campanian (Late Cretaceous) nostoceratid ammonoids from the Toyajo Formation in Wakayama, southwest Japan. Pp. 223–231 in K. Tanabe, Y. Shigeta, T. Sasaki & H. Hirano (eds) *Cephalopods—Present and Past*. Tokai University Press, Tokyo.
- Mohamed, O & Wagreich, M.** 2013. Organic-walled dinoflagellate cyst biostratigraphy of the Well Höflein 6 in the Cretaceous–Paleogene Rhenodanubian Flysch Zone (Vienna Basin, Austria) *Geologica Carpathica*, **64**(3), 209–230.
- Mohamed, O., Piller, W. E. & Egger, H.** 2013. Dinoflagellate cysts and palynofacies across the Cretaceous/Palaeogene boundary at the neritic Waidach section (Eastern Alps, Austria). *Review of Palaeobotany and Palynology*, **190**, 85–103.
- Monks, N. & Young, R. J.** 1998. Body position and the functional morphology of Cretaceous heteromorph ammonites. *Paleontologia Electronica*, **1.1.1A**, 1–15.
- Moradian, F. & Allameh, M.** 2010. Palynology of the Abderaz Formation in Hamam Ghaleh in Kopet Dagh sedimentary basin. *1st International Applied Geological Congress*, Department of Geology, Islamic Azad University, Mashad Branch, Iran, 920–924.
- Morgan, R.** 1977. Elucidation of the Cretaceous dinoflagellate *Diconodinium* Eisenack and Cookson, 1960, and related peridinioid species from Australia. *Palynology*, **1**, 123–138.
- Morgenroth, P.** 1966. Mikrofossilien und Konkretionen des nordwesteuropäischen Untereozäns. *Palaeontographica, Abteilung B*, **119**(1–3), 1–53, pls 1–11.
- Morgenroth, P.** 1968. Zur Kenntnis der Dinoflagellaten und Hystrichosphaeridien des Danien. *Geologisches Jahrbuch, Hannover*, **86**, 533–578.
- Morozumi, Y.** 1985. Late Cretaceous (Campanian and Maastrichtian) ammonites from Awaji Island, southwest Japan. *Bulletin of the Osaka Museum of Natural History*, **39**, 1–58, 18 pls.
- Morton, S. G.** 1842. Description of some new species of organic remains of the Cretaceous group of the United States: with a tabular view of the fossils hitherto discovered in this formation. *Journal of the Academy of Natural Sciences of Philadelphia*, **8**, 207–227, pls 10–11.

- Mourik, C. A. van, Brinkhuis, H. & Williams, G. L.** 2001. Mid- to late Eocene organic walled dinoflagellate cysts from ODP Leg 171B, offshore Florida. Pp. 225–251 in D. Kroon, R. D. Norris & A. Klaus, A. (eds) *Western North Atlantic Palaeogene and Cretaceous Palaeoceanography*. Geological Society, London, Special Publications, **183**.
- Muller, J.** 1959. Palynology of Recent Orinoco delta and shelf sediments: reports of the Orinoco Shelf expedition. *Micropaleontology*, **5**(1), 1–32.
- Muller, J. E. & Jeletzky, J. A.** 1970. Geology of the Upper Cretaceous Nanaimo Group, Vancouver Island and Gulf Islands, British Columbia. *Geological Survey of Canada, Paper*, **69-25**, 1–77.
- Mustard, P. S.** 1994. The Upper Cretaceous Nanaimo Group, Georgia Basin. Pp. 27–95 in J. W. H. Monger (ed.) *Geology and Geological Hazards of the Vancouver Region, Southwestern British Columbia, Geological Survey of Canada Bulletin*, **481**.
- Mustard, P., Haggart, J., Katnick, D., Treptau, K. & MacEachern, J.** 2003. Sedimentology, paleontology, ichnology and sequence stratigraphy of the Upper Cretaceous Nanaimo Group submarine fan deposits, Denman and Hornby islands, British Columbia. Pp. 103–145 in J. Woodsworth (ed.) *Guidebook for Geological Field Trips in Southern British Columbia*. Geological Association of Canada, Cordilleran Section, Vancouver.
- Naidin, D. P.** 1959. Cephalopoda. Pp. 166–220, pls 1–23 in M. M. Moskvina (ed.) *Atlas of the Upper Cretaceous fauna of the northern Caucasus and Crimea*. Trudy VNIIGAZ, Moscow.
- Nesis, K. N.** 1986. On the feeding and the causes of extinction of some heteromorph ammonites. *Paleontological Journal*, **20**, 5–11.
- Niebuhr, B.** 2003. Late Campanian and early Maastrichtian ammonites from white chalk of Kronsmoor (northern Germany)—taxonomy and stratigraphy. *Acta Geologica Polonica*, **53**(4), 257–281.
- Niebuhr, B.** 2004. Late Campanian nostoceratid ammonites from the Lehrte West Syncline near Hannover, northern Germany. *Acta Geologica Polonica*, **54**(4), 473–487, 4 pls.
- Niebuhr, B., Hampton, M. J., Gallagher, L. T. & Remin, Z.** 2011. Integrated stratigraphy of the Kronsmoor section (northern Germany), and the reference point for the base of the Maastrichtian in the Boreal Realm. *Acta Geologica Polonica*, **61**(2), 193–214.
- Nøhr-Hansen, H.** 1993. Dinoflagellate cyst stratigraphy of the Barremian to Albian, Lower Cretaceous, north-east Greenland. *Grønlands Geologiske Undersøgelse, Bulletin*, **166**, 1–171.

- Núñez-Betelu, K. & Hills, L. V.** 1998. A late Coniacian ceratioid dinoflagellate cyst, *Odontochitina octopus* sp. nov., from the Kanguk Formation, Canadian Arctic. *Canadian Journal of Earth Sciences*, **35**, 923–930.
- Núñez-Betelu, L. K., Hills, L. V., Krause, F. F. & McIntyre, D. J.** 1994. Upper Cretaceous palaeoshorelines of the northeastern Sverdrup Basin, Ellesmere Island, Canadian Arctic Archipelago. In K.V. Simakov & D. K. Thurston (eds) *Proceedings of the international conference on Arctic margins, Stratigraphy and Paleogeography*, Magadan, Russia, 43–49.
- Nunnallee, D.** 1983. *Eubostrychoceras*: a genus of uncoiled Santonian ammonoids of southeastern Vancouver Island, British Columbia. Unpublished manuscript, 94 pp.
- Oboh-Ikuenobe, F. E., Yepes, O. & Gregg, J. M.** 1998. Palynostratigraphy, palynofacies and thermal Pp. 277–318 in J. Mascle, P. Clift & M. Moullade (eds) *Proceedings of the Ocean Drilling Program, Scientific Results*, **159**.
- Odin, G. S.** 2001. The Campanian-Maastrichtian stage boundary: characterization at Tercis (Landes, SW France). Pp. 785–804 in G. S. Odin (ed.) *The Campanian-Maastrichtian stage boundary, characterization at Tercis les Bains (France) and correlation with Europe and other continents. Developments in Palaeontology and Stratigraphy*, **19**.
- Odin, G. S.** 2010. Traces de volcanisme explosif dans le Campanien pyrénéen aux alentours du stratotype de limite Campanien–Maastrichtien à Tercis (SO France, N Espagne). Repérage biostratigraphique avec une étude particulière du foraminifère *Radotruncana calcarata*. *Carnets de Géologie*, 2010/02, 1–35.
- Odin, G. S. & Lamaurelle, M. A.** 2001. The *global Campanian-Maastrichtian stage boundary. Episodes*, **24**(4), 229–238.
- Odin, G., Courville, P., Machalski, M. & Cobban, W. A.** 2001. The Campanian-Maastrichtian ammonite fauna from Tercis (Landes, France); a synthetic view. Pp. 550–567 in G.S. Odin (ed.) *The Campanian-Maastrichtian Boundary. Characterisation at Tercis les Bains (France) and Correlation with Europe and other Continents. Developments in Palaeontology and Stratigraphy 19*. Elsevier, Amsterdam.
- Odin, G. S, Hancock, J. M., Antonescu, E., Bonnemaïson, M., Caron, M., Cobban, W. A., Dhondt, A. V., Gaspard, D., Ion, J., Jagt, J. W. M., Kennedy, W. J., Melinte, M., Néraudeau, D., von Salis, K., Ward, P. D.** 1996. Definition of a global boundary stratotype section and point for the Campanian/Maastrichtian boundary. *Bulletin de l'Institut Royal des Sciences Naturelles de Belgique*, **66**, 111–117.
- Ogg, J. G., Hinnov, L.A., & Huang, C.** 2012. Chapter 27: Cretaceous. Pp. 793–853 in F. M. Gradstein, J. G. Ogg, M. D. Schmitz & G. M. Ogg (eds) *The Geologic Time Scale 2012*. Elsevier, Amsterdam.

- Ogg, J. G., Ogg, G. M. & Gradstein, F. M.** 2016. Cretaceous. Pp. 167–186 in J. G. Ogg, G. M. Ogg & F. M. Gradstein (eds) *A Concise Geologic Time Scale 2016*. Elsevier, Amsterdam.
- Okada, H.** 1997. High sedimentation rates vs. high sea-level during the Cretaceous. *Memoirs of the Geological Society of Japan*, **48**, 1–6.
- Okamoto, T.** 1988a. Changes in life orientation during the ontogeny of some heteromorph ammonoids. *Palaeontology*, **31**(2), 281–294.
- Okamoto, T.** 1988b. Developmental regulation and morphological saltation in the heteromorph ammonite *Nipponites*. *Paleobiology*, **14**(3), 272–286.
- Okamoto, T.** 1989. Comparative morphology of *Nipponites* and *Eubostrychoceras* Cretaceous nostoceratids. *Transactions and Proceedings of the Palaeontological Society of Japan, New Series*, **154**, 117–139.
- Okamoto, T.** 1996. Theoretical Modeling of Ammonoid Morphology. P. 225–249 in Landman, N. H., Tanabe, K. & Davis, R. A. (eds) *Ammonoid Paleobiology, Topics in Geobiology*, **13**. Plenum Press, New York.
- Okamoto, T. & Shibata, M.** 1997. A cyclic mode of shell growth and its implications in a Late Cretaceous heteromorph ammonoid *Polyptychoceras pseudogaultinum* (Yokoyama). *Paleontological Research*, **1**(1), 29–45.
- Olivero, E. B. & Zinsmeister, W. J.** 1989. Large heteromorph ammonites from the Upper Cretaceous of Seymour Island, Antarctica. *Journal of Paleontology*, **63**(5), 626–636.
- Olivero, E. B., Medina, F. A. & López, M. I.** 2009. The stratigraphy of Cretaceous mudstones in the eastern Fuegian Andes: new data from body and trace fossils. *Revista de la Asociación Geológica Argentina*, **64**(1), 60–69.
- Oloto I. N.** 1989. Maastrichtian dinoflagellate cyst assemblage from the Nkporo shale on the Benien Flank of the Niger Delta. *Review of Palaeobotany and Palynology*, **57**, 173–186.
- Olsson, R. K.** 1963. Latest Cretaceous and earliest Tertiary stratigraphy of New Jersey coastal plain. *American Association of Petroleum Geologists, Bulletin*, **47**(4), 643–665.
- Packard, A.** 1972. Cephalopods and fish: the limits of convergence. *Biological Reviews*, **47**, 241–307.
- Pascher, A.** 1914. Über Flagellaten und Algen. *Deutsche Botanische Gesellschaft, Berichte*, **32**, 136–160.
- Pasternak, S. I.** 1954. *Ancyloceras bipunctatum* Schluter iz Maastrichta Volino-Pdolskoi pliti. *L'vovskoye Geologicheskoye Obshchestvo Geologicheskii Sbornik*, **1**, 157–169.

- Pavlishina, P.** 1995. Maestrichtian dinoflagellate cysts from North Bulgaria: Taxonomy biostratigraphical and palaeoenvironmental interpretations. *Geologica Balcanica*, **25**(3), 125–143.
- Pearce, M. A.** in T. H. Donders *Advanced Course in Jurassic–Cretaceous–Cenozoic Organic-Walled Dinoflagellate Cysts: Morphology, Paleocology and Stratigraphy*. Unpublished data. Dinocourse 2012, LPP Foundation and TNO, Utrecht, Netherlands.
- Peyrot, D.** 2011. Late Cretaceous (late Cenomanian–early Turonian) dinoflagellate cysts from the Castilian Platform, northern Spain. *Palynology*, **35**(2), 267–300.
- Piasecki, S.** 1980. Dinoflagellate cyst stratigraphy of the Miocene Hodde and Gram Formations, Denmark. *Geological Society of Denmark, Bulletin*, **29**, 53–76.
- Pons, J. M., Vicens, E., Martínez, R., García-Barrera, P., Nieto, I.-E. & Avendaño-Gil, M. J.** 2016. The Campanian–Maestrichtian rudist bivalve succession in the Chiapas Central Depression, Mexico. *Cretaceous Research*, **60**, 210–220.
- Pospelova, V., Chmura, G. L. & Walter, H. A.** 2004. Environmental factors influencing the spatial distribution of dinoflagellate cyst assemblages in shallow lagoons of southern New England (USA). *Review of Palaeobotany and Palynology*, **128**, 7–34.
- Pospelova, V., Chmura, G. L., Boothman, W. & Latimer, J. S.** 2005. Spatial distribution of modern dinoflagellate cysts in polluted estuarine sediments from Buzzards Bay (Massachusetts, USA) embayments. *Marine Ecology Progress Series*, **292**, 23–40.
- Pospelova, V., de Vernal, A. & Pedersen, T. F.** 2008. Distribution of dinoflagellate cysts in surface sediments from the northeastern Pacific Ocean (43–25°N) in relation to sea-surface temperature, salinity, productivity and coastal upwelling. *Marine Micropaleontology*, **68**, 21–48.
- Pospelova, V., Esenkulova, S., Johannessen, S. C., O'Brien, M. C. & Macdonald, R. W.** 2010. Organic-walled dinoflagellate cyst production, composition and flux from 1996 to 1998 in the central Strait of Georgia (BC, Canada): A sediment trap study. *Marine Micropaleontology*, **75**, 17–37.
- Powell, A. J., Lewis, J. & Dodge, J. D.** 1992. The palynological expressions of post-Palaeogene upwelling: a review. Pp. 215–226 in C. P. Summerhayes, W. L. Prell & K.-C. Emeis (eds) *Upwelling Systems: Evolution Since the Early Miocene*. Geological Society, London, Special Publications, **64**.
- Powell, A. J., Brinkhuis, H. & Bujak, J. P.** 1996. Upper Paleocene–Lower Eocene dinoflagellate cyst sequence biostratigraphy of southeast England. Pp. 145–183 in R. W. O'Brien, R. M. Corfield & R. E. Dunay (eds), *Correlation of the Early Paleogene in Northwest Europe*, Geological Society, London, Special Publications, **101**.

- Prince, I. M., Jarvis, I. & Tocher, B. A.** 1999. High-resolution dinoflagellate cyst biostratigraphy of the Santonian–basal Campanian (Upper Cretaceous): new data from Whitecliff, Isle of Wight, England. *Review of Palaeobotany and Palynology*, **105**, 143–169.
- Pross, J. & Brinkhuis, H.** 2005. Organic-walled dinoflagellate cysts as paleoenvironmental indicators in the Paleogene; a synopsis of concepts. *Paläontologische Zeitschrift*, **79**(1), 53–59.
- Puckett, T. M.** 1991. Absolute paleobathymetry of Upper Cretaceous chalks based on ostracodes-evidence from the Demopolis Chalk (Campanian and Maastrichtian) of the northern Gulf Coastal Plain. *Geology*, **19**(5), 449–452.
- Quattrocchio, M. E. & Sarjeant, W. A. S.** 2003. Dinoflagellates from the Chorrillo Chico Formation (Paleocene) of southern Chile. *Ameghiniana*, **40**(2), 129–153.
- Raub, T. D., Kirschvink, J. L. & Ward, P. D.** 1998. New paleomagnetic results from the Nanaimo Group, British Columbia: additional localities for testing the Baja-British Columbia Hypothesis. *Eos (Transactions, American Geophysical Union)*, **79**(45), supplement, 223.
- Rauscher, R. & Doubinger, J.** 1982. Les dinokystes du Maestrichtien phosphaté au Maroc. *Sciences Géologiques, Bulletin*, **35**(3), 97–116.
- Remin, Z.** 2011. *Diplomoceras maximum* and *D. cylindraceum*; the giant Upper Cretaceous heteromorph ammonites and their stratigraphic significance. *Geological Society of America, Abstracts with Programs*, **43**(5), 640.
- Remin, Z., Machalski, M. & Jagt, J. W. M.** 2015. The stratigraphically earliest record of *Diplomoceras cylindraceum* (heteromorph ammonite)—implications for Campanian/Maastrichtian boundary definition. *Geological Quarterly*, **59**(4), 843–848.
- Reyment, R. R.** 1954. Notes on fossils from the northern and eastern regions. *Annual Report of the Geological Survey of Nigeria*, **1952-53**, 20–22.
- Reyment, R. R.** 1955. The *Cretaceous Ammonoidea of southern Nigeria* and the southern Cameroons. *Geological Survey of Nigeria, Bulletin*, **25**, 1–112.
- Riding, J. B. & Fensome, R. A.** 2002. A review of *Scriniodinium* Klement 1957, *Endoscrinium* (Klement 1960) Vozzhennikova 1967 and related dinoflagellate cyst taxa. *Palynology*, **26**, 5–33.
- Riding, J. B. & Kyffin-Hughes, J. E.** 2004. A review of the laboratory preparation of palynomorphs with a description of an effective non-acid technique. *Revista Brasileira de Paleontologia*, **7**(1), 13–44.

- Rochon, A., de Vernal, A., Turon, J. L., Matthiessen, J. & Head, M. J.** 1999. Distribution of recent dinoflagellate cysts in surface sediments from the North Atlantic Ocean and adjacent seas in relation to sea-surface parameters. *American Association of Stratigraphic Palynologists, Contribution Series*, **35**, 152 pp.
- Roemer, F. A.** 1841. Die Versteinerungen des norddeutschen Kreidegebirges. Hahn'sche Hofbuchhandlung, Hannover, 145 pp.
- Roncaglia, L. & Corradini, D.** 1997. Correlation of key dinoflagellate events with calcareous nannoplankton and planktonic foraminiferal zones in the Solignano Formation (Maastrichtian, Late Cretaceous) northern Apennines, Italy. *Review of Palaeobotany and Palynology*, **97**, 177–196.
- Roncaglia, L., Field, B. D., Raine, J. I., Schiøler, P. & Wilson, G. J.** 1999. Dinoflagellate biostratigraphy of Piripauan–Haumurian (Upper Cretaceous) sections from northeast South Island, New Zealand. *Cretaceous Research*, **20**, 271–314.
- Rossignol, M.** 1964. Hystrichosphères du Quaternaire en Méditerranée orientale, dans les sédiments Pléistocènes et les boues marines actuelles. *Revue de micropaléontologie*, **7**(2), 83–99, pls 1–3.
- Rouse, G. E.** 1957. The application of a new nomenclatural approach to the Upper Cretaceous plant microfossils from western Canada. *Canadian Journal of Botany*, **35**, 349–375.
- Rouse, G. E., Hopkins, W. S., Jr. & Piel, K. M.** 1970. Palynology of some Late Cretaceous and Early Tertiary deposits in British Columbia and adjacent Alberta. Pp. 213–246 in R. M. Kosanke & A. T. Cross (eds) *Symposium on Palynology of the Late Cretaceous and Early Tertiary, Geological Society of America Special Paper*, **127**.
- Sarjeant, W. A. S.** 1970. The genus *Spiniferites* Mantell, 1850 (Dinophyceae). *Grana*, **10**, 74–78.
- Sarjeant, W. A. S.** 1974. Fossil and living dinoflagellates. Academic Press, London, 182 pp.
- Sarjeant, W. A. S.** 1982. The dinoflagellate cysts of the *Gonyaulacysta* group: a morphological and taxonomic restudy. *American Association of Stratigraphic Palynologists, Contributions Series*, **9**, 81 pp.
- Sarjeant, W. A. S.** 1984. A restudy of some dinoflagellate cysts and an acritarch from the Malm (Upper Jurassic) of southwest Germany. *Palaeontographica, Abteilung B*, **191**(5–6), 154–177, pls 1–4.
- Sarjeant, W. A. S.** 1985. A restudy of some dinoflagellate cyst holotypes in the University of Kiel collections: VI. Late Cretaceous dinoflagellate cysts and other palynomorphs in the Otto Wetzel collection. *Meyniana*, **37**, 129–185.

- Saunders, W. B. & Spinosa, C.** 1979. Nautilus movement and distribution in Palau, Western Caroline Islands. *Science*, **204**(4398), 1199–1201.
- Scheiner, S. M.** 1993. Genetics and evolution of phenotypic plasticity. *Annual Review of Ecology and Systematics*, **24**, 35–68.
- Schiller, J.** 1937. Dinoflagellate (Peridineae). Pp. 1–590 in R. Kolkwitz (ed) *Dr. L. Rabenhorst's Kryptogamen-Flora of Deutschland, Österreich und der Schweiz*, **10**(3), Part 2.
- Schiøler, P. & Wilson, G. J.** 1993. Maastrichtian dinoflagellate zonation in the Dan Field, Danish North Sea. *Review of Palaeobotany and Palynology*, **78**(3–4), 321–351.
- Schiøler, P. & Wilson, G. J.** 2001. C2b. Dinoflagellate biostratigraphy around the Campanian-Maastrichtian boundary at Tercis les Bains, southwest France. Pp. 221–234 in G. S. Odin (ed) *The Campanian-Maastrichtian stage boundary, characterization at Tercis les Bains (France) and correlation with Europe and other continents. Developments in Palaeontology and Stratigraphy*, **19**.
- Schiøler, P., Brinkhuis, H., Roncaglia, L. & Wilson, G. J.** 1997. Dinoflagellate biostratigraphy and sequence stratigraphy of the type Maastrichtien (Upper Cretaceous), Enci Quarry, The Netherlands. *Marine Micropaleontology*, **31**, 65–95.
- Schlüter, C.** 1872. Cephalopoden der oberen deutschen Kreide. *Palaeontographica*, **21**, 25–120, pls 9–35.
- Schnoor, D.** 2013. Funde unserer Mitglieder: *Diplomoceras cylindraceum* (Defrance 1816) aus Kronsmoor. *Arbeitskreis Paläontologie Hannover*, **41**(2), 65.
- Schreck, M & Mattheissen, J.** 2013. Batiacasphaera micropapillata: Palaeobiogeographic distribution and palaeoecological implications of a critical Neogene species complex. Pp. 301–314 in J. M. Lewis, F. Marret & L. Bradley (eds) *Biological and Geological Perspectives of Dinoflagellates. The Micropalaeontological Society, Special Publications*. Geological Society, London.
- Schwendemann, A. B., Wang, G., Mertz, M. L., McWilliams, R. T., Thatcher, S. L. & Osborn, J. M.** 2007. Aerodynamics of saccate pollen and its implications for wind pollination. *American Journal of Botany*, **94**(8), 1371–1381.
- Shcherbinina, E., Gavrilov, Y., Iakovleva, A., Pokrovsky, B., Golovanova, O. & Aleksandrova, G.** 2016. Environmental dynamics during the Paleocene–Eocene thermal maximum (PETM) in the northeastern Peri-Tethys revealed by high-resolution micropalaeontological and geochemical studies of a Caucasian key section. *Palaeogeography, Palaeoclimatology, Palaeoecology*, **456**, 60–81.

- Scott, G. R. & Cobban, W. A.** 1965. Geologic and biostratigraphic map of the Pierre Shale between Jarre Creek and Loveland, Colorado. *U.S. Geological Survey, Miscellaneous Geological Investigations Series*, Map I-439, 1:48,000 scale, separate text, 1–4.
- Shigeta, Y.** 1993. Post-hatching and early life history of Cretaceous ammonoidea. *Lethaia*, **26**, 133–145.
- Shigeta, Y.** 2014. *Morewites*, a new Campanian (Late Cretaceous) heteromorph ammonoid genus from Hokkaido, Japan. *Paleontological Research*, **18**(1), 1–5.
- Shigeta, Y. & Nishimura, T.** 2013. A new species of the heteromorph ammonite *Phylloptychoceras* from the lowest Maastrichtian of Hokkaido, Japan. *Paleontological Research*, **17**(2), 173–178.
- Shigeta, Y., Nishimura, T. & Nifuku, K.** 2015. Middle and late Maastrichtian (latest Cretaceous) ammonoids from the Akkeshi Bay area, eastern Hokkaido, northern Japan and their biostratigraphic implications. *Paleontological Research*, **19**(2), 107–127.
- Shigeta, Y., Izukura, M., Nishimura, T. & Tsutsumi, Y.** 2016. Middle and Late Campanian (Late Cretaceous) Ammonoids from the Urakawa Area, Hokkaido, Northern Japan. *Paleontological Research*, **20**(4), 322–366.
- Shimizu, S.** 1929. Cretaceous deposits of North and South Saghalin; a comparison. *Saito Ho-on Kai, Annual Report of the Work*, **5**, 30–43.
- Shumard, B. F.** 1861. Descriptions of new Cretaceous fossils from Texas. *Proceedings of the Boston Society of Natural History*, **8**, 188–205.
- Slimani, H.** 1994. Les dinokystes des craies du Campanien au Danien à Halebay, Turnhout (Belgique) et à Beutenaken (Pays-Bas). *Mémoires pour servir à l'explication des cartes géologiques et minières de la Belgique*, **37**, 1–173.
- Slimani, H.** 1995. *Les dinokystes des craies du Campanien au Danien à Halebay et Turnhout (Belgique) et à Beutenaken (Pays-Bas): Biostratigraphie et systématique*. Ph.D. Thesis, Laboratorium voor Paleontologie, Rijksuniversiteit Ghent, 461 pp.
- Slimani, H.** 2000. Nouvelle zonation aux kystes de dinoflagellés du Campanien au Danien dans le nord et l'est de la Belgique et dans le sud-est des Pays-Bas. *Memoirs of the Geological Survey of Belgium*, **46**, 1–88.
- Slimani, H.** 2001. Les kystes de dinoflagellés du Campanien au Danien dans la région de Maastricht (Belgique, Pays-Bas) et de Turnhout (Belgique): biozonation et corrélation avec d'autres régions en Europe occidentale. *Geologica et Palaeontologica*, **35**, 161–201.

- Slimani, H.** 2003. A new genus and two new species of dinoflagellate cysts from the Upper Cretaceous of the Maastrichtian type area and Turnhout (northern Belgium). *Review of Palaeobotany and Palynology*, **126**, 267–277.
- Slimani, H., Louwye, S. & Toufiq, A.** 2010. Dinoflagellate cysts from the Cretaceous–Paleogene boundary at Ouled Haddou, southeastern Rif, Morocco: biostratigraphy, paleoenvironments and paleobiogeography. *Palynology*, **34**(1), 90–124.
- Slimani, H. & Louwye, S.** 2011. New dinoflagellate cysts of the *Microdinium* and *Phanerodinium* complexes (Evitt) from the Upper Cretaceous–Lower Paleogene Chalk Group in the Meer borehole, northern Belgium. *Review of Palaeobotany and Palynology*, **168**, 41–50.
- Slimani, H., Louwye, S., Duser, M. & Lagrou, D.** 2011. Connecting the Chalk Group of the Campine Basin to the dinoflagellate cyst biostratigraphy of the Campanian to Danian in the Meer borehole (northern Belgium). Pp. 129–164 in J. W. M. Jagt, E. A. Jagt-Yazykova & W. J. H. (eds) *A tribute to the late Felder brothers – pioneers of Limburg geology and prehistoric archaeology*. *Netherlands Journal of Geosciences*, **90** (2–3).
- Slimani, H., Louwye, S. & Toufiq, A.** 2012. New species of organic-walled dinoflagellate cysts from the Maastrichtian–Danian boundary interval at Ouled Haddou, northern Morocco. *Alcheringa*, **36**, 337–353.
- Slimani, H., Guédé, K. É., Williams, G. L., Asebriy, L. & Ahmamou, M.** 2016. Campanian to Eocene dinoflagellate cyst biostratigraphy from the Tahar and Sekada sections at Arba Ayacha, western External Rif, Morocco. *Review of Palaeobotany and Palynology*, **228**, 26–46.
- Sliter, W. V.** 1973. Upper Cretaceous foraminifers from the Vancouver Island area, British Columbia, Canada. *Journal of Foraminiferal Research*, **3**(4), 167–186.
- Sluijs, A., Pross, J. & Brinkhuis H.** 2005. From greenhouse to icehouse; organic-walled dinoflagellate cysts as paleoenvironmental indicators in the Paleogene. *Earth-Science Reviews*, **68**, 281–315.
- Sluijs, A. & Brinkhuis, H.** 2009. A dynamic climate and ecosystem state during the Paleocene–Eocene Thermal Maximum: inferences from dinoflagellate cyst assemblages on the New Jersey Shelf. *Biogeosciences*, **6**, 1755–1781.
- Sluijs, A., Brinkhuis, H., Crouch, E. M., John, C., Handley, L., Munsterman, D., Bohaty, S. M., Zachos, J. C., Reichert, G. -J., Schouten, S., Pancost, R. D., Damsté, J. S. S., Welters, N. L. D., Lotter, A. F. & Dickens, G. R.** 2008. Eustatic variations during the Paleocene–Eocene greenhouse world. *Paleoceanography*, **23**, PA4216.

- Smith, S. W.** 1992. Microplankton from the Cape Lamb Member, López de Bertodano Formation (Upper Cretaceous) Cape Lamb, Vega Island. *Antarctic Science*, **4**(3), 337–353.
- Snape, M. G.** 1992. Dinoflagellate cysts from an allochthonous block of Nordenskjöld Formation (Upper Jurassic), northwest James Ross Island. *Antarctic Science*, **4**(3), 267–278.
- Sobral, A. C. S., Zucon, M. H. & Barreto, A. M. F.** 2010. Amonóides da Bacia de Pernambuco-Paraíba, NE, Brasil. *Estudos Geológicos*, **20**(1), 27–46.
- Sobral, A. C. S.** 2011. *Os amonóides da Bacia da Paraíba: implicações cronoestratigráficas, paleoecológicas e paleobiogeográficas*. M.Sc. thesis, Federal University of Pernambuco, Recife, Brasil, 74 pp., 9 pls.
- Sohl, N. F.** 1985. An overview of the use of mollusks in biostratigraphy. Pp. 248–257 in T. W. Broadhead (ed.) *Molluscs, Notes for a Short Course*. Department of Geological Sciences, University of Tennessee, Studies in Geology, **13**.
- Song Zhichen, He Chengquan, Quian Zeshu, Pan Zhaoren, Zheng Guoguang & Zheng Yuefang.** 1978. *On the Paleogene dinoflagellates and acritarchs from the coastal region of Bohai*. Science Press, Beijing, 190 pp.
- Srivastava, S. K.** 1981. Evolution of Upper Cretaceous phytogeoprovinces and their pollen flora. *Review of Palaeobotany and Palynology*, **35**, 155–173.
- Srivastava, S. K.** 1994. Evolution of Cretaceous phytogeoprovinces, continents and climate. *Review of Paleobotany and Palynology*, **82**, 197–224.
- Spath, L. F.** 1921. On Cretaceous Cephalopoda from Zululand. *Annals of the South African Museum*, **12**(7), 217–321, pls 19–26.
- Spath, L. F.** 1925. On Senonian Ammonoidea from Jamaica. *Geological Magazine*, **62**, 28–32, 1 pl.
- Spath, L. F.** 1926. On new ammonites from the English Chalk. *Geological Magazine*, **63**(2), 77–83.
- Spath, L. F.** 1953. The Upper Cretaceous cephalopod fauna of Graham Land. *Falkland Islands Dependencies Survey, Scientific Reports*, **3**, 1–60, 13 pls.
- Stanley, E. A.** 1965. Upper Cretaceous and Paleocene plant microfossils and Paleocene dinoflagellates and hystrichosphaerids from northwestern South Dakota. *Bulletin of American Paleontology*, **49**(222), 179–384, pls 19–49.

- Stephen, D. A., Bylund, K. G., Garcia, P., McShinsky, R. D. & Carter, H. J.** 2012. Taphonomy of dense concentrations of juvenile ammonoids in the Upper Cretaceous Mancos Shale, east-central Utah, USA. *Geobios*, **45**(1), 121–128.
- Stephenson, L. W.** 1941. The larger invertebrate fossils of the Navarro Group of Texas (exclusive of corals and crustaceans and exclusive of the fauna of the Escondido Formation). *University of Texas Publication*, **4101**, 641 pp.
- Stinnesbeck, W., Ifrim, C. & Salazar, C.** 2012. The last Cretaceous ammonites in Latin America. *Acta Palaeontologica Polonica*, **57**(4), 717–728.
- Stinnesbeck, W., Frey, E. & Zell, P.** 2016. Evidence for semi-sessile early juvenile life history in Cretaceous ammonites. *Palaeogeography, Palaeoclimatology, Palaeoecology*, **457**, 186–194.
- Stover, L. E.** 1977. Oligocene and Early Miocene dinoflagellates from Atlantic Corehole 5/5B, Blake Plateau. *American Association of Stratigraphic Palynologists, Contributions Series*, **5A**, 66–89.
- Stover, L. E. & Evitt, W. R.** 1978. Analyses of pre-Pleistocene organic-walled dinoflagellates. *Stanford University Publications, Geological Sciences*, **15**. 1–300.
- Stover, L. E. & Hardenbol, J.** 1994. Dinoflagellates and depositional sequences in the Lower Oligocene (Rupelian) Boom Clay Formation, Belgium. *Bulletin Société belge de géologie*, **102**(1–2), 5–77.
- Stover, L. E. & Helby, R.** 1987. Some Australian Mesozoic microplankton index species. Pp. 101–134 in P. A. Jell (ed.) Studies in Australian Mesozoic palynology. *Memoir of the Association of Australasian Palaeontologists*, **4**.
- Stover, L. E. & Williams, G. L.** 1995. A revision of the Paleogene dinoflagellate genera *Areosphaeridium* Eaton 1971 and *Eatonicysta* Stover and Evitt 1978. *Micropaleontology*, **41**(2), 97–141.
- Stover, L. E., Brinkhuis, H., Damassa, S. P., de Verteuil, L., Helby, R. J., Monteil, E., Partridge, A., Powell, A. J., Riding, J. B., Smelror, M. & Williams, G. L.** 1996. Mesozoic–Tertiary dinoflagellates, acritarchs and prasinophytes. Pp. 641–750 in J. Jansonius & D. C. McGregor (eds) *Palynology: Principles and Applications*. American Association of Stratigraphic Palynologists Foundation, Dallas.
- Summesberger, H. & Kennedy, W. J.** 2004. More ammonites (Puzosiinae, Pachydiscidae, Placenticeratidae, Nostoceratidae, Diplomoceratidae) from the Campanian (Late Cretaceous) of the Gschlifgraben (Ultrahelvetic Nappe; Austria). *Annalen des Naturhistorischen Museums in Wien*, **106A**, 167–211.

- Summesberger, H., Machalski, M. & Wagreich, M.** 2007. First record of the late Campanian heteromorph ammonite *Nostoceras hyatti* from the Alpine Cretaceous (Grünbach, Gosau Group, Lower Austria). *Acta Geologica Polonica*, **57**(4), 443–51.
- Summesberger, H., Wagreich, M. & Bryda, G.** 2009. Upper Maastrichtian cephalopods and the correlation to calcareous nannoplankton and planktic foraminifera zones in the Gams Basin (Gosau Group; Styria, Austria). *Annalen des Naturhistorischen Museums in Wien. Serie A für Mineralogie und Petrographie, Geologie und Paläontologie, Anthropologie und Prähistorie*, **111**, 159–178, 180–181.
- Sun Xeukun.** 1994. Paleogene dinoflagellate cysts from the Liaohe Depression, northeast China. *Palynology*, **18**, 67–86.
- Surlyk, F., Rasmussen, S. L., Boussaha, M., Schiøler, P., Schovsbo, N. H., Sheldon, E., Stemmerik, L. & Thibault, N.** 2013. Upper Campanian–Maastrichtian holostratigraphy of the eastern Danish Basin. *Cretaceous Research*, **46**, 232–256.
- Tabără, D. T. & Slimani, H.** 2017. Dinoflagellate cysts and palynofacies across the Cretaceous–Paleogene boundary interval of the Vrancea Nappe (Eastern Carpathians, Romania). *Geological Quarterly*, **61**(1), 39–52.
- Tabără, D. T., Slimani, H., Mare, S. & Chira, C. M.** 2017. Integrated biostratigraphy and palaeoenvironmental interpretation of the Upper Cretaceous to Paleocene succession in the northern Moldavidian Domain (Eastern Carpathians, Romania). *Cretaceous Research*, **77**, 102–123.
- Takahashi, K. & Shimono, H.** 1982. Maastrichtian microflora of the Miyadani-gawa Formation in the Hida District, Central Japan. *Bulletin of the Faculty of Liberal Arts, Nagasaki University, Natural Science*, **22**(2), 11–118.
- Tanabe, K.** 1979. Palaeoecological analysis of ammonoid assemblages in the Turonian *Scaphites* facies of Hokkaido, Japan. *Palaeontology*, **22**(3), 609–630.
- Tanabe, K., Obata, I. & Futakami, M.** 1981. Early shell morphology in some Upper Cretaceous heteromorph ammonites. *Transactions and Proceedings of the Palaeontological Society of Japan, New Series*, **124**, 215–234, pls 35–38.
- Tanabe, K., Landman, N. H., Mapes, R. H. & Faulkner, C. J.** 1993. Analysis of a Carboniferous embryonic ammonoid assemblage from Kansas, U.S.A. Implications for ammonoid embryology. *Lethaia*, **26**(3), 215–224.
- Trueman, A. E.** 1941. The ammonite body chamber, with special reference to the buoyancy and mode of life of the living ammonite. *Quarterly Journal of the Geological Society of London*, **96**, 339–383.

- Tschudy, R. H.** 1981. Geographic distribution and dispersal of Normapolles genera in North America. *Review of Paleobotany and Palynology*, **35**, 283–314.
- Tsujita, C. J. & Westermann, G. E. G.** 1998. Ammonoid habitats and habits in the Western Interior Seaway: a case study from the Upper Cretaceous Bearpaw Formation of southern Alberta, Canada. *Palaeogeography, Palaeoclimatology, Palaeoecology*, **144**, 135–160.
- Tuomey, M.** 1854. Description of some fossils, from the Cretaceous rocks of the southern states. *Proceedings of the Academy of Natural Sciences, Philadelphia*, **7**(5), 167–172.
- Tzankov, C.V.** 1982. Cephalopoda (Nautiloidea, Ammonoidea) et Echinodermata (Echinoidea). Pp. 1–136 in *Les Fossiles de Bulgarie, Va. Crétacé Supérieur*. Académie Bulgare des Sciences, Sofia.
- Usher, J. L.** 1952. Ammonite faunas of the Upper Cretaceous rocks of Vancouver Island, British Columbia. *Geological Survey of Canada, Bulletin*, **21**, 182 pp.
- Valencia-Giraldo, Y.P., Escobar-Arenas, L.C., Mendoza-Ramírez, J., Delgado-Sierra, D. & Cárdenas-Rozo, A.L.** 2016. Revisión de las localidades fosilíferas del departamento de Antioquia, Colombia. *Boletín de Ciencias de la Tierra*, **40**, 46–54.
- Vellekoop, J., Smit, J., van de Schootbrugge, B., Weijers, J. W. H., Galeotti, S., Sinningh-Damsté, J. S. & Brinkhuis, H.** 2015. Palynological evidence for prolonged cooling along the Tunisian continental shelf following the K–Pg boundary impact. *Palaeogeography, Palaeoclimatology, Palaeoecology*, **426**, 216–228.
- Voight, S. & Weise, F.** 2000. Evidence for Late Cretaceous (Late Turonian) climate cooling from oxygen-isotope variation and palaeobiogeographic changes in Western and Central Europe. *Journal of the Geological Society*, **157**, 737–743.
- Voronina, E., Polyak, L., de Vernal, A. & Peyron, O.** 2001. Holocene variations of sea-surface conditions in the southeastern Barents Sea, reconstructed from dinoflagellate cyst assemblages. *Journal of Quaternary Science*, **16**(7), 717–726.
- Vozzhennikova, T. F.** 1963. Klass Peridineae (Dinoflagellateae). Peridinei, ili dinoflagellaty. In A. Kiselev (ed.) *Tip Pyrrophyta. Pirrofitovye Vodorosli* in V. A. Vakhrameeva, G. P. Radchenko & A. L. Tachmadzhana (eds) *Tip Pyrrophyta. Pirrofitovye Vodorosli. Vodorosli, Mochoobraznie, Psilofitovie, Plaonovidnie, Chlenistostebelnie, Paporotniki*; in A. Orlov (ed.). *Osnovy Paleontologii*, **14**, 171–186.
- Vozzhennikova, T. F.** 1967. *Iskopaemye peridinei Yurskikh, Melovykyh i Paleogenovykh otlozheniy SSSR*. Izdatelstvo Nauka, Moskow, 347 pp., 121 pls. [Translation Lees and Sarjeant, 1971].
- Wade, B. S., Houben, A. J. P., Quaijtaal, W., Schouten, S., Rosenthal, Y., Miller, K. G., Katz, M. E., Wright, J. D. & Brinkhuis, H.** 2012. Multiproxy record of abrupt sea-

- surface cooling across the Eocene–Oligocene transition in the Gulf of Mexico. *Geology*, **40**(2), 159–162.
- Wahl, W. R.** 2011. A new species of the heteromorph ammonite *Eubostrychoceras* from the Upper Cretaceous Frontier Formation, Natrona County, Wyoming. *Geological Society of America, Rocky Mountain / Cordilleran Section combined meeting, Abstracts with Programs*, **43**(4), 13.
- Wall, D.** 1967. Fossil microplankton in deep-sea cores from the Caribbean Sea. *Palaeontology*, **10**(1), 95–123, pls 14–16.
- Wall, D., Dale, B., Lohmann, G. P. & Smith, W. K.** 1977. The environmental and climatic distribution of dinoflagellate cysts in modern marine sediments from regions in the North and South Atlantic Oceans and adjacent seas. *Marine Micropaleontology*, **2**, 121–200.
- Wall, D. & Dale, B.** 1968. Early Pleistocene dinoflagellates from the Royal Society Borehole at Ludham, Norfolk. *New Phytologist*, **67**, 315–326, 1 pl.
- Wall, D. & Evitt, W. R.** 1975. A comparison of the modern genus *Ceratium* Schrank, 1793, with certain Cretaceous marine dinoflagellates. *Micropaleontology*, **21**(1), 14–44.
- Wang, S. C. & Marshall, C. R.** 2004. Improved confidence intervals for estimating the position of a mass extinction boundary. *Paleobiology*, **30**, 5–18.
- Ward, P. D.** 1976a. *Stratigraphy, paleoecology and functional morphology of heteromorph ammonites of the Upper Cretaceous Nanaimo Group, British Columbia and Washington*. Unpublished Ph.D. thesis, McMaster University, Hamilton, Ontario, 194 pp.
- Ward, P. D.** 1976b. Upper Cretaceous ammonites (Santonian–Campanian) from Orcas Island, Washington. *Journal of Paleontology*, **50**(3), 454–461.
- Ward, P. D.** 1978a. Revisions to the stratigraphy and biochronology of the Upper Cretaceous Nanaimo Group, British Columbia and Washington State. *Canadian Journal of Earth Sciences*, **15**(3), 405–423.
- Ward, P. D.** 1978b. Baculitids from the Santonian–Maestrichtian Nanaimo Group, British Columbia, Canada and Washington State, USA. *Journal of Paleontology*, **52**(5), 1143–1154.
- Ward, P. D.** 1979. Functional morphology of Cretaceous helically-coiled ammonite shells. *Paleobiology*, **5**(4), 415–422.
- Ward, P. D.** 1986. Cretaceous ammonite shell shapes. *Malacologia*, **27**, 3–28.

- Ward, P. D.** 1996. Ammonoid Extinction. Pp. 815–824 in Landman, N. H., Tanabe, K. & Davis, R. A. (eds) *Ammonoid Paleobiology, Topics in Geobiology*, **13**. Plenum Press, New York.
- Ward, P. D., Hurtado, J. M., Kirschvink, J. L. & Verosub, K. L.** 1997. Measurements of the Cretaceous paleolatitude of Vancouver Island: consistent with the Baja–British Columbia hypothesis. *Science*, **277**(5332), 1642–1645.
- Ward, P. D. & Kennedy, W. J.** 1993. Maastrichtian ammonites from the Biscay region (France, Spain). *Paleontological Society, Memoir*, **34**, 1–58.
- Ward, P. D. & Westermann, G. E. G.** 1977. First occurrence, systematics, and functional morphology of *Nipponites* (Cretaceous Lytoceratina) from the Americas. *Journal of Paleontology*, **51**(2), 367–372.
- Ward, P. D., Haggart, J. W., Mitchell, R., Kirschvink, J. L. & Tobin, T.** 2012. Integration of macrofossil biostratigraphy and magnetostratigraphy for the Pacific coast Upper Cretaceous (Campanian–Maastrichtian) of North America and implications for correlation with the Western Interior and Tethys. *Geological Society of America, Bulletin*, **124**(5/6), 957–974.
- Ward, P. D., Haggart, J. W., Mitchell, R. & Catlin, E.** 2015. Quantitative morphological description of the Late Cretaceous ammonite *Baculites inornatus* Meek from western North America: implications for species concepts in the biostratigraphically important Baculitidae. *Journal of Paleontology*, **89**(4), 594–610.
- Wedekind, R.** 1916. Über Lobus, Suturallobus und Inzision. *Zentralblatt für Mineralogie, Geologie, und Paläontologie*, **8**, 185–195.
- Westermann, G. E. G.** 1990. New developments in ecology of Jurassic–Cretaceous ammonoids. Pp. 459–478 in G. Pallini, E. Cecca, S. Cresta & M. Santantonio (eds) *Fossili, Evoluzione, Ambiente, Atti del secondo convegno internazionale, Pergola, 1987*. Tecnostampa, Ostra Vetere.
- Westermann, G. E. G.** 1996. Ammonoid life and habitat. Pp.608–695 in Landman, N. H., Tanabe, K. & Davis, R. A. (eds) *Ammonoid Paleobiology, Topics of Geobiology*, **13**. Plenum Press, New York.
- Wetzel, O.** 1933. Die in organischer Substanz erhaltenen Mikrofossilien des baltischen Kreide-Feuersteins mit einem sediment-petrographischen und stratigraphischen Anhang. *Palaeontographica, Abteilung A*, **78**, 1–110, pls 1–7.
- White, H. H.** 1842. On fossil *Xanthidia*. *Microscopical Journal, London*, **11**, 35–40, pl. 4.

- Whiteaves, J. F.** 1879. On the fossils of the Cretaceous rocks of Vancouver and adjacent islands in the Strait of Georgia. Geological Survey of Canada, *Mesozoic Fossils*, **1**(2), 93–190, pls 11–20.
- Whiteaves, J. F.** 1895. Notes on some fossils from the Cretaceous rocks of British Columbia, with descriptions of two species that appear to be new. *Canadian Record of Science*, **6**(6), 313–318, pl. 2.
- Whiteaves, J. F.** 1903. On some additional fossils from the Vancouver Cretaceous, with a revised list of the species therefrom. Geological Survey of Canada, *Mesozoic Fossils*, **1**(5), 309–415, pls 40–51.
- Whitfield, R. P.** 1877. Preliminary report on the paleontology of the Black Hills, containing descriptions of new species of fossils from the Potsdam, Jurassic, and Cretaceous formations of the Black Hills of Dakota. *U.S. Geographical and Geological Survey of the Rocky Mountain Region, Report* (J. W. Powell), 49 pp., 16 pls.
- Whitfield, R. P.** 1892. Gasteropoda and Cephalopoda of the Raritan Clays and Greensand Marls of New Jersey. *U. S. Geological Survey Monographs*, **18**, 402 pp., 50 pls.
- Wiedmann, J.** 1962. Ammoniten aus der Vascogotischen Kreide (Nordspanien). 1. Phylloceratina, Lytoceratina. *Palaeontographica*, **118**, 119–237, pls 8–14.
- Wiedmann, J.** 1966. Stammesgeschichte und System der posttriadischen Ammonoideen. Ein Überblick in Überblick (2. Teil). *Neues Jahrbuch für Geologie und Paläontologie Abhandlungen*, **127**, 13–81, pls 3–6.
- Wiedmann, J.** 1969. The heteromorphs and ammonoid extinction. *Biological Reviews*, **44**(4), 563–602, 3 pls.
- Wiedmann, J. & Kakabadzé, M. V.** 1993. Suture investigations and the classification of Cretaceous heteromorph ammonites. *Geobios*, **26**, Supplement 1, 393–399.
- Williams, T. B.** 1924. The Comox coal basin. Unpublished Ph.D. thesis, University of Wisconsin, Madison, Wisconsin, 143 pp.
- Williams, G. L. & Downie, C.** 1966. Further dinoflagellate cysts from the London Clay. Pp. 215–236, pls 24–26 in R. J. Davey, C. Downie, W. A. S. Sarjeant & G. L. Williams (eds) *Studies on Mesozoic and Cainozoic dinoflagellate cysts. British Museum (Natural History) Geology, Bulletin, Supplement 3*.
- Williams, G. L., Fensome, R. A. & MacRae, R. A.** 2017. The Lentini and Williams index of fossil dinoflagellates 2017 edition. *American Association of Stratigraphic Palynologists, Contributions Series*, **48**, 1097 pp.

- Williams, G. L., Brinkhuis, H., Pearce, M. A., Fensome, R. A. & Weegink, J. W.** 2004. Southern Ocean and global dinoflagellate cyst events compared: index events for the Late Cretaceous–Neogene. In N. F. Exon, J. P. Kenneth & M. J. Malone (eds) *Proceedings of the Ocean Drilling Program, Scientific Results*, **189**, 1–98.
- Wilpshaar, M. & Leereveld, H.** 1994. Palaeoenvironmental change in the Early Cretaceous Vocontian Basin (SE France) reflected by dinoflagellate cysts. *Review of Palaeobotany and Palynology*, **84**(1–2), 121–128.
- Wilson, O. J.** 1971. Observations on European Late Cretaceous dinoflagellate cysts. *Proceedings of the Second Planktonic Conference, Roma*. 1259–1275.
- Wilson, O. J.** 1974. *Upper Campanian and Maastrichtian dinoflagellate cysts from the Maastricht region and Denmark*. Unpublished Ph.D. thesis, University of Nottingham, Nottingham, United Kingdom, 601 pp.
- Wolfe, J. A.** 1975. Some Aspects of Plant Geography of the Northern Hemisphere During the Late Cretaceous and Tertiary. *Annals of the Missouri Botanical Garden*, **62**(2), 264–279.
- Wrenn, J. H.** 1988. Differentiating species of the dinoflagellate cyst genus *Nematosphaeropsis* Deflandre & Cookson 1955. *Palynology*, **12**, 129–150.
- Wrenn, J. H. & Hart, G. P.** 1988. Paleogene dinoflagellate cyst biostratigraphy of Seymour Island, Antarctica. *Geological Society of America, Memoir*, **169**, 321–447.
- Wright, E. K.** 1987. Stratification and paleocirculation of the Late Cretaceous Western Interior Seaway of North America. *Geological Society of America, Bulletin*, **99**, 480–490.
- Wright, C. W. & Matsumoto, T.** 1954. Some doubtful Cretaceous ammonite genera from Japan and Saghalien. *Memoirs of the Faculty of Science, Kyushu University, Series D, Geology*, **4**(2), 107–134, pls. 7–8.
- Wright, C. W., Calloman (sic = Callomon), J. H. & Howarth, M. K.** 1996. Systematic descriptions of the Order Ammonoidea. Pp.1–277 in R. L. Kaesler (ed.) *Treatise on Invertebrate Paleontology, Part L, Mollusca 4 Revised*. Geological Society of America, Boulder and University of Kansas Press, Lawrence.
- Xu Jinli & Mao Shaozhi.** 1989. A new understanding of the bohaidinioid dinoflagellates. *Acta Botanica Sinica*, **31**(3; 4), 215–222; 300–306, pls 1–3.
- Yabe, H.** 1901. Note on three Upper Cretaceous ammonites from Japan, outside of Hokkaido. *Journal of the Geological Society of Tokyo*, **8**, 1–4.
- Yabe, H.** 1902. Note on three Upper Cretaceous ammonites from Japan, outside of Hokkaido. *Journal Geological Society of Tokyo*, **9**, 1–7, 1 pl.

- Yabe, H.** 1904. Cretaceous cephalopoda from the Hokkaido. Part II. *Turrilites*, *Helicoceras*, *Heteroceras*, *Nipponites*, *Olcostephanus*, *Desmoceras*, *Hauericeras*, and an undetermined genus. *Journal of the College of Science, Imperial University of Tokyo*, **20**(2), 1–45, pls 3–6.
- Yabe, H.** 1927. Cretaceous stratigraphy of the Japanese Islands. *Science Reports of the Tohoku Imperial University, Second Series (Geology)*, **11**(1), 27–100, pls 3–9.
- Yokoyama, M.** 1890. Verdteinerung aus der japanischen Kredie. *Palaeontographica*, **36**, 159–202, pls 18–25.
- Yun Hyesu.** 1981. Dinoflagellaten aus der Oberkreide (Santon) von Westfalen. *Palaeontographica, Abteilung B*, **177**, 1–89, pls 1–16.
- Zaborski, P. M. P.** 1985. Upper Cretaceous ammonites from the Calabar region, south-east Nigeria. *Bulletin of the British Museum (Natural History), Geology Series*, **39**(1), 1–72.
- Zaitzeff, J. B. & Cross, A. T.** 1970. The use of dinoflagellates and acritarchs for zonation and correlation of the Navarro Group (Maestrichtian), of Texas. Pp. 341–377 in R. M. Kosanke & A. T. Cross (eds) *Symposium on Palynology of the Late Cretaceous and Early Tertiary*. Geological Society of America, Special Paper, **127**.
- Zakharov, Y. D., Haggart, J. W., Beard, G. & Safronova, P. P.** 2013. Late Cretaceous climatic trends and a positive carbon isotope excursion at the Santonian-Campanian boundary in British Columbia, northeastern Pacific. *Sedimentary Geology*, **295**, 77–92.
- Zittel, K. A. von.** 1884. Handbuch der Palaeontologie. Pp. 329–522 in W. P. Schimper, A. Schenk & S. H. Scudder (eds) Abtheilung I, II (Lief. III) *Cephalopoda*. Oldenburg, Munich and Leipzig.

Appendix I List of heteromorph ammonite specimens

Ordered alphabetically by family, taxon, institutional abbreviation, and institutional accession number.

Repository	Accession No.	In-text No.	Family	Taxon
RBCM	RBCM.EH2008.011.09934.03		Baculitidae Gill, 1871	<i>Fresvillia constricta</i> Kennedy, 1986
RBCM	RBCM.EH2008.011.09934.05		Baculitidae Gill, 1871	<i>Fresvillia constricta</i> Kennedy, 1986
RBCM	RBCM.EH2008.011.10672.001	RBCM.3	Baculitidae Gill, 1871	<i>Fresvillia constricta</i> Kennedy, 1986
RBCM	RBCM.EH2014.003.0001.002	RBCM.2	Baculitidae Gill, 1871	<i>Fresvillia constricta</i> Kennedy, 1986
RBCM	RBCM.EH2014.003.0001.003		Baculitidae Gill, 1871	<i>Fresvillia constricta</i> Kennedy, 1986
RBCM	RBCM.EH2014.003.0001.004		Baculitidae Gill, 1871	<i>Fresvillia constricta</i> Kennedy, 1986
RBCM	RBCM.EH2014.003.0001.005		Baculitidae Gill, 1871	<i>Fresvillia constricta</i> Kennedy, 1986
RBCM	RBCM.EH2014.003.0001.006		Baculitidae Gill, 1871	<i>Fresvillia constricta</i> Kennedy, 1986
RBCM	RBCM.EH2014.003.0001.007		Baculitidae Gill, 1871	<i>Fresvillia constricta</i> Kennedy, 1986
RBCM	RBCM.EH2014.003.0001.008		Baculitidae Gill, 1871	<i>Fresvillia constricta</i> Kennedy, 1986
RBCM	RBCM.EH2014.003.0001.009		Baculitidae Gill, 1871	<i>Fresvillia constricta</i> Kennedy, 1986
RBCM	RBCM.EH2014.003.0001.010		Baculitidae Gill, 1871	<i>Fresvillia constricta</i> Kennedy, 1986
RBCM	RBCM.EH2014.003.0001.011		Baculitidae Gill, 1871	<i>Fresvillia constricta</i> Kennedy, 1986
RBCM	RBCM.EH2014.003.0001.012		Baculitidae Gill, 1871	<i>Fresvillia constricta</i> Kennedy, 1986
RBCM	RBCM.EH2014.003.0001.013		Baculitidae Gill, 1871	<i>Fresvillia constricta</i> Kennedy, 1986
RBCM	RBCM.EH2014.003.0001.014		Baculitidae Gill, 1871	<i>Fresvillia constricta</i> Kennedy, 1986
RBCM	RBCM.EH2014.003.0001.015		Baculitidae Gill, 1871	<i>Fresvillia constricta</i> Kennedy, 1986
RBCM	RBCM.EH2014.003.0001.016		Baculitidae Gill, 1871	<i>Fresvillia constricta</i> Kennedy, 1986
RBCM	RBCM.EH2016.006.0002.001		Baculitidae Gill, 1871	<i>Fresvillia constricta</i> Kennedy, 1986
CDM	993.79.1		Diplomoceratidae Spath, 1926	<i>Diplomoceras (Diplomoceras) cylindraceum</i> (Defrance, 1816)
CDM	993.111.2		Diplomoceratidae Spath, 1926	<i>Diplomoceras (Diplomoceras) cylindraceum</i> (Defrance, 1816)
CDM	993.169.1		Diplomoceratidae Spath, 1926	<i>Diplomoceras (Diplomoceras) cylindraceum</i> (Defrance, 1816)
CDM	996.219.1		Diplomoceratidae Spath, 1926	<i>Diplomoceras (Diplomoceras) cylindraceum</i> (Defrance, 1816)
CDM	998.1.508 COP		Diplomoceratidae Spath, 1926	<i>Diplomoceras (Diplomoceras) cylindraceum</i> (Defrance, 1816)
CDM	2002.76.1		Diplomoceratidae Spath, 1926	<i>Diplomoceras (Diplomoceras) cylindraceum</i> (Defrance, 1816)
CDM	2008.1.4 HUN		Diplomoceratidae Spath, 1926	<i>Diplomoceras (Diplomoceras) cylindraceum</i> (Defrance, 1816)
CDM	2008.1.5 HUN		Diplomoceratidae Spath, 1926	<i>Diplomoceras (Diplomoceras) cylindraceum</i> (Defrance, 1816)
CDM	2008.1.12 HUN		Diplomoceratidae Spath, 1926	<i>Diplomoceras (Diplomoceras) cylindraceum</i> (Defrance, 1816)
CDM	2008.1.23 HUN		Diplomoceratidae Spath, 1926	<i>Diplomoceras (Diplomoceras) cylindraceum</i> (Defrance, 1816)
CDM	2008.1.29 HUN		Diplomoceratidae Spath, 1926	<i>Diplomoceras (Diplomoceras) cylindraceum</i> (Defrance, 1816)
CDM	2008.1.30 HUN		Diplomoceratidae Spath, 1926	<i>Diplomoceras (Diplomoceras) cylindraceum</i> (Defrance, 1816)

Continued

RBCM	RBCM.EH2008.011.10238.001	RBCM.21	Diplomoceratidae Spath, 1926	<i>Diplomoceras (Diplomoceras) cf. cylindraceum</i> (Defrance, 1816)
RBCM	RBCM.EH2008.011.00425.001	RBCM.25	Diplomoceratidae Spath, 1926	<i>Exiteloceras (Exiteloceras) densicostatum</i> sp. nov.
RBCM	RBCM.EH2015.003.0002.001	RBCM.28	Diplomoceratidae Spath, 1926	<i>Exiteloceras (Exiteloceras) densicostatum</i> sp. nov.
RBCM	RBCM.EH2015.003.0003.001	RBCM.26	Diplomoceratidae Spath, 1926	<i>Exiteloceras (Exiteloceras) densicostatum</i> sp. nov.
RBCM	RBCM.EH2016.005.0017.001	RBCM.27	Diplomoceratidae Spath, 1926	<i>Exiteloceras (Exiteloceras) densicostatum</i> sp. nov.
RBCM	RBCM.EH2008.011.00424.001	RBCM.30	Diplomoceratidae Spath, 1926	<i>Exiteloceras (Neancyloceras) aff. bipunctatum</i> Schlüter, 1872
RBCM	RBCM.EH2008.011.10206.006		Diplomoceratidae Spath, 1926	<i>Exiteloceras (Neancyloceras) aff. bipunctatum</i> Schlüter, 1872
RBCM	RBCM.EH2008.011.10206.007		Diplomoceratidae Spath, 1926	<i>Exiteloceras (Neancyloceras) aff. bipunctatum</i> Schlüter, 1872
RBCM	RBCM.EH2008.011.10206.008		Diplomoceratidae Spath, 1926	<i>Exiteloceras (Neancyloceras) aff. bipunctatum</i> Schlüter, 1872
RBCM	RBCM.EH2008.011.10212.001	RBCM.33	Diplomoceratidae Spath, 1926	<i>Exiteloceras (Neancyloceras) aff. bipunctatum</i> Schlüter, 1872
RBCM	RBCM.EH2008.011.10218.001	RBCM.29	Diplomoceratidae Spath, 1926	<i>Exiteloceras (Neancyloceras) aff. bipunctatum</i> Schlüter, 1872
RBCM	RBCM.EH2016.009.0004.002	RBCM.32	Diplomoceratidae Spath, 1926	<i>Exiteloceras (Neancyloceras) aff. bipunctatum</i> Schlüter, 1872
RBCM	RBCM.EH2016.009.0019.002		Diplomoceratidae Spath, 1926	<i>Exiteloceras (Neancyloceras) aff. bipunctatum</i> Schlüter, 1872
RBCM	RBCM.EH2016.009.0022.001	RBCM.31	Diplomoceratidae Spath, 1926	<i>Exiteloceras (Neancyloceras) aff. bipunctatum</i> Schlüter, 1872
RBCM	RBCM.EH2016.009.0025.005		Diplomoceratidae Spath, 1926	<i>Exiteloceras (Neancyloceras) aff. bipunctatum</i> Schlüter, 1872
RBCM	RBCM.EH2016.009.0025.006		Diplomoceratidae Spath, 1926	<i>Exiteloceras (Neancyloceras) aff. bipunctatum</i> Schlüter, 1872
CDM	998.292.1		Diplomoceratidae Spath, 1926	<i>Phylloptychoceras horitai</i> Shigeta & Nishimura, 2013
CDM	2013.84.1		Diplomoceratidae Spath, 1926	<i>Phylloptychoceras horitai</i> Shigeta & Nishimura, 2013
RBCM	RBCM.EH2008.011.00334.001	RBCM.52	Diplomoceratidae Spath, 1926	<i>Phylloptychoceras horitai</i> Shigeta & Nishimura, 2013
RBCM	RBCM.EH2008.011.00338.001	RBCM.50	Diplomoceratidae Spath, 1926	<i>Phylloptychoceras horitai</i> Shigeta & Nishimura, 2013
RBCM	RBCM.EH2008.011.00389.002		Diplomoceratidae Spath, 1926	<i>Phylloptychoceras horitai</i> Shigeta & Nishimura, 2013
RBCM	RBCM.EH2008.011.00420.001		Diplomoceratidae Spath, 1926	<i>Phylloptychoceras horitai</i> Shigeta & Nishimura, 2013
RBCM	RBCM.EH2008.011.09759.006	RBCM.51	Diplomoceratidae Spath, 1926	<i>Phylloptychoceras horitai</i> Shigeta & Nishimura, 2013
RBCM	RBCM.EH2008.011.10200.001		Diplomoceratidae Spath, 1926	<i>Phylloptychoceras horitai</i> Shigeta & Nishimura, 2013
RBCM	RBCM.EH2008.011.10201.001		Diplomoceratidae Spath, 1926	<i>Phylloptychoceras horitai</i> Shigeta & Nishimura, 2013
RBCM	RBCM.EH2008.011.10202.001	RBCM.38	Diplomoceratidae Spath, 1926	<i>Phylloptychoceras horitai</i> Shigeta & Nishimura, 2013
RBCM	RBCM.EH2008.011.10202.002		Diplomoceratidae Spath, 1926	<i>Phylloptychoceras horitai</i> Shigeta & Nishimura, 2013
RBCM	RBCM.EH2008.011.10202.003		Diplomoceratidae Spath, 1926	<i>Phylloptychoceras horitai</i> Shigeta & Nishimura, 2013
RBCM	RBCM.EH2008.011.10202.004		Diplomoceratidae Spath, 1926	<i>Phylloptychoceras horitai</i> Shigeta & Nishimura, 2013
RBCM	RBCM.EH2008.011.10202.005		Diplomoceratidae Spath, 1926	<i>Phylloptychoceras horitai</i> Shigeta & Nishimura, 2013
RBCM	RBCM.EH2008.011.10203.001	RBCM.49	Diplomoceratidae Spath, 1926	<i>Phylloptychoceras horitai</i> Shigeta & Nishimura, 2013
RBCM	RBCM.EH2008.011.10215.002		Diplomoceratidae Spath, 1926	<i>Phylloptychoceras horitai</i> Shigeta & Nishimura, 2013
RBCM	RBCM.EH2008.011.10216.001		Diplomoceratidae Spath, 1926	<i>Phylloptychoceras horitai</i> Shigeta & Nishimura, 2013
RBCM	RBCM.EH2008.011.10216.002		Diplomoceratidae Spath, 1926	<i>Phylloptychoceras horitai</i> Shigeta & Nishimura, 2013
RBCM	RBCM.EH2008.011.10216.003		Diplomoceratidae Spath, 1926	<i>Phylloptychoceras horitai</i> Shigeta & Nishimura, 2013

Continued

RBCM	RBCM.EH2008.011.10216.008		Diplomoceratidae Spath, 1926	<i>Phylloptychoceras horitai</i> Shigeta & Nishimura, 2013
RBCM	RBCM.EH2008.011.10217.001		Diplomoceratidae Spath, 1926	<i>Phylloptychoceras horitai</i> Shigeta & Nishimura, 2013
RBCM	RBCM.EH2008.011.10440.002		Diplomoceratidae Spath, 1926	<i>Phylloptychoceras horitai</i> Shigeta & Nishimura, 2013
RBCM	RBCM.EH2014.003.0001.001		Diplomoceratidae Spath, 1926	<i>Phylloptychoceras horitai</i> Shigeta & Nishimura, 2013
RBCM	RBCM.EH2015.003.0004.001	RBCM.48	Diplomoceratidae Spath, 1926	<i>Phylloptychoceras horitai</i> Shigeta & Nishimura, 2013
RBCM	RBCM.EH2015.003.0005.001	RBCM.46	Diplomoceratidae Spath, 1926	<i>Phylloptychoceras horitai</i> Shigeta & Nishimura, 2013
RBCM	RBCM.EH2015.003.0006.001		Diplomoceratidae Spath, 1926	<i>Phylloptychoceras horitai</i> Shigeta & Nishimura, 2013
RBCM	RBCM.EH2015.003.0007.001	RBCM.44	Diplomoceratidae Spath, 1926	<i>Phylloptychoceras horitai</i> Shigeta & Nishimura, 2013
RBCM	RBCM.EH2015.003.0008.001	RBCM.41	Diplomoceratidae Spath, 1926	<i>Phylloptychoceras horitai</i> Shigeta & Nishimura, 2013
RBCM	RBCM.EH2015.003.0009.001		Diplomoceratidae Spath, 1926	<i>Phylloptychoceras horitai</i> Shigeta & Nishimura, 2013
RBCM	RBCM.EH2015.003.0010.001	RBCM.47	Diplomoceratidae Spath, 1926	<i>Phylloptychoceras horitai</i> Shigeta & Nishimura, 2013
RBCM	RBCM.EH2015.003.0010.002		Diplomoceratidae Spath, 1926	<i>Phylloptychoceras horitai</i> Shigeta & Nishimura, 2013
RBCM	RBCM.EH2015.003.0013.001	RBCM.37	Diplomoceratidae Spath, 1926	<i>Phylloptychoceras horitai</i> Shigeta & Nishimura, 2013
RBCM	RBCM.EH2015.021.0003.001	RBCM.43	Diplomoceratidae Spath, 1926	<i>Phylloptychoceras horitai</i> Shigeta & Nishimura, 2013
RBCM	RBCM.EH2015.021.0004.001	RBCM.45	Diplomoceratidae Spath, 1926	<i>Phylloptychoceras horitai</i> Shigeta & Nishimura, 2013
RBCM	RBCM.EH2016.005.0001.001	RBCM.39	Diplomoceratidae Spath, 1926	<i>Phylloptychoceras horitai</i> Shigeta & Nishimura, 2013
RBCM	RBCM.EH2016.005.0001.002	RBCM.35	Diplomoceratidae Spath, 1926	<i>Phylloptychoceras horitai</i> Shigeta & Nishimura, 2013
RBCM	RBCM.EH2016.005.0001.003		Diplomoceratidae Spath, 1926	<i>Phylloptychoceras horitai</i> Shigeta & Nishimura, 2013
RBCM	RBCM.EH2016.006.0004.001		Diplomoceratidae Spath, 1926	<i>Phylloptychoceras horitai</i> Shigeta & Nishimura, 2013
RBCM	RBCM.EH2016.009.0004.006		Diplomoceratidae Spath, 1926	<i>Phylloptychoceras horitai</i> Shigeta & Nishimura, 2013
RBCM	RBCM.EH2016.009.0005.002	RBCM.36	Diplomoceratidae Spath, 1926	<i>Phylloptychoceras horitai</i> Shigeta & Nishimura, 2013
RBCM	RBCM.EH2016.009.0006.001	RBCM.40	Diplomoceratidae Spath, 1926	<i>Phylloptychoceras horitai</i> Shigeta & Nishimura, 2013
RBCM	RBCM.EH2016.009.0006.003		Diplomoceratidae Spath, 1926	<i>Phylloptychoceras horitai</i> Shigeta & Nishimura, 2013
RBCM	RBCM.EH2016.009.0008.001	RBCM.34	Diplomoceratidae Spath, 1926	<i>Phylloptychoceras horitai</i> Shigeta & Nishimura, 2013
RBCM	RBCM.EH2016.009.0018.001	RBCM.42	Diplomoceratidae Spath, 1926	<i>Phylloptychoceras horitai</i> Shigeta & Nishimura, 2013
RBCM	RBCM.EH2016.009.0018.002		Diplomoceratidae Spath, 1926	<i>Phylloptychoceras horitai</i> Shigeta & Nishimura, 2013
RBCM	RBCM.EH2016.009.0025.007		Diplomoceratidae Spath, 1926	<i>Phylloptychoceras horitai</i> Shigeta & Nishimura, 2013
RBCM	RBCM.EH2008.011.00337.001	RBCM.58	Diplomoceratidae Spath, 1926	<i>Solenoceras exornatus</i> sp. nov.
RBCM	RBCM.EH2008.011.10204.001		Diplomoceratidae Spath, 1926	<i>Solenoceras exornatus</i> sp. nov.
RBCM	RBCM.EH2008.011.10205.001		Diplomoceratidae Spath, 1926	<i>Solenoceras exornatus</i> sp. nov.
RBCM	RBCM.EH2008.011.10206.001		Diplomoceratidae Spath, 1926	<i>Solenoceras exornatus</i> sp. nov.
RBCM	RBCM.EH2008.011.10206.005		Diplomoceratidae Spath, 1926	<i>Solenoceras exornatus</i> sp. nov.
RBCM	RBCM.EH2008.011.10208.001	RBCM.61	Diplomoceratidae Spath, 1926	<i>Solenoceras exornatus</i> sp. nov.
RBCM	RBCM.EH2008.011.10209.001		Diplomoceratidae Spath, 1926	<i>Solenoceras exornatus</i> sp. nov.
RBCM	RBCM.EH2008.011.10210.001	RBCM.53	Diplomoceratidae Spath, 1926	<i>Solenoceras exornatus</i> sp. nov.

Continued

RBCM	RBCM.EH2008.011.10210.004		Diplomoceratidae Spath, 1926	<i>Solenoceras exornatus</i> sp. nov.
RBCM	RBCM.EH2008.011.10213.001		Diplomoceratidae Spath, 1926	<i>Solenoceras exornatus</i> sp. nov.
RBCM	RBCM.EH2008.011.10215.003	RBCM.60	Diplomoceratidae Spath, 1926	<i>Solenoceras exornatus</i> sp. nov.
RBCM	RBCM.EH2016.009.0004.003	RBCM.64	Diplomoceratidae Spath, 1926	<i>Solenoceras exornatus</i> sp. nov.
RBCM	RBCM.EH2016.009.0004.004		Diplomoceratidae Spath, 1926	<i>Solenoceras exornatus</i> sp. nov.
RBCM	RBCM.EH2016.009.0004.005		Diplomoceratidae Spath, 1926	<i>Solenoceras exornatus</i> sp. nov.
RBCM	RBCM.EH2016.009.0004.007	RBCM.54	Diplomoceratidae Spath, 1926	<i>Solenoceras exornatus</i> sp. nov.
RBCM	RBCM.EH2016.009.0005.001	RBCM.65	Diplomoceratidae Spath, 1926	<i>Solenoceras exornatus</i> sp. nov.
RBCM	RBCM.EH2016.009.0005.003		Diplomoceratidae Spath, 1926	<i>Solenoceras exornatus</i> sp. nov.
RBCM	RBCM.EH2016.009.0006.002		Diplomoceratidae Spath, 1926	<i>Solenoceras exornatus</i> sp. nov.
RBCM	RBCM.EH2016.009.0009.001	RBCM.57	Diplomoceratidae Spath, 1926	<i>Solenoceras exornatus</i> sp. nov.
RBCM	RBCM.EH2016.009.0009.003	RBCM.55	Diplomoceratidae Spath, 1926	<i>Solenoceras exornatus</i> sp. nov.
RBCM	RBCM.EH2016.009.0011.001	RBCM.59	Diplomoceratidae Spath, 1926	<i>Solenoceras exornatus</i> sp. nov.
RBCM	RBCM.EH2016.009.0015.001		Diplomoceratidae Spath, 1926	<i>Solenoceras exornatus</i> sp. nov.
RBCM	RBCM.EH2016.009.0015.002		Diplomoceratidae Spath, 1926	<i>Solenoceras exornatus</i> sp. nov.
RBCM	RBCM.EH2016.009.0016.001	RBCM.56	Diplomoceratidae Spath, 1926	<i>Solenoceras exornatus</i> sp. nov.
RBCM	RBCM.EH2016.009.0019.001	RBCM.63	Diplomoceratidae Spath, 1926	<i>Solenoceras exornatus</i> sp. nov.
RBCM	RBCM.EH2016.009.0022.002		Diplomoceratidae Spath, 1926	<i>Solenoceras exornatus</i> sp. nov.
RBCM	RBCM.EH2016.009.0023.001	RBCM.62	Diplomoceratidae Spath, 1926	<i>Solenoceras exornatus</i> sp. nov.
RBCM	RBCM.EH2016.009.0023.002		Diplomoceratidae Spath, 1926	<i>Solenoceras exornatus</i> sp. nov.
RBCM	RBCM.EH2016.009.0025.001		Diplomoceratidae Spath, 1926	<i>Solenoceras exornatus</i> sp. nov.
RBCM	RBCM.EH2016.009.0025.002		Diplomoceratidae Spath, 1926	<i>Solenoceras exornatus</i> sp. nov.
RBCM	RBCM.EH2016.009.0025.003		Diplomoceratidae Spath, 1926	<i>Solenoceras exornatus</i> sp. nov.
RBCM	RBCM.EH2016.009.0025.004		Diplomoceratidae Spath, 1926	<i>Solenoceras exornatus</i> sp. nov.
RBCM	RBCM.EH2015.003.0011.001	RBCM.66	Diplomoceratidae Spath, 1926	<i>Solenoceras</i> cf. <i>reesidei</i> Stephenson, 1941
RBCM	RBCM.EH2015.003.0011.002		Diplomoceratidae Spath, 1926	<i>Solenoceras</i> cf. <i>reesidei</i> Stephenson, 1941
RBCM	RBCM.EH2015.003.0011.003		Diplomoceratidae Spath, 1926	<i>Solenoceras</i> cf. <i>reesidei</i> Stephenson, 1941
CDM	2008.1.102 HUN		Nostoceratidae Hyatt, 1894	<i>Nostoceras (Didymoceras?) adrotans</i> sp. nov.
CDM	2008.1.104 HUN		Nostoceratidae Hyatt, 1894	<i>Nostoceras (Didymoceras?) adrotans</i> sp. nov.
GSC	GSC 5955		Nostoceratidae Hyatt, 1894	<i>Nostoceras (Didymoceras?) adrotans</i> sp. nov.
RBCM	RBCM.EH2008.011.00429.001	RBCM.69	Nostoceratidae Hyatt, 1894	<i>Nostoceras (Didymoceras?) adrotans</i> sp. nov.
RBCM	RBCM.EH2008.011.10210.002	RBCM.73	Nostoceratidae Hyatt, 1894	<i>Nostoceras (Didymoceras?) adrotans</i> sp. nov.
RBCM	RBCM.EH2008.011.10650.001		Nostoceratidae Hyatt, 1894	<i>Nostoceras (Didymoceras?) adrotans</i> sp. nov.
RBCM	RBCM.EH2008.011.10651.001		Nostoceratidae Hyatt, 1894	<i>Nostoceras (Didymoceras?) adrotans</i> sp. nov.
RBCM	RBCM.EH2008.011.10652.001		Nostoceratidae Hyatt, 1894	<i>Nostoceras (Didymoceras?) adrotans</i> sp. nov.

Appendix II Heteromorph ammonite specimen measurements

Morphological abbreviations

Ap: apical angle; **C**: direction of helical whorl progression expressed as either dextral (**dx**) or sinistral (**s**); **Cd**: coil diameter of helical whorl; **Ci**: costal index; **Cu**: angle of gyroconic coil curvature; **Cv**: the number of costae per quarter volution transecting the ventrolateral margin. Values in brackets denote the number of costae per 360° volution which may be obtained through extrapolation expressed as $(Cv \times 4) - 3$ to account for the costae beginning subsequent quarterly volution increments; **D**: dorsum; **Dp**: dorsum at body chamber aperture (peristome); **Di**: angle of limb divergence from elbow axis; **F₁–F₂**: flank-to-flank whorl breadth measurement transversal along helical axis of final volution; **Fb**: constriction furrow breadth as a measurement of costal interspace; **H**: angle between helical whorl and retroversal axes; **P**: phragmacone terminus at lowest septal saddle; **T**: intact shell thickness; **U**: umbilical diameter; **V**: venter; **Wb**: whorl breadth; **Wh**: whorl height; **Xr**: whorl expansion rate. Measurement approximations are median values indicated as follows: **a**: the figure is an extrapolation where a portion of the shell is absent; **d**: the figure is an inference based on a measured section with deformation; **e**: the figure is an estimate where structural dimensions are not fully exposed from surrounding matrix.

Blank cells denote zero value or no data.

Family *Baculitidae* Gill, 1871

Table 1.1

<i>Fresvillia constricta</i> Kennedy, 1986b			Shaft			Tube Dimensions					
Repository	Accession No.	In-text No.	Constrictions			Expansion Rate				Length	Shell
			Wh	Wb	Fb	Wh ₁	Wh ₂	L	Xr	L	T
RBCM	RBCM.EH2016.006.0002.001	RBCM.1				0.3	2	24.6	6.91	25.2	0.1
RBCM	RBCM.EH2014.003.0001.002	RBCM.2				3	3.5	15.7	3.18	15.7	0.2
RBCM	RBCM.EH2008.011.10672.001	RBCM.3	6.9	6.9		5.2	7	43	4.18	43	0.3 e
RBCM	RBCM.EH2014.003.0001.014					0.9	1.7	12.2	6.56	12.3	0.3
RBCM	RBCM.EH2014.003.0001.016					1.8	2.2	6.8	5.88	11.9	0.2
RBCM	RBCM.EH2014.003.0001.013					1.9	2.4	6.8	7.35	8	0.2
RBCM	RBCM.EH2014.003.0001.012					2.3	3.4	16.3	6.75	18.6	0.2
RBCM	RBCM.EH2014.003.0001.010					2.7	3.2	10.5	4.76	12.2	0.2
RBCM	RBCM.EH2014.003.0001.006					2.8	3.6	15	5.33	15	0.2
RBCM	RBCM.EH2014.003.0001.003					3.1	4.1	20.7	4.83	39.5	0.2
RBCM	RBCM.EH2014.003.0001.015					3.1	3.7	14.6	4.11	14.6	0.2
RBCM	RBCM.EH2014.003.0001.007					3.4	4	11	5.45	13.1	0.2
RBCM	RBCM.EH2014.003.0001.011					3.4	3.7	7.8	3.85	13.1	0.2
RBCM	RBCM.EH2014.003.0001.009					3.7	4.1	10	4	12.7	0.2
RBCM	RBCM.EH2014.003.0001.004					3.9	5.6	33.6	5.06	39	0.2
RBCM	RBCM.EH2014.003.0001.008					4.2	4.4	13.1	1.53	16.4	0.2
RBCM	RBCM.EH2014.003.0001.005					5.2	5.4	12.5	1.6	23.5	0.2

Table 1.3 Continued

RBCM	RBCM.EH2008.011.10282.001	4	43.3	37.5	0.87	14											116 d	0.5
RBCM	RBCM.EH2008.011.10670.001	4	44.2 a	36.4 d	0.82 d												40.6 d	0.6
RBCM	RBCM.EH2008.011.06043.001	4	44.4	36.5	0.82	16	44.4	37.5	1.6								178	0.5
RBCM	RBCM.EH2008.011.10246.001	4	45.6	40.8 a	0.89 a	17 a											92	0.5
CDM	2008.1.23 HUN	4	46.7	39.1	0.84	16 a											304.3 d	0.5
RBCM	RBCM.EH2008.011.10269.001	4	46.7 d	37 d	0.79 d	13 d											57.7 d	0.6
GSC	GSC 10064	4	47.2	39.2	0.83	14	39.2	47.3	1.7	47.3	57.5	201.8	5.05				280	0.5
			55.6	45.8	0.82	13	55		1.7									
CDM	2008.1.70 HUN	4	48	39.4	0.82	13				45.6	60.8	382	7.9				450	0.8
			55	47.1	0.85	12												
			58	51	0.88	11												
			59			10												
			60	51	0.85													
RBCM	RBCM.EH2008.011.10260.001	4	47.8	37.2 a	0.78 a	14	38 e		2.2								114 d	0.6
			51.7	42.7	0.83	12	54 a		2.3								108	0.5
RBCM	RBCM.EH2008.011.10315.001	4	48.1	39.7	0.83	15 a											270 d	0.7
			75			16												
RBCM	RBCM.EH2008.011.10313.001	4	48.9 a			16 a											193	0.7
RBCM	RBCM.EH2008.011.10281.001	4	49 a			11 a											47	
RBCM	RBCM.EH2008.011.10308.001	4	49 a	46 a	0.86 a	15 a	54 a		2.3								111 d	0.5
							38 e		2.2								216 d	0.6
RBCM	RBCM.EH2008.011.10264.001	4	50	40 d	0.80	15 a											77.5 d	
RBCM	RBCM.EH2004.012.0102.001	4	50 d			12 d											33.3	0.5
CDM	2008.1.65 HUN	4	50.3	40	0.8	15											70.1	
RBCM	RBCM.EH2004.012.0093.001	4	50.4	37.8	0.75	13											58	0.4
RBCM	RBCM.EH2008.011.10274.001	4	51	45 a	0.88 a	16 a											38.9 d	0.6
CDM	2008.1.72 HUN	4	51.7	43.8	0.85	12 a											39.4 + 112.8 d	0.7
CDM	2008.1.30 HUN	4	53			15 a	50		2.6								189	0.5
RBCM	RBCM.EH2008.011.10270.001	4	53.4	46 d	0.86 d	15											69	0.6
RBCM	RBCM.EH2008.011.10248.001	4	54 a			11 d											63 d	0.7
RBCM	RBCM.EH2008.011.10304.001	4	56 a			17 a											190 d	0.7
			59 a			15 a												
RBCM	RBCM.EH2008.011.10303.001	4	55 a			12 a											110.5 d	0.6
CDM	998.1.508 COP	4	56 d	48 d	0.86 d	16 d	56 d	48 d	2.5								178	0.8
RBCM	RBCM.EH2008.011.10284.001	4	56.4	47.5	0.84	12											70.5	0.6
RBCM	RBCM.EH2008.011.10266.001	4	56.5	48.6	0.86	13 a											29.6	0.5
RBCM	RBCM.EH2008.011.10247.001	4	57 a			16 a	60 e	54 a	3								140	
RBCM	RBCM.EH2008.011.10255.001	4	58 a			14 a											96 d	0.6
RBCM	RBCM.EH2008.011.10280.001	4	59.2	50 d	0.84 d	14											144	0.5
RBCM	RBCM.EH2016.006.0005.001	4	60 d			12 d											183	0.6
RBCM	RBCM.EH2008.011.10328.001	4	61.6	50 d	0.81	14											150 ±10	0.7
CDM	996.219.1	5	70 e			12 e											92.3	
RBCM	RBCM.EH2008.011.10291.001	5	70 d			17 e											209 d	0.6
RBCM	RBCM.EH2008.011.10256.001	5	72 a			10 a											68 d	
RBCM	RBCM.EH2008.011.10314.001	5	72 a			10 d											63.5 d	0.4
RBCM	RBCM.EH2004.012.0104.001	5	75 a			13 a											153	
RBCM	RBCM.EH2004.012.0106.001	5	79 a			14 a											112	0.6
RBCM	RBCM.EH2008.011.10297.001	5	79 a			15 a											67.8 d	
RBCM	RBCM.EH2008.011.10338.001	5	82 a			12 d											190 d	0.8
RBCM	RBCM.EH2008.011.10283.001	5	86 a			12 e											145	0.7
RBCM	RBCM.EH2008.011.10306.001	5	86 a			14 e											189	0.8
RBCM	RBCM.EH2008.011.10257.001	5	92 a			13 a											142	
RBCM	RBCM.EH2008.011.10298.001	5	92 a			17 e											258 d	0.7
RBCM	RBCM.EH2008.011.10668.001	5	97 a			11 a											80 d	
RBCM	RBCM.EH2016.005.0029.001	3	19.6	18	0.92	12	18.1	16.6	2.1								71	0.3
		4	46 d			16 e	42 d		2.1								225	0.8
RBCM	RBCM.EH2008.011.10302.001	5	102 a			12 a											103 d	0.6

Table 1.4

<i>D. (Diplomoceras) cf. cylindraceum</i> (Defrance, 1816)			Tube Dimensions													
			Independent Limb Points				Constrictions			Expansion Rate				Length		Shell
Repository	Accession No.	In-text No.	Wh	Wb	Wb/h	Ci	Wh	Wb	Fb	WH ₁	WH ₂	L	Xr	L	T	
RBCM	RBCM.EH2008.011.10238.001	RBCM.21	23.6	22.2	0.94	11				20.7	26.6	46.5	12.69	105.2 + 86.7 d	0.3	

Table 1.5

<i>E. (Exiteloceras) densicostatum</i> sp. nov.			Whorls									Tube Dimensions							
Repository	Accession No.	In-text No.	Independent Points				Constrictions					Expansion Rate				Length		Shell	
			Cu	Wh	Wb	Wb/h	Ci	Wh	Wb	Fb	Wh ₁	Wh ₂	L	Xr	L	T			
RBCM	RBCM.EH2008.011.00425.001	RBCM.25	29°	16			9	5.4						3.3	6.9	27.4	13.14	117.4	0.3
								12.5	8.6 e	1	11.3	17.3	49	12.24					
								16.5	11.2 e	1.1									
RBCM	RBCM.EH2015.003.0003.001	RBCM.26	35°	19	16 e	0.89 e	8	21.4 d		1.5								53.7	0.3
RBCM	RBCM.EH2016.005.0017.001	RBCM.27	28°	7.7	7.1	0.92	10	6.8 a	5.8 a	1.1								42.5	0.1
RBCM	RBCM.EH2015.003.0002.001	RBCM.28	38°	10.4			10	10.6 d		0.6	24.6 d	31.7 d	66.6 e	10.66 e	108.3 + 78.2 d				0.3
				30			18 e	12 d		0.6									
								14.6 d		0.6									
								24.5 d		1									
								26.3 d		1.1									

Table 1.6

<i>E. (Neancyloceras) aff. bipunctatum</i> (Schlüter, 1872)			Whorls									Tube Dimensions							
Repository	Accession No.	In-text No.	Independent Points				Constrictions					Expansion Rate				Length		Shell	
			Cu	Wh	Wb	Wb/h	Ci	Wh	Wb	Fb	Wh ₁	Wh ₂	L	Xr	L	T			
RBCM	RBCM.EH2008.011.10218.001	RBCM.29	15°	5.4	4.9	0.91	5	2.7		0.2	4.5	5.9	14.5	9.66	43				0.2
RBCM	RBCM.EH2008.011.00424.001	RBCM.30	23°	13.8			6	7.9 a		1.2	13	20	78.1	8.96	134				0.4
				18.2			7	13.7											
				19.9	18.4 e	0.92 e	8	15.6		1.3 a									
								18.5		1.4									
								19.3		1.4									
								23 a		1.7									
RBCM	RBCM.EH2016.009.0022.001	RBCM.31	19°	3	2.8	0.93	4				3.6	5.4	15.6	11.54	27.5				0.1
				4.9	4.5	0.92	4												
RBCM	RBCM.EH2016.009.0004.002	RBCM.32	14°	6.3			5	4		0.8	4.9	6.9	21.5	9.3	26.1				0.1
RBCM	RBCM.EH2008.011.10212.001	RBCM.33	12°	7.1			6	6		0.5	5.5	8.1	33	7.88	48.2				0.3
								7.5		0.8									
RBCM	RBCM.EH2008.011.10206.007		20°	6.4	5.4 e	0.84 e	5				5.3	7.3	16.6	12.05	19.3				0.2
RBCM	RBCM.EH2008.011.10206.006			4.5	3.9	0.87	4								13.3				
RBCM	RBCM.EH2016.009.0019.002			8.5 a			6 a		7.5	1					19.7				0.2
RBCM	RBCM.EH2016.009.0025.005		15°	5.6	5.7	1.02	4				5	5.7	17	4.12	17				
RBCM	RBCM.EH2016.009.0025.006			5.1			4								9.7				

Table 1.5

<i>Phylloptoceras horita</i> Shigeta & Nishimura, 2013			Elbows											Limbs					Tube Dimensions													
Repository	Accession No.	In-text No.	Order	D ₁ -V ₁				D ₂ -V ₂				D ₃ -V ₃			Limb Proximity	Order	Independent Limb Points				Constrictions			Expansion Rate				Length		Shell		
				Wh	Wb	Wb/h	Ci	Wh	Wb	Wb/h	Ci	Wh	Wb	Wb/h			Ci	D ₁ -D ₂	Wh	Wb	Wb/h	Ci	Wh	Wb	Fb	Wh ₁	Wh ₂	L	Xr	L	T	
CDM	2013.84.1		5	7.2 a			3 a	6.9	8.3	1.2	8.3				0.4	5.6								7.2	8.9	30.6	5.56	38.9	0.2			
RBCM	RBCM.EH2016.009.0008.001	RBCM.34													1									0.3	0.5	10	2	10.7				
RBCM	RBCM.EH2016.005.0001.002	RBCM.35	1	0.8			0.9				1				1-3				1.4		0.3	0.7	1.6	23.6	3.81	42.5						
			2	1.4	1.8	1.29	3	1.6	1.9	1.19	1.6 e																					
RBCM	RBCM.EH2016.009.0005.002	RBCM.36	2	1.4	1.7	1.21	3	1.5			1.7			4	2,3															14		
RBCM	RBCM.EH2015.003.0013.001	RBCM.37	1	0.9	0.8	0.89		0.9	0.8	1	1	1	1		1-3								1	2.5	33.8	4.44	39.4					
			2	1.4	1.4	1		1.6	1.6	1	1.7																					
RBCM	RBCM.EH2008.011.10202.001	RBCM.38	2	1.4	1.7	1.21	2	1.4	1.7	1.21	1.7			3	0	2,3								1.1	1.4	12	2.5	24.4				
RBCM	RBCM.EH2016.005.0001.001	RBCM.39	3	2			3	1.9	2.3	1.21					0.2	3,4								1.8	2.3	22.6	2.21	22.6				
RBCM	RBCM.EH2016.009.0006.001	RBCM.40	3	2.8	2.9	1.04	4	2.7	3.2	1.19	3.2	3.3	1.03		0.2	3,4														7.4		
RBCM	RBCM.EH2015.003.0008.001	RBCM.41	3	3.6			3	3.3	3.7	1.12	3.6				3,4									3.9	4	14.5	0.69	23				
RBCM	RBCM.EH2016.009.0018.001	RBCM.42	3				2.8	2.8 d	1 d	2.9	2.9	1		1.1	3,4								2.6	2.6	0.4	2.8	3	16.1	1.24	16.7		
RBCM	RBCM.EH2015.021.0003.001	RBCM.43	1				0.9								1-4								1.7	0.2	0.6	2.8	53	4.15	55.1	0.2		
			2	1.3			2	1.5	1.5	1	1.6												1.5	0.1								
			3	2.3			2.3	2.4	1.04	2.7				0.8																		
RBCM	RBCM.EH2015.003.0007.001	RBCM.44	1				0.8 e								1-4									1.6	2.5	29.7	3.03	44.1 + 13 e				
			2				1.4																									
			3				2.1																									
RBCM	RBCM.EH2015.021.0004.001	RBCM.45	1				0.9								1-4									1.3	1.7	0.3	1.8	2.7	27.8	3.24	69.7	0.2
			2	1.7	1.7	1	2	1.5	1.7	1.13	1.3	1.7	1.3	2																		
			3	2.6	2.6	1		2.4			2.8	2.8	1																			
RBCM	RBCM.EH2015.003.0005.001	RBCM.46	4				3.8	3.8	1	4.2	4.2 e	1 e			4,5	3.6			3					3.3	4.2	29	3.1	64.4				
RBCM	RBCM.EH2015.003.0010.001	RBCM.47	5	6.7	6.7 e	1 e	4	5.6	7.1	1.27	6.9			0.5	5,6									5.9	6.4	35.7	1.4	44.1				
RBCM	RBCM.EH2015.003.0004.001	RBCM.48	5	6.4	6.5	1.02	4	6.4	6.5	1.02	6.4			0.3	5,6									6.3	6.4	36.4	0.27	41.3				

Table 1.8 Continued

RBCM	RBCM.EH2016.009.0023.001	RBCM.62	5.8			4	6.5	9	1.38	8.3	10 e	4	1			3	0.3	3	6.5	52.3	6.69	99.4	0.2			
													1			3.2 e	0.3									
													1			4	0.5									
													1			4.8	0.6									
													2			9.7	1.2	8.3	10.5	37	5.95					
RBCM	RBCM.EH2016.009.0019.001	RBCM.63	5.8	7.8	1.34	4	6.2	8.7	1.4				1	5.8	5.8	1	4		5.6	6.4	12.3	6.5	24.8	0.2 <		
													2	6.9	8.3	1.2										
													2	9.5 a			4 a						9.2			
RBCM	RBCM.EH2016.009.0004.003	RBCM.64	5.1	6.8 a	1.33 a	4	5.1 a	6.7 a	1.31 a	6.6	9.2 a	1.39 a	4	1	4.5	5	1.11	4		4.4	5.4	31.8	3.14	66.4		
													2	4.9	5.6	1.14										
													2	5	6.6 a	1.32 a										
RBCM	RBCM.EH2016.009.0005.001	RBCM.65											1	4.5	5.5	1.22	4	2.5	2.6	0.3	2.9	5.4	23	10.87	26.5	0.2 <
													1													
													1													
RBCM	RBCM.EH2016.009.0025.002												1		4.6		4	2.6								
													1					2.9		2.4	5	32.3	8.05	32.3	0.2	
													1					3.1								
													1					3.6								
													1					1.3								
RBCM	RBCM.EH2016.009.0025.003												1					1.7	0.2	1.3	1.9	7.8	7.69	14.3		
													1					1.8	0.3							
RBCM	RBCM.EH2016.009.0015.002					6.6 a	8.7 a	1.32 a	6.5	9.2 a	1.42 a	4	2											19		
RBCM	RBCM.EH2008.011.10206.001												1					1	0.1 e					5.5		
													1					1.3	0.1 e							
RBCM	RBCM.EH2008.011.10210.004												1					1.7	0.4	1.6	2	8.6	4.65	12.2		
													1					2	0.4							
RBCM	RBCM.EH2016.009.0023.002												1	3			4	2.4	0.3	2.4	3.4	11.3	8.85	11.3		
													1					3	0.3							
RBCM	RBCM.EH2016.009.0025.001												1	5	5.9	1.18	4	4.8	5.5	0.7	3.9	5.1	18.2	6.59	18.2	0.2 e
RBCM	RBCM.EH2008.011.10204.001												1	3.8 e	4.2 e		4 e								16.7	
RBCM	RBCM.EH2016.009.0015.001												1	4.2	5.2	1.23	4								25.8	
RBCM	RBCM.EH2016.009.0005.003												1	4.6 e	5.6 e	1.22	4 e								9.9	
RBCM	RBCM.EH2016.009.0004.004												1	4.7 e			4 e								11.3	
RBCM	RBCM.EH2016.009.0004.005												1	5.3	6.5 d	1.23	4								11.1	
RBCM	RBCM.EH2016.009.0006.002												1	5.3			4								11	
RBCM	RBCM.EH2016.009.0022.002												1	5.9			4								15.5	0.2
													2	8.9			4								14.5	0.4

Table 1.9

<i>Solenoceras cf. reesidei</i> Stephenson, 1941			Elbows										Limbs						Tube Dimensions										
Repository	Accession No.	In-text No.	D ₁ -V ₁				D ₂ -V ₂				D ₃ -V ₃				Order	Independent Limb Points				Constrictions			Expansion Rate				Length		Shell
			Wh	Wb	Wb/h	Ci	Wh	Wb	Wb/h	Ci	Wh	Wb	Wb/h	Ci		Wh	Wb	Fb	Wh ₁	Wh ₂	L	Xr	L	T					
RBCM	RBCM.EH2015.003.0011.001	RBCM.66												1	3.5	3.8 e	1.09 e	6	3.7 e	0.3	3.4	4.4	18.2	5.49	23.3				
														2	6.8	8.2 e	1.21 e	7	3.9 e	0.3					14.3				

Table 1.11 Continued

RBCM	RBCM.EH2008.011.10503.001	29.4	26.8 a	0.91 e	5	32.5	33 a	1.01 e	28.3	7	7.7	6.2 a	38 a	54.5 e	13.5 e	26 d	s	0.8	⊕				
RBCM	RBCM.EH2008.011.10506.001	30.3 e			8 e	31.5 e			33.8 e	8 e	24.7	19.7	53	53 e ±5	19.3	27.8	s		⊕				
RBCM	RBCM.EH2008.011.10572.001	31.3			7	37.5			37.5	9	19.5	14.7 a	42.5 a				dx		⊕				
RBCM	RBCM.EH2008.011.10641.001	31.5	32.4	1.03	6	31.8	39.3	1.24	29.6	27.9	0.94	6	6.2	3.8	40.5				⊕				
RBCM	RBCM.EH2016.010.0006.004	32.4			4	32.4	29.4 d		33	30.2	0.92	6	10.3	5.8	44.9				⊕				
RBCM	RBCM.EH2008.011.10563.001	32.9	36.3	1.11	9	32.4 a	35.8	1.11	32.4	35.4	1.1		13.2		28.7	41.4	29.5	32.7	1.11				
RBCM	RBCM.EH2008.011.10507.001	33 d			7	31.8	35 e	1.1 e	32	32.6 e	1.02 e	7 a	4.8 e				s	0.7	⊕				
RBCM	RBCM.EH2008.011.10561.001	34.1	31 e	0.91 e	9	37.6 e			38.5	40.8 a	1.06 e	10	19.8	19	38.9	45.6	16.5 e	15	5	20.5	0.24		
RBCM	RBCM.EH2008.011.10612.001	34.5			7	34.4			36.4	8	10.7	9.7 a	35.5 a	36.8	24 e ±1		dx	1					
RBCM	RBCM.EH2008.011.10554.001	35.5 a	32 a	0.90 e	6 a												dx	1					
RBCM	RBCM.EH2008.011.10550.001	35.5 d			7 d	37 d			38 d	10 d							dx	0.5					
RBCM	RBCM.EH2008.011.10532.001	36.3 e			6 e	37 d			37 e	7 e	20.5 e	17.8	41.5	56	27.2	30 a	dx	1.1					
RBCM	RBCM.EH2008.011.10564.001	36.4	36.7	1.01	8	37.6	38.9	1.03	36.7	35.1	0.96	9	20.4	20.4	32.3	29.3	17.6	26.8	28.8 d	15 e	31°		
RBCM	RBCM.EH2008.011.10588.001	36.8	35	0.95	6	40.8			40.8					51			s	1.6					
RBCM	RBCM.EH2008.011.10580.001	37.7	35.4	0.94	8	37.7 a	39.9 a	1.06	38	38.5	1.01	9	20	39	11 d ±2		s	0.8					
RBCM	RBCM.EH2008.011.10504.001	39			7	37.4			39.7	8	15.9	15.7 e	38.7 e	40.5 e			dx	0.8					
RBCM	RBCM.EH2008.011.10607.001	40			8 e	42.6 e																	
RBCM	RBCM.EH2008.011.10353.001	40 a			8 e	48 e			47 e	11 e	40.9 e	41.2	61.9	72			s						
RBCM	RBCM.EH2008.011.10552.001	40 e			7 e	41.6	46.2 a	1.11 e	45.3	8	17.6	14.2 e	44.9 e		19.5 e	36 e	dx	0.9					
RBCM	RBCM.EH2008.011.10648.001	41.1 a			7 e						18.8 a						s						
RBCM	RBCM.EH2008.011.10568.001	45			7	44.4			45.5 a	9 a	15.5 e	11.7 e	50.4	32.4	44 e	37 e	12° e	s	1.5				
RBCM	RBCM.EH2008.011.10593.001	45.7 d			6 e	51.5 d			48.7	8	42.7	43 e	60	33 e ±1	35.3	39.5 d	14 a	s	2.6				
RBCM	RBCM.EH2008.011.10556.001	50 e			8 e	57.8			56.5 e	9 e	36 e	35.7 e	54.6 e	61 e	40		s	1.4					
RBCM	RBCM.EH2008.011.10553.001	50.5 a	48.9 a	0.97 e	7												s						
RBCM	RBCM.EH2008.011.10494.001	51 e			7 e	49.4			52.2	10	34.5		59.8				s	1.1					
RBCM	RBCM.EH2008.011.10589.001	53 a			9 a	54.3 a			55 d	9 d	43.4	42.9 a	65.6 a				s	0.8					
RBCM	RBCM.EH2008.011.10549.001								38.6	41.6	1.08	10		48 d			s	0.5		15 d			
RBCM	RBCM.EH2008.011.10606.001								41 e	8 e													
RBCM	RBCM.EH2008.011.10497.001					42 a			42 a	8 a	25.8 e												
RBCM	RBCM.EH2008.011.10560.001								44 e	7 e			69 e								0.6		
RBCM	RBCM.EH2008.011.10492.001								44.5 d	40.5 d													
RBCM	RBCM.EH2008.011.10578.001					45 d			45 d	9 d											0.9		
RBCM	RBCM.EH2008.011.10496.001					45 a			45 a	9 e	25 e												
RBCM	RBCM.EH2008.011.10558.001						46.2	51.4	1.11														
RBCM	RBCM.EH2008.011.10576.001						47.9	55 d	1.15 e								dx						
RBCM	RBCM.EH2008.011.10562.001						48.3	50.4	1.04												2.7		
RBCM	RBCM.EH2008.011.10581.001						50.8		51 a	11 a	37 d ±2												
RBCM	RBCM.EH2008.011.10582.001	53 d			7 e	53 a			58 a	10 e	29 d	25 d	66.9	35.9 e ±2			dx	1.4					
RBCM	RBCM.EH2008.011.10573.001					54 d			55 a	7 a	40.3 a		38 d								2		
RBCM	RBCM.EH2008.011.10566.001					55.6			55 e	9 e	39.7 e		57.2								1.5 e		
RBCM	RBCM.EH2016.005.0020.001	22.4 a	21.4 a	0.96 a	5 a	22.5 a			23.9 a	6 a	3.3 a		24.7 a	41.5 d	14.5 a	20.8 e	s	0.5					
RBCM	RBCM.EH2016.005.0008.001	23.7	24.8 a	1.05 a	6	22.9	25 a	1.09 a	23.7	24 a	1.01 a	8	1.9	1.6	27.5		s	0.6					
RBCM	RBCM.EH2016.008.0006.001	25 a			4 a	26.3	24.2	0.92	26 a	5 a	6.8 d ±2										0.6		
RBCM	RBCM.EH2016.005.0019.001	25.9 d			5 d	28.6 d			27.8 a	5 a	11.4 a	9.5 a	33.5 a		49.2		s	0.7					
RBCM	RBCM.EH2016.007.0003.001	34.7 a	35.1 a	1.01 a	6 a									< 16 a		29 d	28.1 d	0.97 d	14	72°	20° e	s	0.9
RBCM	RBCM.EH2016.007.0001.001	51 a			7 a	52.9 d			52.7 a	10 a	39 a						dx	1					

Table 1.12

<i>Nostoceras (Nostoceras) aff. pauper</i> (Whitfield, 1892)			Limbs & Body Chambers														Helical Whorls							Shell							
Repository	Accession No.	In-text No.	D ₁ -V ₁				D ₂ -V ₂				D ₃ -V ₃				Limb Proximity						F ₁ -F ₂			Cv	U	Cd	U/Cd	Ap	H	C	T
			Wh	Wb	Wb/h	Ci	Wh	Wb	Wb/h		Wh	Wb	Wb/h	Ci	D ₁ -D ₃	-Dp-Dp	Dp-D ₂	P-D ₂	F ₂ -Dp	Wh	Wb	Wb/h									
RBCM	RBCM.EH2008.011.10356.001	RBCM.86																				12	5.1	27.1	0.19	40°			dx		
RBCM	RBCM.EH2008.011.10358.001	RBCM.87																				12	7	36.7	0.19	60°			s		
RBCM	RBCM.EH2015.003.0012.001	RBCM.88	22.7 e	29.6 e	1.3 e	6 e	27.5 a									29 e ±1					27.9	13	2.9	15.5	0.19	52°	15°	s			
RBCM	RBCM.EH2008.011.06049.001	RBCM.89	24.9	23.8	0.96	6	23.5	24.1	1.03	24.3 a			7 a	13.8	13.8	14.9	27.3 e ±1.7					11	7.6	43	0.18	52°	12°	dx	0.7		
RBCM	RBCM.EH2015.021.0002.001	RBCM.90					29.3									15.1	19.6 a			19		13	9.5	53	0.18	40°	15° d	dx			
RBCM	RBCM.EH2008.011.10364.001	RBCM.91																			28.5	28.4	12				50°	11°	dx	0.6	
RBCM	RBCM.EH2008.011.10362.001	RBCM.92																				11	5.9	36.1	0.13	50°		s			
RBCM	RBCM.EH2008.011.10368.001	RBCM.93											20.7	26.7 e								12	9.5	49.9	0.19	50° d	18°	dx	0.8		
RBCM	RBCM.EH2008.011.10359.001		26.4 d			5 d	25.5 d			25.8 d			6 d	12.5	12.5	19	16.8			7.7		12	9.5	49.9	0.19	50° d	18°	dx	0.8		
RBCM	RBCM.EH2008.011.10365.001		20.9			5 d	24 d			24 d			6 d	5.3 d	5.3 d	23			5.8 d	18.7 d		12	9.5	49.9	0.19	50° d	18°	dx	0.6		
RBCM	RBCM.EH2008.011.10357.001																				11	4.3	30.9	0.14			dx				
RBCM	RBCM.EH2008.011.10361.001																				12	5.3	41.1	0.13	48° d		s	0.4			
RBCM	RBCM.EH2008.011.10411.001																				11	5.9	42.6	0.16	56°		s				
RBCM	RBCM.EH2008.011.10366.001																				11				46°		dx				
RBCM	RBCM.EH2016.006.0001.001																				13				60°		dx	0.3			

Appendix III *Nostoceras* (*Nostoceras*) species

Literature-based overview of diagnostic traits of species assignable to the heteromorph ammonite subgenus *Nostoceras* (*Nostoceras*) Hyatt, 1894 for which helical whorls have been recovered. * = inferred from plate image(s) when not explicitly noted in the species' description.

Species	Whorl Contiguity	Apical Angle	Total Volutions	Constrictions per Volution	Ribs per 360° Volution	Costal Bifurcation / Recombination	Costal Intercallation	Inferred Dimorphism	Retroversal Body Chamber	Retroversal Body Chamber RI	Age	Additional Characteristics	References
<i>N. (N.) alternatum</i> (Tuomey, 1854)	high	moderate to high (45°–90°)	≥ 5*	absent*	40–50	yes	yes	no	unknown	unknown	early Maastrichtian	Possesses a minute, loosely coiled apex. ^{1,2} "An equal number of coarse, radially elongated tubercles lie close to umbilical margin. The two rows link across a concave zone by weak zig-zag ribs. Tubercles next to umbilicus give rise to coarse single ribs that extend across inner side of whorl, weakening progressively." ³ Whorl cross-section rhomboidal. ⁴	¹ Cobban 1974a ² Kennedy <i>et al.</i> 2000b ³ Cobban & Kennedy 1995 ⁴ Ifrim <i>et al.</i> 2004
<i>N. (N.) angolense</i> Haughton, 1925	moderate to high*	unknown	≥ 5*	2	indiscernable*	no	indiscernable*	no	unknown	unknown	late Campanian –early Maastrichtian	"Ribs are oblique, bent at the umbilical edge. Each pair of tubercles does not necessarily lie on the same rib . . . between each pair of tuberculate costae are one or two ribs without tubercles. The tubercles of the left side increase in importance as the shell grows, approaching nearer to the venter." ¹	¹ Haughton 1925
<i>N. (N.) approximans</i> (Conrad, 1855)	moderate to high	moderate to high (53°–92°)	4–5	2–4	45–60	yes	yes	no	elongated; U-shaped	6	late Campanian	"Whorl section is round, thick or fat, with round flanks and a round dorsum, and a slightly rounded venter. Diameter of the whorls remains small, giving the species a tall, high spire. Ventrolateral tubercles are small, prominent on the last whorl before the body chamber, and weak on the body chamber itself." ¹	¹ Larson 2012 Other: Cobban 1974b Kennedy & Cobban 1993c Cobban & Kennedy 1994a
<i>N. (N.) archiacianum</i> (d'Orbigny, 1842)	low to moderate*	low to moderate*	unknown	absent	32	yes	no*	no	compact; C-shaped	~4–5*	late Campanian	"Ribs are weak on the upper whorl face but sweep back across the juncture of upper and outer whorl faces in a broad convexity, strengthening and passing obliquely across the outer whorl face . . . all but one or two of the ribs are single, and bear strong equal tubercles about one third way down the outer whorl face." ¹	¹ Kennedy & Cobban 1993d
<i>N. (N.) arkansanum</i> Kennedy & Cobban, 1993c	high*	low	unknown	3–4	50–55	yes	yes	no	unknown	unknown	late Campanian	The species is "ornamented by numerous fine ribs . . . oblique and sinuous on the outer whorl face, with a row of bullate tubercles on the upper third of the exposed whorl face and a second row at the juncture of outer and lower whorl faces." ¹	¹ Kennedy & Cobban 1993d
<i>N. (N.) awajiense</i> (Yabe, 1901)	low	moderate (60°–70°)	≥ 6*	≥ 4	~ 113*	yes	yes	no	compact; C-shaped	9–10*	late Campanian	"The body chamber is . . . slightly higher than broad in section, with the aperture facing obliquely upward to the base of the spire . . . the shell is ornamented with numerous radial ribs and two rows of tubercles . . . shallow constrictions occur irregularly, being associated with flared ribs, the last one of which is discernible near the aperture." ¹	¹ Morozumi 1985

Continued

<i>N. (N.) collignoni</i> Klinger <i>et al.</i> , 2007	moderate*	moderate (~80°)	4-5*	absent*	~43*	no*	no*	no	compact; C-shaped*	2*	early Maastrichtian	"The upper, adapical row of tubercles may be slightly stronger than the lower. Ornament becomes conspicuously coarse on the recurved body chamber, consisting of sharp, widely spaced ribs each bearing a pair of ventrolateral tubercles." ¹	¹ Klinger <i>et al.</i> 2007
<i>N. (N.) colubriformis</i> Stephenson, 1941	high	low (20°-35°)	≥5*	3-4	65-70	yes	yes	no	compact; C-shaped	~10*	late Campanian -early Maastrichtian	"Tiny tubercles present just below mid-flank at point where whorl profile changes; most borne on single ribs but in a few cases, pairs of ribs link at these tubercles, whence ribs pass forward to a second row of tubercles, close to first, but displaced aperturally." ¹ "Juvenile whorl section is rounded to slightly subrectangular . . . whorl sections are flattened at the contact between whorls." ²	¹ Kennedy & Cobban 1993c ² Ifrim <i>et al.</i> 2004
<i>N. (N.) danei</i> Kennedy & Cobban, 1993b	high	moderate (~60°)*	≥6*	1-2	30-35	yes	yes	Yes	unknown	unknown	late Campanian	"Whorls in contact throughout with broad impressed zone occupying much of upper whorl face. Outer whorl face markedly flattened with an angulation separating upper, middle, and lower sectors. Umbilicus narrow . . . tubercles of upper and lower rows widely separated and linked by a single coarse prorsiradial rib." ¹	¹ Kennedy & Cobban 1993b
<i>N. (N.) gracilis</i> Lewy, 1967	low*	high (>110°)*	≥4*	absent*	~60*	no	yes	no	unknown	unknown	late Campanian	"Loosely to faintly touching whorls with a smaller umbilical diameter in the last whorl of the phragmocone than in those before . . . the first half whorl is free and the following quarter touches slightly the whorl below . . . the first half of the whorl is ornamented by fine radial ribs and its section is round. Later a pair of ventrolateral tubercles appear on each rib bordering an almost flat ventral (frontal) side." ¹	¹ Lewy 1967
<i>N. (N.) helicinum</i> (Shumard, 1861)	low to moderate*	high (92°-115°)	4	4	68	yes	yes	no	elongated; U-shaped	6-8	late Campanian	"Ribs may be linked by a simple transverse rib, or ribs may join in pairs at tubercles, zig-zagging across outer whorl face, or loop, which gives a variable appearance to this part of shell." ¹ "Body chamber has umbilical bullae and rounded ventral tubercles located on the same ribs and separated by two or three nontuberculate ribs. Tubercles are strongest on the elbow, and ribs coarsen near the aperture." ²	¹ Kennedy & Cobban 1993c ² Cobban & Kennedy, 1994a Other: Cobban 1974b Larson 2012
<i>N. (N.) hetonaiense</i> Matsumoto, 1977	low to moderate*	moderate to high*	≥4*	absent*	indiscernable*	yes	yes	no	elongated; U-shaped	10-15*	early Maastrichtian	"The ribs are fine, crowded and numerous on the septate whorl, numbering 11 to 14 in the distance as long as the whorl-breadth . . . the bullate tubercles are developed at every third to fifth rib in two rows; the upper row somewhat below the mid-line of the external surface and the lower one at the lower margin." ¹ "The intensity and frequency of tubercles on the body chamber also vary by specimens." ²	¹ Matsumoto 1977 ² Morozumi 1985

Continued

<i>N. (N.) hornbyense</i> (Whiteaves, 1895)	low to moderate	moderate to high (62°–94°)	6–7	3	~45–85 a	yes	yes	Yes	elongated; U-shaped	5–10	late Campanian	"Surface marked with simply, not very flexuous transverse ribs. Upon the last volution one or two continuous ribs without tubercles alternate with a rib or pair of ribs which bears, or bear, at small but rather prominent tubercle on each side of the periphery. Usually two ribs coalesce, both above and below, at each tubercle, but occasionally a single thickened rib bears a pair of tubercles." ¹	¹ Whiteaves 1895; herein
<i>N. (N.) hyatti</i> Stephenson, 1941	moderate*	moderate (65°–80°)	4–5	3–5	43–60	yes	yes	yes; some specimens 3/5th the size of others ²	elongated; U-shaped	3–4	late Campanian	"Spires have much coarse ribbing and tuberculation. Body chambers are characterized by very coarse distant ribs that bear widely separated spinose tubercles borne on simple ribs or with ribs zig-zagging between tubercles, notably on the beginning of the final hook." ¹ The helical whorls of some specimens may exhibit "irregular, periodic, weak constrictions that are somewhat disguised, because of . . . very high ribs." ²	¹ Kennedy & Cobban 1993c ² Larson 2012 Other: Cobban 1974b
<i>N. (N.) irregulare</i> Kennedy & Cobban, 1995	high	indiscernable*	unknown	absent*	~34–50*	no*	no*	no	unknown	unknown	early Maastrichtian	"Whorls rounded and ornamented by crowded flexuous, prorsiradiate ribs and striae; numerous tubercles at base of outer whorl face on phragmocone; body chambers irregularly ribbed and bituberculate." ¹	¹ Cobban & Kennedy 1995
<i>N. (N.) larimerense</i> Kennedy et al., 2000a	moderate to high	low to moderate (40°–55°)	≥7*	3–4	40–58	yes*	yes*	Yes	compact, C-shaped	~5–6*	late Campanian	"Whorls in tight contact except for the last part of the body chamber which is slightly uncoiled . . . ornament of narrow, rursiradiate ribs and, in addition, two rows of minute tubercles on the body chamber . . . constrictions . . . may or may not be bordered by high, thickened ribs." ¹	¹ Kennedy et al. 2000a
<i>N. (N.) magdaliae</i> Lefeld & Uberna 1991	moderate*	moderate*	unknown	≥1	~18*	no*	no*	no	unknown	unknown	early Maastrichtian	"Ribs rather weak . . . every second one ends in a tubercle while the intermediate ones vanish upwards. In addition to two rows of ventral tubercles there are weaker ventrolateral ones but only where spiral whorls contact evolving whorls like cogs in a gearwheel." ¹	¹ Lefeld & Uberna 1991
<i>N. (N.) malagasyense</i> (Collignon, 1971)	low to moderate*	high (110°)	3–4*	absent*	~75*	yes*	yes*	no	elongated; U-shaped*	5–6*	early Maastrichtian	"Ornament consists of thin, thread-like ribs bearing two rows of tubercles in irregular fashion . . . the tubercles are small, and in cases hardly wider than the ribs . . . the body chamber is suspended obliquely below the base of the spire and ends in a simple collared aperture at a distance nearly equal to that of the height of the last helical whorl." ¹	¹ Klinger et al. 2007
<i>N. (N.) mariatheresianum</i> Haas, 1943	moderate	moderate (45°)	≥4*	2–3	indiscernable*	yes	indiscernable*	no	unknown	unknown	late Campanian –early Maastrichtian	"The dominant features of the ornamentation are two rows of obliquely elongated, sharp tubercles. Some of those near the anterior end become decidedly spinous . . . as a rule there are only indistinct folds or fine riblets connecting the upper tubercles with the lower ones obliquely from the upper left to the lower right, in the same direction as the elongation of the tubercles." ¹	¹ Haas 1943

Continued

<i>N. (N.) mendryki</i> Cobban, 1974b	high*	unknown	unknown	1	50	yes*	yes*	no	compact; C-shaped*	unknown	late Campanian	"Ribs are sharp, narrow, singular on the underside of the whorl, and singular or branched on the upper side. Tubercles are sharp and conspicuously bullate." ¹	¹ Cobban 1974b
<i>N. (N.) monotuberculatum</i> Kennedy & Cobban, 1993b	high	low (18°)	unknown	3	44	yes*	yes*	no	unknown	unknown	late Campanian	The "precise relationship between ribs and tubercles varies both within and between specimens." ¹ "Ornament consists of constrictions, closely spaced ribs, and a row of small tubercles at midflank . . . the lower and outer whorl faces are broadly rounded . . . ribs are wirelike and narrower than the interspaces." ²	¹ Kennedy & Cobban 1993b ² Kennedy et al. 2000b
<i>N. (N.) natalense</i> Spath, 1921	moderate	moderate to high (70°–130°)	≥ 3*	≥ 1	~ 25*	yes	no*	no	unknown	unknown	late Campanian –early Maastrichtian	"Wide-angled low-spined phragmocone with curved retroversal body-chamber. Ornamented by two rows of tubercles, connected by looped ribs which eventually appear as single low blunt ribs." ¹ "Ribs continue over the base of the spire in a prorsiradiate fashion, narrowing towards, and continuing over the whole of the umbilical wall." ²	¹ Klinger 1976 ² Klinger & Kennedy 2003
<i>N. (N.) aff. pauper</i>	high	low to moderate (40°–60°)	6–7	3	41–57 a	yes	yes	no	compact; C-shaped	unknown	late Campanian	Helical whorls are rhomboidal in cross-section possessing a narrow umbilicus with Wb exceeding Wh at all stages. U/Cd ratio averaging 0.17.	herein
<i>N. (N.) pauper</i> (Whitfield, 1892)	high	low (20°–42°)	unknown	≥ 2	34–44	yes	yes	no	elongated; U-shaped	unknown	late Campanian	"Upper whorl face concave . . . outer whorl face broadly rounded; lower whorl face somewhat flattened. Umbilicus narrow." ¹ "Ribbing is strongest at the outer margin of the impressed area. Two rows of small pointed bullate tubercles are present, one near the middle of the side and the other lower. Tubercles tend to form on alternate ribs, and those of one row form on different ribs than those of the other row." ²	¹ Kennedy & Cobban 1993c ² Cobban 1974b
<i>N. (N.) plerucostatum</i> Kennedy & Cobban, 1993b	high	moderate (~ 56°)*	≥ 6*	2	60–65	yes*	yes*	no	unknown	unknown	late Campanian	Lacking tubercles with "crowded prorsiradiate, sinuous ribs . . . on lower whorl face, ribs prorsiradiate and convex; some terminate before reaching umbilicus, others merge in pairs . . . constrictions . . . parallel to growth lines, with flared collar ribs of which adapical is the stronger . . . terminal apertural constriction present." ¹	¹ Kennedy & Cobban 1993b
<i>N. (N.) pulcher</i> Kennedy & Cobban, 1993b	moderate	moderate (~ 75°)*	≥ 4*	1	~ 55–60*	yes	yes	no	unknown	unknown	late Campanian	"Occasional nontuberculate ribs intercalate . . . ribs . . . pass more or less straight across upper exposed whorl face and link in groups of two or three to large rounded to transversely elongated flat-topped tubercles that were bases of septate spines." ¹	¹ Kennedy & Cobban 1993b
<i>N. (N.) puzosiforme</i> Kennedy & Cobban, 1994	high	low (15.5°)	Unknown	2	30–50	yes	yes	no	unknown	unknown	late Campanian –early Maastrichtian	"Outer whorl face flattened; ornament of crowded, flexuous, prorsiradiate ribs that may branch, joining in pairs at oblique tubercles at juncture of outer and lower whorl face; periodic constrictions have associated collar-ribs." ¹	¹ Kennedy & Cobban 1994

Continued

<i>N. (N.) rotundum</i> Howarth, 1965	moderate*	moderate (45°)*	≥ 6*	absent	indiscernable*	no*	no*	no	compact; C-shaped	4*	late? Campanian	"Ornament consists of obliquely aligned pairs of tubercles forming two rows . . . ribs are poorly developed on all whorls. Between the rows of tubercles on the spire and the loop only vague undulations occur, but above and below the rows of tubercles weak ribs occur on the spire . . . just before the end of the body chamber the whorl contracts laterally, then flares out and ends in a gently sinuous mouth border of exactly circular section." ¹	¹ Howarth 1965
<i>N. (N.) rugosum</i> Cobban & Kennedy, 1991	high	low (32°–40°)	5–6*	3–4	45–50	yes	yes	yes	compact; C-shaped*	4–6*	late Campanian –early Maastrichtian	"Ribs join in pairs at prominent transversely elongated tubercles located just below midflank . . . the last whorl of the body chamber is uncoiled and slightly recurved . . . the adult aperture is commonly preceded by a strong constriction." ¹ Macroconch "ribs fork into pairs at bullae at or directly above the whorl suture" resulting in a "rounded to square-shaped whorl section" ²	¹ Cobban & Kennedy 1991 ² Ifrim <i>et al.</i> 2004
<i>N. (N.) sanctaeluisense</i> (Klinger, 1976)	low to high	high (120°–140°)	≥ 4*	absent	100–130	yes	yes*	no	compact; C-shaped*	8–13	early Maastrichtian	"The tubercles of the . . . retroversal loop are usually much larger than the ventrolateral tubercles of the phragmocone and are clavate." ¹ "The aperture is preserved in several specimens . . . first forming a slight constriction and then a simple flare." ²	¹ Klinger 1976 ² Klinger & Kennedy 2003
<i>N. (N.) saundersorum</i> (Stephenson, 1941)	moderate	low (37°)	≥ 7*	1–2*	50–60*	yes	yes	no	unknown	unknown	late Campanian	Sides of volutions very broadly rounded. Umbilicus small . . . surface covered with numerous, low, rounded costae of somewhat irregular prominence and spacing . . . at about every half volution there is a deep wide interspace bordered on the rear by a wide, rounded, prominent rib. low on the side of the largest volution of the holotype is a row of weak nodes." ¹	¹ Stephenson 1941
<i>N. (N.) schloenbachi</i> (Favre, 1869)	high	low	unknown	1	34	yes	yes	no	compact; C-shaped*	unknown	late Campanian –early Maastrichtian	"At the smallest diameter, the ribs link in pairs to prominent bullate lateral tubercles, with occasional ribs unattached. As size increases the ribbing becomes less regularly looped, with alternately long and short ribs dominating, the latter stronger than the former. Nontuberculate ribs decline on the lower part of the outer whorl face . . . the last completely preserved rib lacks well-developed tubercles . . . succeeded by a constriction." ¹	¹ Kennedy & Summesberger 1987
<i>N. (N.) splendidus</i> (Shumard, 1861)	high	low (23°–35°)	10–14	1–2*	24–28	yes	no*	no	unknown	unknown	late Campanian	"A short distance behind the aperture is a prominent ring . . . ribs bearing each two small elongated tubercles, one situated near the inferior edge and the other near the middle." ¹ "The diameter of the smallest volution preserved . . . bears a contact groove . . . although the larger volutions are more loosely coiled than the earlier ones there is no indication of an uncoiled senile stage." ²	¹ Shumard 1861 ² Stephenson 1941
<i>N. (N.) subangulatum</i> Spath, 1921	high	low	≥ 3*	absent*	~ 24*	no	yes	no	unknown	unknown	late Campanian –early Maastrichtian	"Whorl section is almost rounded, except for the double row of tubercles on the ventral area, slightly below the middle, and the impressed zone on the supper surface . . . costation is very irregular." ¹	¹ Spath 1921

Continued.

Excluded Taxa

Taxa excluded on the basis of questionable assignment and lack of data are as follows:

Species	Remarks
<i>N. (N.) attenuatum</i> Brunnschweiler, 1966	Helical whorl contiguity is unknown therefore this taxon may belong within <i>N. (Didymoceras)</i> .
<i>N. (N.) draconis</i> Stephenson, 1941	This taxon was reassigned to <i>N. (Didymoceras)</i> by Kennedy <i>et al.</i> (2000c).
<i>N. (N.) ellipticum</i> Kennedy & Lunn, 2000	Specimens are compressed and contiguity cannot be clearly discerned. Irregular, elliptical coiling in the helical stage is characteristic of <i>N. (Didymoceras)</i> .
<i>N. (N.) fisheri</i> Brunnschweiler, 1966	Helical whorl contiguity is unknown therefore this taxon may belong within <i>N. (Didymoceras)</i> . Klinger & Kennedy (2003b) have suggested close affinity with body chambers of <i>N. (N.) sanctaesusiense</i> (Klinger, 1976).
<i>N. (N.) liratum</i> Föllmi <i>et al.</i> , 1992	Described from crushed fragments, this taxon likely belongs within <i>N. (Anaklinoceras)</i> Stephenson, 1941 as the recurved body chamber is situated in contact with the last helical whorl, curving over it in approach to the apex.
<i>N. (N.) major</i> Kennedy & Cobban, 1993a	Described from a single specimen, this ambiguous taxon bears close affinity to the <i>N. (Didymoceras)</i> due to the early helical whorl obliquity. An apparent lack of tuberculation may be a function of faintly expressed ornamentation combined with poor preservation.
<i>N. (N.) platycostatum</i> Kennedy & Cobban, 1993d	This taxon was reassigned to <i>N. (Didymoceras)</i> by Kennedy <i>et al.</i> (2000b).
<i>N. (N.) schloenbachi</i> (Favre, 1869)	Machalski (2012) contends that this taxon is a very close ally of <i>N. (N.) mendryki</i> Cobban, 1974b noting it as “probable that the two forms are conspecific in spite of some differences in ornament and size (Kennedy & Summesberger 1987; Küchler & Odin 2001), but the scarcity of material on both sides of the Atlantic prevents any firm conclusions.”

Appendix IV Glossary of heteromorph ammonite terms

Terminology modified from Henderson & Henderson (1920), Landman *et al.* (1996b) and Arkell *et al.* (1957b).

Ancylocone: a shell characterized by a planispiral or helical coil followed by a shaft or hook.

Ammonitella: The embryonic shell of an ammonoid terminating at the nepionic—or primary—constriction.

Antidimorph: one of the two opposite members of a sexually dimorphic pair.

Aperture: the shell opening at the end of the body chamber.

Apical: refers to the area of the apex near the early whorls of a shell.

Benthic: relating to organisms living on or near the ocean floor.

Bifurcate: to divide in two; relating to ribs which split apart as they approach the venter.

Body chamber: the portion of the shell which accommodates the bulk of the organism.

Camerae: the gas and fluid chambers within the phragmocone used by the organism to control buoyancy.

Costa: a radial rib or ridge on the shell exterior which is not present on the internal mould.

Coil: relating to a whorl turning around a central axis (see *planispiral*, *helical*).

Contiguity: The degree to which whorls are in contact and defined as follows: *Low* = whorls predominantly only slightly touching or with evidence of costal depression on subsequent volutions; *Moderate* = whorls predominantly bearing flattened or slightly concave zones of impression on subsequent volutions; *High* = whorls predominantly tightly impressed with deep, concave furrows on subsequent volutions.

Dextral: pattern of coiling to the right, in a clockwise direction.

Dimorphism: the presence of two distinct forms within the same species generally attributed to sexual differences.

Elbow: a section of limb recurvature in a heteromorph ammonoid conch characterized by a bend of at 90° or less.

Foliolate: a minor incision within a saddle (see *septal suture*).

Furrow: a channel or groove characterized as a concave point of contact between two shell surfaces or the interspatial depression between costae.

Gyrocone: or *criocone*; a heteromorphic shell consisting of a planispiral coil with multiple whorls.

Hamiticone: a shell consisting of two or more straight shafts.

Helical: relating to whorl progression turning around an axis in a three-dimensional spiral.

Heteromorph: an ammonoid with a shell which is not planispirally coiled with successive whorls in contact with one another.

Limb: a straight section of heteromorph ammonoid shell free of helical coiling belonging to a conch characterized by multiple elongated sections.

Lira: a fine costa characterized as a minor ridge on the shell surface.

Lobe: a posteriorly (or apically) directed incision on the septal suture.

Lobule: a minor incision within a lobe (see *septal suture*).

Macroconch: the larger shell in a sexually dimorphic species considered to be the female.

Microconch: the smaller shell in a sexually dimorphic species considered to be the male.

Multicostate: having costae that are numerous and closely spaced.

Neanoconch: the juvenile shell extending up to two volutions beyond the ammonitella.

Nektic: relating to pelagic, free-swimming organisms capable of moving independently of ocean currents.

Orthocone: a shell consisting of a single, straight or curving shaft.

Paucicostate: having costae that are widely spaced.

Pelagic: relating to organisms living in the open ocean independent of the bottom; distinguished as being either planktic (floating) or nektic (swimming) in their mode of life.

Peristome: the outer edge of the ammonoid aperture.

Planispiral: relating to bilaterally symmetrical whorl progression around an axis on a single plane.

Plication: a furrow, or costal interspace which is present on the internal mould.

Phragmocone: the portion of an ammonoid shell consisting of the gas and fluid chambers, or camerae.

Prorsiradiate: the direction of a costa that is slanting forward (more adaperturally) toward the venter than it is from the dorsum.

Polymorphism: the presence of a range of forms within the same species.

Rectiradiate: a radial costa perpendicular to the direction of shell growth that is slanting neither forward nor backward.

Retroversal: the terminal portion of a mature heteromorph ammonoid shell which curves backwards in the direction of the juvenile conch.

Rursiradiate: the direction of a costa that is slanting backward (more adapically) toward the dorsum than it is from the venter.

Saddle: an anteriorly (or adaperturally) directed incision on the septal suture.

Septa: the walls which separate the camerae and provide structural support to the phragmocone in shelled cephalopods.

Septal Suture: the often complex pattern occurring at the point of contact between the septal wall and the outer shell; in heteromorph ammonoids, the septal suture consists of four distinct undulating lobes and three saddles.

Septal Approximation: the crowding of septal walls occurring at the onset of sexual maturity.

Sinistral: a pattern of coiling to the left, in a counter clockwise direction.

Torticone: a shell coiled in a three-dimensional spiral.

Umbilicus: in ancyloconic and torticonic heteromorph ammonoids, the breadth of space between the helical whorls centered on the axis of coiling.

Volution: a complete 360° revolution of shell.

Whorl: generic term for any segment of the shelled tube which at one point enclosed the animal; in ammonoid taxonomy, applied when considering shell dimensions—coiled, helical or otherwise—having origins in the premise of curvature.

Total Other Marine Palynomorphs						
	<i>Fromea</i> spp.	<i>Michrystidium</i> sp.	<i>Parlecaniella indentata</i>	Misc. Acritarchs	Indet. Translucent Bodies	Total Foraminifer Linings
6	6					
38	20			18		
16	8		8			1
18	16	1		1		7
61	52		3	6		2
9	2		7			
18	9		4	2	3	1
55	52			3		
15	8			6	1	
8	6		2			
27	17		3	7		
73	17		52	4		
8	3		4	1		3
13	5		8			1
22	17		5			
72	46		10	12	6	1
3	1		2			
2	2					
8	6			2		1
						2
33	8		1	4	20	1
43	4		4	4	31	3
63	2		61			14
53	12		5		36	
63	57		1	5		9
	5			3	7	2
9	3		6			13

